A Top-Down, Hierarchical, System-of-Systems Approach to the Design of an Air Defense Weapon

A Thesis
Presented to
The Academic Faculty

by

Tommer Rafael Ender

In Partial Fulfillment
of the Requirements for the Degree
Doctor of Philosophy

School of Aerospace Engineering
Georgia Institute of Technology
August 2006

A Top-Down, Hierarchical, System-of-Systems Approach to the Design of an Air Defense Weapon

Approved by:

Prof. Dimitri Mavris
Committee Chair
School of Aerospace Engineering
Georgia Institute of Technology

Prof. Daniel Schrage
School of Aerospace Engineering
Georgia Institute of Technology

Dr. Neil Weston
School of Aerospace Engineering
Georgia Institute of Technology

Dr. Kevin Massey
Aerospace, Transportation,
and Advanced Systems Laboratory
Georgia Tech Research Institute

Dr. E. Jeff Holder
Sensors and Electromagnetic
Applications Laboratory
Georgia Tech Research Institute

Date Approved: 03 July 2006

ב"ה

for my family

ACKNOWLEDGEMENTS

The work presented in this document could not have been completed without the love and support of my parents, Judy and Ilan, my best friend and brother Roy, and my bashert Sonja. I would not have even considered pursuing a Ph.D. without the encouragement of my advisor Dr. Dimitri Mavris, who has supported my academic progression since my first undergraduate term at Georgia Tech. He has taught me to expect more from myself, and certainly more for myself in life. Thanks Doc.

I'd also like to thank the other members of my committee who helped me along the process: Dr. Neil Weston, who was instrumental in the final round of iterations of editing this document; Dr. Daniel Schrage, who took an inspiring interest in this topic very early on and provided encouraging feedback throughout; Dr. Jeff Holder, GTRI, for helping me begin to understand the complex radar concepts I decided to tackle in this thesis; and finally, a very special thank you to Dr. Kevin Massey, GTRI, not only for the encouragement to pursue this specific topic for a Ph.D., but also for working with me every step of the way to formulate a very interesting and important problem to apply the methodology developed in this thesis. That being said, the 6-DoF trajectory analysis in this document would not have been possible without the hard work of Mike Hieges of GTRI, and the co-op students working at GTRI that I've had to pleasure to work with over the past few years: Kevin Guthrie, Patrick O'Leary, Ben DiFrancesco, and Kyle French - I am still very impressed how quickly you guys were able to catch on and contribute to the development of the codes used in this study. Thank you to the U.S. Army-AMRDEC and GTRI for additional computational and financial support.

And many thanks to the friends I've made at ASDL over the years, especially

those that helped out with my thesis review: Andrew Frits, Brian German, Peter Hollingsworth, Hernando Jimenez, Rob McDonald, Janel Nixon, Holger Pfaender, and Jack Zentner. Also a special thanks to the other students I worked with in the original methodology used in this thesis: Bjorn Cole, David Culverhouse, Jared Harrington, and to Patrick Biltgen for helping shape the story telling aspect of the method, as well as the members of the AFICE team I've left out. Thank you to Dr. Michelle Kirby for always making herself available for answering questions and guidance. I would finally like to thank Liz and Jason Billman for proving the occasional retreat from my normal surroundings, giving me the much needed boost to get the thesis proposal started.

TABLE OF CONTENTS

LIST OF TABLES

LIST OF FIGURES

LIST OF SYMBOLS OR ABBREVIATIONS

AAA Anti Aircraft Armament.

ANOVA Analysis of Variance.

ASDL Aerospace Systems Design Laboratory (Georgia Tech).

C-RAM Counter Rockets, Artillery, and Mortars.

CCD Central Composite Design.

CDF Cumulative Density Function.

CEP Circular Error Probable.

CIWS Close-In Weapons System.

DoD Department of Defense.

DoE Design of Experiments.

DoF Degrees of Freedom.

DSE Design Space Exploration.

EAPS Extended Area Protection & Survivability.

FANNGS Function Approximating Neural Network Generation System.

G_r Receive antenna gain [dB].

G_t Transmit antenna gain [dB].

GTRI Georgia Tech Research Institute.

GUI Graphical User Interface.

IADS Integrated Air Defense System.

INS Inertial Navigation System.

IPP Impact Point Prediction.

LHS Latin Hypercube Sample.

LRIT Long Range Inner Tier.

MSPH Multiple Shot Probability of Hit.

P_{avg} Transmitted average power [W].

PDF Probability Density Function.

P_H Probability of Hit.

PID Proportional Integral Derivative (Controller).

P_K Probability of Kill.

$P_{K|H}$ Probability of Kill if Hit.

PNG Proportional Navigation Guidance.

P_S Probability of Survival.

RAM Rocket, Artillery, and Mortar.

RCS Radar Cross Section.

RoF Rate of Fire.

RPG Rocket Propelled Grenade.

RPM Rounds Per Minute.

RSE Response Surface Equation.

SAM Surface to Air Missile.

SEAL Sensors and Electromagnetic Applications Laboratory (GTRI).

SLID Small Low-cost Interceptor Device.

SNR Signal-to-Noise Ratio.

SRIT Short Range Inner Tier.

SSPD Single Sortie Probability of Damage.

SSPH Single Shot Probability of Hit.

THEL Tactical High Energy Laser.

TIF Technology Impact Forecasting.

USAF United States Air Force.

SUMMARY

Systems engineering introduces the notion of top-down design, which involves viewing an entire system comprised of its components as a whole functioning unit. This requires an understanding of how those components efficiently interact, with optimization of the process emphasized rather than solely focusing on micro-level system components. The traditional approach to the systems engineering process involves requirements decomposition and flow down across a hierarchy of decision making levels, in which needs and requirements at one level are transformed into a set of system product and process descriptions for the next lower level. This top-down requirements flow approach therefore requires an iterative process between adjacent levels to verify that the design solution satisfies the requirements, with no direct flow between nonadjacent hierarchy levels.

This thesis will introduce a methodology that enables decision makers anywhere across a system-of-systems hierarchy to rapidly and simultaneously manipulate the design space, however complex. A hierarchical decision making process will be developed in which multiple operationally and managerially independent systems interact to affect a series of top level metrics. This takes the notion of top-down requirements flow one step further to allow for simultaneous bottom-up and top-down design, enabled by the use of neural network surrogate models to represent the complex design space. Using a proof-of-concept case study of employing a guided projectile for mortar interception, this process will show how the iterative steps that are usually required when dealing with flowing requirements from one level to the next lower in the systems engineering process are eliminated, allowing for direct manipulation

across nonadjacent levels in the hierarchy.

In many cases, the analysis tools used to model those particular system components can be very complex and require a nontrivial amount of time for a single execution. Neural network based surrogate models are emerging as a viable method to capturing complex design spaces in the form of surrogate models. Unlike polynomial based surrogate models which are widely used for data regression, neural network based surrogate models give the user the ability to model highly nonlinear, multimodal, and discontinuous design spaces. The use of neural network based surrogate models to represent more complex analysis tools serves as the prime enabler of rapid cross hierarchical manipulation for the methodology developed in this thesis. This is done using a Monte Carlo simulation to sample from bounded distributions on the inputs used to create those surrogate models, populating the design space with the resulting responses. When designing to a specific goal in an extremely multimodal and/or discontinuous design space, this method is more efficient than making use of an optimizer that relies on smooth continuous functions and which often only finds local optima. This gives the user the ability to apply requirement constraints in real time, revealing how the feasible design space of every other response and variable changes, all the while maintaining a family of design options.

As a proof-of-concept, the methodology developed has been applied to the specific case of designing a gun launched guided projectile to intercept a small, indirect fire mortar target. It has not traditionally been the function of air defense weapons to defend against these types of unguided, low radar cross section targets. For this type of threat, one would ideally defeat the source of fire, however, this may not be a feasible option in a densely populated area where the attackers can quickly blend in with civilians, therefore a midair intercept is required. Notional metrics of interest identified for this type of air defense system include a balance between effectiveness against the target, the mobility to be moved to new locations as threats arise, all while

minimizing cost. The 6-DoF trajectory modeling and simulation environment used to study this weapon will be constructed as part of an effort underway at the Georgia Tech Research Institute and Georgia Tech Aerospace Systems Design Laboratory to meet this urgent requirement by the United States Army. This 6-DoF tool gives projectile performance against a mortar target, as a function of errors introduced by the gun and radar. In addition, the radar subsystem properties that define the radar measurement accuracy will be defined as part of the functional decomposition process.

For this system-of-systems environment comprised of a Monte Carlo based design space exploration employing rapid surrogate models, both bottom-up and top-down design analysis may be executed simultaneously. This process enables any response to be treated as an independent variable, meaning that information can flow in either direction within the hierarchy. For bottom-up design, the effect of manipulating weapon design variables on weapon performance (or other metrics of interest, such as cost), as well as the effect of the weapon performance on higher level metrics within an operational environment (for example, the combined effect of using multiple weapons against a single target) can be evaluated. For top-down design, placing limits or constraints on high-level metrics will drive the required weapon performance, with the effects cascading all the way down to the radar subsystem level properties, showing the ability to conduct rapid top-down design among nonadjacent levels in the design hierarchy. When the design space is completely populated, any design region may be visualized using a multivariate scatter plot. As constraints are now used to limit the remaining design space, the identification of not just the variables that are key drivers to response variability, but also those variables that are dependent on the settings of other variables is possible.

CHAPTER I

MOTIVATION

1.1 Introduction

1.1.1 Top-Down Systems Engineering

Systems engineering involves the orderly process of bringing a system into being, and is meant to provide "a structure for solving design problems and tracking requirements flow through the design effort" [35]. A primary function of the systems engineer is to document the requirements of a system, which involves laying out the initial system design in such a manner that the system will do what it is intended to do - for as long as it is required to operate. As Blanchard [40] states:

> *Broadly defined, system engineering is the effective application of scientific and engineering efforts to transform an operational need into a defined system configuration through the top-down iterative process of requirements definition, functional analysis, synthesis, optimization, design, test, and evaluation.*

Systems engineering introduces the notion of *top-down* design, which involves viewing an entire system comprised of its components as a whole functioning unit [40]. This requires an understanding of how those components efficiently interact, with optimization of the *process* emphasized rather than solely focusing on micro-level system components [47]. This drives the need for having a complete identification of system requirements, and relating these requirements to specific design goals and developing of appropriate design criteria. However, it is difficult to develop models that are sufficiently general to be applied to multiple systems [50]. Follow-on analysis

may be required to ensure system effectiveness of early decision making within the design process. This last point can best be described in this context using the on going *paradigm shift* in conceptual design (discussed in further detail later in this chapter). The "current", or traditional way of doing systems design involves very little, if any, front end engineering analysis effort. This requires much greater design effort by individual component designers downstream in the system design process, or even in the life cycle of the system itself. This after-the-fact decision-making may not necessarily integrate well with other design activities and may require many modifications, which may prove expensive in both time and money. Therefore, rather than rely on individual point design solutions, it is desired to keep families of solutions for a given design space of interest giving decision makers the flexibility to observe the impacts of various requirements and constraints on the entire solution space.

To summarize, the entire system design and development process requires an interdisciplinary effort to meet all design objectives effectively. This requires a complete understanding of the various design disciplines, and most importantly for the systems engineer, how the interrelationships between those disciplines affect overall system capability. The same conclusions can be drawn for the interrelationships of the components within a *system-of-systems*, where individually operated and managed systems interact to affect an overall metric (discussed in further detail in Chapter II).

1.1.2 Initial Research Formulation

In the author's opinion, part of developing a novel systems engineering process is in the investigation of its application to the development of a revolutionary concept, and then identifying deficiencies that the new process addresses in whichever process is currently in place, accepted, or in practice. The desire now is to find out how the related community approaches applying the systems engineering process to a complex problem, leading to the first research question.

Research Question 1: *What is the systems engineering process that can be applied to set the design requirements of a complex hierarchical system, and what are the major deficiencies associated with that process?*

For example, designing an air defense weapon system to complete a function in an operational environment not usually associated with air defense weapons, while accounting for uncertainties throughout the design hierarchy, requires several different systems to function together efficiently, and drives the need to utilize a top-down design approach and view the entire process as the system. As will be explained in more detail throughout this chapter, the specific case of launching a gun fired guided projectile to intercept a small, indirect fire target will serve as the primary proof-of-concept of the methodology developed. To help answer this question, several sources were discovered leading to an accepted process. The Department of Defense defines three characteristics of systems engineering [113]. First, systems engineering transforms an operational need into a description of system performance parameters and a system configuration. This process is achieved through an iterative process of definition, synthesis, analysis, design, test, and evaluation. Second, systems engineering integrates related technical parameters and must ensure compatibility of the physical, functional, and program interfaces. This is to be done in such a manner as to optimize the total system definition and design. Finally, systems engineering integrates reliability, maintainability, safety, survivability, human, and other related factors into the total effort to meet specific program objectives, such as cost, schedule, and technical performance goals.

In an effort to apply the general systems engineering process to the design of an air defense weapon capable of defeating small targets, Baumann [35] breaks down the systems engineering process into a hierarchy of decision making levels, using

information from multiple sources. The highest level is the *overall capability level*[1], which identifies the overall need or function that must be addressed. This system concept description is created with the intent of meeting a requirement at the overall capability level. Next below is the *system level*, which produces a system description, for example a performance requirement. At the lowest level is the *subsystem level* that produces a subsystem performance description. Baumann states that the systems engineering process is applied to each level in the design hierarchy, *one level at a time*. This is a "top-down, comprehensive, iterative and recursive" process and is "applied sequentially through all stages of development". It transforms needs and requirements into a set of system product and process descriptions. Figure 1 takes this systems engineering concept, showing the iteration step that must be taken across each hierarchical level. This figure depicts an important fact about this systems engineering process: requirements are decided upon and flowed from the top-down in the design hierarchy, and at each level there must be an iteration to make sure that the design solution satisfies the requirement, one level at a time.

In addition, Figure 1 applies this top-down structure to a notional air defense weapon, where the primary weapon system metric of interest is the probability of hitting a target. This notional weapon system may consist of a projectile, a gun firing that projectile, and a radar that tracks both target and interceptor trajectory throughout the engagement. Each one of those systems has an individual performance capability, for example the gun firing the projectile may experience pointing errors, or the radar may have some error in the location measurements of the interceptor or target. Therefore, only certain combinations of the individual system capabilities will achieve the top level capability requirement, and the iteration process is not required between that high level goal and each system. Once the system level requirements are

[1]Baumann [35] actually refers to this first level as the *concept level*, however for the purposes of remaining within the context of this thesis, it is referred to in this document as the *overall capability level*.

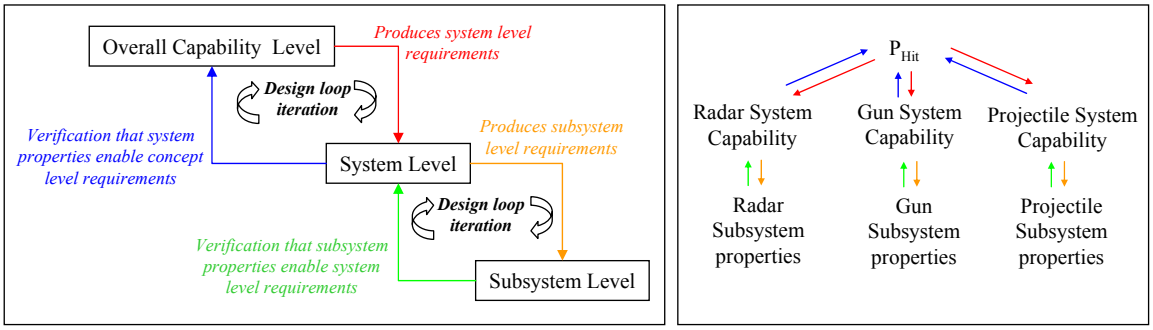

Figure 1: Systems Engineering Process with Top-Down Hierarchical Requirements Flow (adapted from [35]) with Process Applied to a Notional Problem

established, those requirements are then flowed down to the subsystem level properties that enable that individual system performance capability. For example, the radar measurement error can be a function of many of the radar properties, such as antenna gain, operating frequency, transmitted power, etc... Now the next level of iterations is required between each of the required system performance metrics and the variable space among the subsystem level properties.

To further address the question posed in Research Question 1, there are clear deficiencies associated with the traditional systems engineering process as applied to systems that themselves are composed of several component systems that must function together, but contribute individually to the overall process. There must be an iteration between adjacent levels of the hierarchy to make sure that the design solution satisfies the requirement, therefore there can be no direct flow between nonadjacent levels. Therefore, the next Research Question asks how an improved process can be created, encapsulating the overall **research objective** of this thesis.

> **Research Question 2:** *How can a process be created that enables rapid manipulation across a hierarchy of decision making levels?*

This research objective provides the primary motivation for the direction of the literature search chapters in this document. The example discussed of designing an air defense weapon requires several different systems to function together efficiently

within an operational environment in which air defense weapons are not usually used. Each of these systems has its own uncertainties associated with it that affect the combined system's overall capability. In addition, the operational environment may comprise of several high level requirements, such as some measure of effectiveness against a target at a given cost. This requires a more holistic approach to the problem, rather than focusing on the optimization of any of the individual system components.

1.1.3 Overview of Thesis

With the primary research objective introduced in Research Question 2 and the goal of applying this process to the example problem introduced in mind, Chapter II will be dedicated to finding general methods to model and quantify air defense weapon system capability, but do not in themselves allow for a solution to the specific example problem. Chapter III will be dedicated to those advanced design methodologies necessary to fulfilling the primary research objective, addressing the deficiencies in the current process. The motivation discussed in Chapter I and literature reviewed in Chapters II and III led to a another series of research questions and hypotheses discussed in Chapter IV. The questions will be used to refine the problem of interest into specific challenges that must be addressed, and the hypotheses will generally address how to answer those questions, based on information learned throughout the literature search. Chapter V will outline the research formulation and the modeling and simulation approach taken to prove the hypotheses presented. This chapter will also focus all of the information gathered during the literature search into a coherent problem within the scope of this thesis. Chapter VI will discuss the implementation of the methodology developed to solve the problem of interest, as well as any key findings. Finally, Chapter VII will review the research questions with the major elements of the results discussed that prove or disprove the hypotheses. This concluding chapter will also present some recommendations for further study relating to this

thesis.

First however, the remainder of this chapter will provide the reader with some background for an example problem of current interest, benchmarking current proposals for a solution to this problem, and identifying those proposals' shortfalls which drive the need to utilize a revolutionary concept. It is the discovery of a novel systems engineering process to investigate this revolutionary concept that motivates this thesis.

1.2 Background

1.2.1 The Rocket, Artillery, and Mortar (RAM) Threat in Asymmetric Warfare

> *The Army is fast-tracking a lot of technology to send it into Iraq because we are suffering casualties there. Normally, these things would be tested for one, two, three or four years before they were put into the field. So, we are going to be putting many of these new systems into the field in Iraq without complete testing, and some of them are going to work and some of them are probably not going to work very well, but I think it is worth our trouble...any American life saved is worth the effort...Although it is not the ultimate solution, of course, we don't have anything now that will, with 80 to 90 percent accuracy, take these mortars out.*
>
> Brig. Gen. Nick Halley (U.S. Army, Ret.), March 2005 [21]

The 2006 *Quadrennial Defense Review* [26] compiled by senior civilian and military U.S. Department of Defense (DoD) officials discusses attempts of non-state actors to choose irregular warfare in an attempt to break the will of the U.S. military in a protracted conflict. The DoD is therefore refocusing its portfolio of capabilities to address irregular and disruptive challenges in addition to sustaining the ability to address traditional challenges.

> *The [National Defense Strategy] acknowledges that although the U.S. military maintains considerable advantages in traditional forms of warfare, this realm is not the only, or even the most likely, one in which adversaries will challenge the United States during the period immediately ahead. Enemies are more likely to pose asymmetric threats, including irregular, catastrophic, and disruptive challenges.*

Asymmetric strategies toward warfare are "strategies that do not directly engage the full armed forces of a military power, instead taking advantage of anonymity, patience, and willingness to suffer casualties to counter an adversary's advantage in firepower" [123]. The belief that the U.S. has a very limited willingness to suffer causalities may drive an adversary to employ asymmetric strategies. Insurgents usually employ weapons in a war zone that are available in large numbers and simple to operate, and the threat from rockets, artillery, and mortars (RAM) is ever growing. This approach is certainly not a new idea, such as the Vietcong guerrilla attacks on U.S. soldiers during the Vietnam War, however, Vietcong use (and many other historical uses) of asymmetric warfare was in addition to, not in lieu of, a nationally organized military.

The collapse of the Soviet Union strengthened the position for the use of asymmetric warfare, as it was a large driver in the creation of many new centers of arms production in the world making available large numbers of highly sophisticated conventional weapons to anyone willing to pay for them. The Persian Gulf War in 1991 clearly exemplified how the United States, arguably having the most advanced military in the world, likely could not be beaten in a war, in the traditional sense. This traditional military advantage is likely a major factor that makes asymmetric warfare strategy more appealing to insurgents.

The U.N. intervention in Somalia is an early example of this premise. The broadcasts of the bodies of American soldiers getting dragged through the streets of Mogadishu on the news had an immense impact on the American public, limiting its willingness to sustain additional casualties. The civil unrest after Operation Iraqi Freedom is an example of how insurgents with minimally capable conventional weapons are able to successfully stage operations against American troops and interests, as well as attempt to cripple Iraq's fragile economy. This type of warfare attempts to show the world that the U.S. may quickly be victorious in a full scale conventional war, but not when trying to keep the peace in an asymmetric warfare environment.

1.2.1.1 The Baghdad Green Zone

The Green Zone, formally known as the International Zone, is the heavily guarded area of closed-off streets in central Baghdad, Iraq, where U.S. authorities live and work, and includes the main palaces of former President Saddam Hussein (Figure 2). This area houses the civilian ruling authority, as well as the military presence run by the Americans and British, and includes the main offices of major U.S. consulting companies. This area is commonly referred to as the "ultimate gated community" because of the numerous armed checkpoints, razor wire coiled and chain linked fences, and numerous reinforced blast-proof concrete slabs. Security is very tight, and American and British officials rarely leave the Green Zone, only doing so with many body guards and armored vehicles. Civilian traffic is very limited through the Green Zone because of the many terrorist attacks against both Coalition and Iraqi security forces and civilians [22].

The Green Zone is considered to be the safest area within Baghdad, however, terrorists are no longer limiting themselves to planting bombs. On September 27, 2003, insurgents fired three rockets at a Baghdad hotel housing American soldiers and civilians [22]. The attacks did very minimal damage, as the hotel stands hundreds of

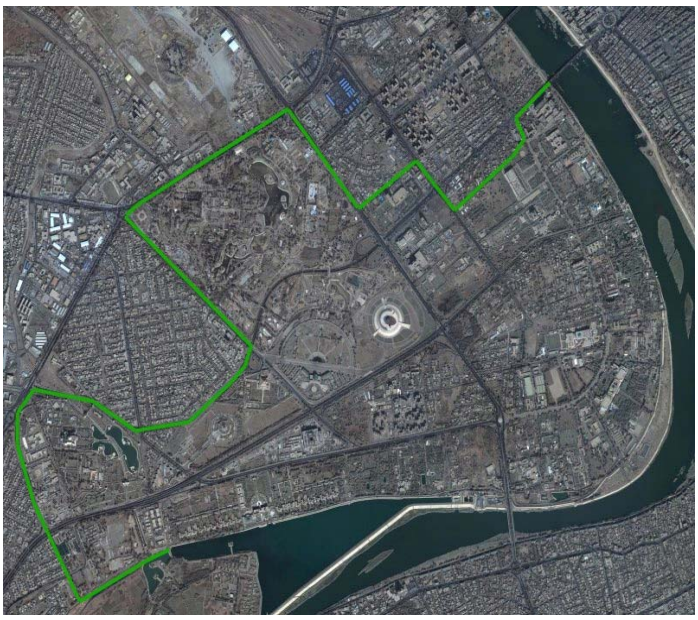

Figure 2: Green Zone in Baghdad, Iraq [22]

yards from high, earth-filled barriers circling that area of the Green Zone. This was the first terrorist attack of this type on coalition forces in this area, and mortar and rocket-propelled-grenade (RPG) attacks are now a common daily occurrence. New defenses against these asymmetric rocket and mortar attacks are sorely needed.

1.2.1.2 The Need for RAM Defense

Historian Major General Robert H. Scales Jr. describes in an interview that "in limited liability wars, most Americans killed in combat were killed by rudimentary weapons; the greatest killer of Americans on the battlefield is the mortar" [77]. He states that a historical pattern has emerged since the Korean War that will continue: most American soldiers killed in combat will die while facing an enemy fighting a close fight on equal terms using simple weapons. General Scales further points out the irony that a B-2 bomber has the ability to fly transcontinental distances to destroy a building with one bomb and return home safely, but that "a platoon under mortar fire is relatively helpless".

As a contemporary example if this, the Green Zone is very large and requires

many types of defense systems, such as M1 Abrams tanks, Bradley fighting vehicles, and 0.50 caliber machine gun armed HUMVEEs. However, these defense systems are not capable of defending against very small targets such as those posed by the RAM threat. It is the very basic nature of these weapons that make them so difficult to defend against. For example, once fired, mortars such as those shown in Figure 3 follow a simple ballistic trajectory. Because mortars do not rely on a guidance package, traditional missile countermeasures can not be used, such as chaffs against radar guided projectiles and flares against infrared guided projectiles. Fortunately, the use of these "dumb" projectiles usually results in a very small amount of direct hits on an intended targets. However, their effective range and the compactness of their launchers, as shown in Figure 4, means that a terrorist may stand off and fire from several kilometers away, making finding the source of fire a difficult task. Mortars provide a source of indirect fire, meaning that an attacker does not aim directly at an intended target. These types of unguided weapons provide rapid, high-angle, steeply dropping fires that have historically proven beneficial to military commanders fighting against dug-in enemy troops or targets with uncertain location, which are far less vulnerable to direct fire. Most mortars and launchers are light enough to be carried by backpack across all terrain.

There is a very urgent need for a weapon system that is able to intercept these small projectiles in mid-flight. Further, the reality of the situation is that this defense system needs to defend against several types of attacks from many directions *simultaneously*. This weapon system needs to be able to detect multiple targets with small radar cross sections (RCS), establish trajectory track for each target, hand off target position to the fire control system, engage each target, and successfully intercept each target with enough kinetic energy to destroy it. Of course, all this must be executed in a very short time (on the order of several seconds, depending on the threat range). All these requirements clearly drive the need for high accuracy and fast response

Figure 3: 60mm (top left), 81mm & 120mm (top right) Fin-stabilized and 4.2 inch Spin-stabilized Mortars (bottom) (photos from FAS [1])

Figure 4: The M252 81mm Medium Extended Range Mortar (photo from FAS [1])

at each level of the engagement, however put simply: hitting many small far away targets is a very difficult task.

1.2.2 Problem Scope: Extended Area Protection & Survivability

> *The Extended Area Protection and Survivability (EAPS) Science and Technology (S&T) Program Architecture Study will provide concept definition, requirements analysis, functional analysis, and design synthesis, and establish a baseline architecture to enable stationary/mobile 360 degree hemispherical extended area protection and survivability of future Army combat unit assets from direct and indirect fires, including rocket, artillery and mortar (RAM), Unmanned Aerial Vehicle (UAV), and Cruise Missile (CM) threats while minimizing cost, weight, and space allowing for improved deployment and mobility.* ***Currently, no existing or programmed system has the capability to negate unguided rockets and mortar/artillery projectiles with mechanical fuzes after they are launched****. Only a limited capability exists to negate UAV reconnaissance capabilities at sufficient range to preclude detection, identification, and targeting. Protection and survivability capabilities in Army combat units faced with this threat needs to be demonstrated to deter or defeat those enemy capabilities.* [138]

Bill Nourse, program manager of the U.S. Army's Extended Area Protection & Survivability (EAPS) program, describes the area air defense operational scenario as being broken down into an inner tier, comprising of the ranges up to 10 km, and an outer tier for defended ranges beyond 10 km [120]. The outer tier is focused on defending against large threats, such as ballistic and cruise missiles, unmanned aerial vehicles, and rotary wing aircraft. The inner tier is primarily focused on the smaller threats, such as rockets, artillery, and mortars, and potentially even on outer tier

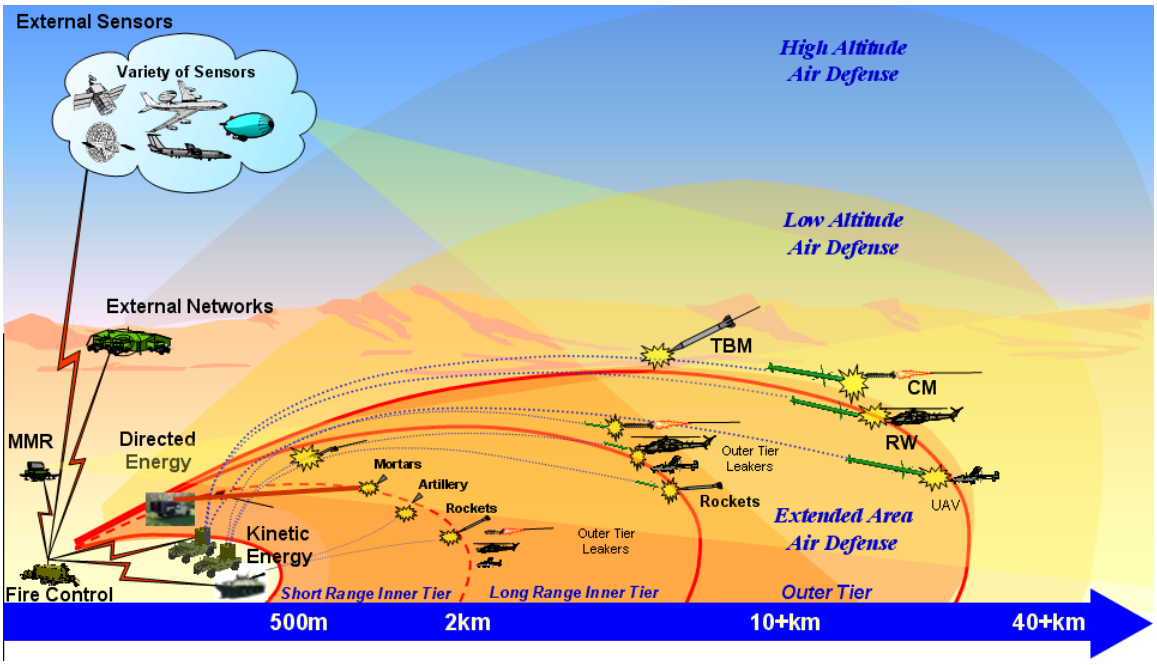

Figure 5: Extended Area Protection & Survivability Operational Scenario [120]

"leakers". As shown graphically in Figure 5, the inner tier is further broken down into a Short Range Inner Tier (SRIT) for ranges between 500-2000 m and a Long Range Inner Tier (LRIT) for ranges between 2-10 km.

Nourse describes several of the potential advantages of solutions addressing each of the inner tier options. A solution required to only defend the SRIT has the attributes of earlier fielding and lower unit cost when compared to a solution designed to defend the LRIT. In addition, threats that have very short times of flight may only operate within the SRIT. However, the ability to protect moving assets may only be addressed by a solution that can defend at the LRIT level. Nourse suggests that a mix of both short and long range shooters might be the most cost effective solution.

In [35], Dr. Jim Baumann, the Deputy EAPS program manager, lays out the basic air defense weapon engagement kinematics as given in Figure 6. This is independent of the type of interceptor solution, for example a gun fired projectile can be launched to intercept the target, or a directed energy (DE) weapon can be used to heat up the target's warhead causing detonation. The basic timeline of events is as follows.

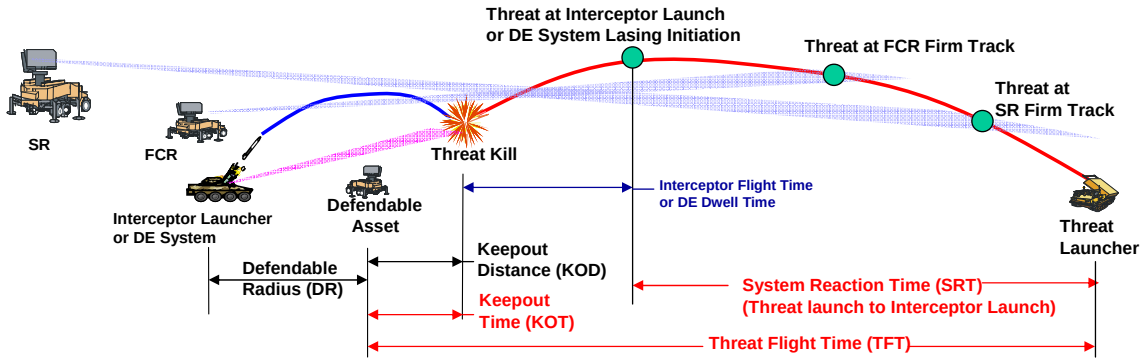

Figure 6: EAPS Engagement Kinematics [35]

A surveillance radar (SR) detects a threat fired from a certain distance with the intention of hitting some defendable asset, and firm track is established. A flight control radar (FCR) establishes a firm track of the threat trajectory to establish a fire control solution. When a solution is established, the air defense interceptor is launched (or if a DE weapon is used, system lasing initiation begins). The time up to this point is known as the System Reaction Time (SRT). The interceptor flight time, or DE lasing dwell time, determines the point at which the threat is killed, and the distance to the defendable asset is the Keepout Distance.

1.2.2.1 Gun vs. Rocket Interceptor Solutions

Baumann [35] compares the use of both gun and rocket interceptor solutions against a notional RAM type target in Figure 7. The red curve shows the intercept velocity versus intercept range for a notional gun firing a 20 mm projectile with a muzzle exit velocity of about 1100 m/s. The black curve shows the same profile for a notional 70 mm bore, 11 kg hypervelocity rocket (HVR). The straight blue curve gives a postulated lethality requirement achieved with a kinetic energy delivered at 800 m/s. Baumann concludes that a gun or rocket system would provide the necessary kinetic energy to destroy this notional target at the shorter range SRIT requirements (0-2 km). From the notional velocity profiles, note that a gun solution is especially better than a rocket at delivering kinetic energy at *very* short range, since the rocket requires

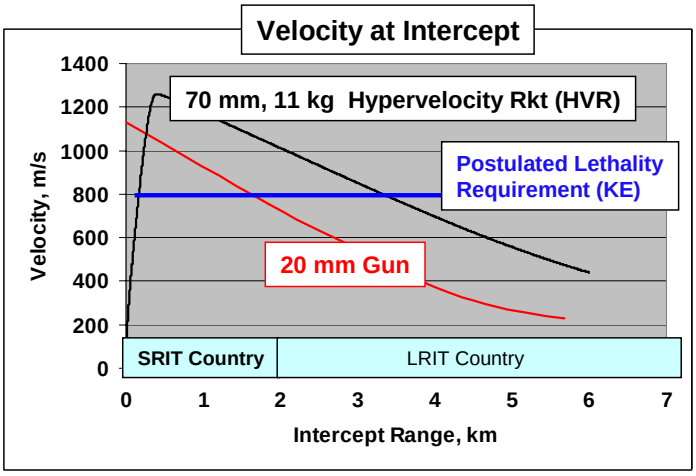

Figure 7: Typical Intercept Velocity Profiles of Guns and Rockets [35]

a certain distance after launch to achieve maximum velocity, where as a gun fires its projectiles at maximum velocity. However, the rapid velocity decay of a bullet as soon as it leaves the gun muzzle severely limits the amount of kinetic energy it can deliver at longer ranges such as those dictated by the LRIT requirement (2-10 km). In fact, the 20 mm gun solution appears to be able to deliver that required kinetic energy up until about 2 km (the boundary of the SRIT/LRIT requirements), and the rocket delivers the required kinetic energy up until about 3.5 km. A self propelled solution such as a rocket may be required to maintain a certain velocity profile at a ceratin range, depending on the amount of kinetic energy required at an intercept range. This clearly shows how the required defendable radius for a single solution drives the weapon design requirements.

1.2.2.2 Radar Accuracy Requirements

The performance of an interceptor projectile, guided or unguided, highly depends on the accuracy of the fire control radar to deliver it to the intended target. To defend an area against the RAM threat, the radar must have 360 degree operation in an urban and mountain environment, against low RCS and low trajectory targets with short times of flight (on the order of 12 to 15 seconds) [75]. These requirements pose several

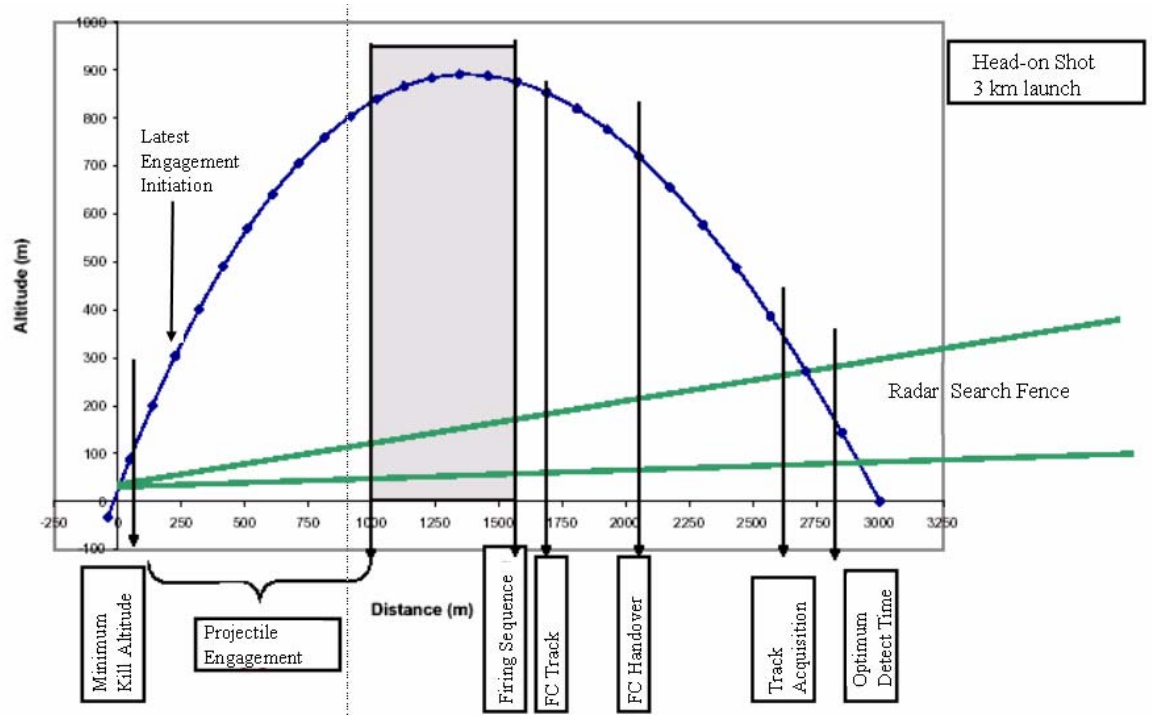

Figure 8: Projectile Timeline Engagement - Typical Mortar [75]

dilemmas. Full 360 degree operation requires a very large coverage volume. The short flight time of the threat requires a high radar search rate. However, finding a low RCS target would likely mean a longer dwell time before detection. A notional projectile timeline engagement against a typical mortar using a surveillance/fire control radar is given in Figure 8. Note a defined minimum kill altitude requirement[2] of 75 m.

Accurate handover to the weapon system requires high radar track accuracy, which in turn drives the need for a narrow antenna beamwidth. Unfortunately, a narrow antenna beamwidth does not readily allow for the large coverage volume and high update rate requirements driven by the threat characteristics. Therefore, the surveillance and weapon handover radar design requirements are incompatible, and drive the design in opposite directions.

The main driver for both surveillance and weapon handover requirements is radar

[2]This 75 m minimum kill altitude is assumed for all scenarios studied in the implementation discussed in Chapter 6.

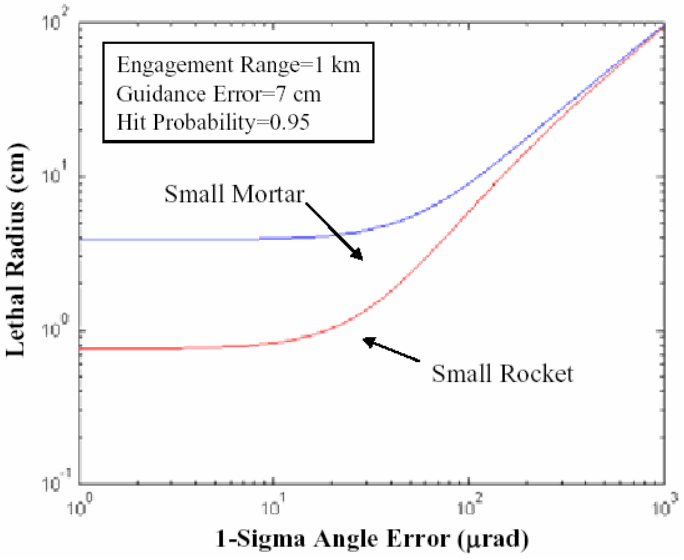

Figure 9: Fire Control Angle Error versus Warhead Lethal Radius [75]

accuracy, which plays an important role as to how close the fired projectile actually ends up to its intended target and its associated probability of direct hit. The use of a warhead would increase the projectile's lethal radius, meaning that a projectile could actually "hit" its intended target without directly intersecting flight paths. This leaves room for error in the radar. Holder [75] therefore states that "warhead size will dictate radar accuracy requirements" as given in Figure 9. The reader will note that for a given target size, as the radar error is reduced, the required lethal radius for a target hit is reduced until a certain point where error reduction does not affect required lethal radius. But the converse can also be stated in that a given radar accuracy might drive the need for a warhead of given lethal radius. The probability of hitting the target with a single projectile will also dictate the number of projectiles required to actually destroy the target. Therefore there is an important tradeoff space to be examined between the lethal radius of one projectile, the number of projectiles fired, and radar accuracy, for a desired probability of hit.

1.2.3 Approaches to the RAM Threat

As can be seen by the shift in how warfare is conducted, one of the most pressing questions facing the modern day war planner is how to defeat the types of weapons posed by the RAM threat. Ideally, one would try to eliminate the source of fire, but as stated previously, this is a particularly daunting task. Therefore the only choice left is to defeat the threat in mid flight, but as the program manager of the U.S. Army's EAPS program states, "currently, no existing or programmed system with a capability to negate RAM projectiles after they are launched" [120]. However, Macfadzean [92], considered one of the primary authorities on the analysis of surface-based air defense systems, states:

> *Surface-launched, direct-fire battlefield missiles are not viable targets for air defense systems. The launcher must be disabled, but this is not an air defense function.*

Nevertheless, as enemy tactics have evolved, so does the required function of air defense weapons. As a reaction to the mortar threat facing coalition forces in the Green Zone within Baghdad, the chief of staff of the U.S. Army has issued a directive for a near term fielding of a Counter Rocket, Artillery, and Mortar (C-RAM) system [19]. This system is in direct response to an operational needs statement from the Multinational Corps-Iraq. Each C-RAM system must identify, track, and engage an incoming threat munition. Additionally, because this defense system will be fielded in crowded areas, it must destroy the incoming threat with minimal collateral damage. The Army has three systems proposed to defeat this threat: the 20 mm Phalanx Close in Weapon System, a Navy anti-ship missile defense gun system; the 35 mm Skyshield, a Swiss rotary wing air defense system; and the Active Protection System, developed by the Defense Advanced Research Projects Agency for anti-tank missile defense. Additionally, the Northrop Grumman Corporation has proposed

using the Tactical High Energy Laser (THEL) developed for destroying Katyusha rockets launched into northern Israel, to counter the total RAM threat. Northrop Grumman has even conducted actual firing tests to prove that a single system can destroy multiple mortars in mid air [18].

One main problem with any of these approaches is the rush to field a system. Retired Army Brig. Gen. Nick Halley, the commanding general of artillery and rocket forces for the 18th Airborne Corps during the first Gulf War, stresses in the opening quotation to the background section of this chapter how the U.S. military would be willing to sacrifice some performance and effectiveness for the ability to deploy a C-RAM weapon system quickly [21]. The following sections will briefly introduce these proposed systems.

1.2.3.1 MK 15 Phalanx Close-In Weapons System (CIWS)

The MK 15 Phalanx Close-In Weapons System (CIWS) built by the Raytheon Systems Company, is a fast reaction, rapid-fire 20 mm gun system designed to provide naval ships a "last-ditch" defense against incoming antiship missiles or aircraft that successfully penetrated longer range defensive systems, such as surface-to-air missiles (SAM). A Phalanx system, shown in Figure 10, includes a fire control that has the ability to automatically detect, track, and engage targets using an advanced search-and-track radar integrated with a stabilized, forward-looking infra-red (FLIR) detector giving a multi-spectral capability. It can also provide an additional sensor and fire-control capability to an existing combat system. Finding specific characteristics on any weapon system used by the U.S. military is very difficult and often conflicting in open-source literature. Therefore, the Phalanx characteristics and description listed in this section are for the latest Block 1B standard derived from Miller [114], and summarized in Table 1.

The Phalanx fire-control system consists of two high frequency Ku-band radars

(discussed later in Chapter 2), which are beneficial when used to track small objects in a high clutter environment [96]. One radar is used to track a target, and the second is used to track its own projectile stream. An internal computer is used to compute the necessary elevation and azimuth required to eliminate the difference between the two, and deliver the projectiles fired to the target. The Phalanx employs a Vulcan Gatling gun element originally designed for use in aircraft. A six barrel cluster rotates at high speed firing projectiles at either continuous fire (4500 rounds per minute) or at burst lengths of 60 or 100 rounds. The gun fires a 20 mm armor-piercing discarding sabot (APDS) projectile consisting of a 15 mm subcaliber tungsten or depleted uranium penetrator. The Phalanx has been issued at several block standards. The latest Block 1B standard introduced many improvements to the gun system, but most notable to this thesis is a man-in-the-loop facility, which makes the system more suitable for use in engagements against small high-speed surface ships, small aircraft, helicopters, and surface mines.

A land based version of the Phalanx, shown in the right side of Figure 10, was selected by the U.S. Army as the interim C-RAM interceptor (and given the C-RAM designation). Tests conducted in December of 2004 showed a 60 to 70 percent shoot down capability of a live mortar [23], and subsequently two of these C-RAM systems were deployed to Iraq in August 2005 [39]. Note that these open source performance reports do not mention the size of the target, the intercept range, and the number of bullets fired (typical bursts of rounds number in the hundreds). As will be discussed much later in this thesis, preliminary studies to determine the effectiveness of a land based Phalanx weapon system using some of the methodologies introduced in Chapter 3 are given in Appendix B.2.

Table 1: MK 15 Phalanx Close-In Weapons System Characteristics [114]

Property	Description
Type	Fast-reaction, rapid-fire 20mm gun system
Date deployed	Block 0: 1980; Block 1: 1988; Block 1b: 1999
Gun type/caliber	M-61A1 Gatling; 20mm
Weight	12,500 lb
Range	4875 ft (horizontal)
Guidance system	Self-contained search-and-track radar with integrated FLIR
Type of fire	4500 rounds/min (Block 1 onwards)
Elevation/depression	+80/-20 degrees
Ammunition	Armor-piercing discarding sabot, tungsten subcaliber penetrator
Magazine capacity	1550 rounds (Block 1 onwards)

Figure 10: MK 15 Phalanx Close-In Weapons System [1]

Figure 11: The Skyshield 35 Air Defence System [2]

1.2.3.2 Skyshield 35 Air Defence System

The Skyshield 35 Air Defence System, manufactured by the Swiss company Oerlikon Contraves [2], was designed for short range air defense against aircraft and cruise missiles. A fully modular Skyshield 35 shown in Figure 11, is based on two 35/1000 Revolver Guns firing 35 mm projectiles at a rate of 1,000 rounds per minute in 24 round bursts and a fire control system consisting of a sensor unit and a detached command post. The sensor unit has an X-band search and track radar (discussed later in Chapter 2) that employs a multi-search unit for radar/TV and/or Laser/FLIR precision tracking. The entire system was designed for rapid deployment by means of trucks, trailers, railway, or aircraft.

The 35/1000 Revolver gun was designed to fire standard 35 mm ammunition, as well as the Ahead Ammunition, show in Figure 12. The Ahead round was specifically developed against small, low, and fast flying targets (here the manufacturer's intended idea of "small" is about the size of a cruise missile). The Ahead round itself, also manufactured by Oerlikon Contraves, is a 35 mm caliber projectile that consists of 152 tungsten submunitions that disperse at a given fuze distance "ahead" of a target. Each projectile is programmed by a muzzle based electromagnetic inductor that sets an electric timer as the projectile exits the gun, to activate and separate the projectile into its 152 submunitions [20]. Weapon characteristics of interest are

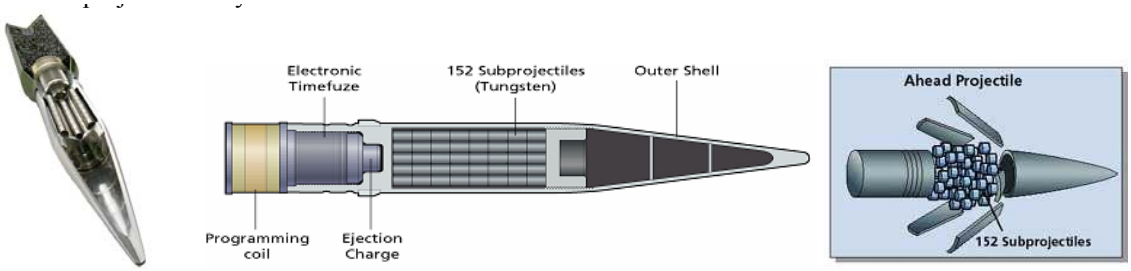

Figure 12: Ahead 35mm Ammunition [2]

Table 2: Ahead 35 mm Ammunition Characteristics [2]

Property	Description
Calibre	35 mm
Length	228 mm
No.Submunition	152
Submunition mass	3.3 g (each)
Payload mass	500 g (all submunitions)
Projectile mass (total)	750 g
Muzzle velocity	1050 m/s

provided in Table 2. Preliminary studies using methodologies introduced in Chapter 3 to determine the effectiveness of the Ahead round against very small targets are given in Appendix B.1.

1.2.3.3 Tactical High Energy Laser (THEL)

The Tactical High Energy Laser (THEL) is a high-energy laser weapon system designed to defeat short range rockets, developed for U.S. Space & Missile Defense Command and the Israeli Ministry of Defense. The THEL uses a high-energy chemical laser that focuses its beam on an incoming threat, the objective of which is to heat up the warhead to point of detonation in mid-flight. The laser beam is created by mixing fluorine atoms with helium and deuterium to generate deuterium-fluoride in an excited state. A resonator is used to extract the deuterium-fluoride and transform it into a coherent, monochromatic beam of light. FAS [12] claims a low-cost per kill (about $3000 per kill), the ability to "fire" 60 shots with a single load of chemical fuel, and a probability for kill near 1 at ranges within 5 km.

The main driving factor for the development of the THEL was the threat that Israel was facing from Hezbollah terrorists firing Katyusha rockets at Israeli towns across the border with Lebanon. These rockets fly very fast and at low altitude ballistic trajectories, and when aimed at crowded towns, can cause considerable damage. These attacks grew so numerous that Israel could not use interceptor missiles, and since the Katyushas flew on ballistic trajectories that landed on Israeli towns unless completely destroyed, they could not deploy an advanced machine gun defense such as the CIWS developed by U.S. Navy against low-flying cruise missiles. In April 1996, Hezbollah fired over two dozen Katyusha rockets at Israel within 17 days. In response, the THEL was designed to handle a large volume of attacks while maintaining a low cost per kill. [8]

The fire control radar would be positioned near the hostile zone, continuously scanning the horizon for threats. For a typical engagement scenario shown in Figure 13, a rocket is launched at a defended area. The THEL fire control radar detects the incoming rocket and establishes trajectory information, which then hands off the target to the pointer-tracker subsystem that includes the laser beam director. This process tracks the target optically, then finely tracks the target for the beam director, placing the high energy beam on the target. The transfer of energy from the high-energy laser causes intense heating of the target, causing the warhead to explode, causing debris from the target to fall to the ground short of the intended impact area.

However, the weapon system has not progressed far beyond the demonstration program. The system's lack of mobility limited the weapon system's effectiveness against targets with various ranges and trajectories. As discussed earlier, a weapon designed to counter the RAM threat must be able to be rapidly mobilized to protect an area. Therefore, Northrop Grummen has proposed a that the weapon system developed beyond the demonstration phase be a mobile version of the THEL, the MTHEL, which would be able to be air transported on a C-17, C-5, or C-130 transport

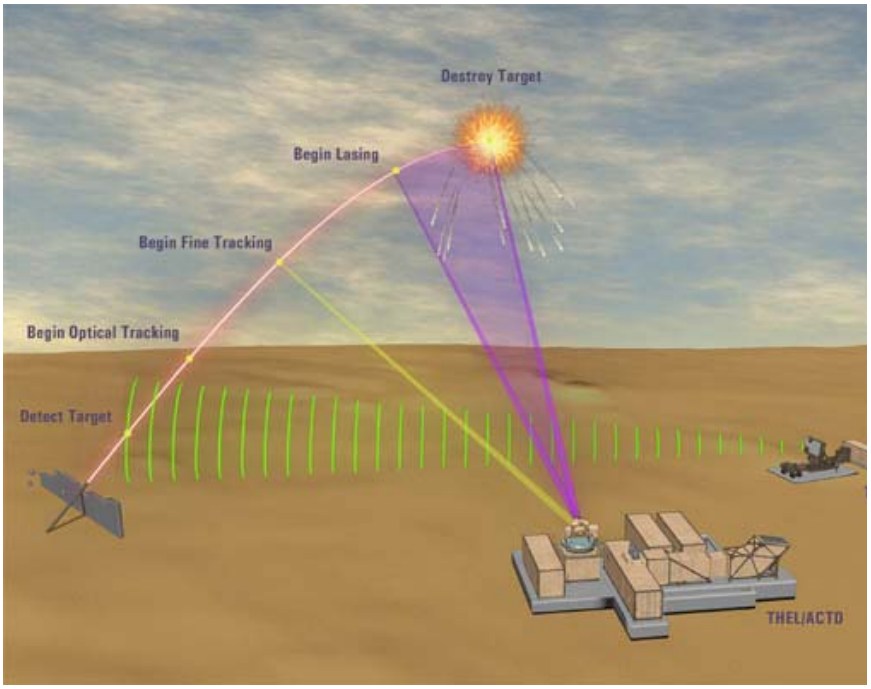

Figure 13: THEL Rocket Interception Process [17]

aircraft [17]. Although originally designed to counter rockets, such as Katyushas, the THEL has successfully shot down multiple mortar rounds in August 2004 during test firings at White Sands Missile Range, New Mexico, proving that the laser weapon could be used to protect against common threats [18]. However, funding for the MTHEL was cut in 2004.

Although no further attention will be paid to laser based weapons in this thesis, the original motivation for the development of the THEL and the difficulty associated with destroying small unguided airborne threats further motivates this thesis.

1.2.4 Guided Projectiles

1.2.4.1 Introducing the Concept

The basic objective of a guided projectile is to increase the accuracy of an otherwise unguided gun-fired projectile in hitting a target. Different approaches to the guided projectile solution have been examined. The projectile may carry a seeker, or on-board tracking sensor that homes in on the target's infrared or radar signature.

Another solution may have a ground based radar sending updates to the projectile as it approaches the target. These updates may include path corrections to adjust for any uncertainties, such as gun firing errors, wind, target tracking location error, etc... For example, Buzzett et al. [44] report that a notional unguided projectile with a Circular Error Probable (CEP)[3] of 200 m could be reduced to under 10 m, using guidance technologies for spinning projectiles using a body fixed guidance approach employing fast impulse thrusters (for control) and a low cost on-board seeker. However, the use of complex components that must be carried on-board the projectile may seriously drive up the cost of a single round. Any on board components or moving parts (i.e. moving fins for control) must be able to stand the high acceleration of being fired from a gun, sometime in the tens of thousands of g's. Nourse [120] identified several technology barriers to a guided projectile solution to the RAM threat, which include:

1. *Low Cost Sensor*: sensors for acquisition of small, short-range, and low trajectory RAM threats
2. *Guidance*: Miniature sensors and control mechanisms for low cost guidance
3. *Lethality*: Lethal kill mechanisms for defeating tough diverse RAM threat
4. *Fire Control*: Algorithms/network for timely impact point prediction/preferential engagement of RAM threat
5. *Shooter trade-off studies*: Efficient and mobile hemispheric protection from engagement of multiple RAM threats arriving simultaneously

A good deal of academic work at the undergraduate level has been conducted at the University of Alabama, including partnerships with other academic, industry, and government institutions. There were specific efforts to equip students with the specific technical skills related to the U.S. Army defined EAPS problem [43]. The efforts of the students to design a guided projectile are discussed in [69] [72] [144].

[3]Circular Error Probable (CEP) is "the radius of a circle, centered on the desired mean point of impact such that 50% of the impact points lie within it" [57].

Owen [121] discusses the use of Response Surface Methodology to represent simple trajectory calculations within more complicated 6-DoF codes, demonstrating a desire to expedite the 6-DoF trajectory process. Tournes [136] discusses using Monte Carlo simulations to quantify uncertainties in guided projectile flight control due to errors in aerodynamics, actuators used to direct control surfaces, wind, radar properties, and mass properties. Costello [51] discusses research at the faculty level at Oregon State University on the dynamic modeling of guided projectiles. Cave [46] introduced a system effectiveness analysis tool to evaluate guided interceptors (both gun-fired and missiles). This tool is designed to provide results that may be used to define defense system architecture and interceptor subsystem requirements.

1.2.4.2 Defense Industry Examples

In a Raytheon presentation explaining the theory of operations of guided projectiles, Geswender [66] compares the different levels of guidance on impact point accuracy, shown in Figure 14. The simplest level, the unguided round, clearly has the worst accuracy (i.e. the largest impact area of uncertainty). As guidance degrees of freedom are added, the impact area of uncertainty is reduced. In the development of the Raytheon Extended Range Guided Munition (ERGM), Geswender points out that the challenge is to "build a projectile with all the functionality of a missile but robust enough to [be] gun fired". The ERGM is a gun-fired, rocket assisted, GPS/INS-guided 127 mm projectile designed to be fired from the MK 45 5-inch gun for the U.S. Navy. The rocket-assisted round extends the range of the 5-inch gun from 13 nmi to 63 nmi, and the GPS/INS can achieve at accuracy of 10-20 m CEP at maximum range [14] [124].

The Boeing Company is developing a defense system which provides protection from missiles and artillery threats, designated the Small Low-cost Interceptor Device (SLID) [7]. The SLID is designed to be a small, low-cost, fully self-contained active

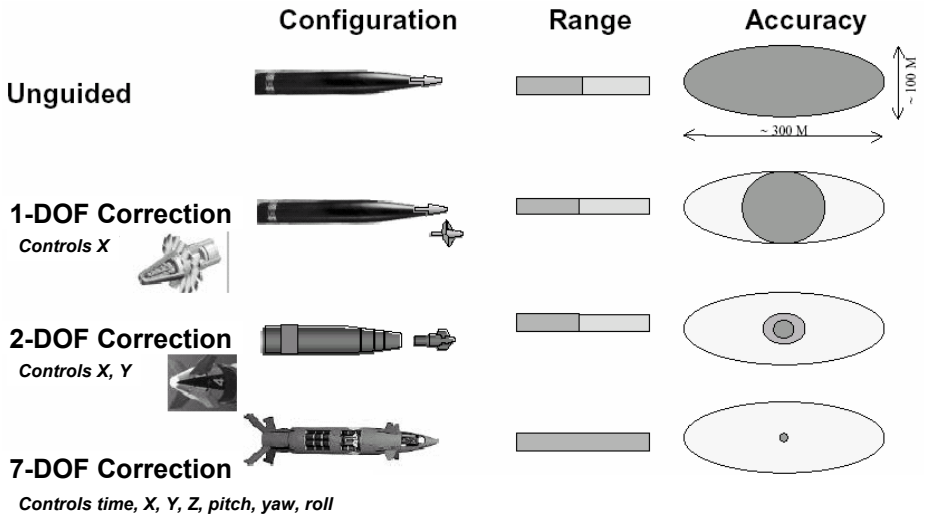

Figure 14: Potential Projectile Guidance Corrections Effect on Accuracy [66]

defense system for military or other high value assets. This system comprises of several components, including a small maneuverable hit-to-kill interceptor, high-speed launcher, passive threat warning sensor, and precision fire control system. Boeing claims that the SLID is designed to defeat threats at standoff ranges up to 250 m, which may include anti-tank guided munitions, high explosive anti-tank rounds, mortar rounds, and artillery shells. At a cost of $10,000 *per round*, the SLID relies on a number of technologies, notably for this thesis is the use of an optofluidic control system for maneuvering [36].

When compared to an unguided gun-fired round, the cost of guided munitions currently labeled "low-cost" would still be too expensive for widespread fielding (about 10-20 times). Even these cost predictions underestimate the cost, as most low cost claims are based on overestimated production volumes that do not materialize when actual procurement begins. Therefore, Horwath et al. [78] state that there is a need to "give up some precision to achieve low cost". Understandably, single shot accuracy and system cost are inversely proportional to each other.

An effort is underway at General Dynamics to study Low Cost Course Correction (LCCC) technologies [78]. The idea is to use off-the-shelf parts already used from

suppliers that build components in "high volume". A restriction is also applied to not use any moving parts, and therefore more suited to high-g gun launch applications. Therefore, there will be several restrictions on performance, such as not being able to employ pursuit guidance (i.e. chasing the target; discussed with the guidance navigation laws in Section 2.6.2). Additionally, it would not likely yield a "one shot one kill" solution, but *if there is confidence of intercepting within a certain miss distance of the target, then a multiple shot scenario could be used*, the "close is good enough" approach. Available literature shows that General Dynamics have applied the LCCC methodology to such smaller 40 mm and 50 mm bore projectiles.

1.2.4.3 Guided Projectile Research at GTRI

The Georgia Tech Research Institute (GTRI) has been investigating the use of pin based actuators to generate forces capable to steer small supersonic projectiles, shown in Figure 15. This section will highlight key findings and information appropriate to this thesis as interpreted from papers by Massey et al. [99], Massey et al. [101], Silton [131], and Silton and Massey [132]. Control of the projectile is achieved through taking advantage of the complex shock-boundary layer interactions produced by mechanical devices, as shown in Figure 16. The forces created by the shock impingement on the fins and body surfaces provide control forces through asymmetric lift. Angle-of-attack control is achieved by deploying two pins placed close to an adjacent fin, and rotation is achieved by deploying two diametrically opposed pins. Range tests of these projectiles fired at Mach 4+ demonstrated the divert required for intercept [100]. As shown in the shadowgraphs of live test firings in Figure 17, the robust pin firing mechanism was able to provide control after withstanding the high g load of being gun fired, and may be a comparatively low cost technology alternative for a guided projectile.

Figure 15: GTRI Guided Projectile with Pin Firing Mechanism [101]

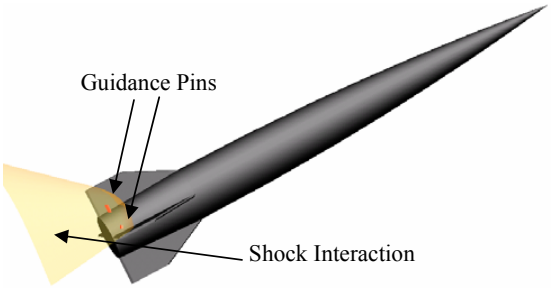

Figure 16: Pin-Fin Shock Interaction Guidance Concept [99]

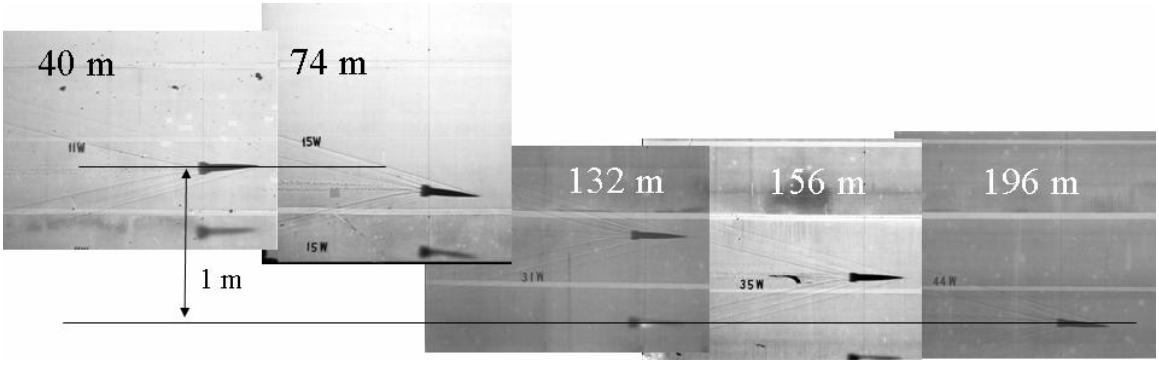

Figure 17: Shadowgraph Ensemble Showing Divert of Pin-Controlled Projectile [100]

1.2.4.4 Concluding Remarks on Guided Projectiles

Clearly, the study of guided projectiles is still in relative infancy compared to mature operational weapons systems. One issue related to the problem defined in this thesis is that most of the literature about industry built guided projectiles is that they are designed to hit fixed *surface* targets at ranges much farther than those outlined by the EAPS SRIT requirements discussed in Section 1.2.2, which address the need to defend against moving airborne targets. This leads to the design of very complicated and expensive projectiles not suited to defend an area against the RAM threat.

1.2.5 Summary of Discussed Solutions

Table 3 reviews the different alternatives discussed as potential solutions to the RAM threat, as well as several of the guided projectiles discussed. As discussed in Section 1.2.2.1, both a gun fired projectile and a self propelled rocket (or missile) could deliver the necessary kinetic energy to destroy a notional RAM threat at distances within the SRIT requirement (<2 km), and in fact at very short distances (within the acceleration period of the rocket) a gun fired projectile would deliver more kinetic energy. A gun fired projectile would certainly be less complex (i.e. less expensive) than a rocket or missile, and therefore more desirable to meet the SRIT requirements. However, with their single shot probability of hit being orders of magnitude lower than that of guided missiles, many gun fired projectiles would have to be used to be effective, something not desirable in an area trying to defend against many incoming targets. Additionally, having to fire many projectiles greatly increases the chances of collateral damage. Therefore, Table 3 includes a review of the guided projectiles discussed in this thesis.

The only directed energy weapon discussed, the THEL, is not capable of being relocated with great effort, probably beyond the effort afforded in a combat situation. For this reason, it is ruled out as a potential possibility for this study.

Table 3: Summary of Relevant Unguided & Guided Alternatives

	Weapon System	**Bore (mm)**	**Guidance**	**Control**	**Kill Mechanism**	**Summary**
Proposed Approaches	Phalanx/C-RAM	20	none	none	hit-to-kill	Inexpensive, low single shot P_H
	Skysheild/Ahead	35	none	none	Submunition burst	Designed to take out target larger than RAM threats
	THEL	-	-	-	Directed Energy	Very expensive, immature and immobile technology
Other Gun Fired Guided Projectiles	SLID	n/a	onboard laser seeker	optofluidic thrusters	hit-to-kill	Max range far short of the EAPS SRIT requirement
	ERGM	127	GPS/INS		submunition burst	Large round fired from large guns; designed to hit targets well beyond EAPS requirement
	GTRI Guided Projectile	TBD	Command updates	pin-firing mechanism	hit-to-kill; warhead req. TBD	

1.3 Paradigm Shift in Conceptual Design

The proposed approaches to defeating the RAM threat discussed in Section 1.2.3 included evolutionary applications to already existing weapon systems that clearly were not designed with the intention of meeting those needs. Those needs are outside the described by the problem of interest are outside the traditional required function of air defense weapons. Therefore, there is a need for a revolutionary solution, such as using a gun launched guided projectile, which serves as an excellent case study example for the implementation of a process desired in Research Question 2.

A paradigm shift is under way in the field of conceptual design to bring knowledge of the system in question up front in the design process, while maximizing design freedom as long as possible, without committing unnecessary cost [106]. Failure to consider all of the requirements for producing a product may result in many changes in the design. Most of the costs associated with developing a product are determined very early in its life cycle, where uncertainty in the design is highest. Chapman et al. [47] states that 80% of the system cost is determined by the initial system design, which is the portion of the system that can no longer be optimized with respect to cost or performance. With only 20% of the product development costs spent, 80% of the total product cost has already been locked. Future optimization of the product during its lifetime will only affect the remaining 20% of the product's cost. Therefore, mistakes made in the initial stages of the design of a system will have a serious negative impact on the total cost and success of the final product. Investing more effort up front in the design cycle, and ensuring that all the aspects of the concept are optimized, a more quality product can be delivered.

Dieter [56] addresses the idea of product cost committed during the phases of the design process as well. He makes the point that true quality must be designed into the product to produce a competitive product that will not have to be redesigned after it goes into the market. Deiter's major points on product design are summarized below:

- Decisions made in the design process cost very little in terms of the overall product cost but have a major effect on the cost of the product.
- Quality cannot be built into a product unless it is designed into it
- The design process should be conducted so as to develop quality cost-competitive products in the shortest time possible.

Today's traditional design process commits cost rapidly at the early stages of design, where knowledge of the system is the lowest. Additionally, design freedom rapidly decreases as important decisions are made in the initial conceptual design stages. Bringing more knowledge of the system forward will enable a designer to make more informed decisions before the final costs are locked in, enabling the freedom to make design changes without a heavy cost for a longer period of time during the design process. This concept is known as a *paradigm shift*, inspired by initiatives in government and industry to focus the engineering design community on system affordability as the overall decision making objective. The evaluation of a design is no longer driven solely by its capability to achieve specific mission requirements or remain within specific product constraints. Rather, a *robust design process*, or one that leads to a design that is least sensitive to influence of uncontrollable factors, is needed to "balance mission capability with other system effectiveness attributes" [106]. This design process would ideally bring more knowledge to the early part of the product design phase where design freedom is highest. Additionally, the designer would like to have the ability to keep a family of designs, rather than a point design, for as long as possible, and keep the design freedom available longer.

Therefore, the following two literature search chapters are dedicated to finding methods to realizing and furthering the spirit of this paradigm shift, as applied to the general systems engineering process development desired in the primary research objective and using the example problem of interest discussed in this chapter as a

proof-of-concept case study.

1.4 Disclaimer

This thesis does not intend to reflect the true performance characteristics of actual weapon systems. It is meant only to show the trends one would expect if actual data was used to conduct the study, data which is usually of a sensitive nature. Every attempt has been made to protect any sensitive data by normalizing or eliminating data on figures and plots, where possible.

CHAPTER II

LITERATURE SEARCH: COMBAT SYSTEM MODELING & SIMULATION

The scientific methods of analysis and optimization have now found acceptance at every level of military operations, starting with the planning of strategies, tactics, and doctrines through force deployment and employment in actual combat. The President of the United States and the National Command Authorities use the results of the extensive analysis when various options for action are submitted by the military departments and the Department of Defense for the final decision. Also, at lower echelons the decision-makers rely heavily on the analytical studies that define measures of system effectiveness and present a process of determining appropriate criteria for choosing preferred alternatives.

Przemieniecki [126]

The intention of this chapter is to introduce general methods to model and quantify air defense weapon system capability, and the various related aspects of combat systems modeling. However, there exists is a lack of literature in modeling of the RAM threat and of the air defense systems designed to defend against this threat, but there is an abundance in the area of aircraft survivability and large scale combat modeling. Although there is not absolute correlation between the two subjects, those topics pertinent to this thesis will be introduced in this chapter, and used as a starting point to identify related topics that are required to be included in any methodology implementation that will address the specific problem. The goal is therefore to find accepted

methods that establish total weapon system accuracy and lethality by modeling the firing of multiple guided projectiles for target intercept, with an additional focus on the modeling of the radar subsystem variables effect on radar system accuracy and cost.

2.1 Modeling Military Operations

2.1.1 General Requirements of Combat Modeling

The planning of successful military operations relies on accurate modeling based on mathematical methods of analysis. Exploring different alternatives for resource allocation or specific force deployments is a useful way to determine the best strategies for use in actual combat engagements. In the opening quote, Przemieniecki [126] underscores the importance of using mathematical methods in defense analysis for decision making, at various levels within the military planning framework.

The basic concept in the mathematical modeling of combat engagements focuses on the *attrition* of combat troops, weapons, vehicles, targets, and any other resource expended in the engagement, according to Przemieniecki. These attrition, or force reduction rates are expressed as number of individual objects (i.e. targets, resources) destroyed per unit time. These rates may vary as a function of time, depending on factors such as: resource allocation (i.e. troop location and concentration); availability of resources (i.e. resupply, or refitting an aircraft returning from a sortie); command, control, and communications; intelligence information about the target area; other major human factors including prior training, and the willingness of combatants to engage in battle to the maximum capabilities constrained only by physical limitations. Much of the data used in these models is generated in terms of probabilities of event occurrence, varying from 0 to 1. A common example of this is using analysis of gun or missile test data to determine the Circular Error Probable (CEP), leading to calculation of probability of hit.

2.1.2 Large Scale Combat Computer Simulations

2.1.2.1 Identification of Large Scale Combat Computer Simulations

There are many modeling and simulation tools that have been developed to attempt to describe the outcome of military encounters at various levels of fidelity. Decision makers can then use the outcomes of these simulations to base important tactical and/or strategic conclusions. The different branches of the United States armed forces have adopted respective theater level analytical campaign simulation tools. The U.S. Air Force uses THUNDER [68] to simulate large-scale application of air and space power in a "joint warfighting context" at the theater level. The Integrated Theater Engagement Model (ITEM) [129] was developed for the U.S. Navy at the request of the Defense Nuclear Agency to model naval nuclear simulations. It has since evolved to model naval surface and subsurface combat, amphibious operations, air combat, and ground combat, and has gained acceptance by the U.S. Pacific Command to model joint expeditions in the Pacific Theater [55].

Janus was one of the first codes developed to simulate low level conflict, primarily used to train platoon and company level commanders to apply tactical doctrines and combat techniques. It is an "event driven simulation that models fighting systems as entities (such as tanks, helicopter, etc)" [13]. The Joint Conflict and Tactical Simulation (JCTS) is an upgrade to Janus giving it an urban combat modeling capability, and gives the user to control thousands of soldiers, aircraft, and naval vessels simultaneously. Although as with Janus, the focus is primarily on the infantry and soldier level, giving the ability to simulate hostage rescues and drug interdiction raids. Many of these simulations or "games can last weeks" and, "sometimes a short game is run dozens of times so that statistical sampling can be used to evaluate a particular tactic or weapon" [71].

These tools are just several examples of large scale simulation tools. The one thing they have in common is that they are meant to provide enough scope to make

high level decisions, such as the ability to defeat an enemy or estimate asset loss.

2.1.2.2 Modeling RAM Defense Using Janus

Baumann [35] discusses the use of Janus to simulate low to mid intensity conflicts having intense RAM barrages. From this study, Baumann concludes that the survivability of assets undergoing an intense RAM barrage was found to be dependent upon asset dispersion, maneuver, concealment and counterfire against only the potentially threatening RAM sources. Because the various RAM projectiles are unguided, they can not be steered into a target and usually have very poor probabilities of hit with a single projectile. It is certainly a waste of resources to engage any RAM threat that is determined to miss any assets. This means that an accurate Impact Point Prediction (IPP) must be used, which uses precision tracking of incoming threats to calculate prediction of threat's flight path and impact point in relation to the location of dispersed assets, both stationary and moving. This means that there are two options to ensure asset survivability on the battlefield: control asset location such that most of the potential RAM fired pose little threat, or only engage the ones that are assessed to threaten the assets.

The key findings of Baumann's Janus study was that effective engagement against RAM considered a threat is dependent on three factors assuming accurate IPP: high threat kill rate, large shooter magazine, and engagement of multiple targets simultaneously. These statements very likely come with a sizable list of assumptions that were not clearly stated in [35], however several assessments can be made as applicable to this thesis. The first statement, that a high threat kill rate is an obvious requirement. For any number of RAM encountered, a high percentage of them must be destroyed. However, this could also be used to set the *confidence* requirement of an individual encounter, saying that the probability of one interception solution destroying a RAM threat must be high. The second statement implies that the likely

case that a single interceptor launched against a RAM threat would not defeat it and requires firing multiple interceptors. However, the statement itself indicates that whatever solutions studied in the Janus simulation must have had a very small Single Shot Probability of Hit (SSPH). Finally, the last statement of engagement of multiple targets simultaneously could lead to the assumption that a specific defendable area was defined. In fact one statement Baumann made was the there was a "need to assess other scenarios". Clearly, there is a need to model an interceptor and target engagement accurately.

2.2 Modeling and Simulation Concepts

It is first necessary to establish definitions to some commonly used terms. The Military Operations Research Society (MORS) [79] explains that according to terminology established by the Department of Defense (DoD), a *model* is a "physical, mathematical, or otherwise logical representation of a system, entity, phenomenon, or process", and a *simulation* is a "method of implementing a model over time. Also, a technique for testing, analysis, or training in which real-world and conceptual systems are reproduced by a model". MORS further breaks down the levels of model aggregation for warfare modeling into four categories: 1) phenomenological models, which describe the behavior of individual physical entities (human or otherwise), 2) single engagement models, 3) battle or multiple-unit engagement models, such as force on force engagements, and 4) campaign or theater level models. These levels may be useful in constructing a hierarchy of models to serve a common purpose of a system-of-systems. This hierarchy may be visualized as a pyramid as shown in Figure 18, with the bottom containing the phenomenological models and the top the campain/theater level functional as the single macro model. This pyramid represents the nesting of models in one interacting whole, showing how results are integrated from one echelon to another, or simply an *abstract* representation of a structure relating independent model

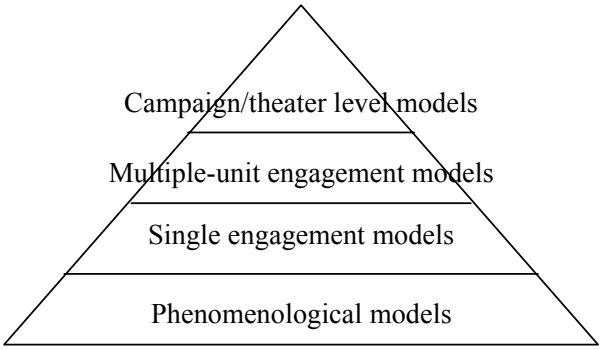

Figure 18: Military Operations Modeling Hierarchy Pyramid (adapted from [79])

operations.

A more generalized approach to defining model types is useful for describing total system effectiveness. Dieter [56] states that "a model is an idealization of part of the real world that aids in the analysis of a problem...Simulation is a manipulation of the model". This manipulation involves subjecting the model to various input conditions to observe its behavior enabling a user to explore the nature of results that would otherwise be obtained from an actual system. In general terms, a model may be either descriptive or predictive. A descriptive model enables an understanding of a real-world system, such as a model of an engine or complete aircraft. A predictive model is used to understand and predict the performance of a system.

Dieter further classifies the model types adapted from [65], as 1) static or dynamic, 2) deterministic or probabilistic, and 3) iconic, analog, or symbolic. Table 4 lists the properties of each of those model classes. The first classification level describes whether or not model properties are affected with time; i.e. static or dynamic. The next level describes whether or not the behavior described by the model is known with certainty; i.e. deterministic or probabilistic. Finally, the physical model is described. If a physically geometric representation is used, such as a wind tunnel model, the model is iconic. An analog model is used when the model only needs to describe the actual behavior without physically representing the actual event, such as a process

Table 4: Model Types (adapted from [56])

Classification	Description
Static	Model with properties that do not change with time
Dynamic	Model in which time varying effects are considered
Deterministic	Model that describes the behavior of a system in which the outcome of an event is known with certainty
Probabilistic	Model that describes situations that have outcomes not known with certainty
Iconic	Model that is a physically geometric representation used to describe the static characteristics of a system
Analog	Model that behaves like the real systems they represent, by either obeying the same physical principles or simulating the behavior of the system
Symbolic	Model with abstractions of the important quantifiable components of a physical system, providing the greatest generality leading to a qualitative result

flow chart. Finally, the greatest qualitative results are obtained by using symbolic models, such as mathematical equations, that are able to model abstractions and quantifiable components of a physical system. Therefore, a mathematical equation used to model a system that uses no random variables would be a static-deterministic-symbolic model.

Symbolic mathematical models, which are usually used to treat a process by logical quantitative relationships, are further classified as analytic or simulation models by Przemieniecki [126]. The analytic model determines exact solutions with deterministic outcomes, whereas the simulation model, as Przemieniecki adopts from [83], is "a series of models that may be used to converge on solutions to very complex problems involving uncertainty (probabilistic occurrence) and risk". Przemieniecki then takes that simulation model, and subdivides it as either a deterministic or stochastic (probabilistic) model, as shown in Table 4. Figure 19 graphically shows the hierarchical relationship between the different model classifications described above

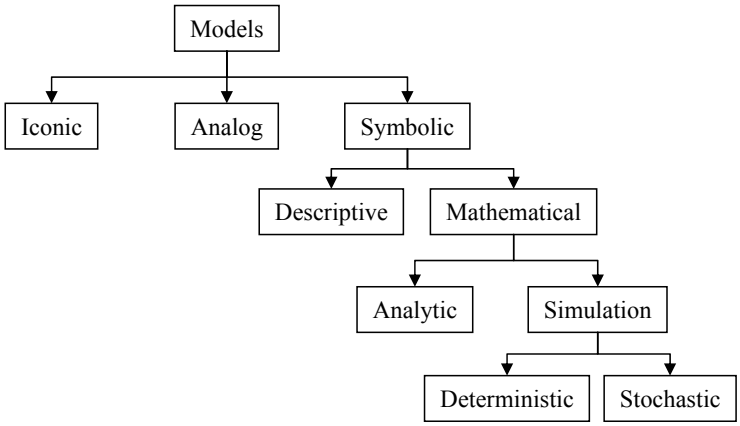

Figure 19: Model Classification Hierarchy [126]

and listed in Table 4, leading down to the model types of interest. As will be discussed in the following subsections, the basic concepts originally developed for the theory of combat were deterministic models. Probability based combat models were developed to simulate more complex situations that take into account the randomness associated with engagements.

2.2.1 Deterministic Models

For simple homogenous combat engagements, a deterministic approach can be used to create a set of differential equations describing the strength of each side of the engaging forces as a function of time. The deterministic approach can be used to model combat engagements only when analytical solutions are possible.

Frederic Lanchester [89] is credited with developing the fundamental model for developing theories of combat and for calculating attrition of forces in military engagements. In 1916, Lanchester developed a mathematical analysis of air combat, the overall concept being based on a simple expression relating attrition rate to the product of the opposing force effective firing rate of a single force (or weapon unit) of time, and the total number of opposing units (or weapons) engaged in combat. The attrition rate is equal to the product of the effective firing rate and number of the

opposing force. The Lanchester equations as applied to notional Blue and Red forces are given in Equations 1 and 2, respectively. The total number of Blue forces m_B is shown as a function of Red force effective firing rate a_R and total number m_R, with similar logic shown for determining the total number of Red forces m_R. Note that the negative sign denotes attrition.

$$\frac{dm_B}{dt} = -a_R m_R \tag{1}$$

$$\frac{dm_R}{dt} = -a_B m_B \tag{2}$$

However fundamental these equations were to the development of modern combat modeling, Przemieniecki points out that they are bound to the following assumptions that quickly show their practical limitations: 1) both sides are homogeneous and are continually engaged in combat; 2) each unit (or individual weapon) is within the maximum weapon range of all opposing units; 3) collateral damage is considered negligible within the target area and ignored; 4) the attrition coefficients include the probabilities of the target being destroyed when hit; 5) the effective firing rates are independent of the opposite force level; 6) every unit is aware of the location and condition of all opposing units - fire is directed only at live targets, and when a target is destroyed, search (or fire direction) is directed at a new target; 7) there is a uniform distribution of fire over the surviving units (i.e. no prioritization of targets). It is evident that all of these assumptions severely limit the practical use of these models, and their very use presumes that an attrition rate can capture all of the pertinent information in an engagement scenario. This drives the need for other types of models that take into account the random nature of engagement models.

2.2.2 Probabilistic (Stochastic) Models

Probabilistic models simulate random processes, such as an endgame, a one-on-one encounter, or a many-on-many scenario. Ball [32] specifies three types of probabilistic

models used for survivability assessment: expected value models, Monte Carlo models, and Markov Chain models.

2.2.2.1 Expected Value Probabilistic Models

Each phase of an engagement may have associated with it a probability that a certain outcome occurs. For example, the probability of detecting an enemy is 0.6, the probability of hitting the target with a weapon is 0.4, and probability of kill if hit may be 0.8. The actual probability of killing the target is the joint probability of each of the battle phases occurring. The *expected value* of a random number is simply its *mean* [74], therefore an expected value engagement model just multiplies the probabilities together to obtain the answer. In the very basic example case above, the probability of a successful kill would be 0.6*0.4*0.8 = 0.192.

2.2.2.2 Monte Carlo Probabilistic Models

When the scenario is too complex because of too many phases in the process that must account for randomness, or too many conditional probabilities are included in the process, a Monte Carlo model is often used. Instead of just multiplying the probabilities of individual events together to determine the joint probability of the combat outcome such as with the expected value model, a Monte Carlo simulation draws a random number [0,1] at each event in the process and compares it to the assigned probability to determine whether that particular event occurs. This process is repeated many times to give a probability distribution. With increased number of trials, the Monte Carlo model results will approach the expected value model results. A more detailed discussion of Monte Carlo simulation as applied to uncertainty quantification will presented in Section 3.2.2 of Chapter 3.

2.2.2.3 Markov Chain Probabilistic Models

A Markov process has a system which can reside in two or more states or conditions, and the values associated with those states are contained in a state vector. A Markov Chain model assumes that a sequence of independent events associated with a system can be modeled as a Markov process. As an event occurs, each state within the system transitions to all other possible states with a specific probability for each transition. The probability of the system existing in each of the possible states is a sequential process, in which the state it will exist in after events $1, 2, 3, ..., J$ is based on the probability the system existed in each of the possible states after the previous events $0, 1, 2, ...J-1$ respectively. This sequential process is the Markov chain process. A transition matrix $[T]$ transforms the current state vector $\{S\}^{\{j\}}$ to the next state $\{S\}^{\{j+1\}}$ as given in Equation 3.

$$\{S\}^{\{j+1\}} = [T]\{S\}^{\{j\}} \text{ for } j = 0, 1, 2, \cdots J-1 \tag{3}$$

As they are not directly applicable to the type of problem studied in this thesis, Markov Chains will not be used, and no more attention will be paid to them[1]. Interested readers should refer to Appendix B in Ball's book [32] for an example engagement scenario modeled as a Markov Chain.

2.3 Survivability as a Discipline

For an aircraft in a combat environment, Ball [32] defines its *survivability* as "the capability of an aircraft to avoid or withstand a man-made hostile environment". The survival of an aircraft on a combat mission is not a deterministic outcome, or something that can be predicted with absolute certainty. Aircraft survivability is

[1] As will be discussed further in the approach chapter, an individual engagement will yield probability of hit as a function of noise on radar measurement and gun firing accuracies. Many executions sampling from distributions of those noises will be required, driving the need for using a Monte Carlo simulation.

influenced by a number of random variables, and is measured by the probability P_S, varying from 0 to 1. The closer P_S has a value to 1, the more likely an aircraft is to survive a combat scenario. The probability that an aircraft is killed, P_K, is the compliment of P_S, as show in Equation 4, and the two are mutually exclusive; the aircraft either survives or it is killed.

$$P_S = 1 - P_K \tag{4}$$

The probability that an aircraft is killed is dependent upon two main factors. The *susceptibility* of an aircraft describes its inability to avoid being hit by enemy fire, and measured by the probability of being hit P_H. Aircraft *vulnerability* describes how easily it is killed if actually hit, and described by the conditional probability of being killed if hit $P_{K|H}$. The actual probability of killing an aircraft is measured by the joint probability of the probability of hit and conditional probability of kill given a hit. Therefore by substitution, survivability may be written as a function of both susceptibility and vulnerability, as in Equation 5.

$$P_S = 1 - P_H P_{K|H} \tag{5}$$

2.3.1 Susceptibility

Susceptibility is "the inability of an aircraft to avoid being hit by one or more damage mechanisms in the pursuit of its mission" [32]. Defined by the probability of hit P_H, the higher the susceptibility, the closer P_H approaches 1. Therefore, the more susceptible an aircraft is, the more likely it will get hit by an enemy weapon. According to Ball, examining an aircraft's susceptibility in a given scenario consists of determining the factors that influence susceptibility, modeling the scenario events to determine the likelihood that the aircraft is hit by each projectile fired at it (called susceptibility assessment), and finally, reduce the aircraft susceptibility through design. An aircraft

Table 5: Probability Factors that Influence Susceptibility [32]

Term	Description
P_A	Prob. that a threat weapon is active, searching, and ready to encounter
$P_{D\|A}$	Prob. that aircraft is detected given an active weapon
$P_{L\|D}$	Prob. that aircraft is tracked, fire control solution obtained, and weapon is launched, given the threat was active and detected the aircraft
$P_{I\|L}$	Prob. that the threat propagator intercepts the aircraft, given a launch
$P_{H\|I}$	Prob. that aircraft is hit by threat, given an intercept

designer desiring to minimize susceptibility would design to reduce the P_H that an air defense weapon would have against it (or probability of fuze P_F for an air burst weapon). An aircraft's susceptibility is primarily affected by the air defense's detection, tracking, and weapon guidance elements. Ball assigns probabilities to several of those key factors, listed in Table 5. Calculating P_H involves the joint probabilities of all the factors listed in Table 5, as shown in Equation 6.

$$P_H = P_A P_{D|A} P_{L|D} P_{I|L} P_{H|I} \tag{6}$$

Each of the probability factors listed in Table 5 correspond to an element in the EAPS engagement kill chain shown back in Figure 5. One of the main factors affecting susceptibility is the probability of detection, which is a function of both the detection capabilities of the air defense system, as well as the aircraft signatures. Aircraft signatures include radar cross section, infrared, visual, and aural. Much can be written on each of these types of signatures, however to limit the scope to the small unguided mortar targets studied in this thesis, special attention will be given to radar signature in Section 2.7.

2.3.2 Vulnerability

Aircraft *vulnerability* is defined as "the inability of the aircraft to withstand the damage caused by the man-made hostile environment, to its vincibility, to its liability to serious damage or destruction when hit by enemy fire" [32]. Vulnerability is described by the probability of being killed if hit $P_{K|H}$, and the higher the aircraft vulnerability, the higher the $P_{K|H}$ as its value approaches 1. It may be thought of as how soft a target is, or how easily it would be destroyed if hit. Therefore, the more vulnerable an aircraft is, the more likely it will get destroyed if hit by enemy fire and the higher its $P_{K|H}$. The Department of Defense [9] defines aircraft attrition kill categories that describe the elapsed time between when an aircraft is hit, and when it is rendered incapable of completing its mission. These are adapted by Ball [32], as given in Table 6. Although these are defined for aircraft, Macfadzean [92] states that these are equally applicable to air-to-surface missiles engaged by air defense weapons, depending on the situation.

Macfadzean [92] does not state that these kill levels are applicable to surface-to-surface indirect fire projectiles, however, this thesis takes this basic idea one step further to describe the attrition to the surface launched RAM threats. Therefore it is important that an air defense system be designed to hit the critical components in an incoming threat so that a "catastrophic" kill occurs sooner, therefore reducing the probability of the threat to be able complete its mission (i.e., destroy the air defense system). The more stringent the kill level desired against a target, the fewer components that will cause that damage if they fail. For example, at extremely short ranges, a catastrophic kill level (KK) may be the only option to defend a given area, and this might only be achieved by directly hitting the fuze or warhead of a mortar or rocket threat. At longer ranges, hits to other sections of the threat might suffice, such as the stabilizers, that would cause the threat to tumble away from the intended mark. To defend against very short range threats, such as mortars, it may be necessary to

Table 6: Attrition Kill Levels (adapted from [32])

Kill Level	Definition
KK kill	Immediate disintegration
K kill	Out of control within 30 sec of a hit
A kill	Out of control within 5 min of a hit
B kill	Out of control within 30 min of a hit
C kill	Aircraft unable to complete mission after a hit, but able to return safely to base (mission kill)

directly impact the fuze and completely destroy it.

2.3.3 Powering-up/Single Sortie Probability of Damage

It may be necessary to use more than one weapon to achieve a desired probability of damaging a target, which Driels [57] terms the "powering-up" or "survivor" rule. This is an important application of the binomial distribution and is used to determine the probability that a target will be hit at least once by n weapons, given the probability of hitting a target with one weapon p. Driels derives the powering-up formula from the Bernoulli distribution, which is a set of repeated trials of the same experiment in which each of the trials are independent. This is obtained by first determining the probability of *not* hitting the target by substituting 0 for x in the binomial equation, given in Equation 32 in Appendix A, such that

$$\frac{n!}{(n-x)!x!}(1-p)^n = (1-p)^n$$

and noting that the probability of hitting the target would be the compliment of this expression where

$$P\,(\text{target hit}) = 1 - P\,(\text{target not hit})$$

Therefore, the probability of hitting the target would be given by the Driels' powering-up rule given in Equation 7.

$$P\,(\text{target hit}) = 1 - (1-p)^n \tag{7}$$

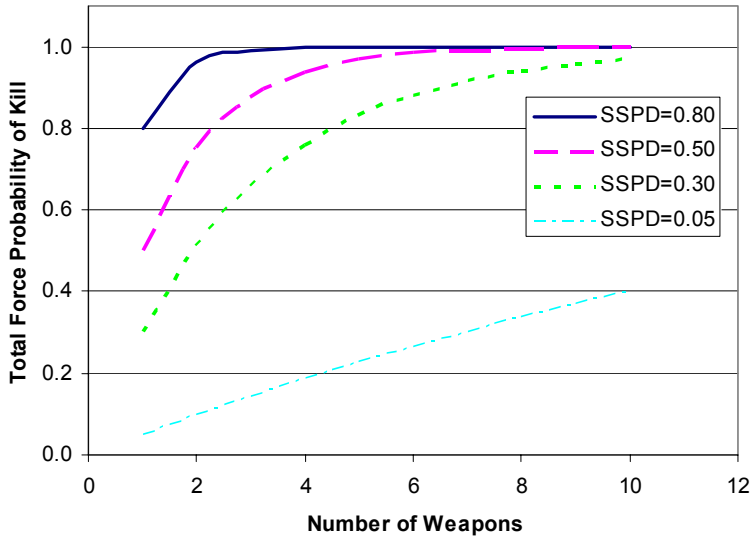

Figure 20: Example of Powering-Up Rule for an SSPD

Driels furthers this technique to a force estimation study, where now P_D is the resulting damage caused by n weapons, and p would be the Single Sortie Probability of Damage (SSPD) for a single weapon, given in Equation 8. A common quantity used in force estimation studies is the probability of damage if only a certain limited number of weapons q is available. An example of powering-up is given in Figure 20. This plot relates the differences in using four different weapons capable of different SSPD's. This allows a user to determine the probability that the target is hit once (or damaged) when 1, 2, etc. weapons are fired. Note that each of the curves approaches unity for increasing numbers of weapons. Recall that the initial assumption was that each of the trials are independent of one another.

$$P_D = 1 - (1 - SSPD)^q \tag{8}$$

Macfadzean [92] applies the idea behind the powering-up equation for Antiaircraft Artillery (AAA) fire, where projectiles are fired from the ground at a moving airborne target. Here it is desirable to determine the cumulative hit probability as a function of range. This is done to determine the range at which some minimum acceptable

probability can be achieved. For a given set of single shot hit probabilities achieved at given ranges $P_{ssh,i}$, the cumulative probability of hit $P_{h,cum}$ at that range is given in Equation 9.

$$P_{h,cum} = 1 - \prod_{i=1}^{N} (1 - P_{ssh,i}) \tag{9}$$

2.4 Air Defense Systems

With the aspects of aircraft survivability pertinent to this problem identified, this section will now describe the subject of defending an area from an airborne attack. Air defenses are "all defensive measures designed to destroy attacking enemy aircraft or missiles in the earth's envelope of atmosphere, or to nullify or reduce the effectiveness of such attack" [15]. The general term *air defense* can be used to describe an entire air defense order of battle in a theater, or to describe a single sensor-weapon combination operating autonomously to both detect and engage threats. Air defense weapons may include large surface based guns known as antiaircraft artillery (AAA), surface-to-air missiles (SAM), and even the air-to-air missiles (AAM) and guns carried by interceptor fighter aircraft. The air defense forces may be assigned to defend a specific area from attacking aircraft, which may include manned figheters/bombers, UAVs/UCAVs, cruise/ballistic missiles, etc...

The resources being protected from air attack may include any land or maritime asset contributing to the capability of an armed force engaged in a conflict. The threat may include manned or unmanned aircraft, air-to-surface missiles, and surface-to-surface missiles. Of course who the "enemy" is depends on the perspective of which side is attacking or being attacked. To successfully defeat an airborne threat, it is necessary to conduct a threat characterization in which probable mission profiles, observability, maneuverability, and vulnerability properties of that threat are identified [92].

2.4.1 Operational Requirement & System Specification

An operational requirement is the identification of the perceived need of an air defense capability as prepared by the military user, and serves as the basis for acquisition of a new system. Macfadzean [92] identifies five issues that the operational requirement must specifically address:

1. Definition of the threat and the specific environment that the threat will be encountered in.

2. Identification of existing systems that can deal with the threat, and any shortfalls to meet this operational requirement.

3. Specification of what the new system would have to do to counter the threat in the expected environment, and the military value it would offer.

4. Estimation of development cost and schedule.

5. Identification of how many systems are needed over a given time frame, for a given cost per system.

The third bullet in the previous list relates directly to the performance requirements of a new system. These generalized statements may be applied to define requirements for the type of threat to engage, the identification of a specific area to be defended, and even the probability of acceptable fratricide and/or level of collateral damage inflicted. Once a concept has been identified, system specifications can be created, which are the explicit requirements placed on the system's design and performance. However, the system requirements do not just restate the operational requirements, but the performance characteristics that ensure meeting the operational requirements.

2.4.2 Types of Air Defense Systems

This section is dedicated to introducing air defense systems that have attributes pertinent to a solution required by the problem statement.

2.4.2.1 Antiaircraft Artillery

Antiaircraft artillery (AAA) systems fire gun-launched unguided, ballistic flight path projectiles at air targets. They are usually found in the role of terminal defense, most effectively for engaging targets within four kilometers. The only controls over a gun-launched projectile flight path are the two gun aiming angles: azimuth and elevation. Guns are considered open loop systems; gun aiming angles are calculated for a predicted target flight path (i.e. predicted future position) such that the projectile will hit the target without any further corrections. Most AAA gun systems employ power-driven mounts to elevate the gun to the commanded azimuth and elevation angles with the smallest possible error. The difference between the commanded angle and the actual response angle is the *position error*. Employing a AAA system successfully requires an accurate error analysis. In addition to target tracking and flight path prediction, Macfadzean [92] lists the following eight major contributions to miss distance of AAA fire.

- Initial velocity
- Air density
- Air temperature
- Range wind
- Projectile weight
- Gun elevation angle
- Crosswind
- Gun azimuth

Both the gun itself and the ammunition fired from it are designed to achieve consistent, predictable firing velocities (the velocity at which the projectile leaves the muzzle) between successive shots. In reality, the initial velocity varies between each gun and each projectile round. One example that Macfadzean points out is that the gun barrel wears more with each shot fired, which increases the barrel diameter and allows some of the gases to escape around the projectile body, thereby reducing the initial firing velocity. Even variations in the temperature of the gun powder can have measurable effects on firing velocity. Manufacturing tolerances drive the variation of the projectile rounds themselves. Macfadzean gives a basic feel for the magnitude of the possible variations in initial velocity. Ammunition from the same manufacturing lot may have small variation from round to round, about 2 to 3 m/s 1σ error (assuming the error is normally distributed around the desired value). Poorly manufactured or mixed lots may have greater than 5 m/s 1σ error.

Differentials in air density and temperature only add a significant contribution to position error when dealing with great variations in altitude over long distances. Range wind, which is the velocity component of wind parallel to the direction that the projectile travels, directly modifies the projectile airspeed and the drag force component in the down range direction (denoted as the X direction). Crosswind is the airspeed component perpendicular to the range axis (denoted as the Y direction). The variation of weight of the projectile results in a change in velocity along the entire trajectory. Macfadzean states that variations from 0.5 to 1 percent are common, and controlled by the manufacturing process and quality control. Gun elevation controls the vertical plane trajectory, and therefore elevation angle variations induce vertical errors that are in the velocity vector normal plane. The azimuth angle controls the motion in the horizontal X-Y plane, and the effect of error produces a lateral effect. Error analysis of AAA trajectories may be based on baseline standard conditions, defined as:

- Projectile specification initial velocity (i.e. fixed exit muzzle velocity)
- Standard atmosphere conditions
- Published drag coefficient versus Mach number
- No wind
- Projectile specification weight
- No aiming error (azimuth or elevation)

2.4.2.2 Surface-to-Air Missiles

Surface-to-Air Missiles (SAM) are missiles that are launched from land (or sea) based platforms [32]. The missiles themselves are self-propelled, and are usually large enough to carry a warhead for long ranges using some type of onboard guidance system. They use movable control surfaces that are deflected by guidance system commands to direct flight, and on board sensors may be used to track the target. However, the complexity of SAM's usually limits their use against large targets, such as a piloted aircraft and cruise missiles, and therefore will not be elaborated on further. The SAM topic is simply included here to show how surface to air guided weapons are generally used.

2.4.2.3 Integrated Air Defense System

A "layered" air defense is a combination of the different types of air defense where one or more point or area defense weapons are assigned overlapping areas. The linking together of the various air defense target sensors, weapon firing platforms, and command centers is known as an *Integrated Air Defense System* (IADS). An IADS consists of 1) surveillance sensors (surface-, air-, and/or space-based); 2) various weapon system installations (including target detection, tracking, and guidance sensors for fire control); 3) filter centers used for data fusion; 4) decision making command centers, or command, control, communication, and information (C3I) centers; and 5) communication links between the sensors, weapon systems, and command centers. [32]

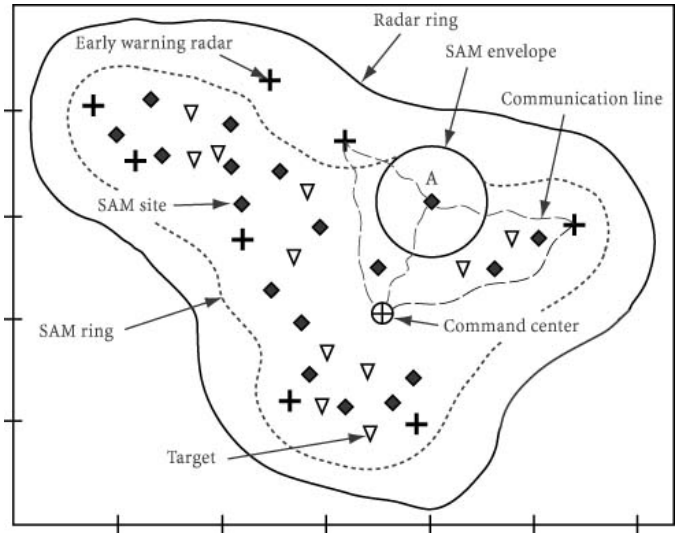

Figure 21: A Generic Integrated Air Defense System [32]

Information gathered within the field of view of any of the sensors is passed to the data fusion nodes. Target location(s) data collected at the data fusion nodes is correlated to determine the number and location of each target, a process called *track correlation* used to create a composite of the defended area sent to the decision node. There, the targets are prioritized after decisions are made as whether the targets are hostile, friendly, or unknown, and whether the targets are likely to attack, how soon, and how much damage they would inflict if they attack. The decision center uses this tactical picture to assign firing units (defensive weapon systems) to targets based on prioritization. The assignments are based on firing unit availability and condition. After the command center assigns the firing units to targets, the individual firing units then attempt to encounter, engage, and kill its assigned target. This process of target prioritization and firing unit assignment is called *classification* [32]. A generic IADS is shown in Figure 21, and shows a complex example of how the different aspects of the kill chain are distributed over various systems to defend an area.

2.5 Weapon System Effectiveness Parameters

Once a particular air defense system is selected, its particular weapon system effectiveness parameters must be identified. The USAF Intelligence Targeting Guide [11] summarizes the *weaponeering* process and its importance in quantification of weapon system effectiveness:

> *Weaponeering is the process of estimating the quantity of a specific type of weapon required to achieve a specific level of damage to a given target, considering target vulnerability, weapon effects, munition delivery errors, damage criteria, probability of kill, weapon reliability, etc.*

This targeting guide stresses that in general, the results of weaponeering studies result in probable outcomes, not the outcome of an individual munition delivery. This is achieved using statistical averages based on many repetitions of models, weapons tests, and real world deliveries.

The most important characteristic parameters of weapons are the ones that describe the weapon accuracy and effectiveness against a target. Przemieniecki [126] lists the parameters that characterize weapon performance as 1) accuracy; 2) range; 3) rate of delivery (rate of fire); 4) warhead or munitions round effectiveness against a given target; 5) time of target acquisition, pointing, and tracking; 6) time of flight to the target; 7) weight and size; 8) cost; and 9) reliability and maintainability. However, Przemieniecki claims that it is the accuracy, effectiveness against a target, and reliability that are most important in defining the weapon system effectiveness.

2.5.1 Weapon Accuracy

Weapon accuracy is "the location of the point of impact for a given aim point on the target" [126]. The actual trajectory that a projectile (either guided or unguided) will likely not coincide exactly with the calculated ideal trajectory, resulting in a point of impact on the target that deviates from the desired aim point. The precise magnitude

of the distance between the desired aim point and actual point of impact can not be determined, however a random function can be used to approximate this distance. Driels [57] states that ballistic errors are only found in unguided weapons, where as the delivery accuracy of guided weapons is mainly influenced by the guidance system of the weapon itself. Common factors that cause this randomness include production tolerances (i.e. no two projectiles in a weapon system are manufactured exactly alike), varying accuracy in aiming, maneuvering target (and the errors associated with tracking a moving target), atmospheric conditions, and human operator error. Measuring the accuracy of weapon delivery can be quantified by measuring the closest point of approach between the weapon and target, or *miss distance*, which is as Ball [32] states "the shortest distance between the aircraft and the missile as the missile flies by the aircraft with no warhead detonation". Delivery accuracy directly relates to the probability of direct hit of a weapon intercept with its intended target.

2.5.2 Lethality

Ball [32] uses the term warhead lethality "to denote the ability of the warhead on the weapon to kill the target given a direct hit or a proximity burst". Weapon lethality against a particular target is basically a measure of the target's vulnerability, or the probability of being killed if hit (as described earlier in Section 2.3.2). Whereas weapon accuracy describes the ability to deliver the weapon as close as possible to the target every time, the lethality describes the probability that the target will be destroyed given that the weapon was delivered accurately (or within some measure of accuracy). Macfadzean [92] identifies three types of damage mechanisms that could be used to destroy a target.

1. Projectiles that directly hit the target
2. Fragments that are ejected by a warhead hit the target
3. Warhead blast creates a pressure wave that is applied to the target skin

The first option that Macfadzean points out is when the projectile directly impacts the intended target, with the transfer of *kinetic energy* as the main source of lethality. This is sometimes referred to as a kinetic kill, or kinetic warhead, even though there is no explosive charge (which is normally associated with warheads). The second item is where the warhead has an explosive charge that when detonated, ejects many small fragments at a high speed. The detonation may occur on impact, timed for certain point after launch, or set to detonate if the weapon comes within in certain distance of the target. Additionally, the direction of fragment ejection may be controlled. These fragments may also be submunitions, such as those discussed for the Ahead round in Section 1.2.3.2. The third item in the list is when the pressure wave created by the explosive charge hits the target, which in some cases is enough to damage the target. With each item in this list, the miss distance accuracy can be alleviated, roughly speaking. For a more thorough discussion of the more exotic types of warheads, Macfadzean [92] may be consulted.

An effective way to defend an area against an incoming mortar is to launch a projectile and impact it in such a manner as to detonate the mortar warhead. This deals with the subject of explosive initiation modeling and its correlation to calculation of probability of detonation (Lloyd [90] [91] are excellent sources on this topic and should be consulted for further detail). Of course, this relies on the level of detail one can afford. In Equation 10, Macfadzean [92] gives a very simple relation between probability of kill and the fragmentation spray density (from the warhead) and vulnerability area of the target. This vulnerability area is the effective area on the target that if hit, could result in a kill. For example a mortar could be detonated by impacting its contact fuze, causing a catastrophic kill (as discussed in Section 2.3.2).

$$P_k = 1 - e^{-\rho A_v} \tag{10}$$

where

$$\rho = \text{fragment spray density (fragments/m}^2\text{)}$$

$$A_v = \text{vulnerable area (m}^2\text{)}$$

2.6 Guidance, Navigation, and Control of Related Weapon Concepts

Guided weapon systems have traditionally been limited to missiles, and many of the concepts discussed in this section were developed specifically for missiles. However, with the emergence of guided projectiles as potential alternatives for shorter range air defense, it is important to review those guidance, navigation, and control concepts that could be employed if a gun fired guided projectile or missile solution are carried through the implementation of this thesis. Since these methods were developed for missiles, this section will use the term "missile" where it would be found in the literature, however the reader is encouraged not to bog down on the term used since it is only the general method that is important. The term "guided projectile" could certainly be used in place of "missile" anywhere in this section.

Guided missiles carry along a guidance package that tries to navigate the weapon on a specific course to successfully intercept an intended target. The trajectory that the weapon would follow is directed by the navigation law used. Finally, the missile itself physically deploys aerodynamic steering surfaces using a specific control logic. This section will describe several alternatives to selecting appropriate guidance, navigation, and control logic for a guided missile (or projectile).

2.6.1 Guidance

Ball [32] describes several possibilities for missile guidance summarized in this section.

2.6.1.1 Inertial Guidance

The inertial guidance method uses gyroscopes and accelerometers to direct the missile over a predetermined path provided to the missile prior to launch. Guidance updates may be sent after launch to correct any errors in the onboard equipment. This method is more suited for long range missiles, such as cruise missiles, where they can cruise for long periods of time with a certain amount of autonomy with occasional course correction updates.

2.6.1.2 Command Guidance

Command guidance logic describes the case where a missile gets its guidance instructions from sources outside the missile. This method relies on a tracking system outside the missile is used to track the missile *and* target along their trajectories. The tracking system may use separate tracking units for the missile and target, or just one to track both objects. The ranges, elevations, and bearing headings are used to calculate position and position rate, leading to the flight path the missile should take to intercept the target. The computed and predicted (based on current tracking information) flight paths of the missile are used to determine how the control surfaces should move to make the corrections required to change the current flight path to the new one. The command guidance signals must be sent to a receiver onboard the missile, using either the tracking system, or some other form of radio command link. There are missiles that get guidance information transferred via a wire connected to the launch site, but this will not be studied as part of this work. The main advantage of command guidance is that there are no sensors on board the missile that have to track the target. Ball notes that the use of command guidance of a missile all the way to the target is usually limited to short ranges, due to the relatively large tracking errors that occur at long range.

2.6.1.3 Beam Rider Guidance

With beam rider guidance, an electromagnetic beam located offboard the missile is used to track the target. A rearward facing antenna senses the tracking beam, and uses the position of the missile with respect to the center of the target tracking beam to compute steering signals used to move control surfaces. One of the main advantages of beam rider guidance is that multiple missiles can be fired at one target, since they can all rely on the same tracking beam. However, Ball notes that this technique has been limited to larger missiles that have the space to carry this guidance package.

2.6.1.4 Homing Guidance

The term homing guidance is used to describe a missile using an onboard guidance package that can determine the target's position and guide itself to interception. The major advantage of homing guidance over the previous methods is that as the missile approaches the target, the error is reduced - the exact opposite is true for the previous methods. There are types of homing guidance that will be discussed here - active, semiactive, and passive.

Active homing is a guidance scheme where by the target is tracked entirely using equipment onboard the missile. Here, a radar on board transmits pulses that illuminate the target, and then uses the echo from the target for navigation. The major advantage of active homing is that the missile is essentially a "fire and forget" weapon and does not require guidance or tracking from an outside source. However, the added weight and expense limit this option to larger missiles going after targets at very long ranges. Semiactive homing differs from active homing in that the source of target illumination is offboard the missile, however the missile does have a system to collect echoes from the target to steer the missile. Passive homing systems are the simplest of the homing systems, and do not employ any type of target illumination.

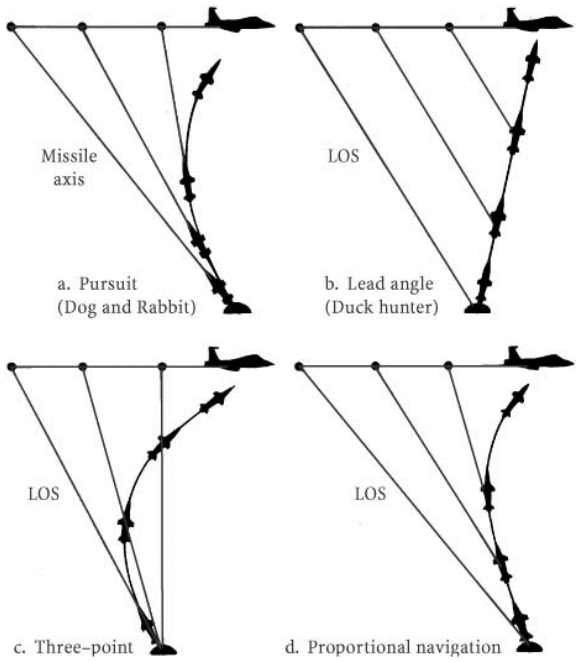

Figure 22: Missile Navigation Laws [32]

Sensors onboard the missile can only use electromagnetic emissions or natural reflections from the target to establish location. Passive homing is limited to large targets such as fighter or bomber aircraft that constantly emit electromagnetic radiation, and have complex shapes ideal for natural reflections. Note that even the simplest homing method requires that the weapon carry onboard complex senors and the capability to compute course corrections.

2.6.2 Navigation

A navigation law is the relationship between the missile and target motion used to generate missile steering commands. If those steering commands are followed such that the navigation laws are satisfied, an intercept will occur [92]. Several types of navigation laws are available for a guidance system to use to steer a missile along a flight path to intercept a target. The four types of navigation laws presented in this section and shown graphically in Figure 22 are also summarized from Ball [32].

2.6.2.1 Pursuit

The pursuit trajectory causes the missile to always fly directly pointing at the target at all times. The guidance package maintains the line-of-sight (LOS) along the heading of the missile. A missile trying to intercept a powered aircraft with pursuit navigation usually ends up in a tail chase, in the same way a dog would chase a rabbit. This drives the need for the missile to have speed considerably larger than its intended target. This method is best used against slow flying targets flying head on toward the missile.

2.6.2.2 Lead Angle

The lead angle navigation routine causes the missile to keep a constant bearing with the target. For a target flying at a constant speed and heading, the LOS between missile and target is constant, and the missile flies a straight collision course. If the target changes direction, a new lead angle is calculated, again assuming a straight flight path, and the missile is steered along that path.

2.6.2.3 Three-Point

Three-point navigation is a routine where the missile is constantly steered along the line between target tracker and target. This method is usually used for short range missiles using a command guidance package where the offboard (i.e. ground or aircraft based) target tracker maintains line of sight with the target.

2.6.2.4 Proportional

Proportional navigation is the most common navigation law used in the final phase of target interception. Here, the guidance package must determine the time rate of change of the LOS between missile and target. The guidance package then tries to maintain a constant LOS angle by making the rate of change of the heading direction proportional to the rate of change of the LOS. A constant of proportionality is unique

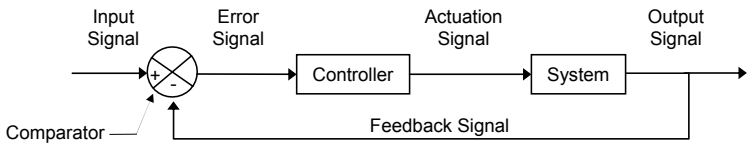

Figure 23: Closed-Loop Control (adapted from [119])

for a missile system, and can change as the missile flies the intercept to efficiently manage the energy used for maneuvers.

2.6.3 Control

There are two basic types of controllers, open-loop and closed-loop. The open-loop controller uses control action completely independent of the output, and is therefore the simplest option. However, it lacks the accuracy of a closed-loop controller. In a close-loop control system (shown in Figure 23), the action that the controller takes depends on the system output. This type of control system is also called a feedback control system, because the output is fed back and compared with the input to generate an error signal. This error signal is used to make the output signal agree with the desired input. This output signal is then used to send signals to control surfaces of an aircraft to actually control the flight path. The method to control the amount of drive signal to use is dependent on the type of controller to use. Two types of controllers will now be discussed as potential option for missile or guided projectile control logic.

2.6.3.1 Bang-Bang

A bang-bang controller is also referred to as on-off control, because the controller has only the option of either applying maximum drive signal, or none at all. A common example of a bang-bang controller is the thermostat of a household heater. If the room temperature drops below a certain temperature, the heater turns on. Once that temperature is reached, the heater turns off, however there is a tendency to overshoot that desired temperature, causing a ripple, or fluctuation of temperature with time.

One attempt to solve this problem is to solve this problem is to set acceptable bounds around the desired temperature, say ±5 degrees around the desired temperature. Now, the heater will not turn on until the lower bound is reached, and will not turn off until the upper bound is reach, letting the temperature fluctuate within those bounds. This is the easier of two control options discussed here, because the only logic the controller must consider is on or off. Likewise to the thermostat example, if a missile using a bang-bang control system is veering off course, the control surfaces would fully deploy until the desired course is reached. Since there is no ability to partially deploy the control surfaces, there is no distinction made between having to correct large or small errors in flight path. [33]

2.6.3.2 Proportional Integral Derivative

The Proportional Integral Derivative (PID) controller is designed to generate a control output signal dependent on the magnitude of the error signal. A PID controller is actually a combination of three controller types. A proportional controller's feedback output is proportional to the error signal, and is the simplest controller type. Its main advantage is its simplicity, however it has the disadvantage that steady-state error may exist. To eliminate steady-state error, an integral controller may be used that creates an output that is proportional to the accumulated error. However an integral controller may cause instability in the system that it is used in. A derivative controller can then be used to provide large corrections before the error becomes too large. Because it relies on the change in error, the derivative controller is at a disadvantage if the error is constant and will not produce control. It also has the disadvantage that is has difficulty with high frequency components of error. Each of the disadvantages of each controller are eliminated when they are combined into a single PID controller. This section is summarized from a section in Nelson [119], which may be consulted for a more in depth description of the mathematical theory

of PID controllers out of the scope of this thesis.

2.7 Radar Concepts

It is evident from studying the problem of interest identified in the motivation chapter that a radar will play an important role in a solution to the RAM threat. One of the key drivers of this thesis is to have the ability to flow top-level requirements directly to subsystem variables (i.e. required operational capability drives required radar capability, which therefore drives the specific radar variables; the notion of top-down design will be discussed further in Chapter 3). Therefore, this section will address the basic radar topics necessary to quantify a solution space relevant to this problem.

2.7.1 Frequency

A radar works by transmitting an electromagnetic wave and using the returned echo picked up by the receiver to locate, identify, and track an aircraft, and is very effective for use against targets at long ranges [125]. The word radar itself is the short form of the phrase *RA*dio *D*etecion *A*nd *R*anging. The number of pulses that a radar transmits as function of unit time is the radar frequency. As given in Table 7, radar frequencies were divided into bands during World War II according to similar power sources, propagation effects, and target reflectivity. The lower frequency bands (HF, VHF, UHF) are primarily used for long range surveillance, but not effective at determining precise target location unless a very large antenna is used. For searching and tracking targets, S-, C-, X-, and Ku-bands are used because the narrow beam widths required can be obtained using much smaller antennas (as compared to the lower frequency radars).

Table 7: Radar Frequency Bands [125]

Band Designation	Frequency Range (GHz)	Wavelength (m)	Usage
HF	0.003-0.03	100-10	Over the horizon surveillance
VHF	0.03-0.3	10-1	Very long surveillance
UHF	0.3-1	1-0.3	Very long range surveillance
L	1-2	0.3-0.15	Long range surveillance, enroute air traffic control
S	2-4	0.15-0.075	Medium range surveillance, terminal air traffic control
C	4-8	0.075-0.037	Long range tracking
X	8-12	0.037-0.025	Short range tracking, missile guidance, airborne intercept
K_u	12-18	0.025-0.017	High resolution mapping
K	18-27	0.017-0.011	Rarely used due to water absorption [73]
K_a	27-40	0.011-0.007	Very high resolution mapping
Millimeter	40-300	0.007-0.001	Experimental [73]

2.7.2 Radar Range

A fundamental topic to radar analysis is the maximum range at which a radar can detect a target is given by the radar range equation in the form given by Paterson [125] in Equation 11. Note that for a given radar with R_0 fixed properties from Equation 11, the maximum detection range of a radar against a 1 m^2 target is proportional to the fourth root of the radar cross section (RCS), given in Equation 12.

$$R_{max}^4 = \frac{P_t G^2 \lambda^2 \sigma}{(4\pi)^3 P_{min}} \tag{11}$$

where

R_{max} = maximum range at which a target can be detected

P_t = transmitted power

G = antenna gain

λ = wavelength

σ = radar cross section of the target

P_{min} = minimum level of received signal based on a signal-to-noise ratio

$$R_{max} = R_0 \sigma^{1/4} \tag{12}$$

The antenna gain and wavelength can be related to physical area of the antenna, A, and the efficiency of the antenna aperture, η, given in Equation 13. The quantity $A\eta$ is a measure of the effective area presented by the antenna to the incident wave [133].

$$G = \frac{4\pi A\eta}{\lambda^2} \tag{13}$$

On the antenna surface of area A, there is an array of antenna elements, usually spaced at $\lambda/2$ [117]. The number of these elements on the radar antenna is the primary driver for the cost of the radar [24].

2.7.3 Signal-to-Noise Ratio

Any unwanted signal that contaminates or competes with the desired signal is known as signal noise. The relative amount of additive noise to the desired signal is the signal-to-noise ratio (SNR) [16]. Barton [34] derives a useful equation relating SNR to pertinent radar properties from a form of radar range equation, given below in Equation 14.

$$SNR = \frac{P_{avg} G_t G_r \lambda^2 \sigma_{rcs} t_0}{(4\pi)^3 R^4 kT} \tag{14}$$

where

SNR = Signal-to-Noise Ratio [dB]

P_{avg} = Transmitted power [W]

G_t = Transmit antenna gain [dB]

$$
\begin{aligned}
G_r &= \text{Receive antenna gain [dB]} \\
\lambda &= \text{Wavelength [m]} \\
\sigma_{rcs} &= \text{Radar Cross Section of the target [m}^2\text{]} \\
t_0 &= \text{Observation time [s]} \\
R &= \text{Transmitter/reciever range to target [m]} \\
k &= \text{Boltzmann's constant [W/(Hz-K)]} \\
T &= \text{System input noise temperature [K]}
\end{aligned}
$$

2.7.4 Radar Cross Section

Most of the properties that make up Equation 14 are controlled by the radar designer, except the only property associated with the target itself, the radar cross section. The *radar cross section* (RCS) of an aircraft (or any object) is the cross-sectional area of a perfectly conducting sphere of radius a that reflects the same amount of energy as that aircraft [92], where RCS (σ) is related to that radius as given in Equation 15[2].

$$\sigma = \pi a^2 \tag{15}$$

The standard unit for RCS is the square meter (m^2), however it is also widely expressed in decibel square meters ($dBsm$), where the two are related in Equation 16.

$$\sigma[dBsm] = 10 \log_{10} \sigma[m^2] \tag{16}$$

For a more practical definition, Skolnik [133] defines the RCS of a target as "the (fictional) area intercepting that amount of power which, when scattered equally in all directions, produces an echo at the radar equal to that from the target".

[2]The symbol σ is usually used to denote RCS, however to avoid confusion with the symbol used for standard deviation, after this section the symbol σ will only be used to refer to standard devation, and RCS will be used for radar cross section.

Table 8: Radar Cross Section Magnitudes[125]

	Ships	**Large Aircraft**	**Small Aircraft**	**Man**	**Birds**	**Insects**
RCS (m^2)	10^4	10^3	10^2,10^1	10^0	10^{-1},10^{-2}	10^{-3},10^{-4}
RCS ($dBsm$)	40	30	20,10	0	-10,-20	-30,-40

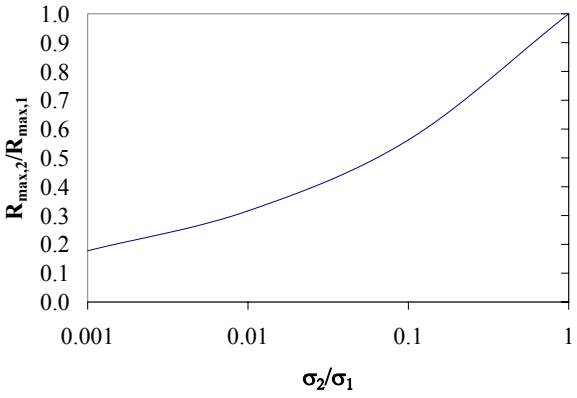

Figure 24: Reduction of Maximum Detection Range with Reduced RCS

Table 8 presents the RCS magnitudes associated with common airborne objects, in the form given by Paterson [125]. This is meant to give the reader an appreciation for RCS order of magnitude in both $dBsm$ and m^2, against the size of several common reference objects. In relation to the types of targets discussed in this thesis, a mortar would likely fit into the "bird" category in Table 8, with an associated RCS somewhere between -10 $dBsm$ and -20 $dBsm$. *While mortars are considered a low technology weapon, their small size and simple smooth shape give them a fairly small RCS that make them difficult to detect* with radars designed to detect conventional aircraft. This puts mortar RCS on the about the same order of magnitude with stealth aircraft, however the detection ranges associated with mortar engagements are far shorter than those associated with stealth aircraft.

Comparatively, a reduced RCS will decrease the radar detection range R_{max}. Using the principle that R_{max} varies with the fourth root of RCS, Figure 24 shows the

comparative ratio of RCS reduction. Minimizing RCS is therefore an important design criterion in the field of military aircraft design. (Knott [86] describes the methods in which an aircraft designer can reduce RCS.) However, these methods will not be exploited in this study, due to the low technology nature of the airborne targets in question, but the information was included to provide the reader with an appreciation for the radar accuracy required to detect a low RCS target.

2.7.5 Tracking Radars

2.7.5.1 Methods of Radar Tracking

A tracking radar measures location of a target, proving data that may be used to determine flight path and future position [133]. The available radar data is usually range, elevation angle, azimuth angle, and doppler frequency shift. Angular error is the difference in magnitude and direction between the target position and a reference direction, usually the direction of the radar antenna which is both the transmitting and receiving device of the radar. During transmission, the antenna's function is to concentrate radiated energy into a shaped beam pointing in a desired direction. The antenna also collects the reflected energy contained in the echo signal (from a target) and delivers it to a receiver (these two antenna parameters are the gain variables in Equations 11 and 14). A tracking radar attempts to line up the antenna with the target in order to make the angular error zero, and the target is located along the reference direction.

There are three methods to determine the direction and magnitude of the angular error. *Sequential lobing* (also called lobe switching and sequential switching) is a method in which the antenna beam is alternately switched between two positions to obtain the angular error in one coordinate. The error is quantified by measuring the difference in signal from the two positions from the reference, or "switching" axis. The antenna is moved to align the switching axis and the target direction. In order to obtain angular error in the orthogonal coordinate, two additional switching positions

are needed. The primary accuracy limitation of a sequential lobing tracking radar is due to noise caused by mechanical and electronic fluctuations. This method was one of the first tracking techniques employed in airborne interception radars, and is not used as often in modern tracking applications.

The *conical scan* radar has the same basic principle as the sequential lobing method, however instead of discontinuously stepping the beam between four discrete positions, the antenna beam is continuously rotating. In both sequential lobing and conical scanning techniques, measuring the angle error in two orthogonal coordinates (i.e. both azimuth and elevation) requires multiple pulses to be processed. If the train of pulses collected over a given time interval contains additional modulation components, the tracking accuracy will be degraded. If the angular measurements are made on the basis of one pulse, rather than multiple pulses, fluctuations in the amplitude of the echo signal between pulses will have no effect on tracking accuracy. Those tracking techniques that derive angle error information from a single pulse are known as simultaneous lobing, or more commonly as *monopulse*. Also unlike sequential lobing and conical scan trackers which use only one antenna beam, monopulse trackers use more than one antenna simultaneously. This way, the location of the target relative to the radar is determined by measuring the relative phase or relative amplitude of the echo pulse received in each beam.

More specifically, a tracking radar that operates with phase information is an *interferometer* radar, since it " deduces information from the coherent interference between the two signals" [16]. The phase difference between the two signals is the relative displacement between the two waves having the same frequency (or wavelength). The complete wave cycle has a phase of 2π radians. To illustrate an interferometer radar, two antennas are shown in Figure 25 separated by a distance D. The line of sight to the target is offset an angle θ from the perpendicular bisector connecting the

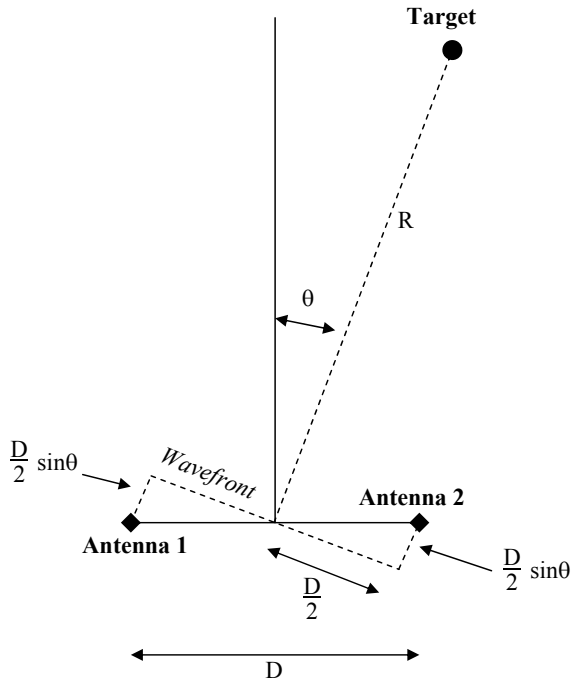

Figure 25: Wavefront Phase Relationship for an Interferometer Radar

two antennas. The wavefront phase at antennas 1 and 2, respectively, are [24]

$$\phi_1 = -\frac{2\pi}{\lambda}\frac{D}{2}\sin\theta$$

$$\phi_2 = \frac{2\pi}{\lambda}\frac{D}{2}\sin\theta$$

with a negative sign associated with ϕ_1 because of the reference origin defined directly between the two antennas. Therefore the measure phase difference for an interferometer radar is given in Equation 17 [133].

$$\Delta\phi = \phi_2 - \phi_1 = \frac{2\pi}{\lambda}D\sin\theta \tag{17}$$

2.7.5.2 Radar Error Analysis

Statistical methods can be used to describe the error of a radar measurement. This error is simply defined "as the difference between the value indicated by the measuring instrument and the true value of the measured quantity" [34]. For the purposes of this thesis, this is the error in determining the location of an object in three dimensional

space. These radar errors may include both systematic and random properties. The systematic property, or *bias*, is present when the radar error is constant with time. For example, the difference in the actual position and radar measurement of an object would be identical at each sample. This level of predictability can be corrected by a process of calibration applied to the measuring instrument. The random property of radar error, or *noise*, changes with each sample in time.

The most accurate method of error measurement is with using actual test data, however this might not be very practical when required for use in a simulation with changing properties. Mathematical approximations can be created that model actual error components and enable accurate analysis of a particular system's error. In most cases, a normal distribution may very accurately approximate radar noise. Of course, the actual shape of the error distribution may not be normal, but Barton [34] states that "the normal distribution is often assumed to represent errors of unknown characteristics, and it closely approximates the distribution of many actual errors".

Using the interferometer phase difference calculated in Equation 17, Holder [24] derives an equation relating the measurement error standard deviation for an interferometer radar, as a function of radar properties. The remainder of this section will summarize that derivation. Taking the expected value of Equation 17 gives the variance (σ^2), of which the square root yields the equation in the form of standard deviation (σ), given as

$$\sigma_{\Delta\phi} = \frac{2\pi D}{\lambda} \cos\theta \sigma_\theta$$

Next, substituting

$$\sigma_\phi = \frac{1}{\sqrt{2SNR}}$$

and

$$\sigma_{\Delta\phi} = \sqrt{2}\sigma_\phi$$

which are obtained from [34][3], results in the following relation

$$\sigma_\theta = \frac{\lambda}{2\pi D \cos\theta \sqrt{SNR}}$$

If the radar is assumed to be pointing directly at the target, the offset angle θ goes to 0, and the $\cos\theta$ term goes to 1, resulting in Equation 18, relating radar measurement error 1σ to wavelength (λ), the distance between interferometer antennas (D, a measure of radar size), and signal-to-noise ratio.

$$\sigma_\theta = \frac{\lambda}{2\pi D \sqrt{SNR}} \tag{18}$$

When the radar properties given in Equation 14 are substituted for SNR, the measurement error can be a direct function of those radar subsystem properties.

2.8 Chapter Conclusions

This chapter reviewed related concepts of combat system modeling and simulation, and discussed particular topics closely related to the problem of short range RAM defense. As mentioned in the opening paragraph of this chapter, there is a lack of literature in modeling of the RAM threat and of the air defense systems designed to defeat those threats, certainly no direct approach exists to model the threat within a weapon design environment. One of the closest ideas discussed in this chapter is the IADS concept, generally showing how defending an area requires the interaction of several key systems, such as a radar and a weapon system. The topic of short to medium range RAM defense is a relatively new field of interest within the combat modeling and simulation community, and the established systems engineering process in place to address the specific problem does not address satisfy the overall research objective of this thesis. Ultimately, an integrated hierarchical environment based on

[3]These substitutions are based on ideas put forth in Chapter 8 of [34], where Barton derives several key relations for tracking radars. The final result in Equation 18 is therefore a derivation specific to an interferometer radar by Holder [24] using many of the relations that can be found in [34].

accepted combat modeling and simulation methods must be created for the various components that need to interact, and allow for rapid manipulation enabling decision making at any level within and across the hierarchy. Because the literature on combat modeling and simulation does not provide enough background to satisfy this need, several concepts from appropriate Advanced Design Methodologies will be discussed in the next chapter.

CHAPTER III

LITERATURE SEARCH: ADVANCED DESIGN METHODOLOGIES

One of the great challenges in planning, managing and developing system-of-systems is to develop an ability to handle traceability when dealing with "big pictures" of defence capability in various contexts and for different purposes.

Chen et al. [48]

3.1 System-of-Systems Approach

There are many modeling and simulation methods that have been developed to attempt to describe the outcome of military encounters at various levels. Decision makers can then use the outcomes of these simulations, and base important tactical and/or strategic decisions on them as described by the first quote in Section 2.1. However, one common problem with most of these tools is that the models themselves are only capable of describing events at one level, such as a theater level tool [68] [129] at the very top level, or an aircraft sizing and synthesis tool [112] at the aircraft system level. A system-of-systems approach can be used to describe events at every level by functionally decomposing the entire system in question into a hierarchy of decision making levels. An attempt now will be made to differentiate between the terms *system* and *system-of-systems*.

Webster [3] defines a system as "a regularly interacting or interdependent group of items forming a unified whole". Chapman et al. [47] simply define a system as

"any process or product which accepts inputs and delivers outputs". A more specific definition by Blanchard [41] is that a system "may be considered as constituting a nucleus of elements combined in such a manner as to accomplish a function in response to an identified need...A system must have a functional purpose, may include a mix of products and processes, and may be contained within some form of hierarchy". Blanchard [40] further describes a system in terms of the following characteristics:

1. A system integrates a complex combination of resources, which may be in the form of data, equipment, software, or even humans, and must be done in an efficient manner.

2. A system is contained within a hierarchy, and is highly influenced by the performance of the higher level system.

3. A system may be broken down into subsystems, the scope of which depending on the complexity and function being performed.

4. The system must have a purpose, meaning it must be able to respond to an identified need.

Despotou [54] defines a system-of-systems as "an organised complex unity assembled from distributed autonomous systems (capable of independent provision of services) collaborating to achieve an overall system purpose", and further making the important distinction from any complex or legacy system. A Department of Defense (DoD) study [49] states that a system-of-systems must have both operational and managerial independence of its individual system components. There also must exist a relationship among the system components, and a common objective or purpose for each component, "above and beyond any individual objective or purpose for each component". Chen et al. [48] add that a system-of-systems is concerned with the

ability to analyze joint effects of system components, have interoperability of levels and analysis, enable information sharing, and have the capability for planning, coordinating, and managing of any systems evolution.

Adding to the DoD principles, Maier [93] defines fives principal characteristics that describe a true system-of-systems:

1. *Operational independence* of the elements: the system-of-systems is composed of systems that can be usefully operated independently if the system-of-systems is decomposed.

2. *Managerial independence* of the elements: the individual systems that comprise the system-of-systems are separately acquired, and therefore are actually run and maintained independently of each other.

3. *Evolutionary development*: the development of the system-of-systems is evolutionary with functions added, removed, and modified with experience, therefore never actually appearing to be fully formed.

4. *Emergent behavior*: the entire system-of-systems performs functions and carries out purposes that are emergent of the entire process, and cannot be localized to any component system. The principal purpose of the system-of-systems is fulfilled by its emergent behavior.

5. *Geographic distribution*: the independent system components can readily exchange information only, and not substantial items like mass or energy.

The additional dimension of managerial control is critical to identifying the appropriate principles of the system-of-systems. This is due to the fact that not all system-of-systems, or the component systems within them, are of similar complexity. Maier further classifies three basic categories of system-of-systems by managerial control: directed, collaborative, and virtual.

Directed systems are built and managed to fulfill specific purposes, with centrally managed operation. The component system maintains the ability to run independently, but their operation within the integrated system-of-systems is subordinate to central management purposes. An integrated air defense systems (IADS), for example, is centrally managed to achieve a common objective, although its component systems, such as the individual radars or surface to air missiles, may still operate independently. An IADS, discussed in Section 2.4.2.3, is an excellent example of a true system-of-systems.

Collaborative systems have a central management organization that does not have the authority to run individual systems. Each component system must voluntarily collaborate to fulfill the central objective. The internet is an example of a collaborative system, where internet component sites exchange information using protocol regulations, adhered to voluntarily.

Virtual systems completely lack a central management authority, although they maintain a common purpose for the system-of-systems. Any large scale behavior emerging from the combined systems must rely on "invisible" mechanisms for maintainability. National economies are virtual systems, as their long term nature is determined by highly distributed mechanisms, that appear to have no central management control.

The fact that the system components have a level of autonomy may have adverse effects on the system-of-systems in that there may be conflicts of responsibility. Each component within the system-of-systems has its own distinct goals, which Alexander [28] lists as including self-preservation and maintenance of a certain level of safety, as well as sub-goals that define the component's contribution to achieving the overall system-of-systems goals. An Unmanned Aerial Vehicle, for example, may assume responsibility for surveying a section of area intended for overall system-of-systems purposes. However, a partially or fully autonomous system can essentially have so

much freedom to govern its own choices that it becomes a risk to itself and other elements in a system [54].

One of the greatest advantages of a system-of-systems approach to problem solving is that it is very adaptable, since it allows improvement within any of its layers, depending on either the evolution of a threat of advancement of an applicable technology. For example, a study of the application of a system-of-systems approach to a national missile defense strategy was conducted by the RAND National Defense Research Institute [67]. The study found that this approach would offer more distinct technological options to improve kill probability in any of the hierarchical layers, thus reducing the required proportion of interceptors required to respond to proportionally more enemy re-entry vehicles.

3.1.1 Functional Decomposition

A system is made up of many components that interact with each other. These interactions make it impossible to effectively design a system in which each component is considered independently. Dividing a system into smaller subsystems allows for a simpler approach relative to the analysis required for all of the system's functional interfaces. The system must be viewed as a whole, broken down into its components, its component interrelationships studied and understood, and only then may the system be put back together. Therefore, a technique will now be introduced to structure the component hierarchy of the system (or system hierarchy within a system-of-systems).

A structured way to break down the components and subcomponents of a system is by utilizing a functional decomposition technique. A *functional decomposition* defines subsystems by the system requirements they enable [45]. The original intent of functional decomposition, developed by Pahl and Beitz [122], and Koller [87], was to describe the direction of information flow in a system. First, a system *function*

must be defined, which describes the process that takes inputs in and transforms these inputs into outputs. This function is a transformation which may involve the changing of the system state, and must contain an activation criterion that describes the availability of resources for the function to execute, and an exit criterion that describes when a function has completed. Dieter [56] considers *function* to be "in the nature of a physical behavior or action", whereby the system's functions are described as a transformation between an initial state and a desired final state. The function describes what the product must do, while its form or structure must describe how it accomplishes it.

A *functionality* is simply a set of functions required to obtain a desired output. *Decomposition* may be thought of as a form of *top-down* structuring, in which a defined top-level system function is partitioned into several subfunctions, as Buede describes [42]. Each function that requires further insight for the production of outputs is decomposed into another level of subfunctions (i.e. not every function must be decomposed, as long as the desired output is obtainable). The decomposition process must conserve all of the inputs to and outputs from the system's top-level function.

This methodology can help in understanding the context in which the term *system* is used, which requires appreciating the perception from which that term is used. Therefore, what is considered a system from one perspective, may actually be a system-of-systems in another. For example, the system may be an aircraft, consisting of engines, wings, landing gear, etc..., that all function to comprise the aircraft system. However, the engine sub-system may be further broken down into its own subsystems such as the compressor, combustor, and turbine. The wing could be broken down to each individual rib and spar. In an engagement, this aircraft may operate in an environment where it carries a weapon with the objective of destroying a target, and this target will likely wish to defend itself. This environment is now the system, comprising of aircraft and missiles, each a system of their own that can

be functionally decomposed into the subsystems that make them up. *Examining the effects of manipulation at any given layer of system/subsystem on every other system in this environment will define the system-of-systems approach taken in this thesis.*

One such tool used to decompose a problem of interest is the morphological matrix, or otherwise described as a matrix of alternatives [137]. A *morphological matrix* lists the key parameters or functions of a system on the vertical scale of the matrix, and alternative methods for satisfying them along the horizontal scale. The purpose of the method is to uncover combinations of design concepts that might not be intuitively generated. The elements of each functionally decomposed system level are arranged in such a manner as to maximize the system effectiveness. Of course, those elements could be systems themselves. Hines et al. [73] state that "system effectiveness has become the prime metric for the evaluation of military aircraft. As such, it is the designer's goal to maximize system effectiveness". In an engagement scenario, each side wishes to maximize its system effectiveness such that it is able to, at the very least survive the conflict, and if possible, destroy its opponent. Therefore, it is necessary to quantify system effectiveness in an engagement scenario, where in this case it would be a measure of how successful a system performs.

3.1.2 Functional Composition

Buede [42] also introduces *functional composition* as the opposite approach to the decomposition of a function. Composition may be thought of as a *bottom-up* approach. This method starts with the identification of simple functionalities associated with scenarios involving only one of the outputs of the system. Each one of these functionalities is a sequence of input, function, output-input, and then the repetition of function, output-input, function, until a final output is reached. Within the functional hierarchy, these functions in functionality are relatively low-level. After a number of

these functionalities are defined, the functions in the functionalities must be aggregated into similar groups. Next, these groups are aggregated into similar groups, and the process is repeated until a hierarchy is formed, *bottom-up*.

The main advantage of the composition approach, over decomposition, is that the composition process may be executed in parallel with the development of the actual physical architecture. This way, the functional and physical hierarchies will match each other. Furthermore, this is a very comprehensive approach in which a designer will be less likely to omit major functions. However, these many functionalities must be easily accessible during the composition process. When there is little experience with the system, or working with a "radical departure" of that system, Buede recommends this approach.

Depending on the situation, it may be useful to use a combination of functional composition and decomposition (which Buede refers to as "middle-out"). The simple functionalities in the composition approach associated with specific scenarios defined in the operational concept may be used to establish a sense of the system. Next, a top-level decomposition may be positioned to match the divisions of the physical architecture, which can be bolstered to assure totality by recurrent reference to the functionalities.

3.1.3 System-of-System Architecture

Proper systems-of-systems analysis requires engineering at the *architecture* level, which deals with allocation of functionality to components and inter-component interaction, rather than the internal workings of individual components. The architecture acts as a framework that constrains the way components interact with their environment, receive and relinquish control, manage data, communicate, and share resources [50]. For a successful design process, the functions or activities that a system has to perform must be considered. As Buede [42] states,

The functional architecture of a system contains a hierarchical model of the functions performed by the system, the system's components, and the system's configuration items; the flow of informational and physical items from outside the system through the transformational processes of the system's functions and on the waiting external systems being serviced by the system; a data model of the system's items; and a tracing of input/output requirements to both the system's functions and items.

The individual elements of a system-of-systems operate independently, collaborating only through information exchange. Although integrated modeling can be used to define a system-of-systems, as Maier describes as a "unified approach to systems engineering" [94], those models in themselves do not provide the guidance necessary for their structuring. The system-of-systems architecture defines the interfaces and composition which guides the implementation and evolution of the system-of-systems [48]. Maier et al. [95] define systems architecting as "the art and science of designing and building systems", and state that the "architect's" greatest concerns and leverage should be with the systems' connections and interfaces which distinguish a system from its components and provide unique system-level functions. Subsystems (or in a system-of-systems, the component systems) specialists will want to concentrate most "on the core and least on the periphery of their subsystems" because they generally view the periphery as external constraints placed on their internal design. Therefore, the subsystem specialists' concern for the entire system effectiveness would be less than that of the architect of the systems. The entire system architecture, as Maier et al. claim, "if not managed well, the system functions can be in jeopardy".

Systems architecting differs from systems engineering in that it relies more on heuristic reasoning and less on use of analytics. There are qualitatively different problem solving techniques required by high and low complexity levels. The lower levels would certainly benefit from purely analytical techniques, but those same techniques

may be overwhelming at higher levels which may benefit more from heuristics derived from experience, or even abstraction. It is important to concentrate on the essentials to simply solve the problem. The system should be modeled at as a high a level as possible, then the level of abstraction should be reduced progressively. "Everything should be made as simple as possible, but not simpler", as Albert Einstein once said [59].

The management of relations between the system components is an architectural issue which does not belong to individual systems, but shared by all the involved components. Chen et al. [48] introduced an architecture-model based approach to systems and capability relation management. *The responsibility of system relation management cannot be the responsibility of developers of individual systems, but at the system-of-systems level.* This architecture management system was designed to store and manage knowledge and information of systems capability in their proper context. The relations are determined by the interfaces between systems, or by the manner by which they are integrated. Chen et al. define the possible manners by which systems and capabilities are related in a system-of-systems manner as structure, function, information, operation, and generation:

1. Structure-related: Two systems are structure-related if one is a component or basis of the other.

2. Function-related: Two systems are function-related if one system requires certain functions or services by another system to perform its own function.

3. Information-related: Two systems are information-related if requirements or information is exchanged between the two.

4. Operation-related: Two systems are operation-related if they are both used in an operation scenario to jointly fulfil a mission.

5. Generation-related: Two systems are generation-related if one system will be a replacement of the other.

As capabilities evolve, the relation between systems can change. Therefore, Chen et al. state that a requirement to achieve good relation management is the development of an environment or system that serves as a basis for: managing concepts and objects in context; conducting analysis, synthesis and evaluation of values and relations of objects; handling complexity; exploring and studying dependency; maintaining traceability; and finally, visualizing concepts, objects and their relations and dependencies.

3.2 Uncertainty Analysis and Quantification in the Design Process

A NASA white paper describes those design problems that have a nondeterministic formulation as *uncertainty-based design* [145]. This survey of the state of the art in uncertainty-based design breaks it down into two major classes. The first is the *robust design* problem, which seeks a design relatively insensitive to small changes in uncertain quantities. Dieter [56] defines a robust design as "one that has been created with system of design tools to reduce product or process variability, while simultaneously guiding the performance toward an optimal setting". A *reliability-based design* seeks one in which the probability of failure is less than a predetermined acceptable value. The two major factors that drive the domain of applicability of each case are the frequency of the event and the impact of the event, as Zang et al. [145] adapts from Huyse [80] shown in Figure 26. A designer would likely design a system with performance insensitive to everyday fluctuations, or robust, such that there is not a catastrophic failure when the system encounters everyday fluctuations. However, a designer would like to minimize the probability of a catastrophic failure

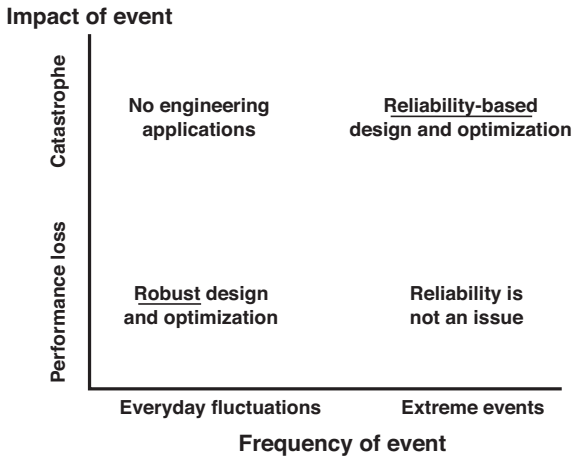

Figure 26: Uncertainty Based Design Domains ([145] adapted from [80])

occurring, or maximizing the design's reliability. Practically, the goal of robust-based design is to maintain acceptable performance levels at off design conditions, whereas reliability-based design aims to prevent catastrophic failure. The design risk is therefore a combination of both the likelihood and consequences of an undesired event.

The two cases can best be illustrated on a probability density function (PDF), as shown in Figure 27. Robust design is concerned with the event distribution around the mean of the PDF, whereas reliability-based design is concerned with the event distribution in the tails of the PDF. Zang et al. state that the mathematical methods for robust design procedures are considerably less developed than those for reliability based design, and "still largely confined to academic studies".

Simulation tools are proving to be useful in providing designers with efficient means to explore the interrelationships among various disciplines. However, uncertainties associated with these computer codes, arising from errors in input parameters and internal uncertainties due to simulation inaccuracy, may propagate through the different codes as shown in Figure 28. Du et al. [58] introduce two methods for managing uncertainty in simulation-based design that formally mitigate uncertainty based on principles of robust design. An extreme condition approach uses an interval

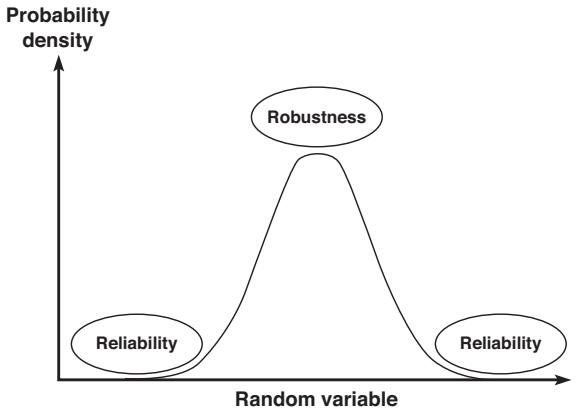

Figure 27: Reliability Versus Robustness in Terms of the Probability Density Function [145]

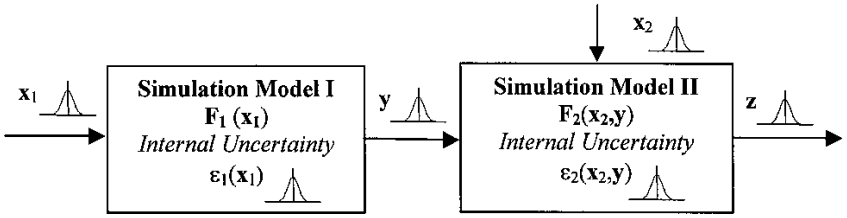

Figure 28: Uncertainty Propagation in the Simulation Model Chain [58]

of the output from a chain of simulations. The second, the statistical approach, provides statistical estimates of the outputs of the various codes, for example, estimating the probability and cumulative density function outputs, terms that will be defined in Section 3.2.2.

3.2.1 Forecasting

In an ideal circumstance, a decision maker would like to know what will happen in the future. The aim of a forecast is to provide a decision maker with the knowledge of whether a particular event happens. Twiss [137] defines four elements that a forecast must contain to adequately provide a basis for decision making: 1) qualitative, 2) quantitative, 3) time, and 4) probability. The qualitative element defines what should be forecast, which selects the events which need to be considered. The quantitative aspect requires selecting a measurement for a given metric. Since forecasting relates

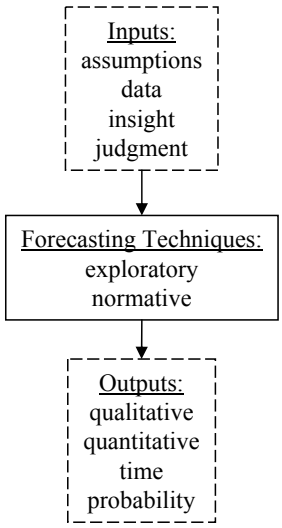

Figure 29: The Forecasting Process (adapted from [137])

future conditions to the time when they occur, the time element is necessary. The probability element is necessary to capture the likelihood of a particular outcome due to uncertainty in the system. The uncertainty aspect is important because it also be used to identify potential causes of discontinuity in the system.

There are two basic forecasting techniques used to achieve the four elements described by Twiss. *Exploratory* techniques rely on selected attributes of historical data, such as functional performance, technical and economic parameters, plotted against time. Progress is assumed evolutionary and not random, enabling the generation of characteristic forecasting curves made with a measure of certainty. *Normative* techniques work backwards from a proposed desired state to determine the steps necessary to reach a required outcome. It possible to have many "paths" of development to reach a desired outcome. The basic forecasting process described by Twiss is shown in Figure 29, where either of the forecasting techniques use assumptions, data, insight, and judgment to achieve the four desired forecasting elements. [135] [137]

3.2.2 Monte Carlo Simulation

A common approach to uncertainty quantification is the Monte Carlo simulation. A Monte Carlo method is a way to generate information for a simulation when events occur in a random way, using random sampling in a computer simulation in which the results are generated repeatedly to develop statistically reliable answers [56]. It is a useful method used to solve problems too difficult to obtain a numerical solution analytically, by observing that fraction of the numbers obeying some property or properties as a result of the random number generation input to a computer simulation [140]. Therefore, the Monte Carlo simulation is employed to approximate solutions to quantitative problems with statistical sampling [4]. The Monte Carlo method has found uses in many fields, as Shonkwiler [130] states, "Monte Carlo methods are used to simulate stochastic processes that occur in science, engineering, business and entertainment, to numerically solve problems in mathematics, science and engineering, and to ensure the security of data".

Variability in input variables, or "control" variables, and in assumptions, or "noise" variables, can be tracked by adding distributions to any point values. A random number generator is used to sample from a bounded distribution assumed for each variable, and then uses those variable settings to run a modeling and simulation environment. Many cases with randomly selected points from these distributions can then give a statistical indication of the probability with which each response will occur. A histogram, or graphical display of tabulated frequencies, can be created by tracking the number of responses in discrete bounded bins, or non-overlapping intervals of some variable. The histogram in this case is actually the Probability Density Function (PDF), which is the probability of observing a particular outcome. The integral of the PDF allows for the generation of a Cumulative Distribution Function (CDF), the mathematical function that maps the probability of obtaining a response to the metric within the given range. Because the sampling of the response into bins

is a discrete process, the more samples, the smoother the PDF and CDF curves, and therefore a confidence can be extracted with more precision.

The distribution shape and bounds for a given variable of interest requires a working knowledge of the system in question, and is usually based on experimental results, expert opinion, and most likely several iterations of trial and error for a system where little knowledge is known. Several of the probability distributions used in this study are described with more detail in Appendix A.

3.2.3 Filtered Monte Carlo Approach

According to Kuhne et al. [88], "Probabilistic Design is the process of accurately accounting for and mitigating the effects of variation in part geometry and other environmental conditions while at the same time optimizing a target performance factor." However, using mathematical methods, the authors state, probabilistic design may prove to be a complex and daunting task. Using logic and graphics along with Monte Carlo simulation, Kuhne et al. demonstrate an alternate visual approach called a "Filtered Monte Carlo" that achieves useful probabilistic design results efficiently and simply. This method assumes the existence of a fast-running simulation model that can be called on many times.

The Filtered Monte Carlo approach shown as a flow chart in Figure 30 works by populating a design space with response values obtained by running a simulation many times with randomly selected values from bounded distributions on input variables. If the output for that particular Monte Carlo simulation trial violates any response constraints defined a priori, that response is discarded. The outputs that do not violate the constraints are then plotted in a scatter plot fashion versus any of the inputs, given the user the ability to visualize sensitivity to variation in the inputs. However, the authors note the biggest challenge to this approach is with problems with large numbers of inputs and responses (i.e. >10), which *drives the need for*

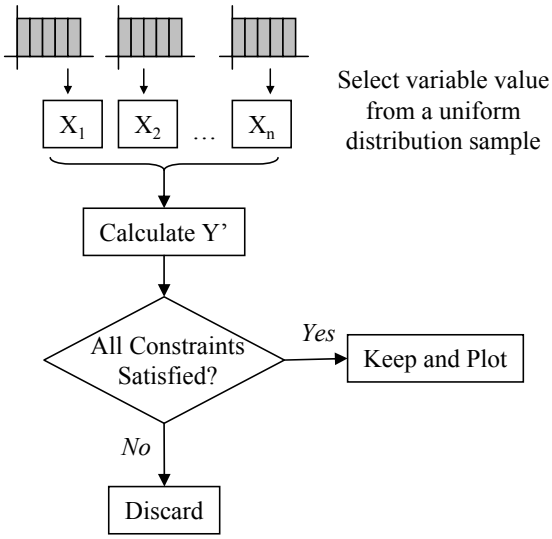

Figure 30: Filtered Monte Carlo Approach (adapted from [88])

improved visualization and data mining tools that would enable the user to simultaneously explore the design space while conducting input variation sensitivity. The authors claim "great success" with Filtered Monte Carlo approach on many application within General Electric Transportation-Aircraft Engines, including optimization, robustness studies, and design space exploration.

3.3 Surrogate Modeling

To be able to conduct an uncertainty quantification or design space exploration, a modeling and simulation tool would have to be executed many times. As stated earlier, the more Monte Carlo simulations run, the smoother the PDF and CDF curves, increasing the accuracy in the trends and confidence in the predictions made from those trends. In many cases, a design related simulation environment may be very large, comprising of many codes running in series, parallel, or both, requiring anywhere from several seconds, to several hours for a single trial run. This may not be a practical, or even feasible option when thousands of runs are required for a solution. Therefore, the use of a surrogate modeling approach is proposed to represent a

modeling and simulation environment, and increase the efficiency of the uncertainty quantification process many times fold. A *surrogate model*, also known as a meta-model, is a model of a small segment of a more complex or sophisticated analysis tool based on a regression of statistical inputs and response metrics. This model allows for quick calculation of responses by employing equations to relate independent variables to those responses. This section will cover two types of surrogate models proposed for use in this thesis 1) polynomial Response Surface Equations, and 2) neural network Response Surface Equations.

Many publications have been published on the use of polynomial Response Surface Equations (RSE), and this thesis will not belabor the theory or derivations involved in the regression techniques to achieve them. Interested readers may visit the Georgia Tech Aerospace Systems Design Laboratory (ASDL) publication webpage [5] for a vast amount of publications on the use of and theory behind polynomial RSE's. However, the use of Neural Networks for data regression is less practised, and therefore this study will explore the theory behind it.

3.3.1 Polynomial Response Surface Equations

A surrogate model is made by regressing against a set of data. In theory, a surrogate model may be built around data collected from a large number of runs with random selection of values within the bounds of input variables. However, for a very complex system model requiring many time consuming computer codes to run, a structured method for data sampling with the minimum number of simulation runs is needed. A statistical approach to experimental design is necessary to draw meaningful conclusions from data. Montgomery [115] defines a statistical Design of Experiments (DoE) as "the process of planning the experiment so that appropriate data will be collected, which may be analyzed by statistical methods resulting in valid and objective conclusions".

The simplest form of DoE is the full-factorial design. Each variable is discretized into two or three levels, and the modeling and simulation environment is executed for every combination of possible values for those discretized variables. A common DoE for creating second order polynomial RSEs with minimum amount of simulation executions is the Central Composite Design (CCD) [116]. This design combines a two-level fractional factorial with center points (point at which all of the factor values are zero, or midrange) and axial or star points (points at which all but one factor are zero, and one point is at an outer axial value).

The polynomial form of an RSE is given in Equation 19. The coefficients that make up the RSE are determined by regressing sample data points taken from a modeling and simulation tool against the input variable used to obtain those data points. The statistical software JMP [127] can be used to generate the required DoE and regress the corresponding data in RSE's, acting as both a pre- and post-processor.

$$R = b_0 + \sum_{i=1}^{n} b_i x_i + \sum_{i=1}^{n} b_{ii} x_{ii}^2 + \sum_{i=1}^{n-1} \sum_{j=i+1}^{n} b_{ij} x_i x_j \tag{19}$$

where

$$\begin{aligned} n &= \text{number of factors} \\ b_0 &= \text{intercept regression coefficient} \\ b_i &= \text{regression coefficients for linear terms} \\ b_{ii} &= \text{regression coefficients for pure quadratic terms} \\ b_{ij} &= \text{regression coefficients for cross product terms} \\ x_i, x_j &= \text{design variables or factors} \end{aligned}$$

3.3.2 Neural Network Response Surface Equations

A neural network is "computational architecture based on the design of the interconnections of neurons in our brains" [64]. Neural networks are emerging as a useful way creating highly nonlinear regression models, and are a good alternative when a polynomial RSE representation does not fit the design space well. When used to create RSE's, a neural network is just a set of nonlinear equations that predict output variables from a set of given input variables using layers of linear regressions and S-shaped logistic functions. The implementation introduced here is the one used by JMP [127] to create neural network regressions, with many concepts and explanations to the equations taken from help guides written by Demuth et al. [53] and Johnson [81].

Neural networks have been applied to various fields. In the aerospace field, neural networks have been used to develop aircraft autopilot routines and control systems, and for defensive uses such as target discrimination and recognition. They have also been used to create image processing software, predict stock market activity, develop speech recognition software, and various other uses in the banking, manufacturing, and medical fields. Many authors that write about neural network applications, even recent works, cite the 1998 DARPA *Neural Network Study* [10] report for the various applications of their use. The application of neural networks used in this thesis proposal is different from most of the "common" applications identified above, since here they will be used to fit, or regress, analytical models to output data from computer simulations, rather than predict future results of additional real-world real-time experiments.

3.3.2.1 Neural Networks Background

The elements of neural networks were inspired by biological nervous systems, in which the connections between elements determines the network function. A neural network

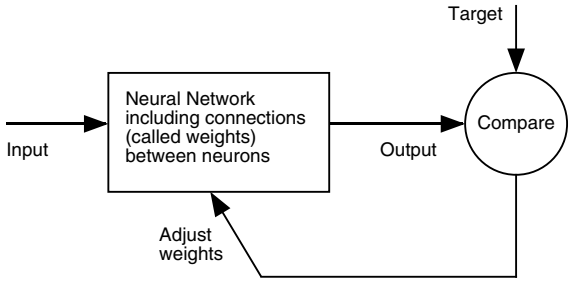

Figure 31: Neural Network Training Process [53]

can be trained to perform a particular function by making adjustments to the values of the connections, or weights, between the elements. This training process involves adjusting the weights so that a particular input leads to a specific target output, as shown in Figure 31. By comparison of the output and target values, the weights are adjusted until a match is made, within a specified tolerance. The collection of outputs that is paired to the inputs is called the *training set*. The algorithm used to find the values of the regression coefficients is called *back propagation*, whereby those values are found in which they minimize the error as compared to the training set. This can be achieved using any one of a number of optimization techniques (some relevant techniques will be discussed in Section 5.3.5).

In a feed-forward network shown in Figure 32, the input layer receives values which it feeds to a *hidden layer*. The hidden layer provides the network's non-linear modeling capabilities [27]. The link between each input and hidden layer has a weight associated with it. Another set of weights are placed on the connections between the hidden and output layers. Note that each input node has an effect on each hidden node, and in turn each hidden node has an effect on each output node.

The logistical function is the way the hidden layer handles the input. An S-shaped or *sigmoid* logistic function works as the weighted sum of the input values increase, the value of the response increases gradually. An alternate approach would use a *threshold* function, where the response is set to 0, and if the weighted sum of the

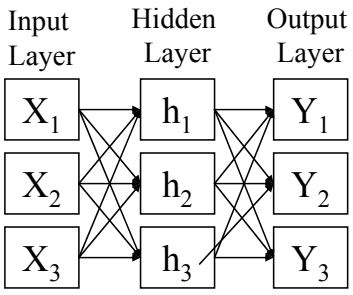

Figure 32: A Simple Feed-Forward Neural Network

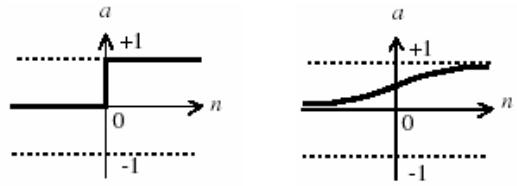

Figure 33: The Threshold (L) and Sigmoid (R) Logistic Functions [53]

inputs exceeds a threshold value, the response is set to 1. The threshold function does closer resemble the actual behavior of the biological neurons, however, the S-shaped function is used for the regression analysis since it is smooth and easily differentiable. These logistic transfer functions, shown in Figure 33, and many other types used in the other applications of neural networks are provided by Demuth et al. [53].

3.3.2.2 Neural Network Equations

The logistic function used to create neural networks, as given in Equation 20, is used to scale the inputs between [0,1], and is referred to in JMP as the "squish" function. As described earlier, this creates the S-shaped logistic function for input manipulation within the hidden layer.

$$S(z) = \frac{1}{1 + e^{-z}} \tag{20}$$

This logistic function is used to calculate the value of each hidden node, as shown in Equation 21 by its application to a linear term related to the input variable.

$$H_j = S_H \left(a_j + \sum_{i=1}^{N_X} (b_{ij} X_i) \right) \tag{21}$$

where

$$
\begin{aligned}
H_j &= \text{the value of hidden node } j \\
S_H &= \text{the logistic function for hidden node } j \\
a_j &= \text{the intercept term for hidden node } j \\
b_{ij} &= \text{the coefficient for design variable } i \\
X_i &= \text{the value of design variable } i \\
N_X &= \text{the number of input variables}
\end{aligned}
$$

The outputs are then calculated as shown in Equation 22. Note that the bracketed portion fits within an interval of [0,1], where as the coefficients c and d are used to scale the magnitude of the response.

$$R_k = c_k + d_k \left[e_k + \sum_{j=1}^{N_H} (f_{jk} H_j) \right] \tag{22}$$

Finally, the steps described can be combined to describe the form of neural network equation that JMP uses, as shown in Equation 23.

$$R_k = c_k + d_k \left[e_k + \sum_{j=1}^{N_H} \left(f_{jk} \left(\frac{1}{1 + e^{-\left(a_j + \sum_{i=1}^{N} (b_{ij} X_i)\right)}} \right) \right) \right] \tag{23}$$

where

$$
\begin{aligned}
a_j &= \text{the coefficient for hidden node } j \\
b_{ij} &= \text{the coefficient for design variable } i \\
c_k &= \text{the response scaling intercept term for response } k \\
d_k &= \text{the response scaling coefficient for response } k \\
e_k &= \text{the intercept term for response } k \\
f_{jk} &= \text{the coefficient for hidden node } j \text{ and response } k \\
N &= \text{the number of design variables}
\end{aligned}
$$

N_H = the number of hidden nodes

X_i = the value of design variable i

3.3.2.3 Overcoming Disadvantages of Neural Network Regression

Neural networks are very useful for creating regression equations when the design space is highly non-linear and/or discontinuous. Any surface can be approximated to any accuracy with the proper amount of hidden nodes [127]. However, this fact is not without its price. Neural networks are not as interpretable as polynomial equations since there is an intermediate (hidden) layer between inputs and outputs, rather than a direct path. It is very easy to "overfit" a set of data with too many hidden nodes, such that it no longer predicts future data well, resulting in an extremely multimodal response surface, as shown in Figure 34. The fit itself is not parametrically stable, meaning that many times the objective function may converge before the parameters settle.

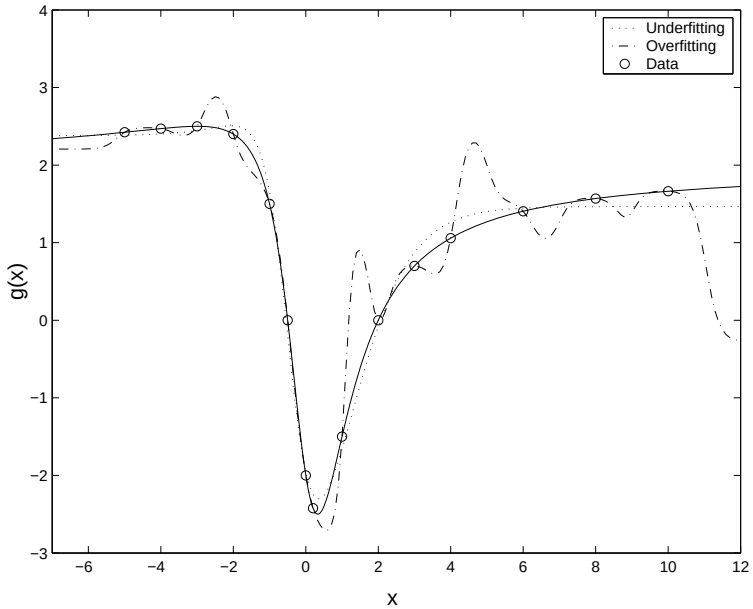

Figure 34: Example of Over- and Underfitting a Neural Network [128]

With a highly multimodal design space, there are many local optima, therefore the optimizer that finds the neural network coefficients must be run with many starting

points. Each one of these starting estimates is called a *tour*. Of course, there is no exact science in determining the appropriate number of tours. Too few will likely not lead to the global optima, where as too many tours may exhaust the available computational resources.

To counter the overfit problem, neural networks will fit with a holdback sample, which is data not used in the estimation process. The holdback sample is called the *validation set* when used along with the training set. An overfit penalty, or weight decay, may be used to avoid overfitting the data. This puts a numerical penalty on the size of the parameter estimates, and usually improves numerical convergence.

Unlike the polynomial RSE's that use a Design of Experiments to define the cases needed to run to get the data needed to build the regression model, there is no well defined methodology for neural network regression. Since the model fits to both a training and validation set, the more random cases run the better the fit. However, Johnson [81] states that it is important to include cases for a neural network regression that include all effects that the model needs to simulate. Running only random cases will lead to a model that does not fit well in the extremes of the design space. Therefore, Johnson suggests running a combination of a Latin Hypercube Sample (LHS), which would provide a list of random cases with as little correlation as possible, along with a two-level Design of Experiments to capture the corners of the design space.

An LHS is one of several space-filling designs, which are configured to uniformly spread design points to the maximum distance possible (within variable limits). The LHS method chooses points to maximize the minimum distance between design points, but with a constraint that involves maintaining the even spacing between factor levels and minimizing the correlation in the design [127]. An example of using an LHS to fill two dimensional space with 1000 design points is given in Figure 35. Similarly in three dimensional space, a cube would appear.

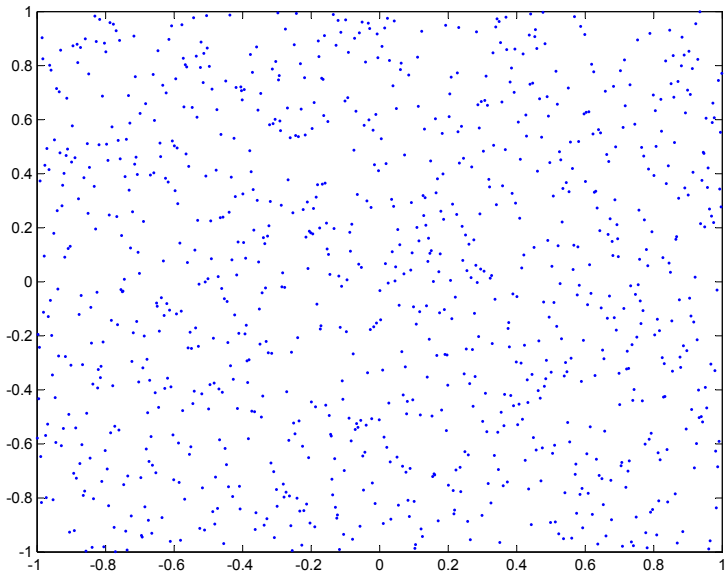

Figure 35: Example Latin Hypercube Used to Fill 2-D Space

3.3.3 Analysis of Variance

One of the major advantages of creating surrogate models is the ability to rapidly run an analysis of variance (ANOVA), which measures the contribution of each variable on the *variability* of each response. A useful way to visualize the results of an ANOVA is in the form of a Pareto Plot, as shown in Figure 36 for an example of contributions of gun accuracy to miss distance. Each horizontal bar shows the individual influence of each error term on the response, listed in descending order, and the cumulative effect of each of the terms is represented as a line (totaling 100%). This is also a useful tool for examining the combined effects of variables. For example, the combination of two variables may affect a response more than the some of each variable.

3.4 Application of Techniques

3.4.1 Response Surface Methodology & Design Space Exploration

Many processes for using surrogate models to expedite a Monte Carlo simulation to quantify uncertainty and provide a robust design have been developed for aerospace vehicle design. A major application of this includes creating the ability of forecasting

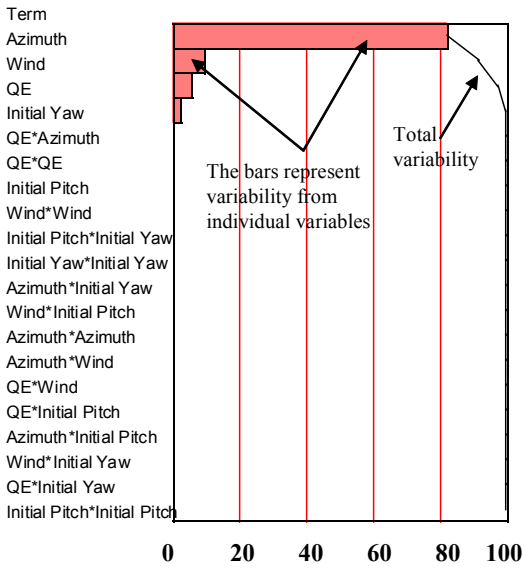

Figure 36: Example Pareto Plot - Gun Accuracy Contributions to Miss Distance

the impact of new or immature technologies on a system to provide increased knowledge to a decision maker in the conceptual and preliminary phases of aircraft design [85]. Mavris et al. [109] have applied the exploratory forecasting technique to select from a list of potential technologies ones that have the most positive impact on the design of a high speed civil transport using a technology impact forecasting (TIF) method. This TIF method was implemented by applying multipliers, or "k" factors, to various disciplinary metrics that are used by an aircraft design tool, using polynomial RSE's for rapid manipulation. This technology impact forecasting methodology has also been applied to other aerospace systems, such as determining the technology impact on subsonic transport affordability [84], on the design of an Uninhabited Combat Aerial Vehicle (UCAV) [111], and on a civil tiltrotor [104]. Surrogate models have also been used to create a parametric environment to integrate disciplinary codes together to size a hypersonic cruise missile [62], as well as quantify the errors associated with disciplinary codes and evaluate the impacts of those errors on the confidence of reaching mission requirements and maintaining within given physical constraints [61]. In addition, one of the major applications of the methodologies introduced in

this chapter is in the field of design for affordability, as will be discussed shortly.

3.4.2 Top-Down Capability Based Design

Soban [134] developed a formulation that links variables and responses across a system-of-systems hierarchy using polynomial based surrogate models. In this formulation, the outputs of one level within the hierarchy feed directly to the next higher level. Manipulating a subsystem level variable, for example the thrust-to-weight ratio of an aircraft, changes it's performance capability which in turn affects the way it capability in the system-of-systems context, for example the way that same aircraft would affect the course of a many-on-many campaign environment. If the system level metrics are represented by surrogate models, the outputs of those surrogate models can then be inputs to the next hierarchical level of surrogate models, essentially enabling a rapid hierarchical modeling and simulation environment.

A Unified Tradeoff Environment (UTE), developed by Baker et al. [30] [31], allows for simultaneous trades between design variables, requirements, and technologies by coupling the customer requirements and technologies to the vehicle concept space. Once again when polynomial surrogate models are able to represent a design tool, rapid trade-offs enable real time decision making. Using a UTE enabled by these surrogate models as a real-time decision making tool, a designer can see the effects of evolving requirements on the design space of a vehicle.

The author has been part of an effort to expand these efforts to a more complex many-on-many campaign scenario by developing a hierarchical, surrogate model enabled environment for systems-of-systems analysis [38], shown graphically in Figure 37. This hierarchical modeling and simulation environment consists of vehicle and missile propulsion subsystem models, missile and aircraft (platform) synthesis and sizing codes, and top-level military campaign analysis tools that are linked together using neural network based surrogate models into a UTE. Real time trades are

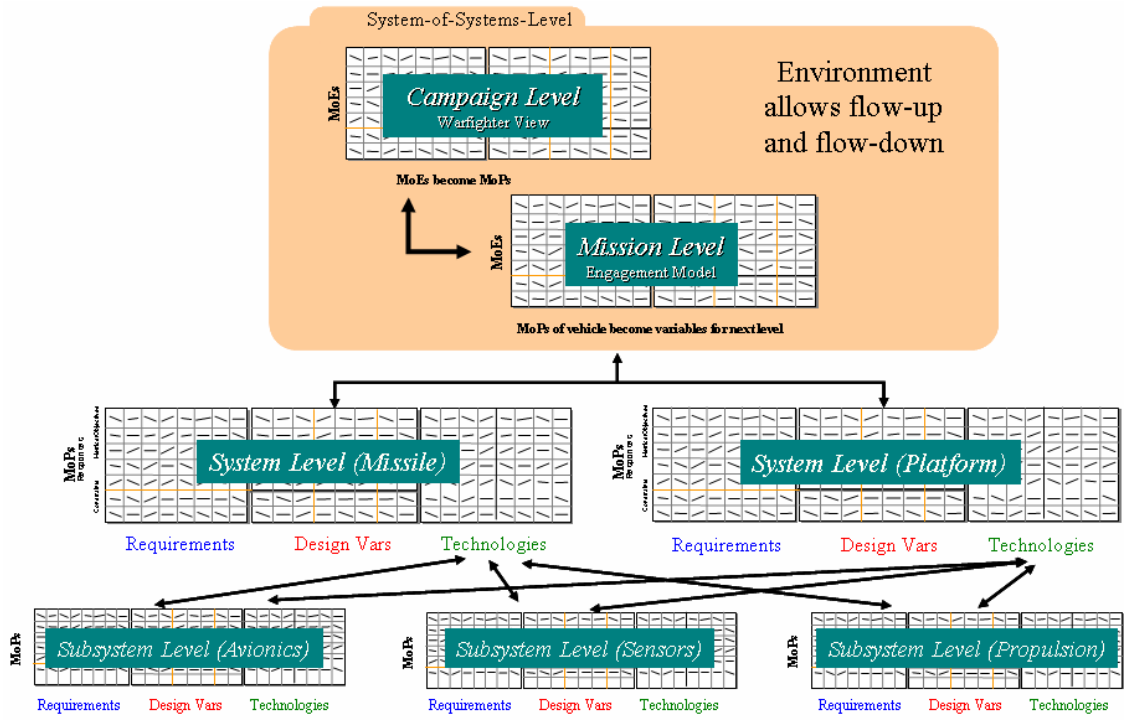

Figure 37: Hierarchical, Surrogate Modeling Environment for Systems-of-Systems Analysis [38]

therefore enabled between design variables, requirements, and technologies at each hierarchical level.

Using surrogate models to link the different subsystem and system models together allows for rapid manipulation of the design space. Now, the value of each design variable can be selected using a Monte Carlo simulation to fill the design space. In the example shown in Figure 38, weapon performance values are output for each Monte Carlo simulation selection of design variables. However, in the system-of-systems context, this one weapon does not operate independently to effect top-level metrics. Subsystem weapon attributes flow up the hierarchy, and additional variables that would affect top-level metrics, such as enemy weapon capability are also selected using a Monte Carlo simulation. In this example, the top-level metrics of platforms lost and targets killed are observed. When this process is repeated many times, the entire system-of-systems design space is filled. The results of this type of study are

best viewed using a multivariate scatter plot, or collection of bivariate plots shown in Figure 38, showing the results of 1,000 Monte Carlo samples. Note that the plots in Figure 38 only represent a fraction of the total design space. Although somewhat overwhelming, when used interactively this process allows a user to perform both bottom-up and top-down design.

From the bottom-up, individual weapon designs may be identified to compete against an enemy capability and the results observed by studying the top-level results. However, with the design space filled at each level in the system-of-systems hierarchy, the notion of *top-down design* comes in, as opposed to top-down requirements flow. Here, a user may highlight a capability region of interest, for example defining desirable and undesirable regions (shown respectively as green and red in Figure 38). Now, the types of targets that may be prosecuted, as defined by their characteristic are identified. Taking this one level lower, the weapon performance requirements are defined. From this, it is evident that regions of improving performance (i.e. higher weapon speed and range capabilities) yield a more desirable outcome, as were defined at the very top of the decision making hierarchy. Finally, at the very bottom, individual weapon designs are identified that yield desirable outcomes at any level in the hierarchy. This top-down design based on desired capability allows for true hierarchical decision making.

Viewing a hierarchical system-of-systems design space populated using a Monte Carlo simulation brings in the notion of total versus partial derivatives, first discussed by previous work conducted by the author [38]. In the field of mathematics, the *partial derivative* of a function of several variables is the derivative of that function with respect to only one of those variables, with all other variables held constant. Generally speaking, a curve on a two-dimensional plot is a partial derivative, because it shows how a function varies with respect to one variable. If any of the other variables that define that function change, the shape of that curve will change. This is like

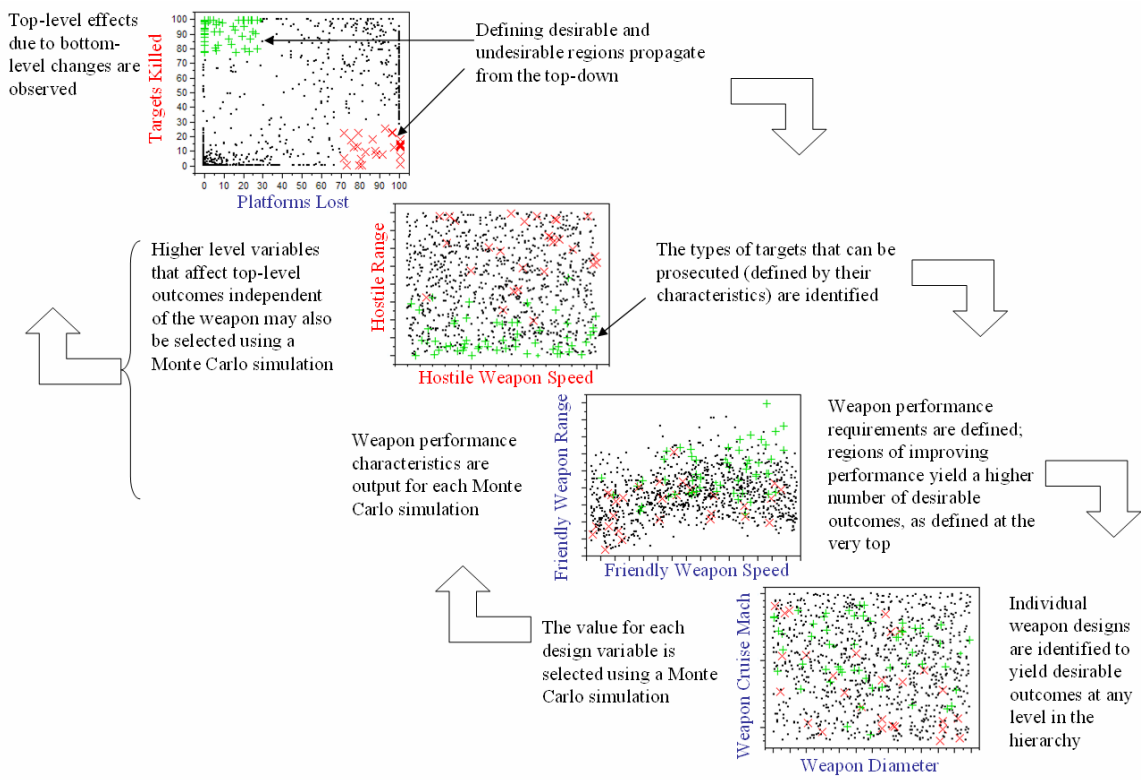

Figure 38: Top-Down Capability Based Design for a Campaign Scenario [110]

a contour plot, where the partial derivative is shown for several fixed values of the other variables that define the function. A *total derivative*, however, is the derivative of that function when all of the variables are allowed to vary [1]. Because every degree of freedom is exploited, it is difficult to view the total derivative design space. For a vector valued function, it's derivatives are vectors as well. This directional derivative is known as the *full derivative*[2]. For a vector function $\vec{f}$ with m functions and variable vector $\vec{x}$ with n variables, Berglund [37] gives the full derivative $D\vec{f}$ as the Jacobian

[1] This also includes indirect dependencies of the function due to intermediate variables. For example, the function y is dependent on variable x, but variable x is a function of t, therefore y is indirectly dependent on t [141].

[2] The terms total and full derivatives are usually interchangeable in much of the literature, and many times slightly different definitions are given to describe them. This thesis will assume the form given in this section.

Matrix:

$$D\vec{f}(\vec{x}) = \begin{bmatrix} \frac{\partial f_1}{\partial x_1}(\vec{x}) & \frac{\partial f_1}{\partial x_2}(\vec{x}) & \dots & \frac{\partial f_1}{\partial x_n}(\vec{x}) \\ \frac{\partial f_2}{\partial x_1}(\vec{x}) & \frac{\partial f_2}{\partial x_2}(\vec{x}) & \dots & \frac{\partial f_2}{\partial x_n}(\vec{x}) \\ \vdots & \vdots & \ddots & \vdots \\ \frac{\partial f_m}{\partial x_1}(\vec{x}) & \frac{\partial f_m}{\partial x_2}(\vec{x}) & \dots & \frac{\partial f_m}{\partial x_n}(\vec{x}) \end{bmatrix} \tag{24}$$

3.4.3 Design for Affordability

There has been a shift in the design industry to design for affordability, and several of the techniques introduced earlier have been applied to this field. Mavris and DeLaurentis [105] state that the design process must not only address interactions between the traditional aerospace disciplines, such as aerodynamics and propulsion, but also include "life cycle" disciplines, such as economics, reliability, manufacturing, safety, and supportability. However, these additional disciplines bring with them a variety of uncertainties into the design problem. The presence of uncertainty demands a stochastic treatment of the design process, handled with uncertainties.

The term *affordability* here is used as a measure of cost effectiveness. It is defined here as the ratio of desired outcome (i.e. performance) over the cost of a given system. A more affordable system therefore is not always the least expensive one. It can be thought of as a measure of how much performance each dollar buys. Designing with affordability concerns in the aerospace industry was driven primarily by military budget cuts and increased competition in the commercial market [108]. So much so, the Defense Manufacturing Council has requested that *cost be treated as an independent design variable* on the same level as traditional design variables [97]. Affordibility can also be a measurement of product effectiveness against both cost and risk [105]. Affordability itself can be thought of as a multiattribute and multidisciplinary process. More on implementing life cycle analysis to reduce total cost within the conceptual design phase of aerospace systems can be found in [98] [107]. However, the notion of treating cost as an independent variable brings forth the desire to have the ability to

treat any response metric, which is a function of independent variables, itself as an independent variable.

3.5 Chapter Conclusions

This chapter reviewed advanced design methodology concepts that could be used to enable the creation of a process to set the design requirements of a complex system across a multilevel decision making hierarchy. The system-of-systems concept was introduced as a methodology for describing events at every level by functionally decomposing the entire system in question into a hierarchy of decision making levels. Several uncertainty analysis and quantification techniques were discussed, including a filtered Monte Carlo approach that uses a Monte Carlo simulation to determine the combination of bounded design variables that do not violate a series of response constraints. Two surrogate modeling techniques were discussed as potential methods for representing bounded segments of complex analysis tools using a series of regression based equations. Finally, an initial study into the topic of top-down capability based design was introduced as a method for implementing the cross hierarchical flow of information. Using the information gathered in the literature sections, a set of additional research questions and hypotheses can now be formed, in an attempt to expound on the primary research objective of this work.

CHAPTER IV

RESEARCH QUESTIONS & HYPOTHESES

4.1 Problem Revisited

The motivation chapter introduced a problem in which a need was established for a process enabling the rapid manipulation across a hierarchy of decision making levels in the systems engineering process. An example problem was presented in which an air defense weapon is required to defeat the threat posed by rockets, artillery, and mortars (RAM) fired from heavily populated areas. Several issues were brought up throughout the chapter that impede a quick solution to this problem, and technology barriers of the proposed solutions that the Department of Defense is studying were reviewed. Formal requirements have been established by the U.S. Army under the Extended Area Protection & Survivability (EAPS) program, describing the needs for different defendable area tiers. Initial studies have been conducted by various organizations under the EAPS program to define general needs, and to examine potential solutions to the problem.

The second chapter was dedicated to presenting methods for modeling and simulation of combat systems pertinent to the topic in question. It was determined, however, that there is no defined method to modeling the RAM threat or air defense systems that could be used to defeat them. This established the need to create a modeling and simulation environment that brings together the various interacting components of this problem. However, this leads to the issue of simulating complex systems, each with its own uncertainty contributions to capabilities at various levels of the hierarchy. Many of these simulations may be physics based tools that would

exhaust most computational frameworks, especially if many executions would be required such as in any uncertainty quantification process. Therefore, various Advanced Design Methodologies were presented in Chapter 3 that could be applied to assist in this problem. Many of these methodologies have been established through many years of use, and several were more recently developed such as those the author was a part of developing.

The purpose of this thesis is not to provide a specific solution down to the detail design level of a specific problem, but a process that may be applied to complex revolutionary problems in which independent components interact with one another in a hierarchy to effect an outcome. The goal is to define capabilities anywhere in a hierarchy, even in many cases where there will be components outside the user's control, and define the requirements of the components within the user's control. The following research questions will formally address this and related issues. First, the initial formulation research questions introduced during the motivation to this thesis will be revisited for consistency. Next, more specific research questions will be presented, inspired by information gathered during the literature search. The set of hypotheses will propose specific answers to those research questions based on literature, evidence, and information concerning related studies collected as part of the literature search conducted for this thesis.

4.2 Research Questions

4.2.1 Initial Formulation Research Questions Reviewed

Section 1.1.2 introduced two research questions that inspired the research objective of this work, as well as the direction of the literature searches reviewed in Chapters 2 and 3.

> **Research Question 1:** *What is the systems engineering process that can be applied to set the design requirements of a complex hierarchical system,*

and what are the major deficiencies associated with that process?

Several deficiencies were identified for the systems engineering process discussed in Section 1.1.2, as applied to a sample complex system. In summary, there must be an iteration between adjacent levels of the hierarchy to make sure that the design solution satisfies the requirement, therefore there can be no direct flow between nonadjacent levels. Therefore, the second Research Question asks how an improved process can be created

> **Research Question 2:** *How can a process be created that enables rapid manipulation across a hierarchy of decision making levels?*

This question drives the need for a specific process to be defined, as opposed to a point design solution for a given set of rigid requirements and constraints. This question also motivated the direction taken as part of the literature searches. As an example problem, a solution designed to satisfy the requirements drawn by the EAPS program requires several independent systems to function together within an operational environment. Each of these systems has its own uncertainties associated with it that affect the combined system's overall capability. The operational environment may comprise of several high level requirements that must be satisfied, as well as any other constraints within the hierarchy.

4.2.2 Additional Research Questions

Based on the methods and techniques discovered during the literature search phase, more specific research question were formulated regarding this thesis, which are included in this section.

> **Research Question 3:** *An ANOVA/Pareto plot technique can be used to quantify the contribution of each variable to the variability of a response, but is there a way to identify which variables drive each other?*

This question is related to the topic of identifying the variables that have the most impact on the variability of a response. The contribution of each variable to the variability of a response can be measured by conducting an Analysis of Variance (ANOVA) based on main effects (i.e. the bounds of the variables), and visualized using a Pareto Plot. This has been proven very useful because the variables that have little or no contribution to response variability can be defaulted to a reasonable value and left out of any further parametric study. However, this gives only a one dimensional representation of the results, listing the percentage of response variability contribution of each variable. This gives no indication of the variability tradeoffs between the variable bounds, or the tradeoff between the variables themselves. More specifically, of the variables that do contribute to the variability of the response (i.e. the variables that drive the response in a particular direction), *are there variable settings that drive any other variable in one direction or another based on response constraints*?

> **Research Question 4:** *Can a tradeoff space be identified interchangeably between variables and responses?*

Question 4 is a natural extension of explanation given for the previous question. Regarding the identification of tradeoff space between variables based on response constraints, the same question can also be asked regarding placing constraints on variables as well as responses, leading to the notion of creating a trade space between any combination of variables and responses based on any constraints placed on any other variables or responses.

> **Research Question 5:** *How can rapid design tradeoffs be assessed in a hierarchical environment composed of independent time consuming models if the design space between them is multimodal or discontinuous?*

The topic of Response Surface Methodology has been well established as a useful way to capture a small segment of the design space of a complex computer code, reducing the wait time for the code to run to fractions of a second. However, this requires that the user bound the design space tightly enough so that it could be accurately be represented using a series of polynomial equations, or transformations thereof. An argument can certainly be made that one could constrain any design space so tightly that even a linear trend would suffice. Across a hierarchy of design levels for interacting systems, however, it may be desirable or even necessary to open up the design space to allow for tradeoffs across the hierarchy and between the systems. This leads to the likely potential that polynomial regressions (or their transformations) cease to accurately represent the design space.

> **Research Question 6:** *How can the effects of uncertainty propagation at any level within a hierarchical decision making design environment be assessed?*

There is a clearly defined need to be able to quantify the effects of uncertainty of a system's performance within its operational environment. Sources of uncertainty may include errors in system attributes or unexpected deviations from expected performance. When dealing with a hierarchical environment in which interacting systems may be decomposed into the subsystems that describe them, there may exist sources of uncertainty at any level that may effect the outcome from the bottom-up. It is important to have the ability to quantify those sources of uncertainty regardless of position in the hierarchy. Another source of uncertainty may also lie in the top-level requirements or constraints. For example, the exact requirement may not be known, but a region of interest may be defined. This drives the need to determine how those top-level regions of interest affect the design space of lower level metrics and variables.

4.3 Hypotheses

The hypotheses presented in this section are an attempt to answer the research questions given in the previous section, using methods collected in the literature search. These hypotheses will shape the research formulation and approach taken for the remainder of this thesis. The first hypothesis encapsulates the overall ***research objective*** of this thesis.

> **Hypothesis 1:** *A system-of-systems approach can be used to create an environment that will allow for both weapon requirements definition and system optimization from top-down requirements that take into account operational environment characteristics, as well as for analyzing the impacts of subsystem level changes on top level metrics from the bottom-up.*

Information acquired about system-of-systems and the overall systems engineering process inspired the approach proposed in this thesis to create a hierarchical decision making design environment in which multiple independent systems interact to affect an overall metric. The notion of top-down design in the field of systems engineering introduces the concept of flowing requirements from high level needs down to system and subsystems. This thesis takes that notion one step further to propose constructing a design environment that enables simultaneous bottom-up and top-down design. To do this, the entire process must be functionally decomposed by degrees of freedom allotted for each component. The ability to conduct rapid or real-time tradeoffs are addressed in Hypothesis 2.

> **Hypothesis 2:** *A hierarchical environment composed of neural network based surrogate models will enable multimodal and/or discontinuous design spaces to be accurately represented, allowing for rapid tradeoffs. These tradeoffs may be conducted with real time application of constraints at*

any level of the hierarchy, for both independent variables and dependent responses.

Assembling a hierarchical design environment as discussed in the first hypothesis usually requires assembling simulation tools of various complexities. Surrogate models based on predetermined simulation runs have proven to be useful in representing small segments of design space by providing parametric polynomial equations. As the complexity of the design space increases, polynomials are less likely to be able to represent the complexity of the design space, and certainly not any multimodal or discontinuous effects. Neural network based surrogate models are emerging as viable alternatives to polynomials, and have the ability to model highly nonlinear, multimodal, and discontinuous design spaces. As noted in the literature search discussing them, the use of neural networks have several drawbacks that must be overcome. Special attention must be paid to not "over fit" the data, leading to a surrogate model that is not able to predict future points not used to create them. Additionally, as the number of variables increases, the complexity of the neural networks requires more computational resource to properly execute the optimizer calculating the neural network coefficients.

Once the technical hurdles will be overcome, neural network based surrogate models will enable rapid tradeoffs of complex design spaces. In conjunction with Hypothesis 1, these neural network based surrogate models will be the prime enabler of rapid cross hierarchical manipulation, and with proper design space allotment, requirement constraints can be applied in real time revealing how the design space of every other response and variable changes.

Hypothesis 3: *A properly constructed system-of-systems environment will allow for the rapid assessment of the effects of uncertainty at any level in the hierarchy on any other level in the hierarchy.*

Many sources of uncertainty may exist among the various interacting components of a system-of-systems design environment. Using a hierarchical system-of-systems design environment composed of neural network based surrogate models, the effects of uncertainty propagation throughout the environment can be rapidly assessed. An even more profound proposal using the combined conjectures of the hypotheses presented in this section is the ability to bound the acceptable errors or uncertainties in individual components based on top-level requirements. This gives the ability to bound an acceptable region of uncertainty anywhere in the system-of-systems hierarchy for a desired level of total system robustness.

CHAPTER V

RESEARCH FORMULATION & APPROACH

5.1 Decomposing the Bounded Problem

5.1.1 Narrowing the Scope of Interest

In an effort to provide an example problem to study to specific systems engineering process identified, Chapter 1 discussed the urgent need to provide an air defense system to protect coalition assets in the Baghdad Green Zone from the threat of rockets, artillery, and mortars. However, it is unfeasible as well as out of the focus of this thesis to propose a complete solution to this specific problem with substantial technical merit expected of this work. Therefore, the need to defend the Green Zone only serves as a motivation to shape a sufficiently bounded problem studied in this thesis. This is an appropriate point to discuss how the problem scope is further bounded to provide attainable goals suitable to proving the hypotheses presented in Chapter 4.

One of the hypotheses stated that a system-of-systems approach can be used to assemble a hierarchical decision making environment composed of interacting systems. This may bring to mind a generic campaign code such as those discussed in Chapter 2, in which any number of the identical or different systems may interact with many opposing threats (i.e. a squadron of fighters aircraft destroying an enemy IADS). This thesis will not study a many-on-many scenario relating to this problem, for example defending a specific area shape and size with multiple air defense systems simultaneously intercepting multiple targets. Only single "instances" of each system type will be examined, such as one gun firing one interceptor projectile type against one target. However, once the a suitable architecture is in place to analyze a single

weapon system and engagement scenario, statistical methods introduced in Chapter 2 will be used to determine the combined effect of firing multiple projectiles at a single target.

Several interceptor solutions and target types falling in the RAM threat category were identified in Chapter 1, and there is obvious benefit to studying each of those in great detail in addition to any new ideas. This is most certainly out of the scope of this thesis, and therefore a representative scenario will be defined in which an air defense weapon intercepts a mortar threat. Additionally, top-down design was introduced as a method of flowing top-level requirements down to the system and subsystem level. There is more than one system interacting in this problem scenario, and each one can certainly be functionally decomposed into any number of desired degrees of freedom. For this to occur for each of the systems would create a daunting task, especially when the time comes to show how top-level requirements impact subsystem level variables. Therefore, only one of the systems will be decomposed to the subsystem level, as will be discussed later in this chapter.

There may be a concern regarding bounding the problem as such, while maintaining a true system-of-systems context. These restrictions are in fact done to enable a thorough study of a top-down/bottom-up flow of requirements and constraints within a hierarchical system-of-systems environment, from subsystems, to systems, to the operational (i.e. system-of-systems) level, as stated by the primary research objective of this thesis.

5.1.2 Morphological Matrix

Section 3.1.1 discussed methods for functionally decomposing a problem or system into the subsystems that enable it. In addition, the morphological matrix, or matrix of alternatives, was introduced as a method for functional decomposition by listing key parameters or functions of a system and the alternative methods for satisfying

them. The morphological matrix of alternatives for the problem of interest is shown in Table 9. Presented in the morphological matrix are all of the methods discussed in this thesis relevant to addressing the problem of interest, namely defending against the RAM threat. This exercise helps identify which degrees of freedom to keep open, and which ones are to be locked down. As will be discussed, many of the factors are locked down for subjective reasons, whereas others simply due to computation limitations. In some cases, more than just one option will be selected in order to maintain that particular degree of freedom.

This exercise suggests the extent of the magnitude of the problem, as the number of potential solutions is calculated by multiplying the number of solutions per row by each other. Some of the selections are not compatible with each other, however several of the rows have multiple options that could be selected simultaneously. The amount of perturbations even in this already constrained design space numbers in the hundreds of billions. Even if a modeling and simulation environment was in place to handle every one of the combinations, it would take many years of computational run time assuming even only one second required to complete a single case. Therefore, it is important to have clear justification of why certain decisions were made about design freedom, and that the proper functional decomposition took place. What follows is a description of each of option discovered in the literature search that could satisfy the functions required of a related air defense system, with justification of concept selection, and and overall functional decomposition of the entire process.

5.1.2.1 General Alternatives

The general problem is first decomposed into the defended range tiers. The EAPS problem definition discussed in Section 1.2.2 defines an inner tier broken down into a short (500 m - 2 km) and long (2 km - 10 km) ranges, and an outer tier for ranges beyond 10 km. The potential intercept solution types discussed included gun

Table 9: Morphological Matrix of System Alternatives

		1	2	3	4	5	6	7
General	**Engagement Range**	Short Range Inner Tier 500m - 2km	Long Range Inner Tier 2km - 10km	Outer Tier 10km +				
	Intercept Solution	Gun Fired Projectile	Rocket/Missile	Directed Energy/Laser				
Projectile	**Guidance**	None	Interital	Beam Rider	Command	Passive Homing	Semi-Active Homing	Active Homing
	Navigation Law	Pursuit	Lead Angle	Three Point	Proportional			
	Controller	Bang-Bang	PID					
	Bore	30mm	40mm	50mm	57mm	Custom		
	Warhead	Kinetic Kill	Blast/Fragmentation	Submunition Dispersal	Calculated Lethal Radius Based Need			
	Collateral Damge Reduction Consideration	None	Self-Destruct Projectile	Forced Tumble				
Gun	**Firing Muzzle Velocity**	Fixed	Adjustable					
	Firing Error	Muzzle Velocity	Air Density	Air Temperature	Range/Cross Wind	Projectile Weight	Elevation	Azimuth
	Gun Firing rate	Calculated for Optimum Performance	Fuction of Specific Selected Gun	Function of Bore (historical database)				
Radar	**Tracker Type**	Sequential Lobing	Conical Scan	Monopulse				
	Radar Error	Elevation	Azimuth	Range	Roll	Pitch	Yaw	
	Radar Error Type	Bias	Random Noise					
Threat	**Threat Types**	Artillery	60 mm Mortar	82 mm Mortar	107 mm Rocket	120 mm Rocket		
	# simultaneous threats	single	multiple					
	Threat Firing angle	head on (0^o)	low slant ($<45^o$)	high slant (45^o-90^o)				

fired projectiles, a self propelled rocket or missile, and a directed energy or laser weapon. The selection of defendable range as defined by the selected engagement range will drive the intercept solution type, as discussed in Section 1.2.2.1 there will be a range at which an unpowered gun fired kinetic kill projectile will not be able to deliver the required kinetic energy to destroy a notional target, driving the need for a self-propelled solution. Additionally, a directed energy solution was discussed, but the immaturity of technology associated with it hinders its use in the desired environment discussed Chapter 1. However, the simplest solution is desirable for many reasons (cost, technology limit, etc...), and therefore a gun fired projectile will only be examined for the SRIT requirement.

5.1.2.2 Projectile Alternatives

One of the major subjects discussed in the EAPS community regarding a gun fired projectile solution is issue of guidance. Namely, the question asked is how to quantify the benefit of having a guided versus an unguided projectile. If in fact guidance is preferred, there are several options discussed as relating to the field of missile design. The first was the use of inertial guidance that relies on gyroscopes and accelerometers to direct the missile over a predetermined path provided to the missile prior to launch. The next option listed is beam rider guidance, where a rearward facing antenna on the projectile senses an electromagnetic tracking beam and uses the position of the missile with respect to the center of the target tracking beam to compute steering signals used to move control surfaces. Command guidance is where a projectile gets its guidance instructions from a tracking system outside the projectile to track itself and the target along their trajectories, aiding the projectile to steer itself to intercept the target. Passive homing uses sensors onboard the projectile that can only use electromagnetic emissions or natural reflections from the target to establish location. The next option is semiactive guidance, whereby a source other than the projectile (i.e.

the ground radar) illuminates the designated target, and a sensor on the projectile sensitive to the energy reflected off of the target guides the projectile. Finally, the active guidance option involves having the target illumination transmitter and target echo receiver co-located on the projectile itself, however this option has historically been restricted to larger weapons that have space to carry those components. Since command guidance only requires a receiver on board to receive commands from a ground radar, it is the simplest solution and allows for a less complex projectile.

Four types of navigation laws were discussed. The pursuit trajectory causes the missile to always fly directly pointing at the target at all times by maintaining the line-of-sight (LOS) along the heading of the missile. The lead angle navigation routine causes the missile to keep a constant bearing with the target with the intention that the missile flies a straight collision course with the target. Three-point navigation is a routine where the missile is constantly steered along the LOS between an offboard target tracker and target. Finally, a proportional navigation law uses a guidance package that tries to maintain a constant LOS angle between projectile and target by making the rate of change of the heading direction proportional to the rate of change of the LOS.

Assuming that a guided projectile is used, the next option to select from is the controller type, and two were discussed as potential options. The first discussed was a bang-bang controller, where the application of control is either full on or off, with no ability for fine adjustments . The other method discussed was the Proportional Integral Derivative (PID) controller, where amount of feedback control applied is proportional to the error in the desired trajectory. Practically, this means that using PID control, the amount of control surface deployed would be a function of desired aerodynamic force required, whereas a bang-bang controller would only have the option of fully deploying the control surfaces. Clearly the PID option is far more complex component wise, but would provide the best course correction for a guided

projectile.

The issue of projectile bore stems from the desire to use a projectile that can be fired from an existing gun. This would limit the projectile to specific discrete bore sizes, which has several disadvantages. The first is that in most likely cases, any one of the existing bore sizes would be either larger or smaller than an ideal calculated bore size (i.e. if a designer could optimize around bore size), which could be a function of internal volumetric packing of guidance components, warhead, etc... and required external aerodynamic forces to steer the guided projectile. However, limiting the projectile bore to one compatible with an existing gun greatly simplifies determining optimal bore size in the simulation process, and is based on the actual practicality that it would be a very expensive venture to design a new gun based on a non-standard projectile bore size. Therefore, the projectile caliber, although a variable, will be discrete to one of the following four existing and standard guns bores:

1. 30 mm
2. 40 mm
3. 50 mm
4. 57 mm

The issue of internal packing leads to the next option for the projectile listed in the morphological matrix. The projectile may or may not carry a warhead. If, for example, a guided round could be designed to directly intercept a target *with a high enough confidence*, and assuming that enough kinetic energy is delivered to detonate the target's warhead or render it incapacitated, a kinetic kill is sufficient and a warhead is not needed. Now the issue of confidence in a direct hit comes into play, and begs the question of how many projectiles would have to be fired at the target to achieve a confidence of *at least* one direct hit. If a warhead is desired, two

options discussed were the blast/fragmentation warhead and a warhead that simply disperses submunition ahead of the target flight path. Of course, the desire for a small inexpensive projectile seriously constrains the ability to use a warhead. The last option listed for the warhead leaves the need for a warhead open, based on a lethal radius required around a projectile to destroy the target based on a calculated miss distance confidence.

Finally is the issue of collateral damage, which is directly stated as an important issue for consideration this problem. One option is designing a self-destruct projectile that is fuzed destroys itself after a certain amount of time after fire, such as the Phalanx based C-RAM discussed in Chapter 1. Another option is deploying an external surface after forcing the projectile into a tumble, decreasing the velocity at which the projectile hits the ground, as well as limiting the range otherwise taken by an unaltered ballistic flight path. However, if the projectile already had a warhead this would not be an issue, as the warhead could be fuzed to detonate after a given time after launch if there was no target intercept. Of course, an ideal kinetic kill projectile would be designed to directly impact the target every time and not need to consider this issue, assuming that both interceptor and target are completely destroyed in the process.

5.1.2.3 Gun Alternatives

Decomposing the functions of the gun firing the projectile is a matter of selecting the desired degrees of freedom. As mentioned earlier, it was difficult to find literature on medium caliber gun design in open literature. However, in a computer simulation, the gun firing the projectile can in many cases be defined simply by the firing position (in azimuth and quadrant elevation) and the velocity at which the projectile leaves the muzzle. The first option in the morphological matrix for the gun is whether to keep open the degree of freedom to select muzzle velocity, or to simply fix it at some

value. The simple option is to assume that a specific gun design firing a specific unpropelled projectile has a single muzzle velocity associated with it, therefore the firing position would be a function of determining the azimuth and elevation required to cause the ballistic flight paths to intersect. For a head on intercept, the problem further simplifies to only adjusting the firing elevation. However, this limits the ability to determine the "optimal" firing muzzle velocity, i.e. a major design variable for the gun.

Another major function of the gun design would be the pointing error accuracy. When information is known about the projectile flight characteristics, desired trajectory, and muzzle exit velocity, a fire control solution can prescribe the gun pointing characteristics (i.e. elevation and azimuth). However, the gun may not be pointing in the exact direction at the time of fire, which result in error surrounding the elevation and azimuth from the intended firing direction. In addition, the velocity at which the projectile leaves the gun muzzle may not be exactly what was intended. These gun firing errors may play a very important role surrounding the trajectory of a non-propelled projectile, and certainly for an unguided projectile following a ballistic trajectory.

Actual guns would have specific error distributions associated with those properties, usually given as normal distributions with the standard deviation given around the desired property. Differing guns would have poorer or better accuracy, depending on that reported standard deviation. Several sources of error for the gun were introduced, and is the second element listed for the gun in the morphological matrix. These can be broken down in to three major groups: firing condition (muzzle velocity, elevation, azimuth), atmospheric condition (wind, air temperature and density), and projectile manufacturing tolerance (the difference in weight from one projectile to the next). Because the projectile/target interception is not meant to happen at very high altitude and at relatively large ranges, the effects of perturbations in density

and temperature will not have a great effect on pointing error and can be eliminated. Sensitivity to randomness in wind is certainly an important aspect in gun design, however to limit the scope it will not be a factor for this study. The errors based on firing conditions are the important factors that define the properties and capabilities of a particular gun system, and can not be eliminated.

Finally, after the capability of one projectile is established, it is possible to statistically determine the capability of multiple projectile fired simultaneously can be determined (Section 2.3.3). This means that for a given engagement time window, the amount of projectiles fired (from a single gun) is an important factor, therefore rate of fire is listed as the third option of the gun in the morphological matrix. The first option is to calculate based on given condition to number of bullets fired, since too few would not result in an acceptable probability of hit, but firing too many would simply waste resources. If a specific gun system is selected, the rate of fire would be fixed for that gun. Finally, a historical database of gun bores can be used to establish a simple relation between bore size and rate of fire.

5.1.2.4 Radar Alternatives

The radar plays an important role in the systems hierarchy in that it relays target information to determine a firing solution (i.e. how to point the gun), and would also be used to track the projectile so that course correction guidance updates could be sent. Three types of radar tracking methods were introduced, including sequential lobing, conical scan, and monopulse. Sequential lobing is a method in which the antenna beam is alternately switched between two positions to obtain the angular error in one coordinate. Instead of discontinuously stepping the beam between four discrete positions, the conical scan method continuously rotates the antenna. To determine angular measurement, both of these methods require receiving multiple pulses, or the received echo, as the antenna translates. The monopulse method requires only

receiving one pulse to make these measurements, however this requires the use of at least two antennas in each dimension measured. This thesis also reviewed some of the methods developed to approximate the error in the received signal using the phase difference in the two signals (per dimension), as is done with an interferometer radar.

A measure of radar capability is in its level of accuracy when taking measurements of an object. All radars have errors associated with the measurements they take of an object. These errors include measurement of information about the target in relation to the radar which identify the key attributes of an object in three dimensional space including elevation, azimuth, and range relative to the radar. The radar can also measure orientation properties including the moments about the axes of the object, including yaw, pitch, and roll orientations. Figures 39 and 40 graphically depict the orientations described here. The errors may be a fixed bias that is the same for every measurement, a random noise that is different for each measurement defined by a distribution, or a combination of the two. As discussed regarding the gun firing errors, a radar may have measured error distributions associated with measurements it takes in any of the dimensions. These errors are commonly normally distributed, with a reported standard deviation about a mean. Radar measurement accuracy can also be rated subjectively as "poor" or "advanced", and a given radar system would fall somewhere in that subjective scale depending on the standard deviations that define its error distributions. However, for this study it is of great interest to leave these values open for design space definition later on.

5.1.2.5 Threat Alternatives

The first chapter defining the motivation for this thesis discussed the need for an air defense system capable of defeating the threat due to rockets, artillery, and mortars, or more commonly referred to as the RAM threat. Ideally, one would design a single weapon that is optimized between the tradeoffs concerning the different target types.

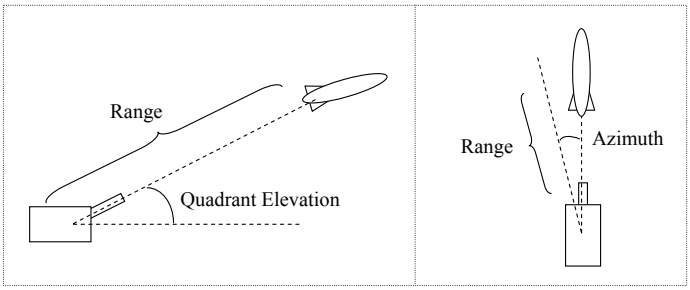

Figure 39: Side (L) & Top (R) Views of Gun and Radar Orientations

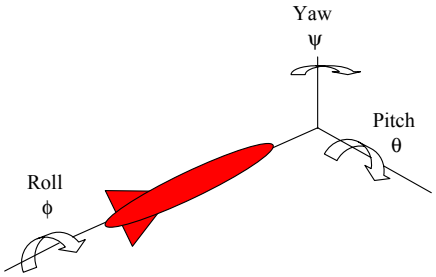

Figure 40: Moments About Projectile Axes

For example, a different firing solution would be obtained for rocket target flying a shallow trajectory than a mortar that is commonly fired at very high trajectories. In the morphological matrix, specific RAM threats are listed. All gun fired projectiles are listed as artillery, and two common mortar sizes are given. Additionally, two common rocket sizes are given as well.

In addition to selecting the target type, for the purposes of assembling a decision making hierarchy the number of simultaneous threats to be encountered must be determined. This is simply listed as either "single" or "multiple". Finally, the potential threat firing angle can be defined. As mentioned in this section, the problem can be greatly simplified if a head on intercept is assumed, however a slant angle between the trajectories of the interceptor and target can be identified. The greater the slant angle, however, the more difficult it would be to ensure interception.

5.1.3 Hierarchical Decomposition of Proposed Solution

5.1.3.1 Identification of Key Metrics

The previous section provided alternatives based on functional decomposition of each independent system. In order to focus the scope of the problem definition, this section will hierarchically decompose the problem by function using the systems discussed in the previous sections. This first requires that certain quantifiable top level requirements be established beyond the qualitative desire to intercept a target with an inexpensive solution. As a result, several high level metrics are now defined to address the problem. The first metric defined will be the minimum miss distance between the interceptor projectile and the target. Since there will be uncertainties to account for in quantifying this metric, there will have to be confidences associated with reporting specific values of intercept miss distance. This one metric allows for direct determination of two key metrics. For one, a lethality radius requirement can be extracted from the miss distance quantification. Nevertheless, since kinetic kill is the ideal option and less complicated than using a warhead to destroy the target, the probability of direct hit must also be quantified. As might be expected, the most intuitive solution to decrease the intercept miss distance and ultimately increase the probability of hit would be to increase the radar and gun accuracies. In lieu of some form of cost metric, the simple answer would be to just design a projectile around the best radar accuracy available. Therefore a form of a cost metric that penalizes for increased radar accuracy must be accounted for.

The system-of-systems hierarchy decomposition used in this thesis is given in Figure 41. At the very top, the capabilities of interest are identified at the operational level, including probability of direct hit, warhead lethality radius, and a measure of weapon system cost as relating to the radar. Probability of direct hit and warhead lethality radius are directly related to miss distance quantification, which is a function of specific properties of the radar, gun, interceptor projectile, and target as well as a

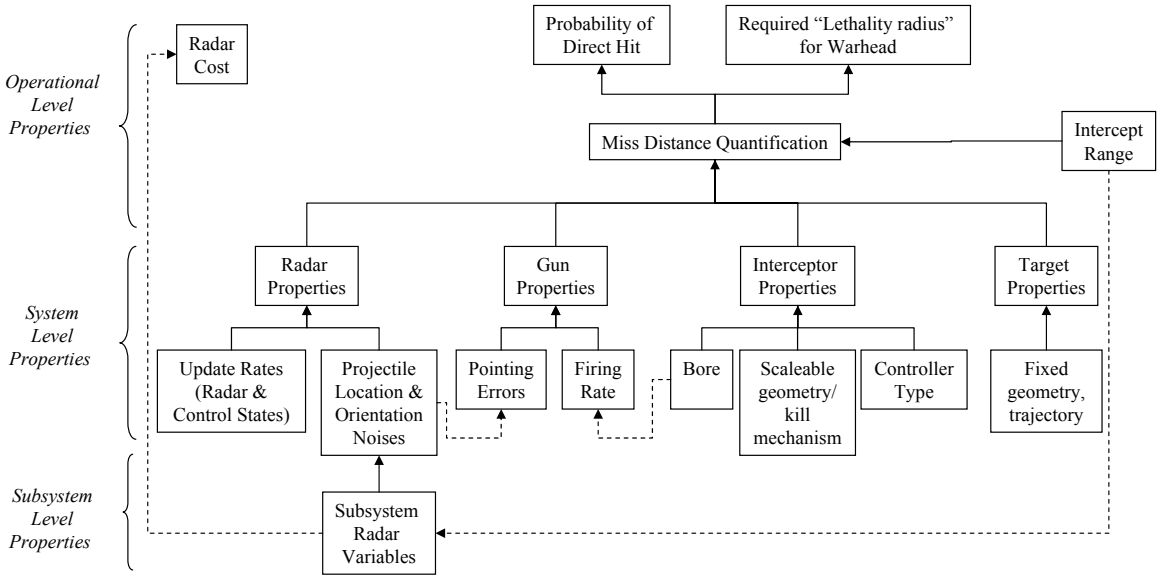

Figure 41: Hierarchical Decomposition of Proposed Solution

specified intercept range. Each of the the systems operating at the system level can further be decomposed to their own properties. When each of the components work together in an assembled environment providing the desired outputs as a function of the desired inputs, the environment is considered functionally composed. The individual components of the simulation will be discussed in this section. Many of the assumptions taken to focus the scope of the problem were taken with the advice and consultation of the thesis committee members in their respective fields of expertise.

5.1.3.2 Radar Decomposition

The radar properties will be decomposed to two separate property types. The first includes the noises describing the errors in measuring the different projectile location and orientation properties. The error in the radar measurements of the target's location directly impacts the position that the gun barrel points to fire the interceptor (this is in addition to the inherent pointing error due to mechanical errors in the gun, discussed in the very next section). The second set of major radar properties are the update rates at which the radar measurements on the position of the projectile and

target, and the rate at which the projectile controller state is updated. The radar accuracy capabilities can be further decomposed to the subsystem level variables that define the radar capability. Those subsystem level variable directly affect the cost of the radar.

5.1.3.3 Gun Decomposition

As shown in Figure 41, the gun was not functionally decomposed below the system capability level, and therefore there are no subsystem variables identified for the gun. As can be deduced from literature search relating to the modeling and simulation of combat systems presented in Chapter 2, there is not much open literature on the design of medium caliber guns. Therefore, this study will not decompose the gun firing system below the gun firing errors, including noises around firing elevation, azimuth, and muzzle velocity. As discussed in the preceding radar decomposition section, there are gun pointing errors inherent to the mechanical properties of the gun itself, and the error due to the noises in the radar measurement of target location.

5.1.3.4 Interceptor Decomposition

The primary interceptor used in this thesis will be the GTRI guided projectile discussed in Section 1.2.4.3[1]. The physical geometrical properties of the projectile will not be modified, as it is presumed from the studies discussed on this projectile that its design is sufficient optimized to be used properly. Recall that the focus of this thesis is not component design, but the formulation and application of a methodology. Additionally, the papers discussing the guidance and control mechanisms, i.e. the actuator controlled pins, show that this guidance concept is validated in both computer simulation and real live gun firings. However, the bore of the of the interceptor will be a considered a variable, and be scaled accordingly in the 6-DoF simulations.

[1]The last portion of this thesis introducing the completed assembled environment will compare the GTRI kinetic-kill/pin-controlled round to a round specifically designed to carry a small warhead, as well as an unguided round, however this will not be addressed until Section 6.7.

Figure 42: 82mm Mortar Geometry Used in 6-DoF Simulations [101]

For this study, it is assumed that there are only nominal variations in inertial and aerodynamic characteristics due to different bore sizes [101]. Therefore, any non-dimensional inertial and aerodynamics information for the baseline interceptor will be used for any bore size projectile (i.e. drag coefficient variation with Mach). As discussed for the morphological matrix of alternatives, the type of controller used is a primary attribute of the interceptor.

5.1.3.5 Target Decomposition

Examining multiple targets is considered outside the scope for this thesis. Therefore, a single representative target of interest was selected. This arguably falls short of proving an all inclusive defense against the stated RAM threat, but it should allow for one to make educated conclusions of the value of the proposed methodology application. An 82 mm mortar was selected as this representative target, as presented in Figure 42.

5.1.4 Review of Morphological Matrix Selections

The morphological matrix was introduced in the beginning of this section in an attempt to decompose the problem and potential solutions into the properties that enable them. What followed was the justification to narrow the design space based

on problem definition, initial studies into notional concepts and solutions discussed in the literature search, or the need to limit the problem within the scope of this thesis. Table 10 revisits the morphological matrix presented in Table 9, but with specific selections based on those justifications discussed all throughout this section. The engagement range was bounded to the Short Range Inner Tier as described by the EAPS program, and therefore will only focus on intercepting targets between 500 m and 2 km. The intercept solution studied will be a gun fired projectile.

The projectile itself will be command guided, meaning that after launch it can receive course correction updates and follow a proportional navigation law, the most commonly used navigation law. At this point, there will be no restriction as the use of a PID or bang-bang controller. However, for the sake of the simulation, an initial study will be conducted in which the projectile will use an onboard PID controller, so that the controller can react according to the magnitude of required control surface force application. A more detailed study will follow in which a bang-bang controller will be used to more accurately represent the actual projectile. The projectile bore will be studied at discrete values based on currently available guns, and not "optimized" for any measure of merit. Therefore, the four gun bore sizes discussed are selected. The decision to employ a warhead will be left as part of the design study requirements. Consequently, a kinetic kill projectile will be studied, with the quantification of intercept miss distance setting the requirement for a lethal radius required of a warhead, if one were to be used. There will be no safety precautions regarding collateral damage onboard the projectile itself.

Each 6-DoF trial in the initial study will examine a fixed gun firing muzzle velocity, as opposed to having the ability to tune the firing velocity based on intercept range. This however does not eliminate the ability to study error around that fixed muzzle velocity. For the more detailed study, the muzzle velocity will be variable, however only to discrete muzzle velocities. Additionally, errors on firing azimuth and elevation

will be considered. For reasons discussed in Section 5.1.2, errors on the remaining factors are not key drivers and will not be examined. The magnitudes of those gun firing errors will be considered as variable, rather than pick notional gun accuracies (i.e. a gun with "poor" accuracy). There is no clear method of determining the firing rate of a gun based on simple design properties, therefore regressions based on a historical database will be used. This is needed in order to calculate the effect of firing multiple rounds at a single target. A rate of fire regression based on historical database, simply as a function of bore size, is given in Appendix C.

An interferometer radar using the monopulse tracking method will be used, and as such any methods, equations, or simulations will include that decision when discussing attributes at the subsystem level. As with the gun, the radar accuracies will be considered variable, bounded between notional "poor" and "advanced" radar accuracy capabilities. All projectile location errors (elevation, azimuth, range) will be examined. For a gun fired projectile that exits the muzzle spinning about its primary axis, the controller must have accurate knowledge as to the roll orientation in order to accurately apply the control surfaces for steering. Any errors associated with the radar's ability to measure roll rate will have an effect on the ability to steer the projectile to a desired impact point, and will be studied. The projectile can be assumed to be flying at negligible angle of attack and sideslip, therefore pitch and yaw will not be studied in this thesis. Only radar noise will be considered as a form of radar error, and bias will not be considered for reasons already discussed.

Finally, the only threat type studied will be an 82 mm mortar, considered a sufficient representative of the RAM threat. The 6-DoF simulation will only consider one simultaneous threat fired head on to the gun firing the guided interceptor.

Table 10: Morphological Matrix of System Alternatives with Selections

		1	2	3	4	5	6	7
General	**Engagement Range**	Short Range Inner Tier 500m - 2km	Long Range Inner Tier 2km - 10km	Outer Tier 10km +				
	Intercept Solution	Gun Fired Projectile	Rocket/Missile	Directed Energy/Laser				
Projectile	**Guidance**	None	Interital	Beam Rider	Command	Passive Homing	Semi-Active Homing	Active Homing
	Navigation Law	Pursuit	Lead Angle	Three Point	Proportional			
	Controller	Bang-Bang	PID					
	Bore	30mm	40mm	50mm	57mm	Custom		
	Warhead	Kinetic Kill	Blast/Fragmentation	Submunition Dispersal	Calculated Lethal Radius Based Need			
	Collateral Damge Reduction Consideration	None	Self-Destruct Projectile	Forced Tumble				
Gun	**Firing Muzzle Velocity**	Fixed	Adjustable					
	Firing Error	Muzzle Velocity	Air Density	Air Temperature	Range/Cross Wind	Projectile Weight	Elevation	Azimuth
	Gun Firing rate	Calculated for Optimum Performance	Fuction of Specific Selected Gun	Function of Bore (historical database)				
Radar	**Tracker Type**	Sequential Lobing	Conical Scan	Monopulse				
	Radar Error	Elevation	Azimuth	Range	Roll	Pitch	Yaw	
	Radar Error Type	Bias	Random Noise					
Threat	**Threat Types**	Artillery	60 mm Mortar	82 mm Mortar	107 mm Rocket	120 mm Rocket		
	# simultaneous threats	single	multiple					
	Threat Firing angle	head on (0^o)	low slant ($<45^o$)	high slant (45^o-90^o)				

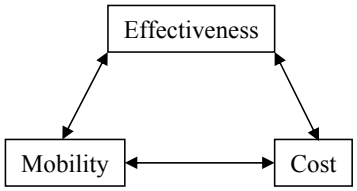

Figure 43: Measures of Merit for Gun System Optimization

5.2 Research Focus

The research in this study will focus on the application of a system-of-systems top-down Monte Carlo based approach to the design of an air defense weapon employing guided munitions with the goal of defeating the RAM threat. Basic requirements assembled from the literature searches for this type of weapon are that it must be lethal enough to destroy the incoming threat, mobile enough to be moved to new locations as threats arise, all while providing an affordable solution[2]. These are certainly vague, but show the conflicts and complexity of the issue, and make for an excellent example to use the methods developed in this thesis. One of the main goals is to optimize between three main system metrics as shown in Figure 43: effectiveness, mobility, and cost. Note that each of these three has some dependency on each of the others, and one can not be improved without some degradation to another metric. For example, to increase effectiveness, a larger radar may be used to improve the accuracy in finding and tracking a target. However, this would result in a less mobile weapon system and certainly would increase cost. On the other hand, a very mobile weapon system may end up being too small to be effective against a target, and the necessity to build very small electronics would increase cost.

The different disciplines may be arranged in a design-structured-matrix (or N^2 matrix), as shown in Figure 44, to show the feed-forward and feed-back coupling of each discipline. In this case, the system is fully coupled. In a traditional design

[2]As summarized by Holder [24].

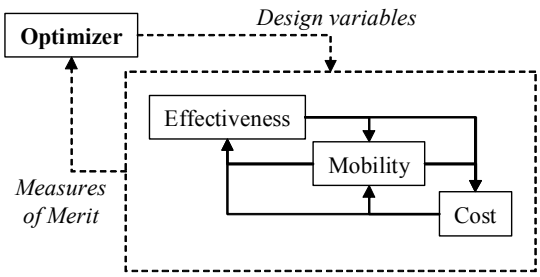

Figure 44: Traditional Application of Optimizer on a Design-Structured-Matrix

optimization problem, an optimizer may be used to determine the values for the design variables that maximize given measures of merit (i.e. effectiveness and mobility, while minimizing cost). The optimizer may even be used to break the feed-back loops for faster convergence. However, most gradient-based optimizers can only be used on a completely smooth, continuous, and unimodal design space. To overcome a complex multimodal design space, the gradient-based optimizer must be coupled with stochastic techniques, such as Genetic Algorithms or random searches, which consume a great deal of computing power, even for simple multimodal problems. Additionally, the traditional approach shown in Figure 44 is best applicable when optimizing on the weapon system itself (or any single "system"). The addition of several interacting systems and the subsystems that compose them, would create a highly combinatorial and complex problem, in which only local optimal solutions would likely be found.

The generic process created as part of this research is given in Figure 45. The first step is to collect which ever modeling and simulation tools are necessary to assemble the hierarchical environment. For those tools not capable of rapid manipulation, surrogate models will be created. To model a highly nonlinear or discontinuous desired design space neural network surrogate models will have to be used, otherwise, polynomial surrogate models may suffice. The next step is to assemble the models of the various interacting systems and subsystems, such that the necessary outputs of subsystems are fed as inputs to the appropriate system level tools. A Monte Carlo

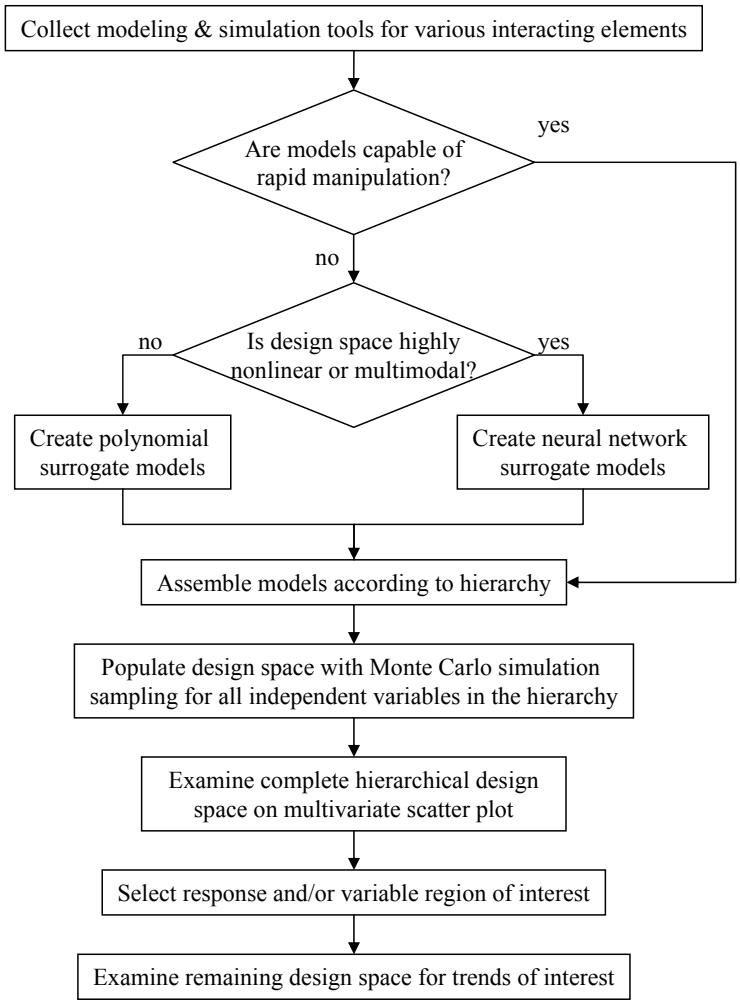

Figure 45: Flow Chart of Research Process

simulation will then be used to sample from bounded uniform distributions on the inputs to the various models. The complete hierarchical design space can then be viewed collectively on an interactive multivariate scatter plot. Here a user may examine any trends of interest. For example, the plot between random variables should be filled uniformly, by virtue of the Monte Carlo sampling. Now, a user may interactively select or highlight design space regions of interest between any combination of responses and variables, and examine the remaining design space for trends that appear.

This study proposes to use this hierarchical system-of-systems decision-making

architecture to examine weapon design requirements based not only on the measures of effectiveness described above, but also taking into account the entire interacting environment. A Monte Carlo simulation will be used to quantify uncertainty in both design tolerances and uncertainties in the scenario as well as be used to explore the design space. A properly conducted design space exploration will eliminate the need for running a gradient-based/stochastic combined optimizer that only produces a point design. Constraints may be placed only after the architecture is fully linked together, rather than during the optimization process.

For a system-of-systems environment comprised of a Monte Carlo based design space exploration employing rapid surrogate models, both bottom-up and top-down design analysis may be executed simultaneously. The general top-down/bottom-up flow of information is shown in Figure 46. *This process enables any response to be treated as an independent variable*, meaning that information can flow in either direction in the hierarchy. From the bottom-up, the subsystem level properties of a particular weapon system component define that component's capability independent of the other components (note: as was discussed earlier, only the radar properties are taken down to the subsystem level). At the next level, each of the weapon system components' capabilities are defined, which collectively yield the weapon system performance. Next, the engagement scenario is defined, in which a weapon of given performance is fired to intercept a target. Other attributes of the scenario independent of the target and weapon are defined in this level, and for this study the intercept range is a major factor. Each of these factors in the scenario definition affect the operational level factors. These operational factors are what the decision maker primarily cares about, including the ability to quantify the ability to hit (and/or destroy) the target, and at what cost. This bottom-approach amounts to nothing more than a traditional approach of linking together several computer codes in a hierarchical fashion, i.e. the outputs of one code feed directly as inputs at the next level in a hierarchy.

From the top-down, the operational requirements will limit the feasible scenarios and drive weapon performance. For example, the limit of intercept range can be identified for a given weapon system capability. Additionally, the weapon performance that meets those operational level requirements can be identified. However, now different combinations of intercept range and weapon capability against a given target may meet the operational requirements. Moving on one level lower, the particular weapon system capability drives the design space of each of the individual weapon system components. However, for a given desired weapon capability, there may be many perturbations of the gun, projectile, and radar capabilities that meet that need. And finally, further decomposing the radar to its composing subsystems will identify the feasible options that provide the required radar capability. Therefore at each level of the hierarchy in the top-down process, a capability is identified, and the feasible options at the adjacent lower level may be filtered out that enable that next higher level capability.

Comparing the bottom-up and top-down approaches in Figure 47 shows that for bottom-up design, selections are made at the lowest level, which then define the capability at each higher level. This results in one design point flowing up through the hierarchy. In the traditional design approaches, this is where an optimizer would use logic to search the design space at each level for options that do not violate any constraints and minimize (or maximize, depending on the problem) the desired response. However, the top-down approach that uses a Monte Carlo based design space exploration linked together with rapid surrogate models will likely define more than one combination of design variables that meet favorable constraints at higher levels. Therefore, an efficient way to identify those feasible combinations is needed. When appropriately populated, the design space can be defined between each of these variables and responses using multivariate scatter plots, i.e. one plot for each variable/variable, variable/response, or response/response combination. The idea is

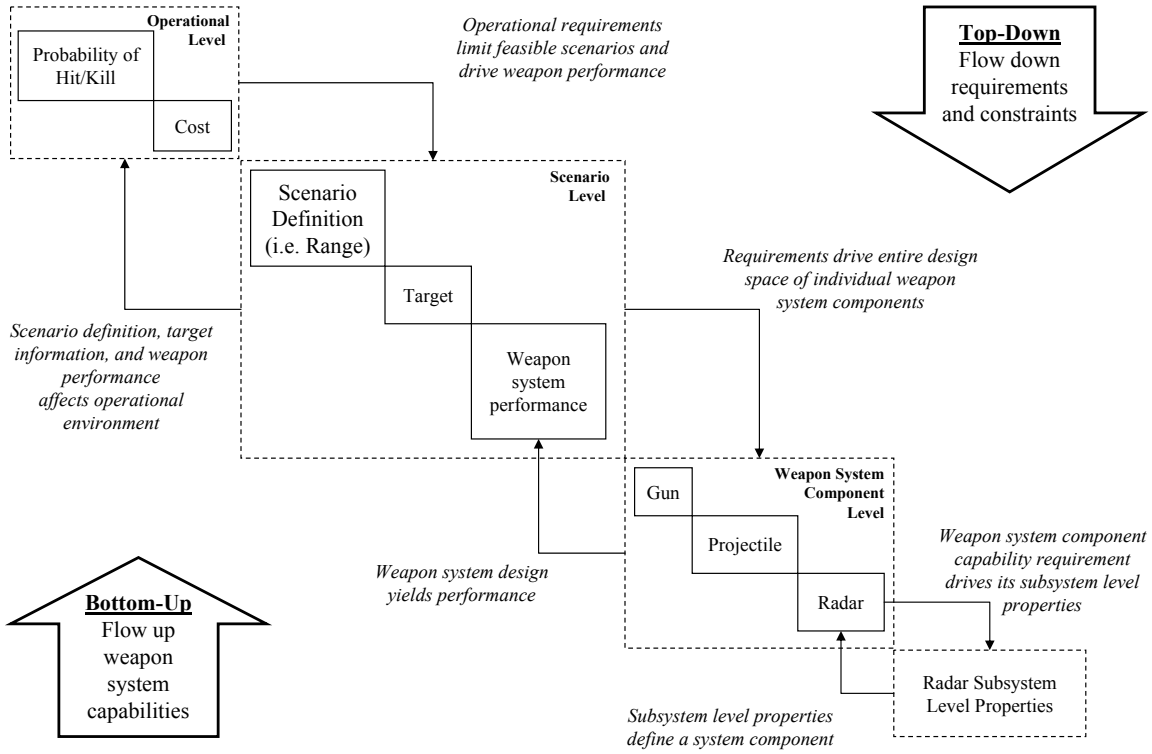

Figure 46: Top-down Requirements Flow and Bottom-Up Weapon Capabilities Flow

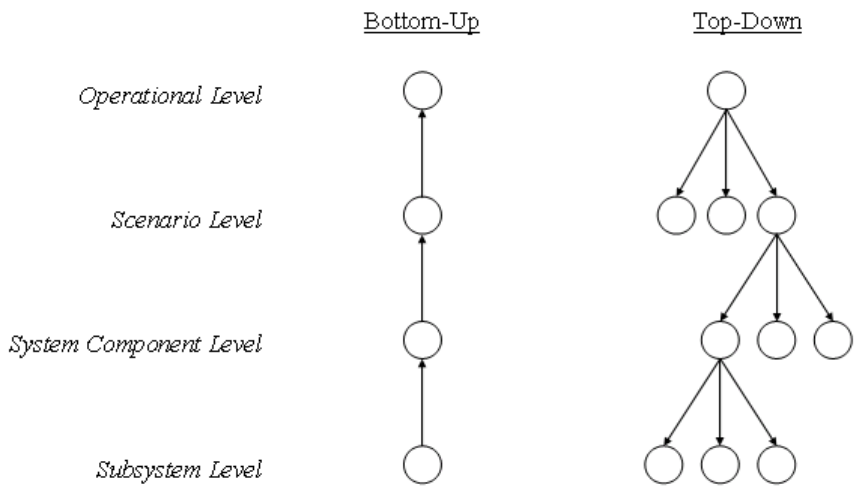

Figure 47: Bottom-up Single Design Point vs. Top-Down Multiple Design Point Hierarchical Flow

to be able to literally carve out the feasible design space as was shown in Figure 38 of Section 3.4.2.

Ultimately, the goal is to optimize a system that strikes the most favorable balance between the metrics identified in Figure 43 by defining the weapon system design requirements to reach those metrics. Lower level design variables drive system effectiveness, but top level requirements may require performance beyond what is available. Therefore the elements in Figure 43 cannot simply be treated as "black boxes" with an optimizer wrapped around them. The elements must be treated as functions that will be decomposed to whatever systems and/or subsystems that enable them, as given previously in Figure 41. An ANOVA approach may be used to determine which variables have the greatest effect on total system-of-systems variability, and this method may be compared to using the multivariate scatter plot technique to identify critical design space tradeoffs. A certain application of this would be the most effective way to apply technologies to narrow the gap between what is currently available and what is ideally required.

5.3 Modeling and Simulation Approach

5.3.1 Modeling and Simulation Requirements

The problem outlined in this chapter drives the need to assemble a specific modeling and simulation environment. The desire to model a projectile intercepting a target in midair drives the need to use a six degree-of-freedom (DoF) trajectory analysis tool. This tool had the requirement to be able to simulate the trajectory of a guided projectile receiving updates from a ground based radar and the trajectory of an unguided threat projectile. Because it was decided that the radar system will be defined down to the subsystem level, there was a need to have the ability to evaluate how radar properties affect radar accuracy. When dealing with capturing the effects of gun and radar accuracy on interception capability, many executions of the 6-DoF are required to adequately populate the design space. As such, the need to employ surrogate models has been well established for this problem, particularly neural network based representative models able to capture multimodal or discrete effects. Therefore a tool is required to create those neural network equations rapidly and efficiently. This section will discuss the various computer based tools required for this thesis study.

5.3.2 6-DoF Modeling

5.3.2.1 PRODAS

PRODAS (PROjectile Design and Analysis System) [29] is a six degree-of-freedom (DoF) trajectory analysis tool, used to calculate the trajectories of gun fired projectiles. PRODAS is a software package that allows a user to create a three-dimensional projectile model, calculate mass properties, estimate a full set of aerodynamics coefficients and stability properties, and simulate test firings, including launch dynamics muzzle velocity calculations, and the ability to fly 4-DoF, 6-DoF, and body fixed trajectories. The software allows for calculation of penetration of kinetic energy projectiles and shaped charged warheads, and allows for control system simulation of

guided projectiles [6]. Although PRODAS has the capability to estimate the ballistic coefficients of the round, the calculated trajectories are more accurate when experimental aerodynamic coefficients are used, as reported by Silton and Massey [132], and Silton [131].

There is very little literature available discussing the detailed capabilities of PRODAS, short of acquiring and using the tool itself. However, Whyte [142] [143] provides an excellent introduction to PRODAS's capabilities.

5.3.2.2 GTRI 6-DoF Multibody Simulation

GTRI has conducted several years worth of research on the effects of pin based actuators generating enough force to steer small supersonic projectiles [99] [131] [132]. In most of these studies, the projectile was modeled using PRODAS to carry out 6-DoF simulations to test the stability and simulate pin forces on the projectile. As researched progressed, it became necessary to implement software that seamlessly embedded the pin force model into the simulations. In addition, PRODAS currently does not support two simultaneous trajectory simulations of two separate bodies, an important aspect of the interceptor/target problem. For this reason, a fully functional custom 6-DoF program was written at GTRI, which includes the pin force model, and has the ability to track an interceptor projectile and target with a radar [101]. This software has been validated using results from actual range tests.

The 6-DoF multi-body simulation code is outlined in the flow chart presented in Figure 48. The first step involves an initialization step, including loading the physical characteristics of the target and interceptor, loading sensor characteristics, and initializing the object states and sensor biases. The next step involves computations regarding the sensors. First, the radar noises are calculated for azimuth, quadrant elevation, and range, by sampling from a normal distributions defining those errors. Because this simulation involves the use of a guided projectile, the orientation of the

projectile must be known in order to accurately direct the projectile control surfaces. Therefore, the sensor noise associated with projectile roll is then computed. Next, the target position with respect to the radar noise is calculated. A filter is then applied to "smooth" the radar error with the number of samples taken. The same process for position calculation with filtered noise is repeated for the interceptor, in addition to the computing the interceptor roll attitude with respect to noise.

Next the guidance routine uses proportional navigation guidance (PNG) laws to calculate inertial acceleration commands, which feeds directly to the controller routine. The interceptor roll command is calculated from inertial acceleration commands. A low pass filter is applied to the roll command and roll attitude. The roll attitude error signal is calculated, and the error rate and integral are calculated. The roll control moment is calculated from a PID controller. This is used to calculate the roll pin (projectile control surface associated with roll control) height from the control moment. The pin vertical acceleration command is then calculated, along with a vertical acceleration error, and followed by a vertical acceleration error rate and integral. Next the pitch pin (projectile control surface associated with pitch control) height is calculated from an open loop acceleration command and PID. A rate limit is then applied to the roll and pitch pin movements. Finally, the pins are deployed, taking into account a "wake up" time from when the deployment command is given. The pin heights are then converted to forces and moments physically applied to the interceptor.

In the 6-DoF routine, the aerodynamic and gravity forces and moments are calculated for both the interceptor and target. A Runge-Kutta time integration is used to determine the trajectory of both bodies. The simulation is performed for a predetermined amount of time, after which the minimum relative distance between the interceptor and target is calculated. In addition, an actual interception hit is determined, with the two bodies assumed to be cylinders. The entire process after the

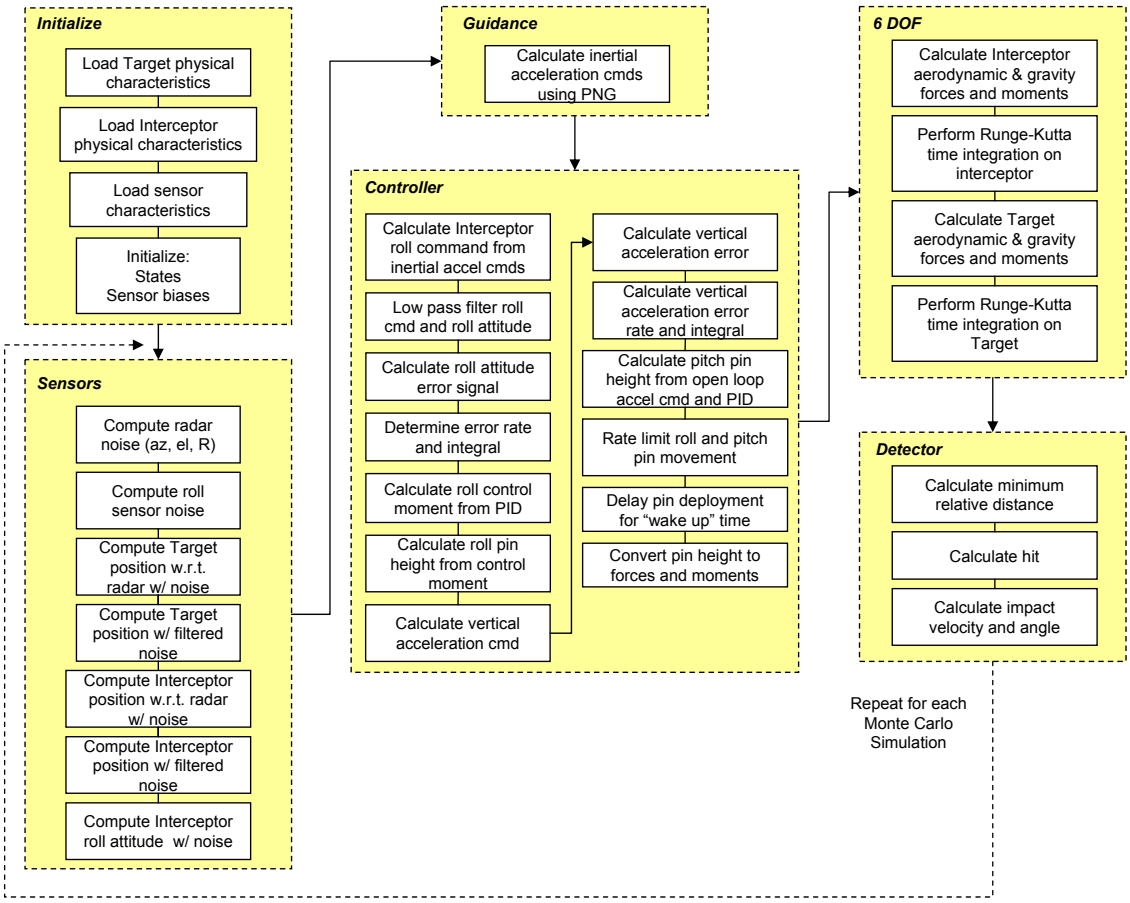

Figure 48: GTRI 6-DoF Multi-Body Simulation (adapted from [102])

initialization step is repeated for the number of Monte Carlo simulations desired to sample from the noises associated with the sensors routine.

5.3.3 Radar Subsystem Model

5.3.3.1 Radar Measurement Error

At the very bottom level in the hierarchy, the subsystem radar variables that result in a given capability can be identified, using radar properties discussed in Section 2.7 and given in Equation 14. The projectile location noise can then be calculated using Equation 18.

5.3.3.2 Radar Cost

An attempt was made to take some measure of system cost into consideration, however an accurate method for cost estimation was not found. It ultimately would be beneficial to take total system (or system-of-systems) cost into account, i.e. breaking down the cost of the guided projectile, the gun, the radar, as well as life cycle costs. This life cycle cost would depend heavily on actual campaign usage, however a complete campaign model is beyond the scope of this work. Therefore, a good candidate for cost tracking in this study was the radar, since as described earlier (and will be proved in the next chapter), radar accuracy is considered a driving factor in determining the accuracy of a guided projectile.

Based on talks with Holder [24], an accepted radar cost estimation is given in Equation 25, and is based solely on the number of antenna array elements on the antenna. This very basic relation shows that radar cost is just four times the number of elements, times the cost of the individual element. From [24], a reasonable estimation for the cost of an individual element is $1000.

$$RadarCost = 4 \cdot N_{elements} \cdot (\text{cost per element}) \tag{25}$$

The total amount of elements in one radar antenna array can be simply calculated as the square of the number of elements along one side of a square shaped antenna array,

$$\text{Number of Elements} = (\#\ \text{Elements on 1 side of an antenna array})^2$$

The number of elements on one side of the array is just the length of one side of the antenna array divided by the space between the elements in the array, plus one, therefore

$$\text{Number of Elements} = \left(\frac{\text{length of 1 side of antenna array}}{\text{space between elements}} + 1\right)^2$$

The length of one side of the antenna array is simply the square root of the calculated antenna area, and the space between elements can be approximated one half the wave length (as discussed in Section 2.7), yielding

$$\text{Number of Elements} = \left(\frac{\sqrt{A}}{0.5 \cdot \lambda} + 1 \right)^2$$

Noting that it takes two antenna arrays for an interferometer to measure angle in one plane (i.e. either elevation or azimuth), it takes at least three to measure both elevation and azimuth.

$$\text{Number of Elements} = \left(\frac{\sqrt{A}}{0.5 \cdot \lambda} + 1 \right)^2 \cdot 3 \tag{26}$$

where antenna area is found by manipulating Equation 13 from Section 2.7

$$A = \frac{G_r \lambda^2}{4\pi\eta}$$

Finally, to determine radar cost as a function of radar subsystem level properties, the number of elements calculated in Equation 26 is substituted into Equation 25.

However, a portion of the implementation chapter (following this chapter) will not study the radar properties down to the subsystem level, but there still needs to be some cost measure that penalizes using a more accurate radar. During this initial implementation study, radar cost will actually be a normalized measure of radar complexity based on a simple relation given in Equation 27. The normalization is based on the bounds used for the radar noises (shown as "max" and "min"). This simple equation assumes that the most accurate (i.e. less noisy) radar has a complexity of +1, and the least accurate (i.e. most noisy) radar has a complexity of -1. The equation is a summation of the separate and independent contributions to radar noise, i.e. elevation noise, azimuth noise, etc..., each weighted according to total contribution to radar complexity. The purpose of the weightings is to normalize the total radar cost between -1 (all radar noises at highest setting) and +1 (all radar noises at lowest setting).

$$RadarCost = \sum_{i=1}^{\#\ noise\ contributions} \left[\frac{(Noise_{i,mid} - Noise_{i,actual}) * 2}{Noise_{i,max} + Noise_{i,min}} \right] * Weight_i \tag{27}$$

5.3.4 Combined Effect of Multiple Projectiles

The methods defined to this point aim to quantify the ability of a single guided projectile to intercept a target as a function of various radar and gun accuracy capabilities. This ability will be measured in the quantification of minimum miss distance between interceptor and target, as well as the probability of a direct hit of the target by a single projectile. Section 2.3.3 discussed the possibility that more than one weapon may be required to achieve a desired probability of damaging or destroying a target. Equation 7 was presented as a means to determine the probability that a target will be hit at least once by n weapons, given the probability of hitting a target with one weapon P_H. This equation was derived using the binomial distribution and the assumption that each trial is independent of every other trial. The same method was also applied in Equation 8 used to determine that damage caused by a multiple sorties, given the single sortie probability of damage (SSPD). Equation 28 uses the same idea given in Equations 7 and 8, with nomenclature more suitable to this problem. Here, the probability of hitting the target at least once using n multiple shots, or the Multiple Shot Probability of Hit (MSPH), is a function of the Single Shot Probability of Hit (SSPH).

$$MSPH = 1 - (1 - SSPH)^n \tag{28}$$

The next step is to determine the number to substitute for n in Equation 28. The maximum number of projectiles that can be fired from a single gun in a given amount of time is a function of the firing rate. Assuming that the firing rate is given using the relation discussed in Appendix C, the number of projectiles that can be

fired at the target is a function of an engagement window time that assumes that all of the projectiles arrive at the target plane at the same time. This is a major assumption necessary to implement this portion of the study in the absence of a 6-DoF simulation capable of modeling a single gun firing multiple projectiles at a single target. Therefore, the maximum number of projectiles fired at the target is simply the product of the rate of fire [projectiles/second] and engagement window [seconds].

The probability of hitting the target will be determined using the SSPH (determined using methods discussed earlier) substituted in Equation 28, and any integer up to the maximum number of projectiles fired. This should result in a trend such as the one given in Figure 20, with the curve bounded by the SSPH for the first projectile up the maximum attainable MSPH at the maximum possible number of projectiles fired.

5.3.5 Creating Surrogate Models

Any surrogate models of more complex computer codes used in this thesis will be in the form of a Response Surface Equation (RSE). As discussed in Section 3.3, the most common form of RSE used to represent a complex design space is the polynomial RSE. However, as the design space becomes high nonlinear, multimodal, or discontinuous, simple polynomials can no longer be used for accurate model representation. Neural networks are emerging as an excellent alternative to polynomial RSE's to model those complex design spaces that often arise when capturing effects across a design hierarchy, such as those that arise in a system of systems formulation.

5.3.5.1 JMP

The statistical package JMP [127] allows for the creation of both polynomial and neural network response surface equations. If during the implementation portion of this work, a design space will be simple enough to be modeled with a polynomial, JMP will be used to create those surrogate models. However, if polynomials are

not suited to approximate a given response, neural network RSE's will have to be used. As noted, JMP has the capability to create neural network RSE's, but it does have its limitations. The only back propagation method used by the JMP software is a momentum-based steepest descent optimization method. The steepest descent is a gradient-based optimization method that uses a search direction within a design space in the direction of the negative of the gradient of the objective function [139]. The use of momentum means that if the optimizer moves in the same direction more than once, it increases its step size. This process helps overshoot local minima and speed up convergence time. This training process is deterministic, however, the initial weight space (or set of regression coefficients) is very highly dimensional, and therefore predicting the outcome of training the randomized initial neural network is extremely unlikely [64]. This back propagation method may work in many cases, but there may arise instances when the design space is so complex that other optimization methods might be required. Additionally, the user has to hand iterate the number of hidden nodes used. As discussed in Section 3.3.2, there is an optimum number of hidden nodes within the neural network topology that would fit the training and validation data with the least error. Recall that too few hidden nodes would cause an underfit model, and too many hidden nodes would cause an overfit mode.

5.3.5.2 FANNGS

The Function Approximating Neural Network Generation System (FANNGS) by Johnson [82], is program written in MATLAB created to automate the generation of neural network regressions. FANNGS allows the user to select a range of hidden nodes to fit data to, and then selects the number of hidden nodes that has the least error when compared to both the training and validation data. Because FANNGS uses the MATLAB Neural Network toolbox [53] for many of its functions, it has a number of training algorithms available to it. All of these algorithms are line search

methods that require many starting points to try to achieve a global optimum, just as JMP. Of the many optimization methods MATLAB has to offer, Johnson [82] notes that the Levenberg-Marquardt with Bayesian Regularization algorithm offers the best generalization, or the ability to predict future data not used in the training process such as the validation data. The MATLAB Neural Network toolbox documentation [53] may be consulted for further detail on the different neural network training algorithms. For the most complex design spaces, FANNGS will be employed to create neural network surrogate models.

CHAPTER VI

IMPLEMENTATION

6.1 Approach Review & Implementation Introduction

The previous chapter outlined a methodology to attempt to answer the research questions outlined in Chapter 4. A specific problem was defined based on the motivation introduced in Chapter 1. To focus the design space, a morphological matrix was used to present alternative approaches to address each decomposed function necessary to provide a problem solution. Options were eliminated for each function based on several factors, including expert opinion, level of technology maturity, and relativity to the scope of this Ph.D. thesis. An approach was outlined that creates an environment that enables top-down design throughout a system-of-systems hierarchy, using a Monte Carlo simulation to populate the design space employing surrogate models for rapid manipulation. Tools were then selected to address the functions necessary to complete the system-of-systems hierarchy.

This chapter is composed of several main sections. The first part will very briefly introduce preliminary results based on related work that served as a proof of concept to begin work on this thesis. The next part shows the implementation of the methodology proposed for individual portions of the systems hierarchy, with the aim of proving its use in each section. The first individual part will be an initial study using the GTRI Multibody 6-DoF code to simulate a guided projectile and mortar interception, using gun and radar noise variables of interest decided on a priori, which will show the benefit of using the top-down decision making approach to identify variable tradeoffs based on various constraints on measures of effectiveness. This same

approach will also identify the variables that contribute the most to variability of the constraints placed on those measures of effectiveness, as well as those variables that contribute little if any. The radar noise variables identified as the main contributors to the metric sensitivity will then be carried through to study the effects of varying radar and guidance update rates. Afterwards, the combined effect of firing multiple projectiles at one target will be studied using the surrogate models created that include the update rates and the radar noise variables of interest.

This is followed by a section that is independent of all of the other work presented up to that point in the chapter, and will apply this method to study the subsystem variables of the radar. These subsystem variables enable the radar accuracy capability that is carried through as the "variables" at the next higher level in the hierarchy (i.e. the level where the radar, gun, projectile, and target interact to cause a particular top-level effect). The design space defined in this section will be carried through to the final section, which will be the final assembled hierarchical environment. Before this final environment is demonstrated, a more detailed 6-DoF model of the interception scenario based on knowledge acquired during the initial interception study will be presented. Finally, the assembled hierarchical model will be demonstrated with relevant discussion about any discoveries made during this process.

6.2 Preliminary Studies

Preliminary work leading to this thesis was conducted to establish the effectiveness of using surrogate models in the uncertainty quantification of the ability of gun fired projectiles to intercept small aerial targets at various distances. The specifics of these preliminary studies are given in Appendix B, which overviews studies relating to two of the systems discussed in Section 1.2.3. This is meant to be understood as results based on simple test cases relating to systems currently being studied as potential solutions to the RAM defense problem. The successful application of a number of

the more basic methods discussed in Chapter 3 to the problem of mortar interception with an unguided, unpowered gun launched projectile served as the preliminary proof of concept for the remainder of the effort undertaken to conduct the implementation portion of this thesis study.

6.3 Initial 6-DoF Study

6.3.1 Variable and Response Identification

This initial study is designed to examine the effects of gun firing and radar accuracies on the confidence of projectile/target interception. As will be addressed several times in this chapter, many code executions are required to create surrogate models of the 6-DoF code that uses an internal Monte Carlo simulation to simulate gun and radar noises. Limitations in computing capabilities and scope restrict the number of the degrees of freedom discussed for the gun and radar accuracies that can be carried to the more detailed analysis level. However, other variables that need to be considered in describing the intercept problem are range from projectile launch to target intercept, and the projectile bore.

The initial analysis studies four radar measurement noises involving error in identifying the location of an object: elevation, azimuth, range, and projectile roll orientation (also referred to by its variable name from the field of dynamics as "phi" for brevity as was shown in Figure 40 for the moments about a projectile's axes). Table 11 shows the bounds for radar noises, shown as the standard deviation (1σ) of a normal distribution around the reported location (elevation, azimuth, and range) and roll orientation of the projectile as it travels along its trajectory. The bounds were selected with consultation with disciplinary experts in the Sensors and Electromagnetic Applications Laboratory (SEAL) of the Georgia Tech Research Institute (GTRI) [24]. The lower bounds of each of the radar noises is intended to represent an advanced technology radar, which represent the lowest noise and therefore highest

Table 11: Radar Noise Errors for Initial Study(1σ)

Property	Minimum	Maximum	units
Elevation	0.015	1.000	mrad
Azimuth	0.015	1.000	mrad
Range	0.00005	0.0001	$m_{error}/m_{downrange}$
Projectile Roll Orientation	0.000045	0.00017	rad/m

accuracy. The upper bound is intended to represent a low cost, low technology radar, which has the highest amount of noise, and therefore also has the least accuracy.

The bounds selected for gun pointing biases for the initial study are given in Table 12. Note that the values given are *not* standard deviations of a distribution around a desired value. They are static deviations from the intended firing position and muzzle velocity. *This initial 6-DoF study does not assume the use of a fire control computer that calculates the gun firing position (i.e. in terms of elevation, azimuth) required for the projectile to intercept the target, assuming an unguided ballistic trajectory.* For each simulation, the gun firing position must be manually set for each desired intercept range. This gun firing position must be calculated depending on the desired intercept range, which is not done automatically in the 6-DoF simulation. Therefore, for each predetermined intercept range, a separate 6-DoF code input file must be created using a precalculated gun firing position. This means that range can not be treated as a continuous variable within the 6-DoF code, and must be treated as a discrete variable. Surrogate models created around these static deviations of gun firing position (rather than stochastic noises) leave the flexibility of sampling from a distribution within the bounds used to create those surrogate models, as well as actually "pointing" the gun away from an ideal firing position. This is the same approach used in the preliminary studies explained with more detail in Appendix B.

The two other variables also noted as a necessary component for the initial study were intercept range and projectile bore. The design of the gun firing the projectile is

Table 12: Gun Pointing Bias for Initial Study

Property	**Minimum**	**Maximum**	**units**
Elevation	-5	5	mrad
Azimuth	-5	5	mrad
Muzzle Velocity	-10	10	m/s

Table 13: Discrete Variable Settings for Initial Study

Bore (mm)	**Range (m)**
30	250
40	500
50	1000
57	1500
	2000

not within the scope of this thesis, and the projectile bore itself is constrained to be compatible with an existing gun. Table 13 lists the discrete settings for the projectile bore and intercept range used for this portion of the study.

Because this portion of the implementation does not examine the radar subsystem variables, radar cost will be based on the complexity relation given in Equation 27 in Section 5.3. Each of the four radar noise components is assumed to contribute equally to radar complexity, and therefore is equally weighted in Equation 29; each noise factor has a weighting of 0.25, summing to 1.0. These weightings could just as easily have been any other value, and can be changed even after the decision making environment is constructed.

$$
\begin{aligned}
RadarCost &= \left[\frac{(AzimuthNoise_{mid} - AzimuthNoise_{actual}) * 2}{AzimuthNoise_{max} + AzimuthNoise_{min}}\right] * 0.25 \\
&+ \left[\frac{(ElevationNoise_{mid} - ElevationNoise_{actual}) * 2}{ElevationNoise_{max} + ElevationNoise_{min}}\right] * 0.25 \\
&+ \left[\frac{(RangeNoise_{mid} - RangeNoise_{actual}) * 2}{RangeNoise_{max} + RangeNoise_{min}}\right] * 0.25 \\
&+ \left[\frac{(PhiNoise_{mid} - PhiNoise_{actual}) * 2}{PhiNoise_{max} + PhiNoise_{min}}\right] * 0.25
\end{aligned} \tag{29}
$$

6.3.2 Surrogate Model Creation & Visualization

The previous sections described seven continuous and two discrete variables needed to describe gun pointing errors, radar noises, intercept range, and projectile bore. Therefore, a seven variable Design of Experiments (DoE) was created to dictate the settings required to model the continuous variables, and was then run for each combination of the two discrete variables. A DoE consisting of 178 runs was created by combining a Central Composite Design (CCD) consisting of 79 runs to capture the corners of the design space, a Latin Hypercube Sample (LHS) consisting of 79 runs to capture multimodal effects within the bounds, and 20 uniformly selected random points to be used as a hold back sample to validate the model fit. Recall that each trial of the DoE executes a Monte Carlo simulation within the 6-DoF code. The more Monte Carlo samples, the greater the resolution of the statistics compiled from those runs. However, the DoE was then required to run 15 times at each combination of the two discrete variables, therefore limiting the number of Monte Carlo runs to 100 to maintain within a feasible amount of computer run time. This means that running the DoE for one range/bore combination executed the 6-DoF 17,800 times, and therefore a total of 267,000 6-DoF executions.

The radar error is represented by random noise, meaning that at each sweep, the reported radar measurement is off by a different amount (as described in Section 2.7). This noise is approximated by a normal (Gaussian) distribution. Therefore, each run

of the DoE input settings results in a different set of radar noises, each one requiring a Monte Carlo simulation to sample from the normal distributions describing each noise variable. Multiple runs are required to quantify the confidence of achieving a response; here the responses of interest are the minimum miss distance of the interceptor and target, and probability of direct hit. Consequently, each DoE run will have as many outputs as Monte Carlo simulations per run. A frequency distribution can be created for each response as a function of each input, and useful statistics can be extracted from these distributions to help analyze the data. A useful way to analyze these responses is by constructing a CDF using the 90%, 75%, 50%, 25%, and 10% confidences due to random radar noise, and calculated using the Monte Carlo simulation results for each DoE run. This required creating a simple MATLAB script to read in the data and run the statistics. At this point, neural network surrogate models were created using the confidences as the responses, and may be visualized using a prediction profiler as shown in Figure 49. Note that results are only shown for the 40, 50, and 57 mm projectile bores. This is because the scaling laws used to model the smaller 30 mm bore did not allow for sufficient control authority, resulting in insufficient data to be used in the surrogate model regression.

Rather than just using a prediction profiler, a more useful way to visually analyze these responses is by constructing a CDF using the neural network surrogate models in a graphical user interface (GUI), shown in Figure 50. This CDF is formed by using the neural network surrogate model fits to the 90%, 75%, 50%, 25%, and 10% confidences of the minimum distance interception due to the randomness caused by radar noise. Using the GUI, a user may use either the slider bars or type in the value of each variable and instantly see the CDF update. When using surrogate models, it is clear to see the benefit of instant results rather than having to wait for a complicated 6-DoF code to execute. It is important to understand that in this case, manipulating the surrogate models is the equivalent of running a Monte Carlo simulation within

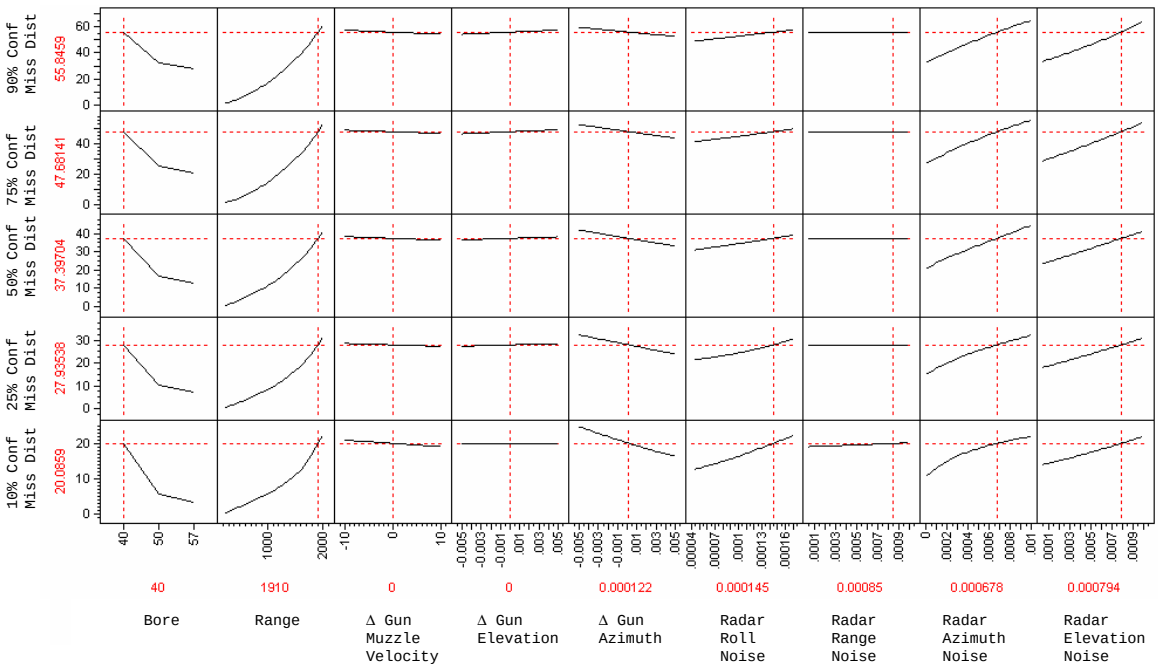

Figure 49: Initial Study - Viewing Surrogate Models Using a Prediction Profiler

the 6-DoF code. In addition to the CDF, the neural network surrogate model created to capture the actual probability of a direct hit is simply displayed on the GUI as well.

One of the more valuable uses of having the minimum miss distance CDF is to be able to determine the confidence of hitting the target with a lethal radius. This can be directly applicable to setting the requirements for a warhead, if needed, by typing a lethal radius value in the GUI that simply interpolates the confidence of achieving that lethal radius. For the example case shown in Figure 50, for a radar with the particular properties specified by the user, the probability of a direct hit is about 0.22, whereas the same projectile employing a warhead with a lethal radius of 1.0 m increases the confidence of hitting the target to 0.40. Creating a tool like the GUI shown in Figure 50 is a very useful way to visualize how radar noise affects the interceptor/target miss distance confidence. However, it still leaves open the question of how constraints on top-level metrics affect the design space on the lower levels of the design hierarchy. The section after next will show how the surrogate models used

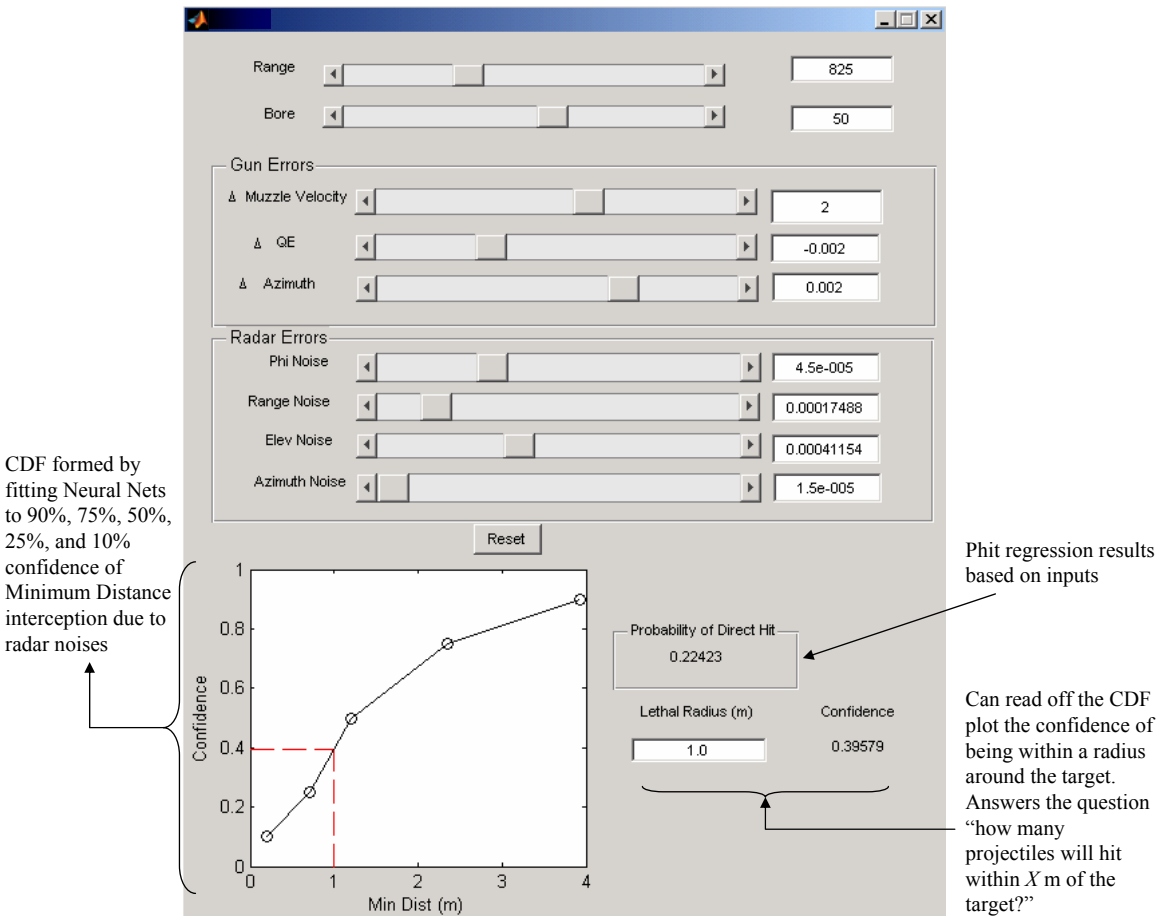

Figure 50: Manipulating the Surrogate Models Using a Bottom-Up GUI

to create the bottom-up GUI can be used to fill the design space throughout the hierarchy, and then constrained from the top-down. First, the introduction of gun firing noise to the gun pointing error will be addressed.

6.3.3 Introduction of Gun Firing Noise

Because the use of a fire control computer was not available to point the gun in the proper direction for a given intercept range, the correct gun firing elevation and azimuth had to be decided on a priori to running the DoE. This eliminated the possibility of using gun "noise" as a variable, as was used for the radar, therefore within the 6-DoF code, gun error was introduced as a controlled bias from the ideal firing condition (gun elevation, azimuth, and muzzle velocity). For this initial 6-DoF study, the introduction of gun firing noise, or randomness on the gun pointing and muzzle velocity was conducted by creating a new set of surrogate models by running a Monte Carlo simulation on the gun biases of the surrogate models already in place, and fitting the new set to the same confidence intervals as those discussed in Section 6.3.2.

Normal distributions extend to positive and negative infinity around the mean, so placing upper and lower bounds on the distributions comes in the form of selecting an appropriate standard deviation. The goal is to ensure that the random number generator in the Monte Carlo simulation selects values within the desired bounds *most* of the time. The number of standard deviations away from the mean value can describe the amount of area under the distribution curve captured. For example, as discussed in Appendix A there is a 99.9994% probability of selecting a random number within 4σ of the mean of a random variable. Using a random variable X with normalized bounds $-1 \leq X \leq 1$ and mean at 0 as an example shown in Figure 51, a standard deviation of 0.25 maintains that 99.9994% of any samples taken from a Monte Carlo simulation to be within the normalized bounds.

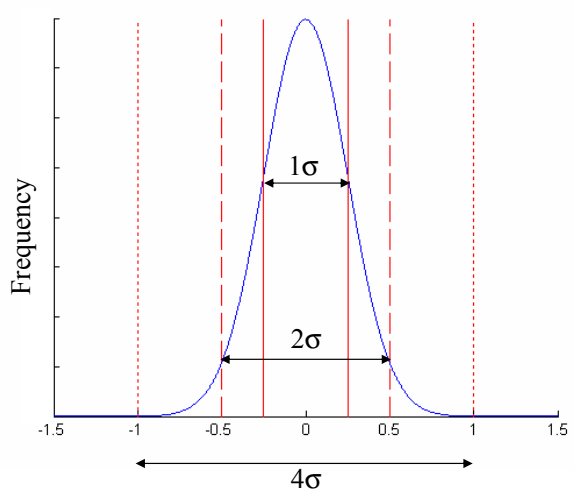

Figure 51: Normal Distribution, μ=0, σ=0.25

Table 14: Gun Firing Noise

Property	**Min**	**Max**	**units**
Elevation	0	1.25	mrad
Azimuth	0	1.25	mrad
Muzzle Velocity	0	2.50	m/s

Using the presumption that 4σ is a suitable upper bound, by conjecture the absolute value of the limits discussed in Table 12 presented earlier can simply be divided by 4. A standard deviation centered about a mean of zero results in equal spread among positive and negative values, therefore one standard deviation value can account for the positive and negative bounds presented in Table 12. As given in Table 14, a standard deviation of zero implies no gun firing noise for a particular variable, and the maximum value is the value selected to stay within the absolute bounds of the gun bias surrogate models.

The problem is now set up to make minimum intercept miss distance quantification a function of both radar and gun *noises*, as well as intercept range and projectile bore. An eight variable DoE was created using the three variable bounds given in Table 14 in addition to the four radar noise variables of Table 11. For the first DoE run

(discussed in Section 6.3.2), range was run as a discrete variable because the 6-DoF code could only accept it as such. However, enough discrete values of intercept range were executed to capture the design space of range and all other variables, and the analysis conducted in Section 6.3.2 resulted in an equation that allows range to now be treated as a continuous variable for the remainder of this initial 6-DoF study. To simplify the problem within the scope of this study, bore was left as a discrete variable and not included in the DoE, however the DoE was executed once for each value of bore: once each using a 40 mm, 50 mm, and 57 mm bore (recall that the 30 mm bore results were invalid and therefore insufficient for creating surrogate models). The results may be visualized using a prediction profiler as shown in Figure 52. Note the relatively flat curves that describe the individual contributions of the gun noises, as compared to those of the radar noises. Those gun errors now have a "_std" suffix in many of the graphics in this section, and are bounded from zero to the maximum value in Table 14. This indicates that the responses are not very sensitive to gun error (this will be expanded on in the coming sections). The surrogate models created in this section that quantify intercept miss distance as a function of both radar and gun noises will be used for the remainder of this initial 6-DoF study.

6.3.4 Response Variability Study

One of the main intentions of this thesis is to have the ability to discover not only which variables are the key drivers to the variability of the responses, but also which variables drive each other. This section will compare the use of Pareto plots and the proposed multivariate scatter plot method to conduct a response variability study.

6.3.4.1 ANOVA with Pareto Plots

Figure 53 shows a Pareto Plot created using an Analysis of Variance (ANOVA) as discussed in Section 3.3.3. This figure lists the variables contributing to the variability of 90% confidence minimum miss distance, in order of most contribution. Range has

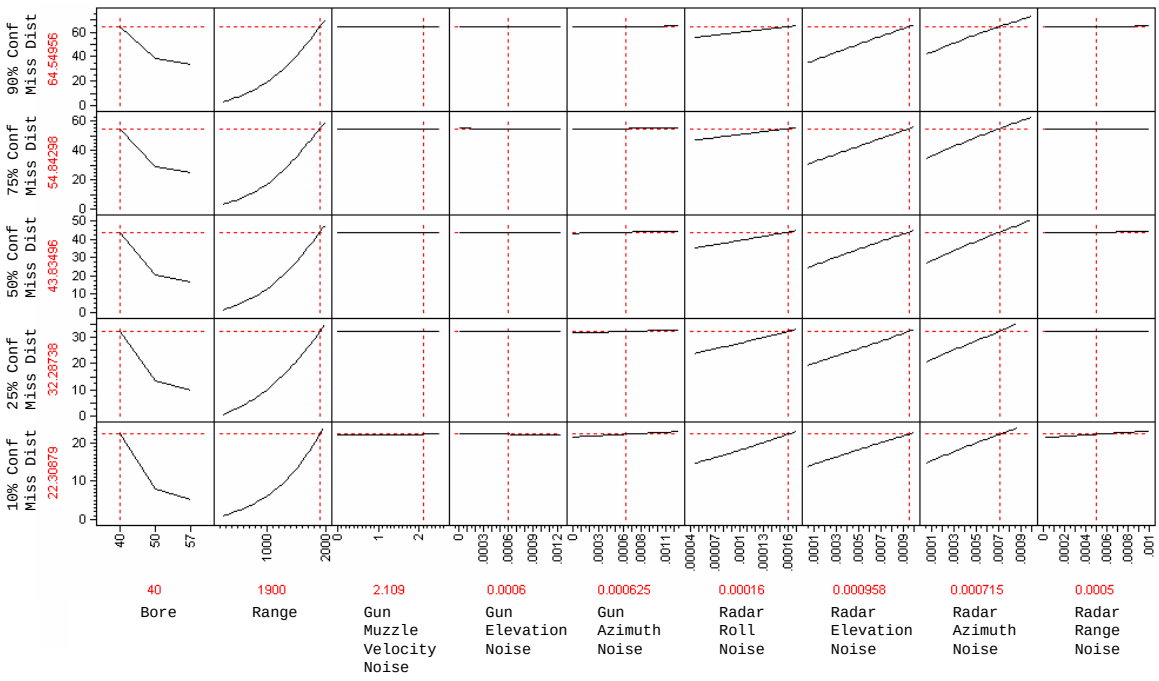

Figure 52: Initial Study - Viewing Surrogate Models Using a Prediction Profiler

the highest contribution with about 42%, and next is bore size at about 18%. Next, the four radar noises are listed, however there is clear step in the contribution of elevation and azimuth noises (both about 17%), and of range noise (4%) and roll (phi) orientation (3%). The contributions to miss distance variability from gun firing error are essentially too small to measure. As indicated by the cumulative contribution to response variability, roughly 90% of the total variability is due to range, bore, radar elevation noise, and radar azimuth noise.

Clearly the discrete variables evaluated dominate the gun and radar noises. One of the problems in evaluating a Pareto plot is that it alone does not indicate which variables drive each other. For example, the question can be asked "at which intercept ranges do the radar noises have more of an impact"? One way to answer this is to conduct the ANOVA for each combination of the discrete variables set to a fixed value, which would allow one to examine the prioritization of the gun and radar properties as range increases. A complete set of Pareto plots for each bore/range combination is given in Figures 121, 122, and 123 in Appendix D.1. Studying those

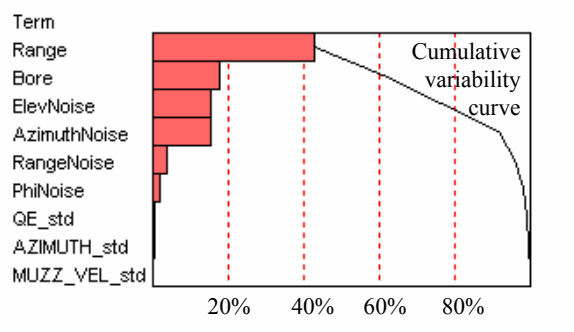

Figure 53: Initial Study - Pareto Plot for Discrete and Continuous Variables on Variability of 90% Confidence Intercept Miss Distance

figures one can extract important information from examining the intercept range extremes, summarized in Figure 54. The first observation made from studying those Pareto plots is that the radar azimuth and elevation noises are the key drivers in each case.

For the 50 mm and 57 mm bore sizes, the gun errors play a much more important role in miss distance at the shorter ranges than at the longer ranges. This is because as range increases, the controller has more time to correct the pointing errors. Interestingly enough, for each of the three bore sizes at 2000 m, the order of the variables is the same. The only difference is that as bore size increases, the amount of variability contributed by radar range and roll noises, and the gun noises reduces. In summary, as range increases, miss distance is less affected by the gun errors due to the controller having more time to correct the trajectory, and as bore size increases, the relative contribution of the radar noises is less due to the increased dynamic pressure on the larger control surfaces giving more control authority.

A Pareto plot showing the results of an ANOVA study is a useful way to prioritize the variables of interest, but it is a very one-dimensional way to make assessments. Additionally, showing how the variables drive each other proves to be a cumbersome process. As this section showed, to do just that, the discrete variables had to be fixed at each of the various settings, and only then could the ANOVA be conducted to see

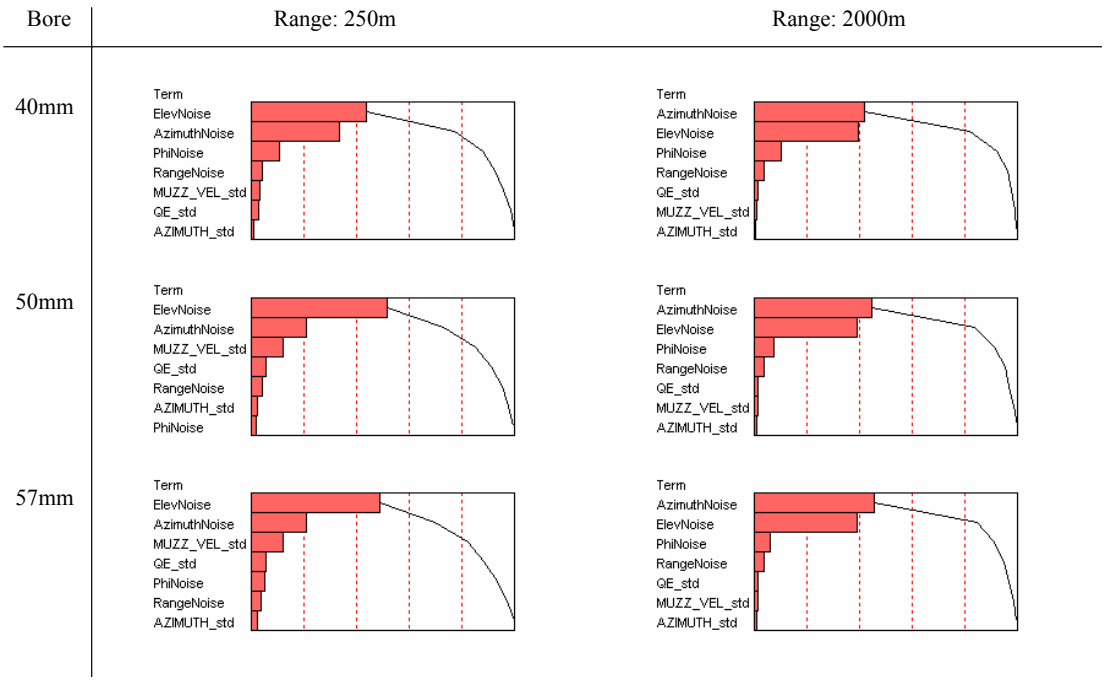

Figure 54: Initial Study - Pareto Plots for Fixed Combinations of Range and Bore on Variability of 90% Confidence Intercept Miss Distance

the way the priority of the other variables changes.

6.3.4.2 Multivariate Design Space Exploration

Another useful way to analyze the data is to conduct a design space exploration using a multivariate scatter plot. A Monte Carlo simulation sampling from a uniform distribution selected 1,000 samples from each variable within the bounds used to create the surrogate models. This includes the three discrete bores, the intercept range, the three gun noises, and the four radar noises. For each combination of variable values selected, the responses of interest are tracked. Therefore, each corresponding Monte Carlo simulation has a unique array of variable and response values, and can be visualized on a multivariate scatter plot, such as the one used for this initial study as given in Figure 55. Note the multivariate plot is actually just a collection of bivariate plots. Because the independent variable values in the blue box are samples from a uniform distribution, the points evenly fill the design space between them.

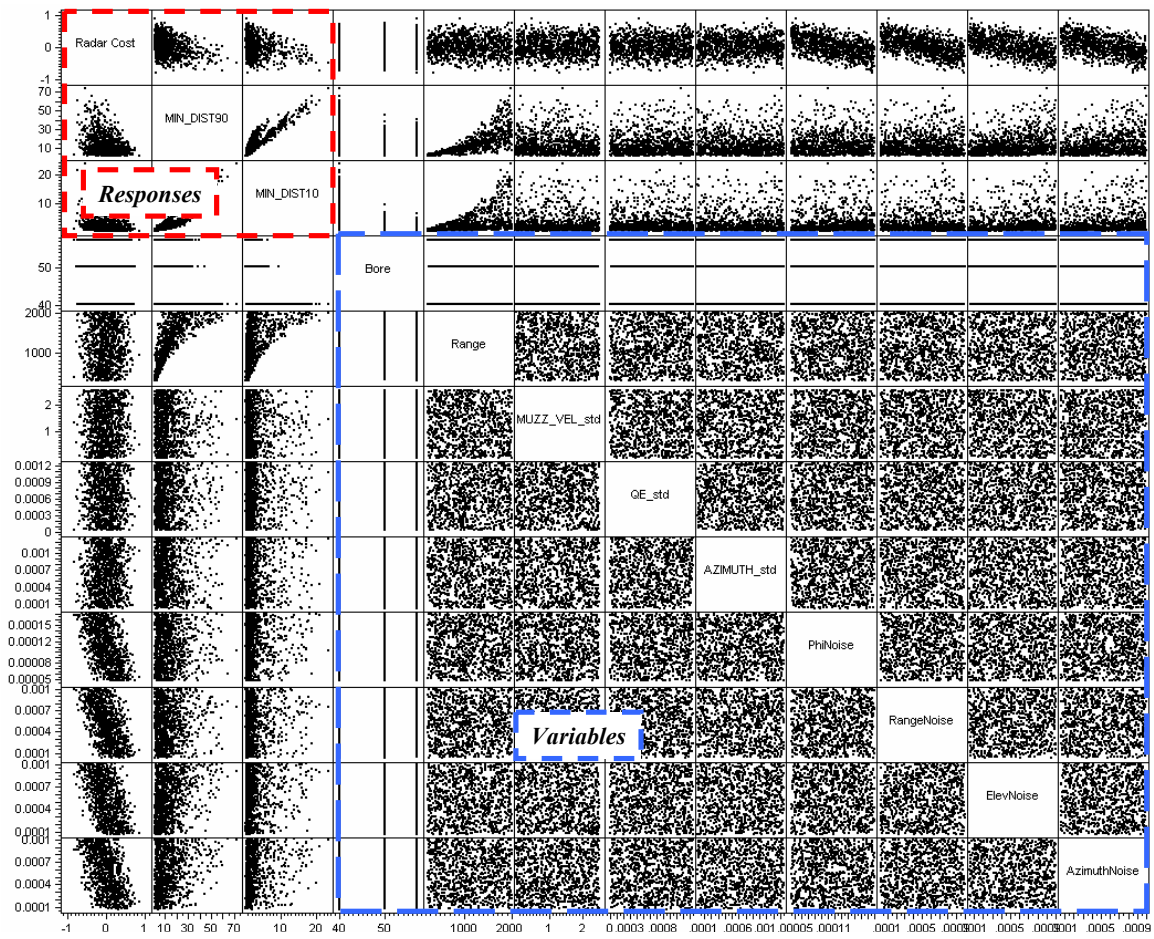

Figure 55: Initial Study - Multivariate Scatter Plot Design Space Exploration

The dependent responses are outlined with a red box, and are calculated using the variable values selected by the Monte Carlo simulation. Note that the individual bivariate plots within the red box show the design space between the responses. Each of the remaining scatter plots show the design space of each of the response/variable combinations, and is synonymous with the total derivative given in Equation 24 of Section 3.4.2.

As an example for using this method, a region of interest can be defined on the multivariate matrix as shown in Figure 56. Here, a region of acceptable performance is defined: the projectile must achieve a 90% confidence minimum miss distance of 7 m, and a 10% confidence minimum miss distance of 0.9 m. The other CDF settings (i.e. 75%, 50%, 25%) could have also been included to refine the shape, however

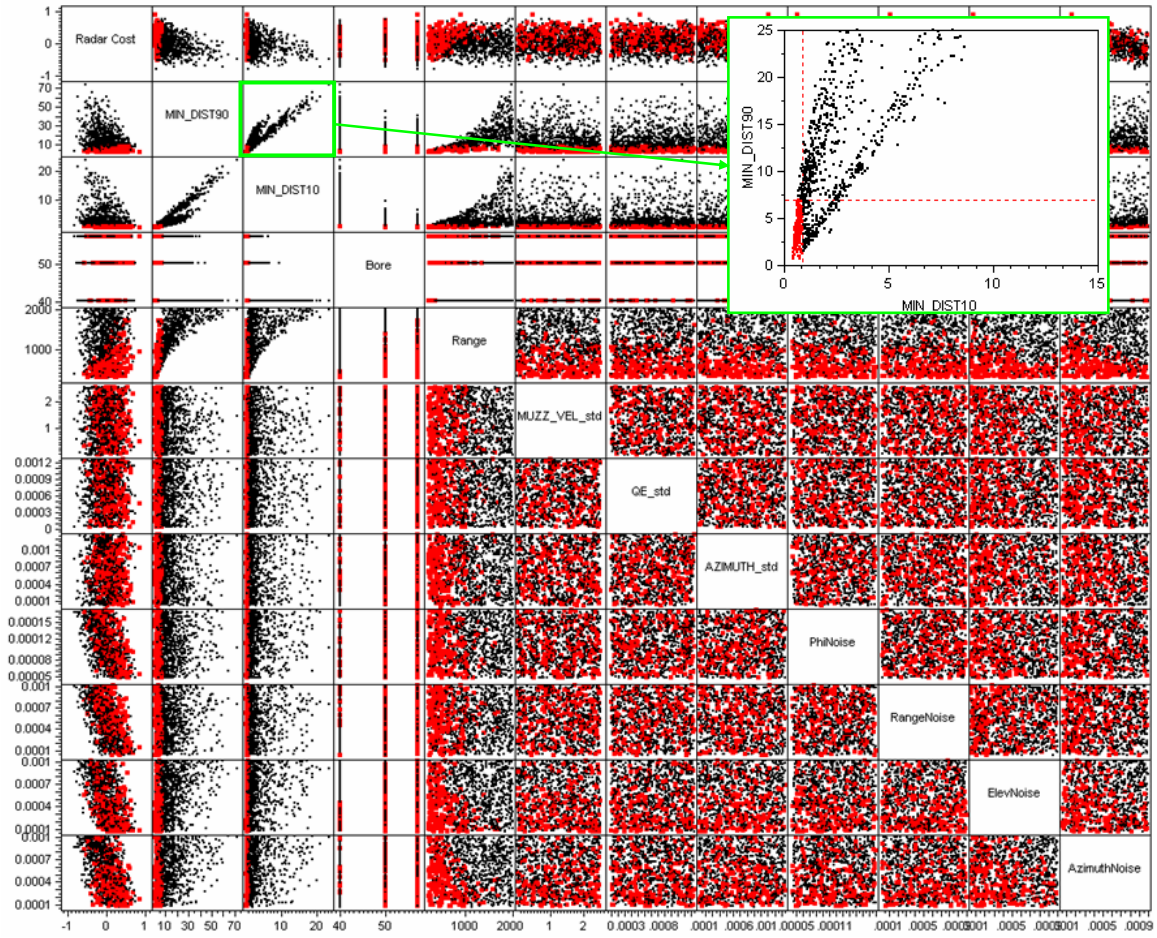

Figure 56: Initial Study - Intercept Miss Distance CDF Shape Constraint

they are omitted for clarity on the graphic. The points that lie within this region of interest are highlighted red, and the corresponding points are then immediately highlighted in every other dimension. This means that every red point in each of the other dimensions corresponds to a design that meets (or exceeds) the requirement set by the initial design space constraint. One can spend a good deal of time examining the tradeoffs in each dimension, but an attempt will be made to highlight some interesting results in the form of bivariate plots taken directly off of the multivariate plot in Figure 56.

For example, as shown in the left plot in Figure 57, note that the miss distance requirement drives a higher concentration of red design points at the lower radar

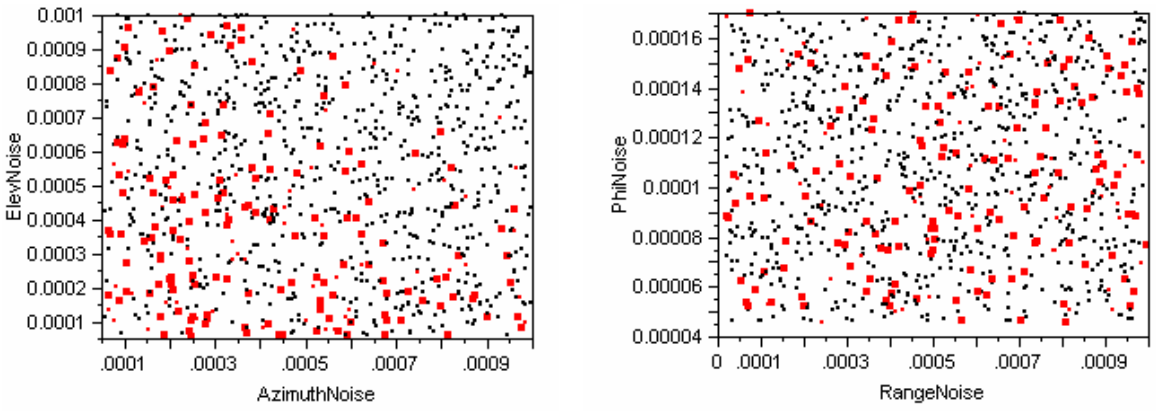

Figure 57: Initial Study - Bivariate Plots of Radar Noises, For Intercept Miss Distance CDF Shape Constraint

elevation and azimuth noises. This does not mean that certain specific values of elevation and azimuth noises must be used, since it is not immediately apparent which red points in this dimension correspond to a red point in another dimension. Although, what is apparent is that these two radar noises have a great effect on minimum miss distance. The remaining radar noises, range and roll (phi) noises (the right plot in Figure 57), and the three gun noises shown in Figure 58 are not concentrated in any specific region, and therefore are not as driven by the top-level constraint. This is the same conclusion drawn using the ANOVA and Pareto plots, however that method only identifies key variables as a function of total response variability, where as this new methodology enables a user to actually specify the CDF shape to discover the variable trade space, shown in the next few examples.

Figure 59 shows the maximum intercept range possible to achieve the minimum miss distance confidence constraint, for both 90% and 10% confidences. Here, the highest intercept range achievable is roughly 1700 m, evident from the red design point with the highest range on both plots. Another key finding from the miss distance constraints placed on the multivariate plot in Figure 56 is the variability of required radar accuracy with range. This is highlighted in Figure 60, where range is plotted against all four of the radar noises. Note that the black unconstrained points

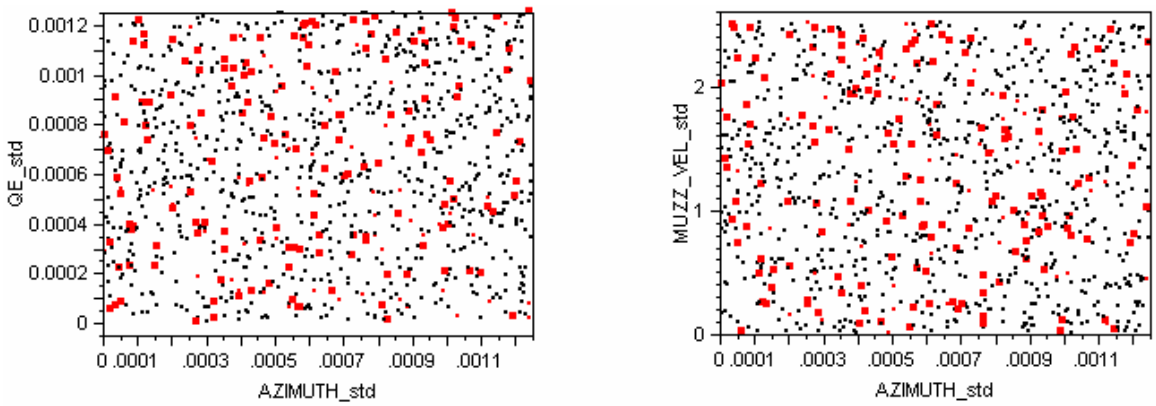

Figure 58: Initial Study - Bivariate Plots of Gun Noises, For Intercept Miss Distance CDF Shape Constraint

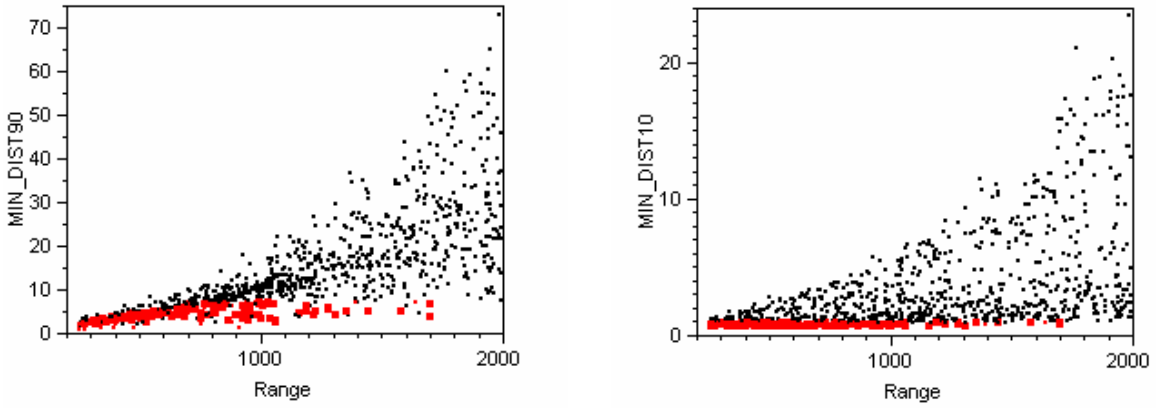

Figure 59: Initial Study - Bivariate Plots of Showing Maximum Range, For Intercept Miss Distance CDF Shape Constraint

from the previous figures are hidden for clarity, leaving only the red points that meet the miss distance constraint. Clearly, at the very low ranges, all radar accuracies are tolerated (i.e. meet the constrained goal), and as range is increased, the upper bound allowable radar azimuth and elevation noises are driven lower (top two graphics in Figure 60). A similar statement can not be made for the effect of increasing range on radar range and roll noises (bottom two graphics in Figure 60), where it is clear that for increased range there are fewer points that meet the range requirement, but it is not clear that increasing range requires higher radar range and roll accuracies.

The design space constrained by the miss distance requirements can further be constrained by other requirements, such as cost. Shown in Figure 61 are the points

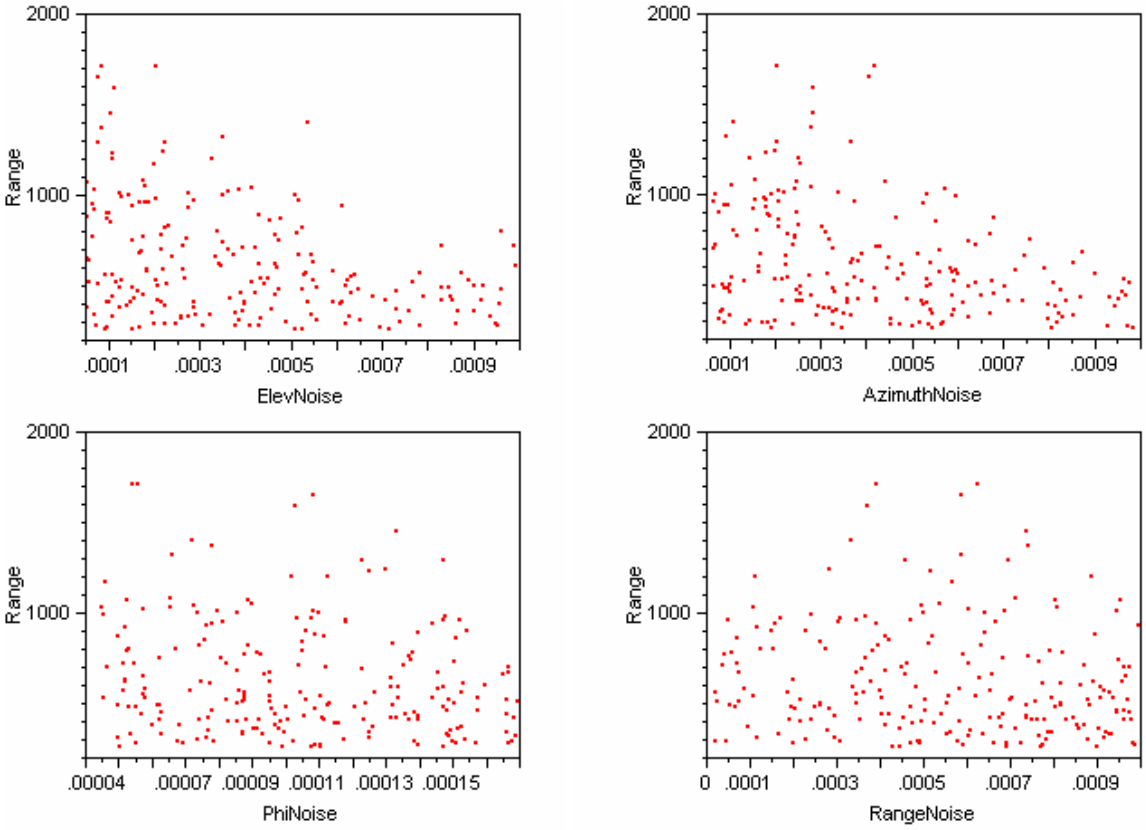

Figure 60: Initial Study - Bivariate Plots of Range and Radar Noises, For Intercept Miss Distance CDF Shape Constraint

within the miss distance constraints divided up into two regions in the radar cost space. The points colored red can be considered the more complex, or expensive options, and the blue points can be considered the less expensive or complex options. It is important to remember that both the red and blue points still satisfy the miss distance requirements identified in Figure 56. Several significant trends appear comparing feasible radar solutions by cost. Figure 62 shows radar cost (left) and 90% confidence miss distance (right) both versus range. Again, the solutions that do not meet the miss distance constraint are hidden for clarity. On the left graphic, a notional frontier has been drawn in to exemplify the nondominated solutions providing maximum range capability for minimum cost. This is a very useful way to determine at what range one would have to switch from using a "cheaper" radar to a more expensive one, depending on how complexity was valued from Figure 61 (in this case at about 850 m intercept range). The right graphic in Figure 62 shows how the more expensive radar (red points) enables a lower intercept miss distance at higher ranges when compared to the less expensive option (blue points).

Figure 63 shows bivariate plots of the radar noises just as shown in Figure 57, except with the distinction made between the two radar cost regions. The less expensive (blue) points dominate the upper right corner of both plots, and the more expensive (red) points dominate the bottom left corner. This is clearly intuitive since the closer a solution is to the bottom left corner of each plot in Figure 63, the more accuracy it has. However, an interesting observation can be made in the plot showing elevation and azimuth noises (left), where blue points do not fill the space completely in the upper right corner (as was pointed out in Figure 57). This shows that the miss distance constraint sets the lowest tolerable radar accuracy, even using the less complex radar. However one of the most useful plots extracted from the original multivariate (Figure 61) is studying radar azimuth and elevation noises versus range, given in Figure 64. Starting at the lower ranges, it is clear that both sets of radar

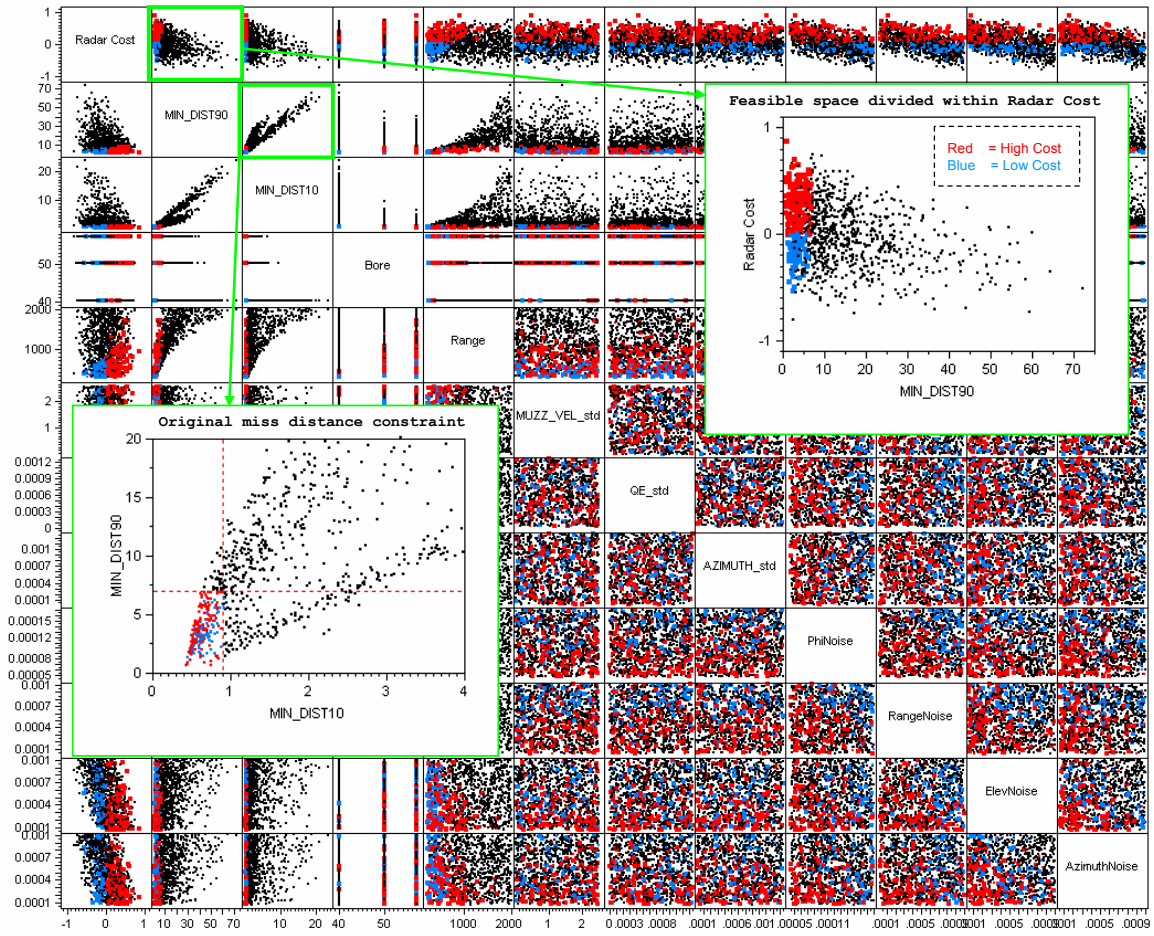

Figure 61: Initial Study - Feasible Designs Separated by Radar Cost

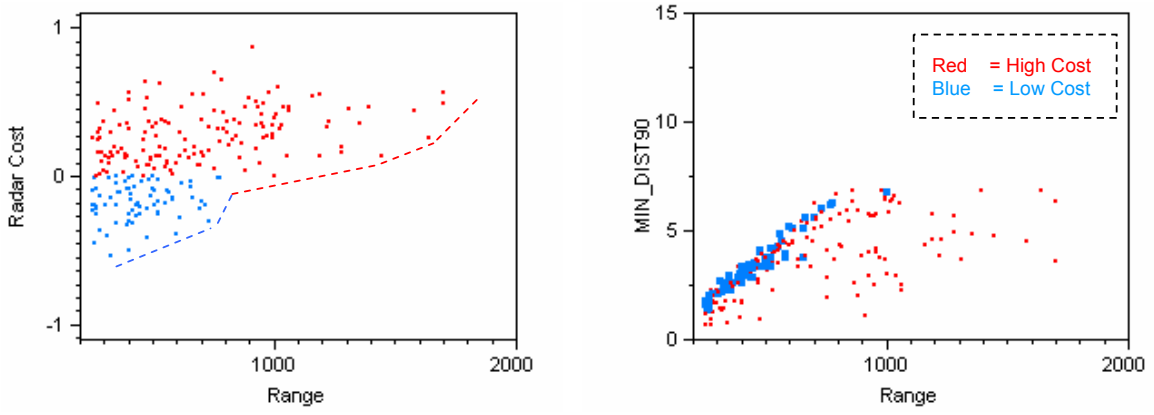

Figure 62: Initial Study - Radar Cost by Range (L) & Minimum Miss Distance by Range (R), Divided by Radar Cost

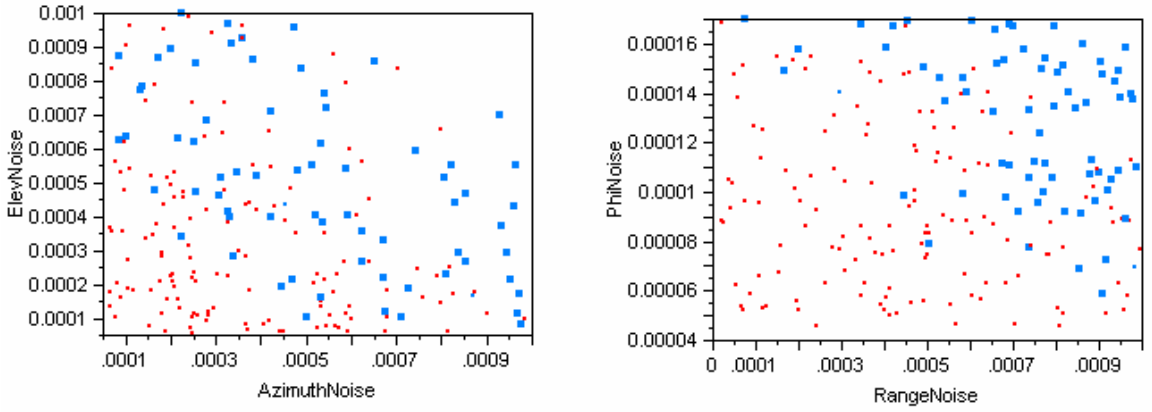

Figure 63: Initial Study - Radar Noises, Divided by Radar Cost

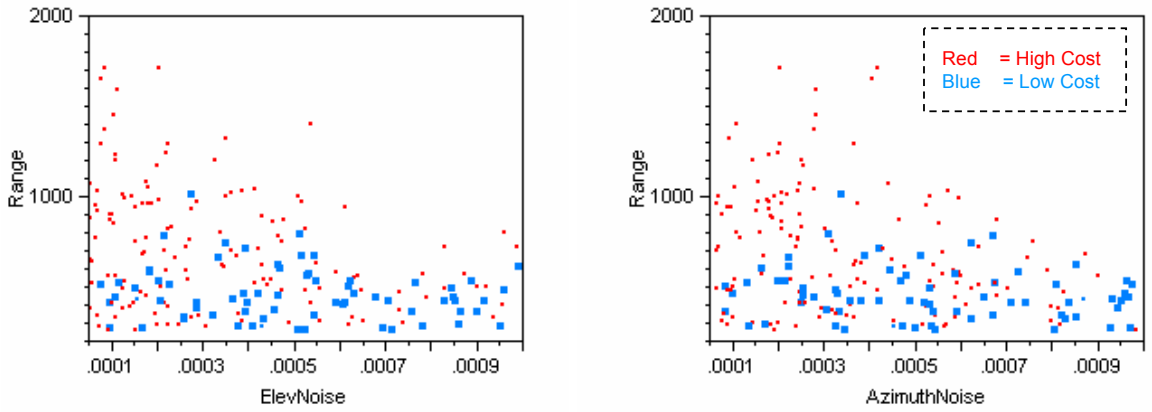

Figure 64: Initial Study - Range by Radar Azimuth & Elevation Noises, Divided by Radar Cost

complexities provide solutions to the minimum miss distance requirements. However, at about 800 m intercept range there is a clear shift from blue to red points, and at about 1000 m there are only red points, indicating the need for more radar accuracy at high ranges.

Other types of constraints can be flowed down to the radar capability level. As shown in Figure 65, a certain maximum allowable 90% confidence miss distance can be defined for a desired intercept range. Immediately, a clear tradeoff Pareto Frontier emerges between the radar elevation and azimuth noises, shown in the left plot of Figure 66. However, there is no apparent sensitivity due to radar roll (phi) and radar range noises, shown in the right plot of Figure 66. And just as discussed for the earlier

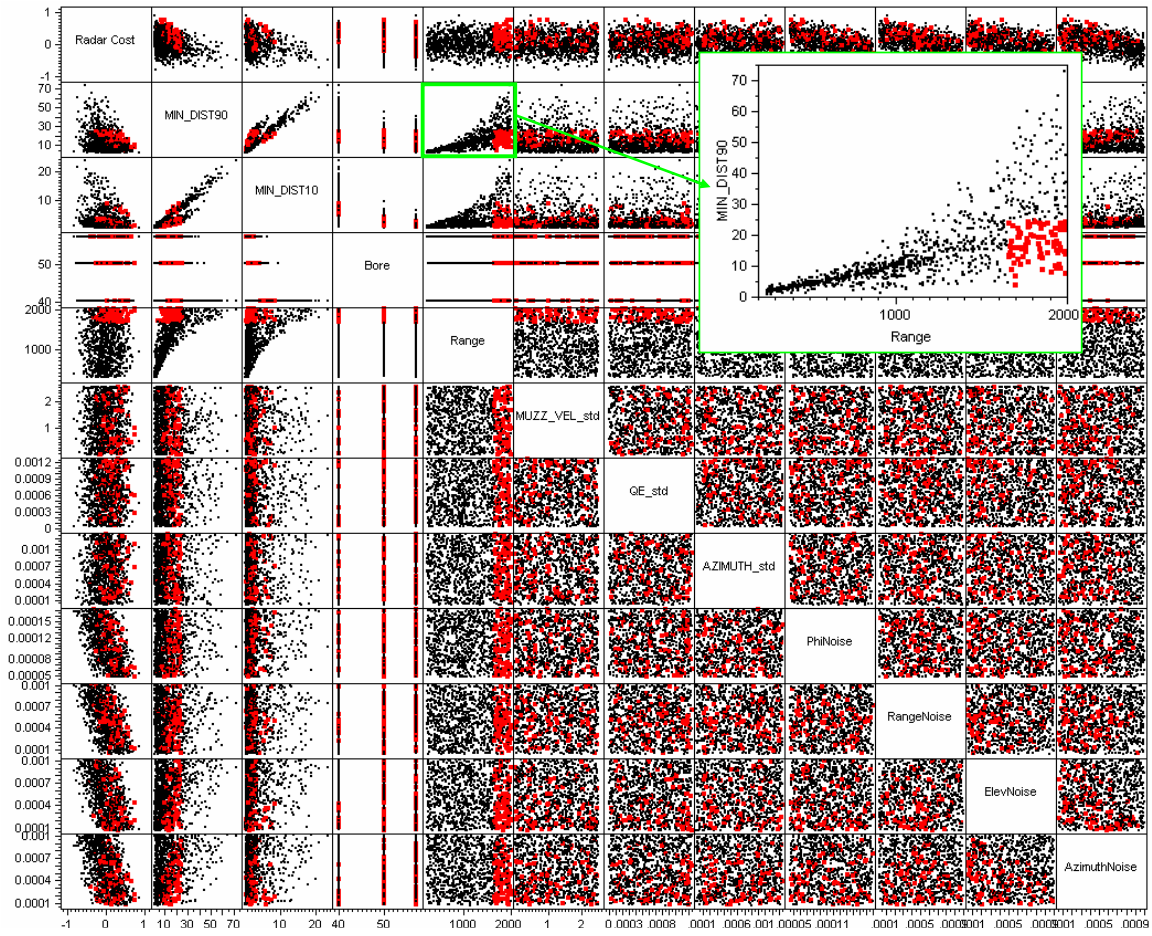

Figure 65: Initial Study - Selection of Required 90% Confidence Miss Distance and Intercept Range

examples in this section, there is no particular shift of feasible points in any direction with regard to the gun errors, shown for gun firing muzzle velocity by gun firing azimuth on the left, and gun firing quadrant elevation by azimuth on the right side of Figure 67. Now when compared to the Pareto plots, this method shows not only the key driveers, but also how the variable trade space varies for multiple response constraints.

Another useful application of this methodology is to use the interactive multivariate scatter plot from the bottom-up. Please note that the minimum miss distance constraints discussed earlier no longer apply to the following examples. In Figure

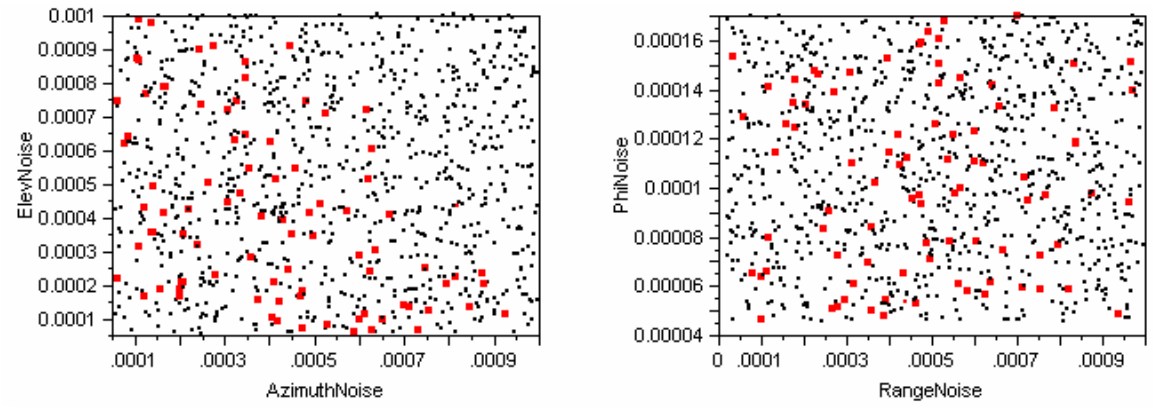

Figure 66: Initial Study - Radar Noises, For Required 90% Confidence Miss Distance and Intercept Range

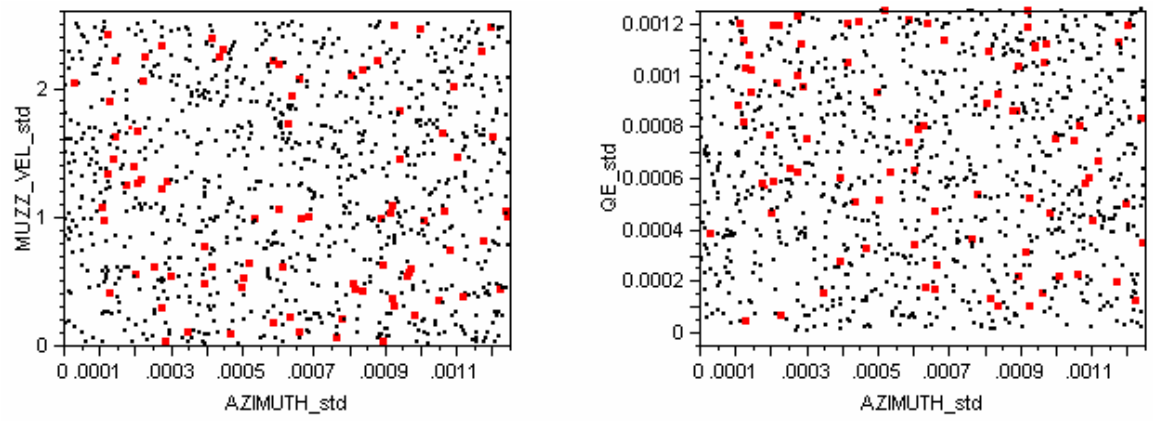

Figure 67: Initial Study - Gun Noises, For Required 90% Confidence Miss Distance and Intercept Range

68, regions of "good" and "bad" radar accuracies are chosen by selecting radar azimuth and elevation noises, in this case notionally. Here, the blue points represent solutions with very low radar elevation and azimuth noises, and red points indicate designs with high noise. Now, the impact can be traced to the upper levels of the hierarchy. In Figure 69, the 90% and 10% confidence minimum miss distances are plotted against intercept range. Especially examining the 90% confidence plot on the left, it is clear that as range is increased, the better radar (blue points) enables solutions staying closer to the x-axis than solutions using the less accurate radars (red points). This is clearly an intuitive result, however this method allows a user to rapidly quantify a statement made that a more accurate radar drives the intercept miss distance down, and with a measurable certainty. Note that both the red and blue points diverge as range is increased (i.e. there is a clear trend, but the points do not form a straight line). This is due to the fact that each variable value is selected from Monte Carlo simulation used to populate the multivariate scatter plot, and each point in the diverging trends will have various values selected for the other variables. However, this can be further examined by studying another trend observed from Figure 68. Figure 70 shows a plot of 90% confidence miss distance and gun bore. Notice that at each discrete bore setting, a majority of the less accurate radars have higher miss distances. The interesting trend here is that the intersection of the majority of blue and red points shifts lower with increased bore size, indicating that a guided projectile with a higher bore can tolerate more radar noise for a given intercept miss distance.

The previous example showed that selected radar azimuth and elevation noise accuracies drive the weapon capability, and define a clear tradeoff space with projectile bore size and intercept range. Now, a similar example is shown to determine whether the other two radar noises have a similar impact. Figure 71 shows regions of higher (blue) and lower (red) radar roll rate (phi) and range noises. In a similar fashion

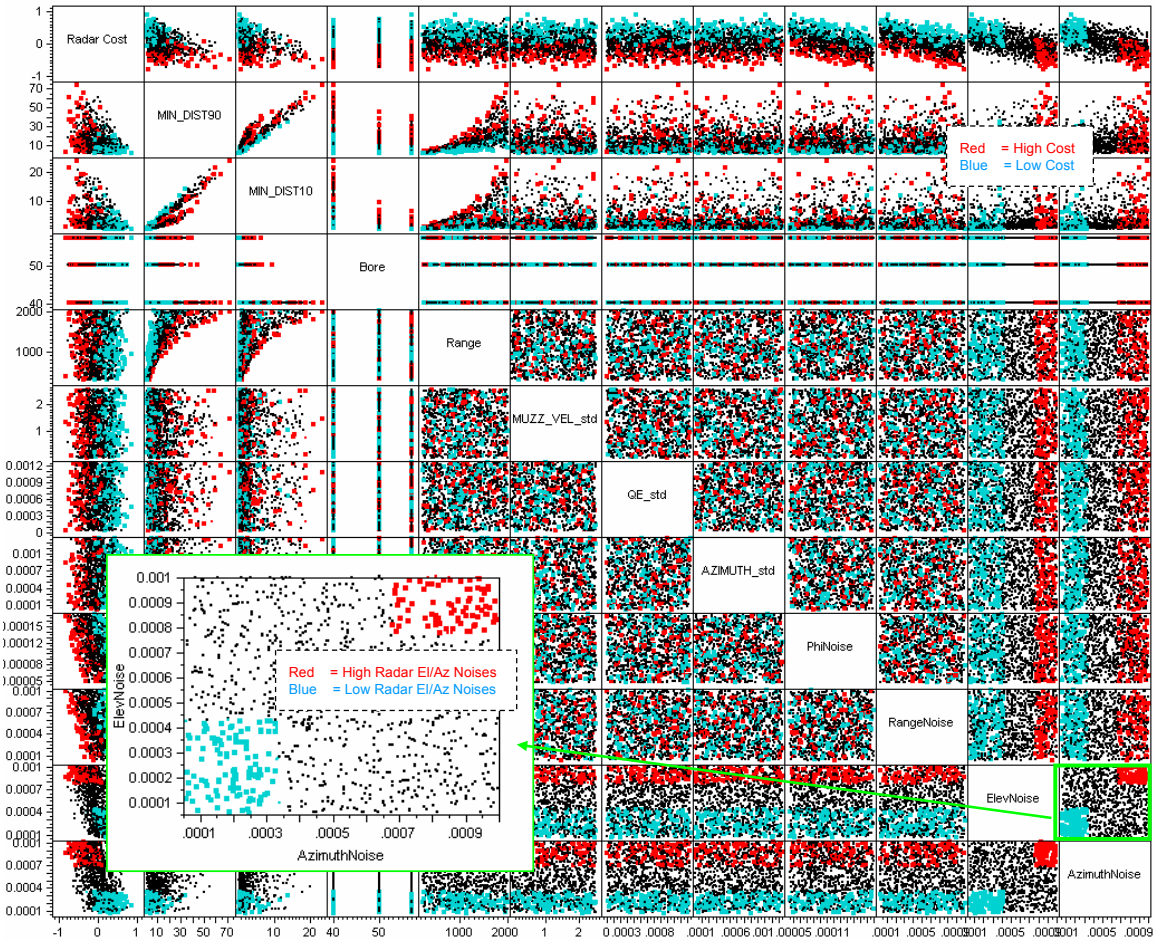

Figure 68: Initial Study - Multivariate Scatterplot DSE, Sorted by Radar Azimuth and Elevation Noises

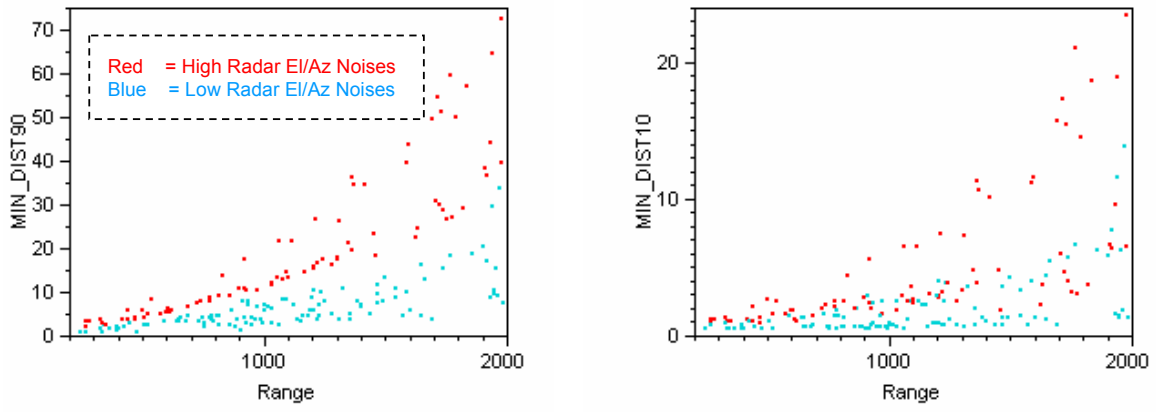

Figure 69: Initial Study - Bivariate Plots of Minimum Miss Distances and Range, Sorted by Radar Azimuth and Elevation Noises

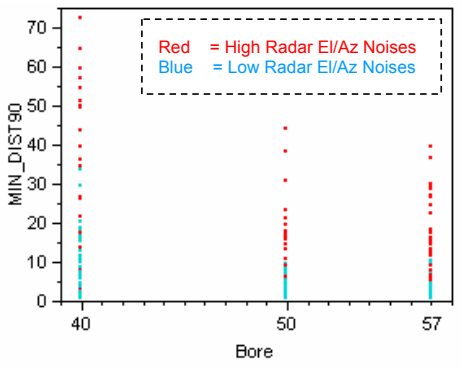

Figure 70: Initial Study - Bivariate Plot of 90% Confidence Miss Distance and Bore, Sorted by Radar Azimuth and Elevation Noises

to the previous example, Figure 72 shows bivariate samples of the resulting design space, showing how minimum miss distance varies with range for both 90% and 10% confidences. There is no evident benefit to selecting more accurate radar roll and range noises with increased range, especially when directly compared to Figure 69.

In a final graphical example exploiting the surrogate models used to create the multivariate scatter plot based design exploration, a study was conducted to isolate the effects of the various bore sizes. Figure 73 shows the design space sorted by bore size, with the 40 mm solutions colored red, the 50 mm ones colored blue, and 57 mm bore size solutions colored black. Even without the color difference, it is evident that increased bore size has a clear advantage of decreasing the miss distance. Figure 74 shows both the 90% and 10% confidence miss distances by bore size. A decreasing "worst case" scenario miss distance decreasing with increased bore size is shown, the effects of which are more prevalent in the 10% confidence miss distance. Figure 75 shows both miss distance confidences by range. Note that the 40 mm bore (red) points rapidly increase in miss distance as range increases for both the 90% and 10% miss distance confidences. However, the advantage of 57 mm over 50 mm bore is not as evident in the 90% miss distance confidence, since with increased range the dispersion of blue and black points is about the same. Looking at the 10% confidence miss distance by range plot for contrast, there is a clear advantage of the 57 mm bore

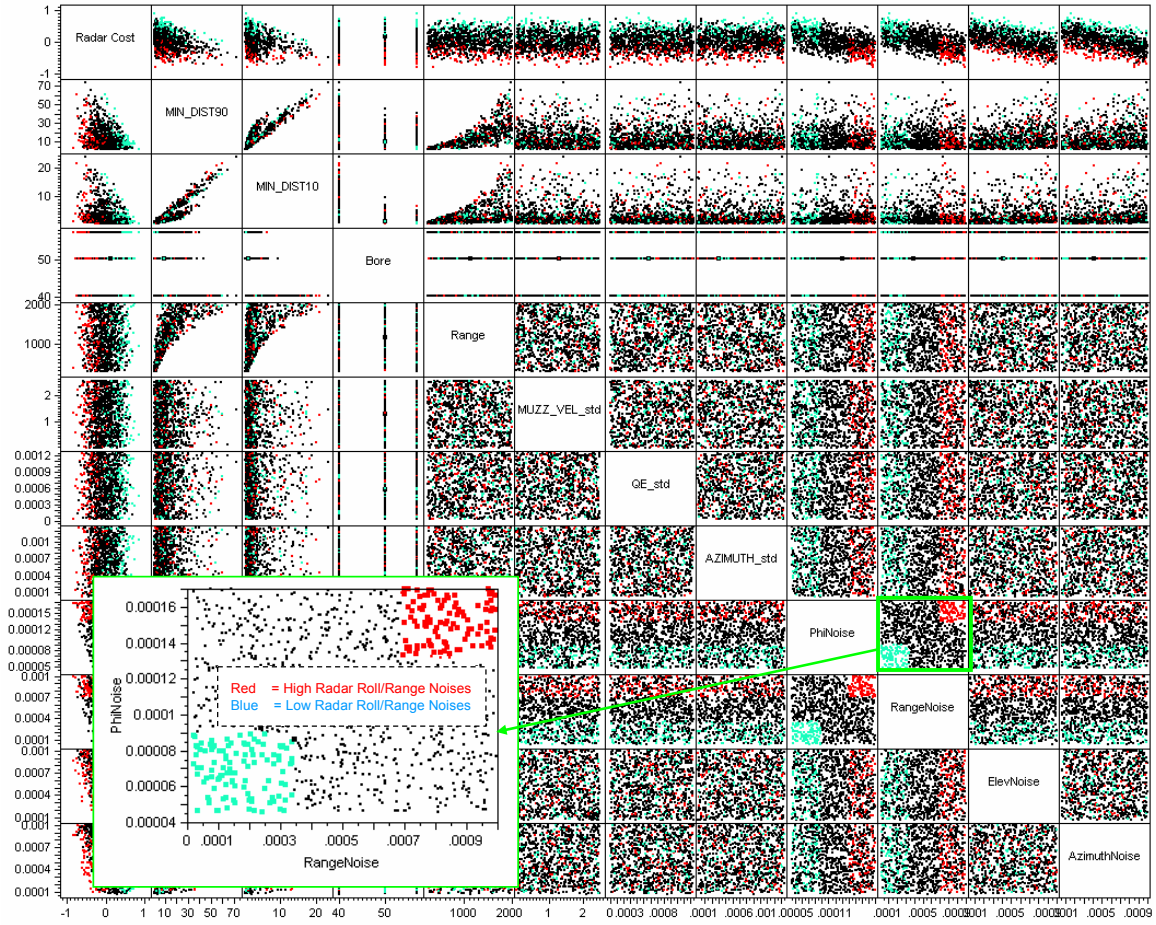

Figure 71: Initial Study - Multivariate Scatterplot DSE, Sorted by Radar Roll and Range Noises

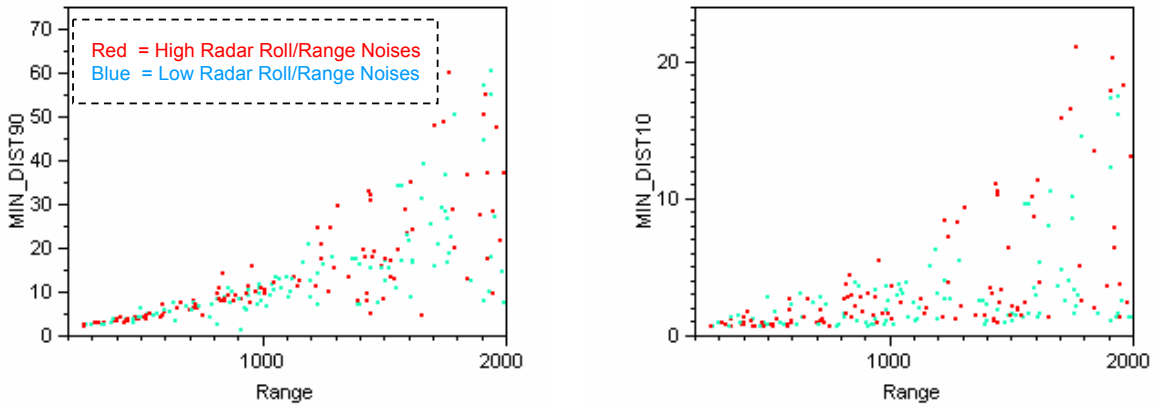

Figure 72: Initial Study - Bivariate Plots of Minimum Miss Distances and Range, Sorted by Radar Roll and Range Noises

over the 50 mm bore, where the dispersion of 57 mm (black) points is not as great with increased range when compared to the 50 mm (blue) points. A more pronounced benefit of increased bore at the lower miss distance confidences may give an indication of the the shape of the CDF, whereby its slope is more gradual with increased bore. This is more evident by studying Figure 76, where the three bores can be compared on a bivariate plot of 90% and 10% miss distance confidences. For the same 90% confidence, a lower 10% confidence is achievable with a larger bore. This has a very clear practical impact. If designing a solution for a single shot kill, 57 mm vs 50 mm bore size does not have as much of an impact, because there is not much difference in their 90% miss distance confidences. However, for a defense system allowing for multiple shots, there is an advantage using the 57 mm over the 50 mm bore projectile, since the value added of each additional bullet has more impact. This methodology clearly enabled the discovery of these tradeoffs.

6.3.4.3 Response Variability Study Concluding Remarks

This purpose of this section was to compare the use of the ANOVA method visualized with Pareto plots and a Monte Carlo simulation design space exploration visualized with a multivariate scatter plot as methods for discovering the variable trade space that drives response variability. The ANOVA method that uses Pareto plots shows a one-dimensional portrayal of the contributions of each variable to the variability of a response. Variables that drive each other can be identified only when certain variables are fixed at their lowest and highest values, with an ANOVA run on the remaining variables. This not only proved to be a very cumbersome process, but also did not yield the tradeoff space between those variables. Running a Monte Carlo simulation, and visualizing the design space on a multivariate scatter plot showed how constraining requirements can identify where design tradeoff spaces lie, and which variables drive the values of other variables. The same variables that were identified

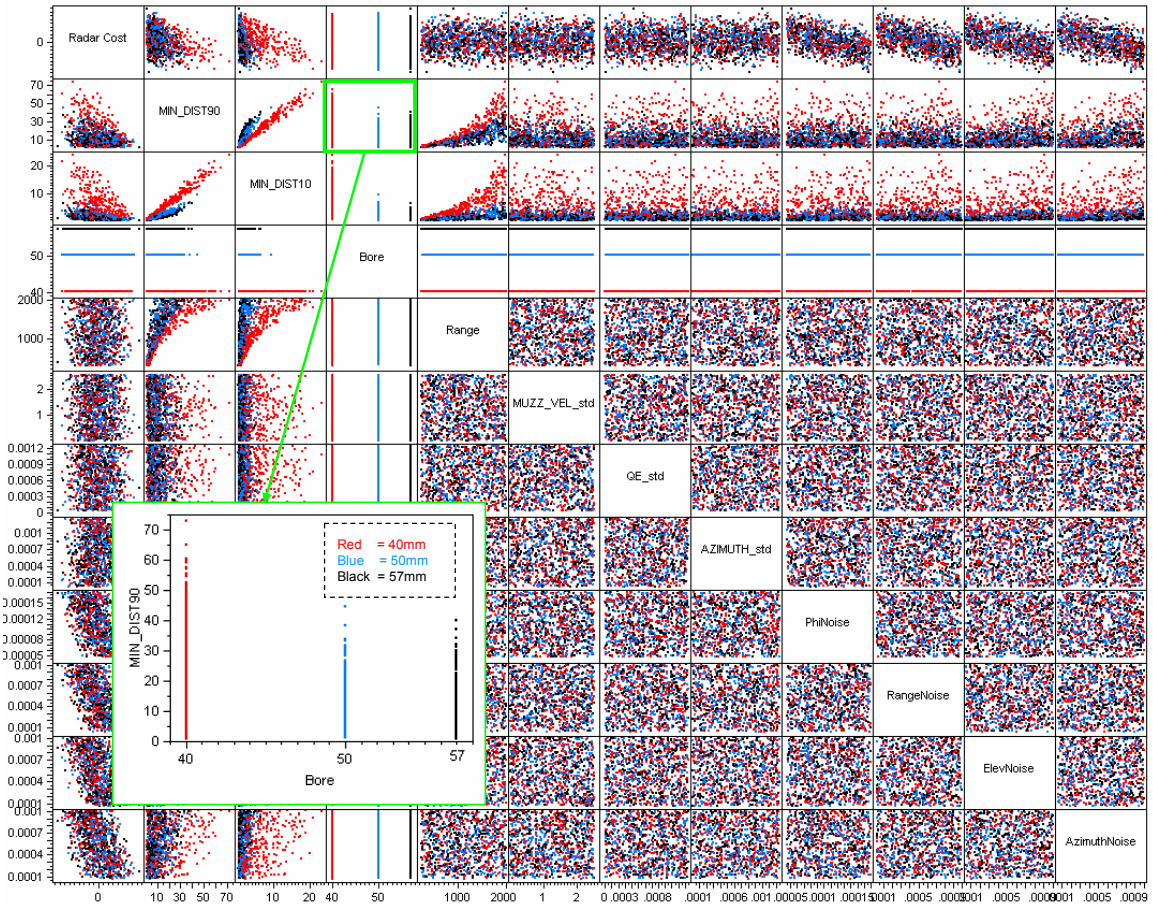

Figure 73: Initial Study - Multivariate Scatterplot DSE, Sorted by Bore

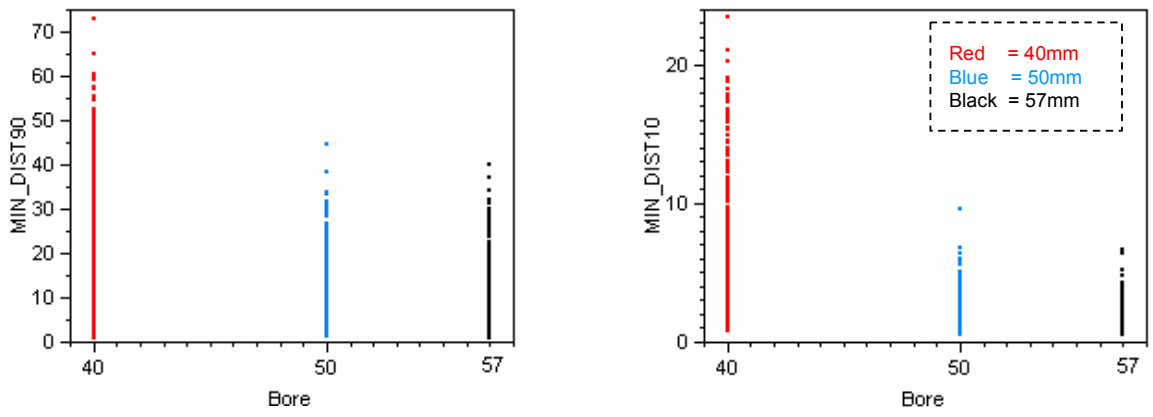

Figure 74: Initial Study - Bivariate Plots of Minimum Miss Distances and Bore, Sorted by Bore

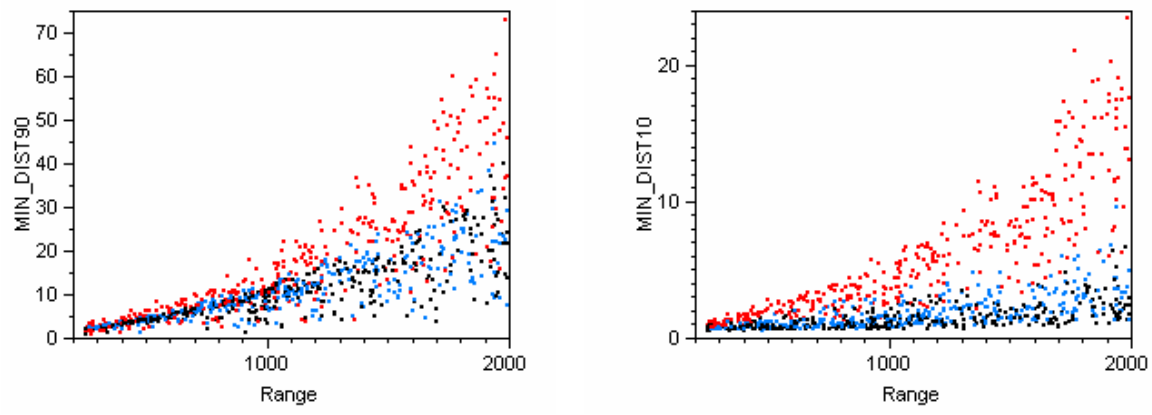

Figure 75: Initial Study - Bivariate Plots of Minimum Miss Distances and Range, Sorted by Bore

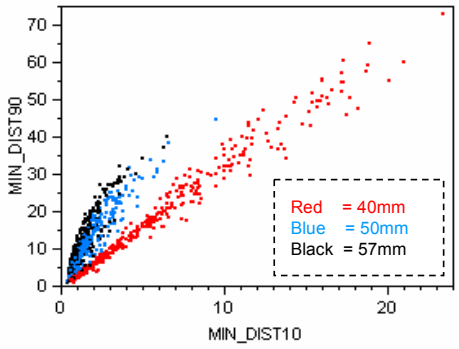

Figure 76: Initial Study - Bivariate Plot of 90% Confidence and 10% Confidence Minimum Miss Distance, Sorted by Bore

as being key drivers on a Pareto plot were also identified on the multivariate scatter plot, however clear tradeoffs were identified using the latter method.

Additionally, a clear benefit of this methodology is the ability to manipulate random functions as independent variables. These random functions result in probabilistic outcomes that can be quantified and bounded in ways previously unavailable. For example, the manipulation of the response CDF can be used to bound the random function independent variables.

6.4 Addition of Radar & Guidance Update Rates

With the methodology showing its usefulness in the previous section, it will now be applied in an attempt to add a degree of freedom to the problem. The next part of the implementation focused on the tradeoff between radar noise and the rate at which the radar and guidance updates occur, With the primary radar noise variables contributing to the variability identified. The radar update rate is the rate at which projectile and target position updates are sent to the fire controller, and the guidance update rate is the rate at which guidance updates are sent to the projectile to allow for course correction. This tradeoff is an important step in determining whether the radar and guidance updates should be included in the parametric capability of the decision hierarchy. Eliminated variables that do not significantly contribute to variability in intercept end game were fixed to default values, shown in Table 15. The gun errors were shown to contribute little compared to the radar noises, and even within the radar noises, two of the four examined proved to provide the majority of the response variability. Therefore these values are fixed, however they are still treated as noises in the 6-DoF code, and therefore still provide an element of variability. In addition for this study, only the 50 mm bore is used.

These restrictions on the design space were necessary to allow for design study to be completed with a limited amount of computing resources, and to focus the

Table 15: Fixed Variables for Radar & Control Update Rate Study

Property	Fixed Value	units
Muzzle Velocity Error (1σ)	8.25	m/s
Firing Azimuth Error (1σ)	0.001	rad
Firing QE Error (1σ)	0.001	rad
Radar Roll Noise (1σ)	87.3	μrad
Radar Range Noise(1σ)	0.001	rad
Bore	50	mm

resources available on fine tuning the parametric models created. For example, with fewer variables needed in the surrogate models, fewer DoE runs would be required when compared with the initial study. With fewer DoE runs than the previous study, more Monte Carlo runs per DoE run could be afforded computationally. This allows for a more precise examination of the statistically based responses. Five hundred Monte Carlo simulations were used for the radar update rate study. For the probability of hit metric which counts the number of hits for each Monte Carlo simulation executed for each DoE run, the resolution is much needed.

This section will be broken down into two sections. The first will simply presume that the projectile controller is slaved to the radar update, in other words the guidance update is set to the radar update. The second part of this section will treat the radar and guidance update rates as independent. In both cases, the radar azimuth and quadrant elevation noises are treated as variable.

6.4.1 Control State Slaved to Radar Update

As stated earlier, this portion of the study focuses on the effects of slaving the projectile controller to the radar update, as opposed to using guidance updates for control. The variable bounds used to examine the effects of radar update rate are given in Table 16. A DoE was created for the 3 continuous variables, including a 15 run CCD, a complimentary 15 run LHS, and 15 random points for a total of 45 runs per each

Table 16: Variables for Radar Update Rate Study with Control State Slaved to Radar Update

Property	Minimum	Maximum	units
Radar Elevation Noise (1σ)	15	150	μrad
Radar Azimuth Noise (1σ)	15	150	μrad
Radar Update Rate	10	100	Hz
Intercept Range	250	2000	m

discrete range setting given in Table 13.

Figure 77 shows a series of surface plots illustrating the study conducted to analyze the effects of radar update rate on required radar accuracy. The three graphics comprising Figure 77 show the required radar update rate varies with intercept range to achieve a desired probability of direct hit, using three notional radar accuracies: advanced, or low radar noise (top), medium radar noise (center), and high radar noise (bottom). A notional P_H of 0.5 is shown as an example to constrain the feasible design space.

For the low radar noise case (top graphic), P_H is not very sensitive to radar update rate. As range increases, there exists a region where only radars with a high radar update rate satisfy the P_H constraint. Also, note how at the very upper bounds of range, even the highest radar update rate does not meet the P_H constraint. With an increased radar noise shown in the center graphic, note how the feasible space above the P_H constraint has diminished. At even higher values of radar noise (bottom graphic), the only feasible design space is with very low intercept ranges. Even a cursory examination of the graphics in Figure 77 should provide an appreciation of using neural network based surrogate models. Capturing this complex design space, with all of its multimodal peaks and discontinuities would have been unimaginable using polynomial fits.

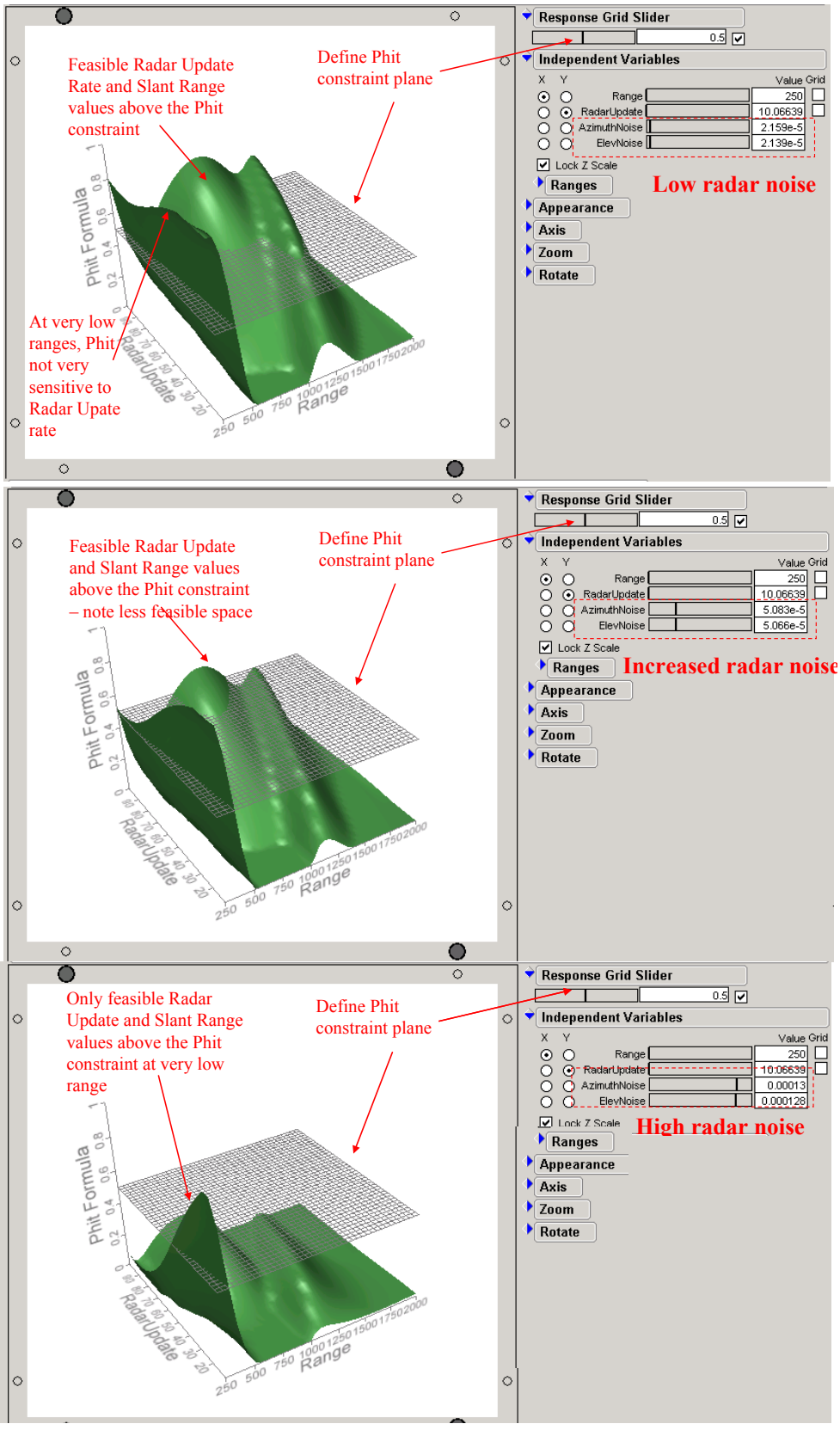

Figure 77: Radar Update Study with Control State Slaved to Radar Update - Surface Plots

Table 17: Variables for Radar Update Study with Independent Radar & Guidance Updates

Property	Minimum	Maximum	units
Radar Elevation Noise (1σ)	0.025	0.500	mrad
Radar Azimuth Noise (1σ)	0.025	0.500	mrad
Radar Update Rate	10	50	Hz
Control Update Rate	90	200	Hz
Intercept Range	500	2500	m

6.4.2 Independent Control and Radar Update Rates

With the importance of radar update established, this section isolates between the effects of the rate of radar position updates and that of the guidance update rate. The higher the frequency of guidance updates, the more corrections the projectile can make to attempt to stay along its intended trajectory. As in the previous section, the radar azimuth and elevation noises and radar update rate are included as variables, but now guidance update rate is included. The bounds selected for the parametric models created for this portion of the study are given in Table 17. An important note to mention at this point is that the originally desired lower bound for control update was 10 Hz, however the 6-DoF simulation tool was not properly set up to handle that lower bound with all other conditions. The value of 90 Hz was selected simply as a lower bound for the capability of the simulation.

6.4.2.1 Surrogate Modeling and Design Space Exploration

To create the neural network surrogate models, a DoE was created for the 4 continuous variables, including a 25 run CCD, a complimentary 25 run LHS, and 25 random points for a total of 75 runs per each discrete range setting. A prediction profiler is given in Figure 78, showing an example setting for how radar capability drives probability of hit. The individual contributions of each variable can be identified. As noted earlier, there will be a minimum distance at which the controller on the projectile

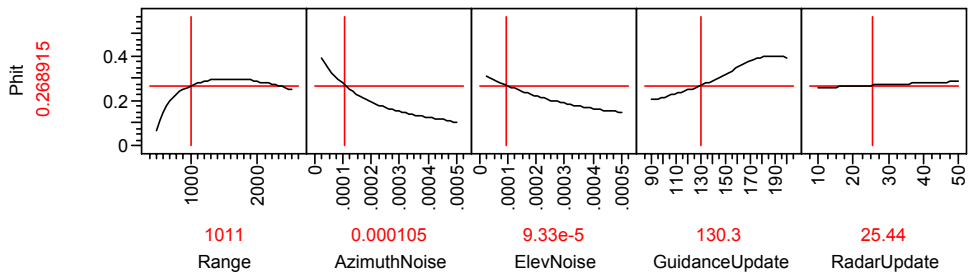

Figure 78: Radar Update Study with Independent Radar & Guidance Updates - Prediction Profiler

can engage and have a steering effect beyond the unguided ballistic path. Clearly reducing the amount of radar noise has a positive effect of increasing the probability of a direct hit, but the impact of azimuth noise clearly has more impact than the elevation noise. The prediction profiler also shows the importance of independently studying the guidance and radar updates. Given the settings of the other variables in this one example, it is just barely evident of the impact of increased on radar update rate on P_H, however increasing the guidance update rate would greatly increase P_H. This graphic gives another appreciation for capturing the multimodal nature of the design space. For instance, holding all other variables constant, there is a benefit to P_H to increasing the guidance update rate up until about 170 Hz, where increasing past that does not provide any additional benefit.

The graphics in Figure 79 show the benefit of using the surface plots to view the effects of two variables at the same time on a response. The surface plot on the left shows azimuth noise and range on P_H. This plot is a good example of showing the minimum steerable intercept range. At poorer (i.e. higher) azimuth noises, there is less variability in P_H with range. However at the much more accurate azimuth noises, effective intercept range bounds can be identified. Also in the left surface plot of Figure 79 a notional P_H constraint is placed roughly at 0.15, and the 3-D surface above that indicates the feasible tradeoff between radar azimuth noise and intercept range. An interesting note on this is that at the intercept range providing the greatest

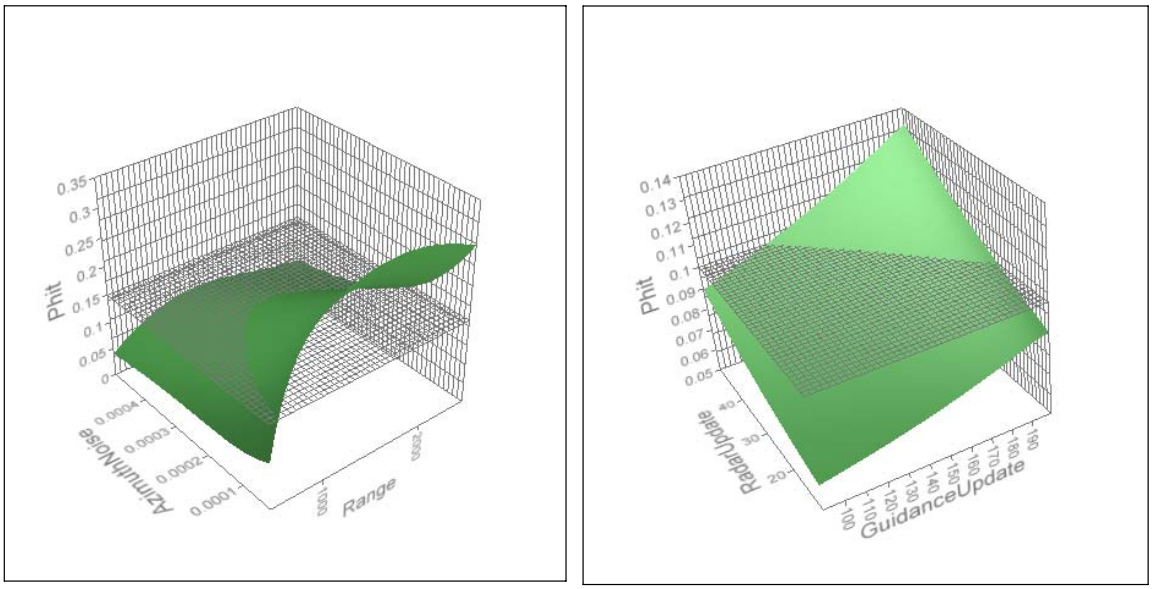

Figure 79: Radar Update Study with Independent Radar & Guidance Updates - Surface Profilers

P_H (about 1500 m), a clear tradeoff curve showing exactly how much radar azimuth noise can be tolerated given the response constraint. This is of course assuming that the other variables are held constant - manipulating those variables would certainly shift the surface. The surface plot on the right side of Figure 79 shows the effects of both radar and guidance update rates on P_H. For the settings of the other variables held constant, there is a benefit to having high radar and guidance update rates. That is certainly the obvious conclusion, however this shows the importance of including these two degrees of freedom in this study.

6.4.2.2 Response Variability Contribution of Variables

A similar response variability study conducted earlier to define the CDF shape is now conducted for this new problem, however here only the contribution of variability to P_H is included as the measure of merit. Figure 80 shows a Pareto plot listing the variables for this portion of the study in order of importance with associated measure of contribution. The two radar noises top the list (radar azimuth noise provides about 22% variability, followed by radar elevation noise at about 10%). Next is the guidance

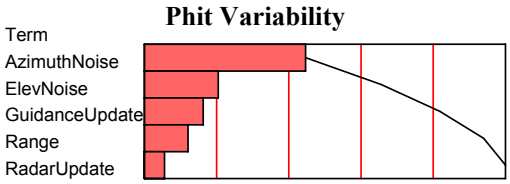

Figure 80: Radar Update Study with Independent Radar & Guidance Updates - Pareto plot

update rate providing about 8%, intercept range at about 6%, and radar update rate at 2% contributions to P_H variability. This is a useful way to prioritize the variables of interest, but it is a very one-dimensional way to make assessments, and begs an important question. For example, in the Pareto plot, the number one driver of P_H variability is radar azimuth noise, but is there another key variable that drives radar azimuth noise? The answer can be found by utilizing the multivariate scatter plot approach to design space exploration.

Figure 81 shows a multivariate scatter plot matrix populated using a Monte Carlo simulation on the neural network surrogate models created for this portion of the study. To illustrate, all of the points in the design space with a P_H above about 0.22 are highlighted red. The points are highlighted in the first row, but the design points corresponding to that value show up red in each of the other bivariate plots. Figure 82 points out two important findings using this multivariate method. These two bivariate plots are taken directly off of the multivariate plot, with the design points not meeting the P_H requirement hidden for clarity. On the left side, elevation noise is shown on a bivariate plot along with guidance update rate, and the right graphic shows azimuth noise compared with guidance update rate. Assuming that less accurate radar accuracy (i.e. higher elevation and azimuth noises) and a lower guidance update rate is desirable for cost and complexity purposes, a black dotted line shows the non-dominated design points. Now it is possible to assess the relative importance of variables to the variability of a response. Azimuth noise was shown

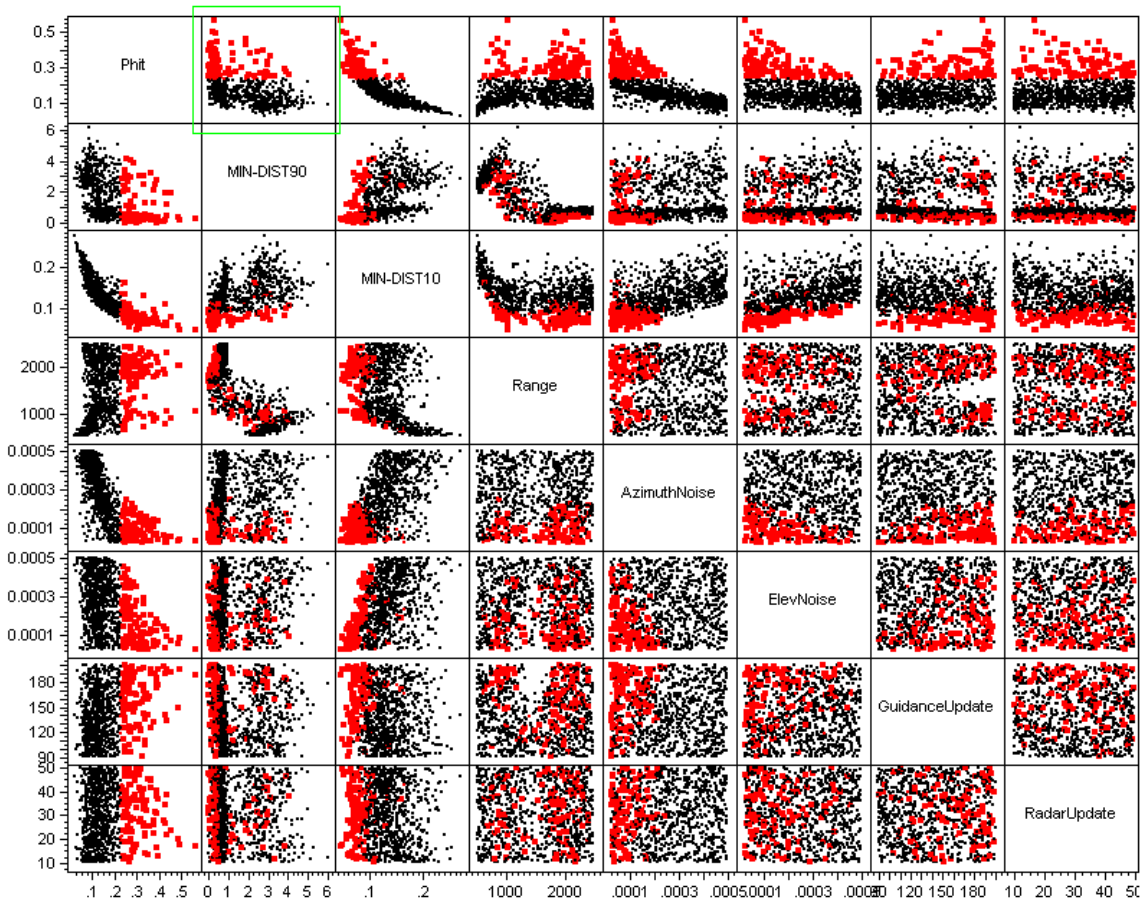

Figure 81: Radar Update Study with Independent Radar & Guidance Updates - Multivariate Scatter Plot with P_H Region of Interest in Red

in the Pareto plot in Figure 80 to be the biggest driver for P_H variability, but using the multivariate method, guidance update proves to be a very important driver in the radar accuracy. The radar accuracies do not stand alone, and their impacts on a guided projectile's performance capability clearly depend on the rates of both radar and guidance updates.

6.5 Effect of Firing Multiple Projectiles

This section is dedicated to taking the results presented for quantifying the ability to hit a target with a single round, and determining the probability of hitting the target with at least one projectile if multiple are fired using the methodology discussed

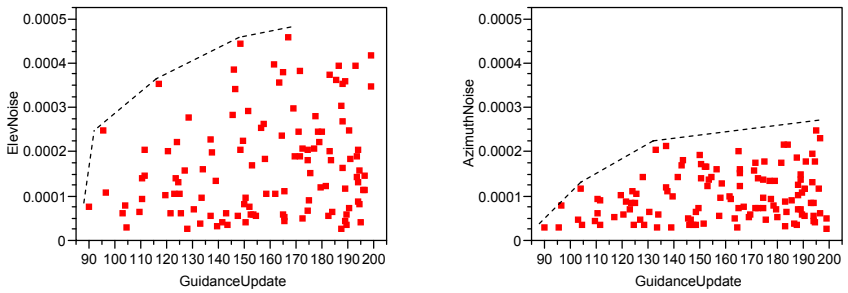

Figure 82: Radar Update Study with Independent Radar & Guidance Updates - Bivariate Plots of Radar Accuracies and Guidance Update

in Section 5.3.4. This section applies the methodology in this thesis to answer the specific question, *what does the single shot probability of hit (SSPH) have to be if many bullets are fired*? Taking this down a level in the design hierarchy, the question can then be asked, *what is the tradeoff in the single projectile design space when using more than one shot fired to achieve a multiple shot probability of hit (MSPH)*?

Equation 28 from Section 5.3.4 is used in this section to quantify the probability of directly hitting the target with at least one projectile if multiple are fired, assuming that the probability of hitting the target is the same for each projectile (a very common assumption made when dealing with "bursts" of projectiles [92]). The maximum number of projectiles that can be fired is a function of the firing rate, and the length of time of fire. Equation 33 (from Appendix C) is used to calculate firing rate as a function of gun bore. In order to use the assumption that each of the projectiles intercept the target with the same probability of hit, a suitable "engagement window" must also be assumed. This section arbitrarily assumes an engagement window of 2 seconds, meaning that any projectiles fired within that window will cross the target plane at (essentially) the same time. This engagement window could have any other value.

For the sake of example, this section will use the surrogate models generated in Section 6.4.2 to show how the methodology used in this thesis can be applied to

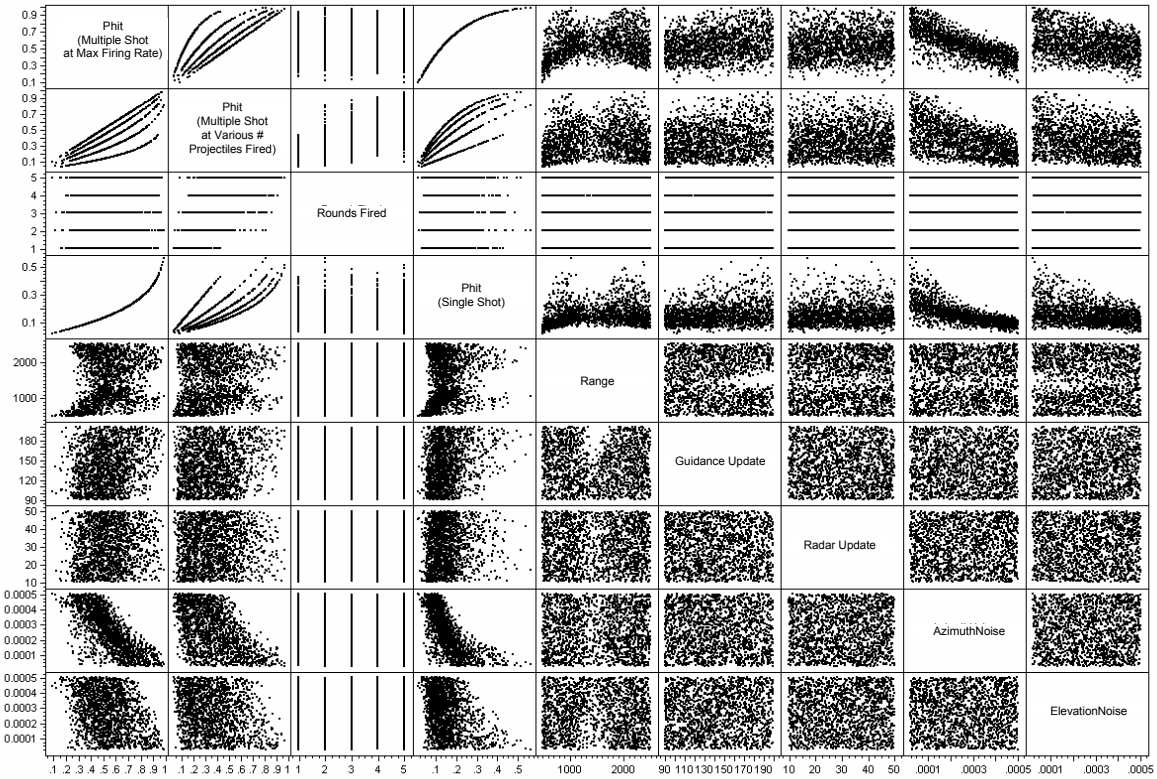

Figure 83: Multiple Projectiles Study - Multivariate Scatter Plot Design Space Exploration

showing tradeoffs between number of projectiles fired and the required accuracy of each projectile. This includes using the variables and bounds given in Table 17. However, now not only is the probability of hit of a single projectile tracked, but the probability that a single shot will hit if many are fired. Using the number of rounds fired at the maximum firing rate as the maximum number of rounds possible, part of the design space exploration includes every integer from 1 to that maximum number fired. As was previously done, a Monte Carlo simulation was used to conduct a design space exploration, using a multivariate scatter plot as shown in Figure 83. Note that for the assumptions used to create these results (i.e. the variable bounds, the engagement window, etc...), the maximum number of shots fired is 5. Therefore, this design space exploration uses the same radar variable bounds using between (and including) 1 and 5 projectiles, and then tracking the responses.

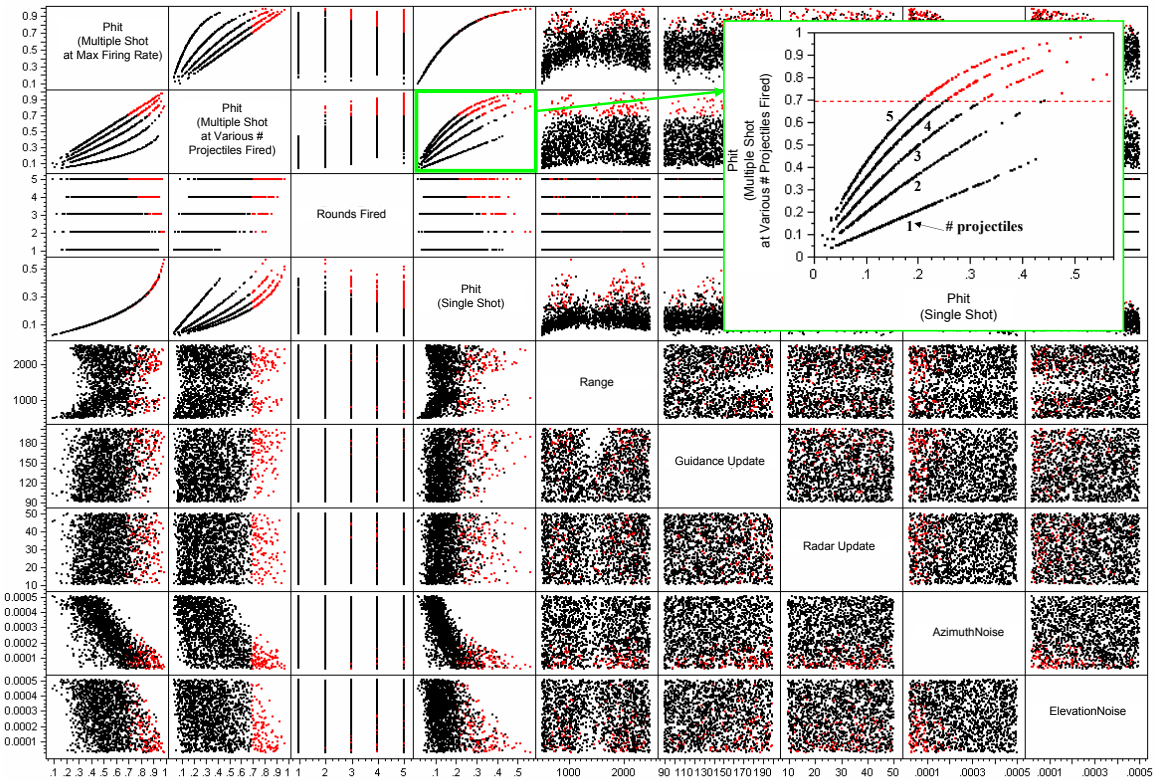

Figure 84: Multiple Projectiles Study - Selection of Required MSPH

Figure 84 shows how an a desired multiple shot probability of hit can be defined, this example showing an MSPH of 0.70. Note that the solution using only 1 projectile does not meet the MSPH requirement cutoff; the maximum attainable SSPH is about 0.42 using only one shot. Another interesting observation made is that as the number of shots is increased, the benefit in MSPH increases less. This figure is reminiscent of Figure 20 (Section 2.3.3), in which the probability of hitting or destroying the target with one weapon (or sortie) is a function of number of weapons (or sorties), for varying SSPH. Figure 85 then isolates the feasible designs that meet the MSPH requirement, hiding all other infeasible points, and color grouping the remaining design points by number of shots fired. Interesting findings appear in the multivariate plot, shown as bivariate plots for clearer examination in the remaining figures in this section.

The tradeoff between the SSPH and the radar properties is given in Figure 86. For both radar accuracy plots (the top two), with fewer number of shots fired the

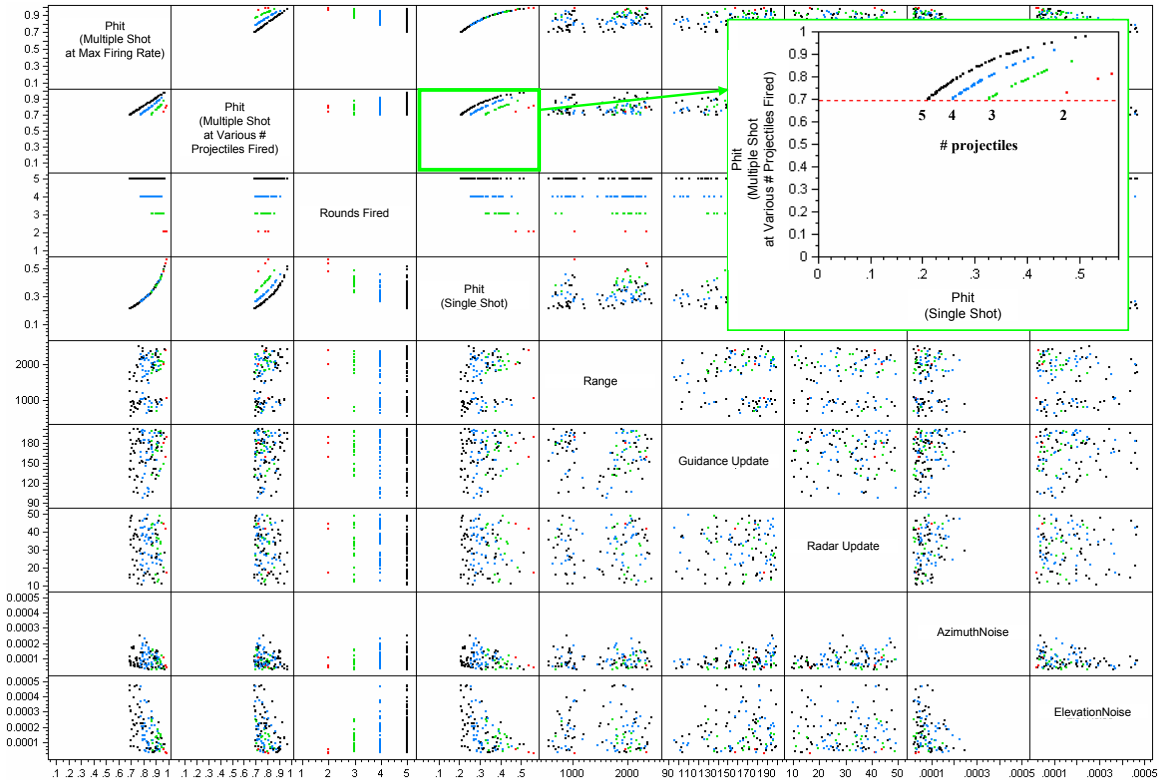

Figure 85: Multiple Projectiles Study - Feasible Design Space Isolated and Grouped by Shots Fired

radar noises are driven lower. This means that the more shots are fired, more noise error can be tolerated in the radar accuracy. The 2 projectile shot solution occupies only the very top left corners of the plots, with more shots fired spreading to higher tolerated radar noise with decreased SSPH. Note that as was pointed out in earlier sections, the design space is more sensitive to variations in radar azimuth noise than of elevation noise, which is indicated in Figure 86 by the fact that higher elevation noises are tolerated than azimuth noises. This is of course more evident with an increased number of projectiles fired. The bottom two plots in Figure 86 show SSPH as a function of both guidance and radar update rates. As the guidance update rate is reduced, note that more projectile shots are required. This same conclusion can not be made of the radar update rate. The reader may have already noticed that one of the 2 shot (red) points is actually shown as a small square. This is shown to illustrate that when using this method, one can easily select one of the design points in one of the dimensions, and immediately see where it is in all other dimensions. The point selected here is the one with the highest required SSPH in the azimuth noise plot (top left). Note that this same design point has the lowest azimuth and elevation noises, and also requires a very high guidance update rate. A high radar update is not required for this design point, however this is not surprising as the radar update rate was found to contribute less to performance variability in previous sections (see Figure 80).

As in previous sections, the radar properties are shown in Figure 87. The left plot shows the two radar accuracies together. With few projectiles, the design space constrains itself to the origin (i.e. fewer projectile shots requires less radar noise and more accurate projectile). With increased number of shots, the feasible design space opens up to allow less accurate radars. The right plot shows the guidance and radar update rates. Here, it is only evident that fewer projectiles constrain the guidance update rate, while not affecting the radar update rate as significantly. The two plots

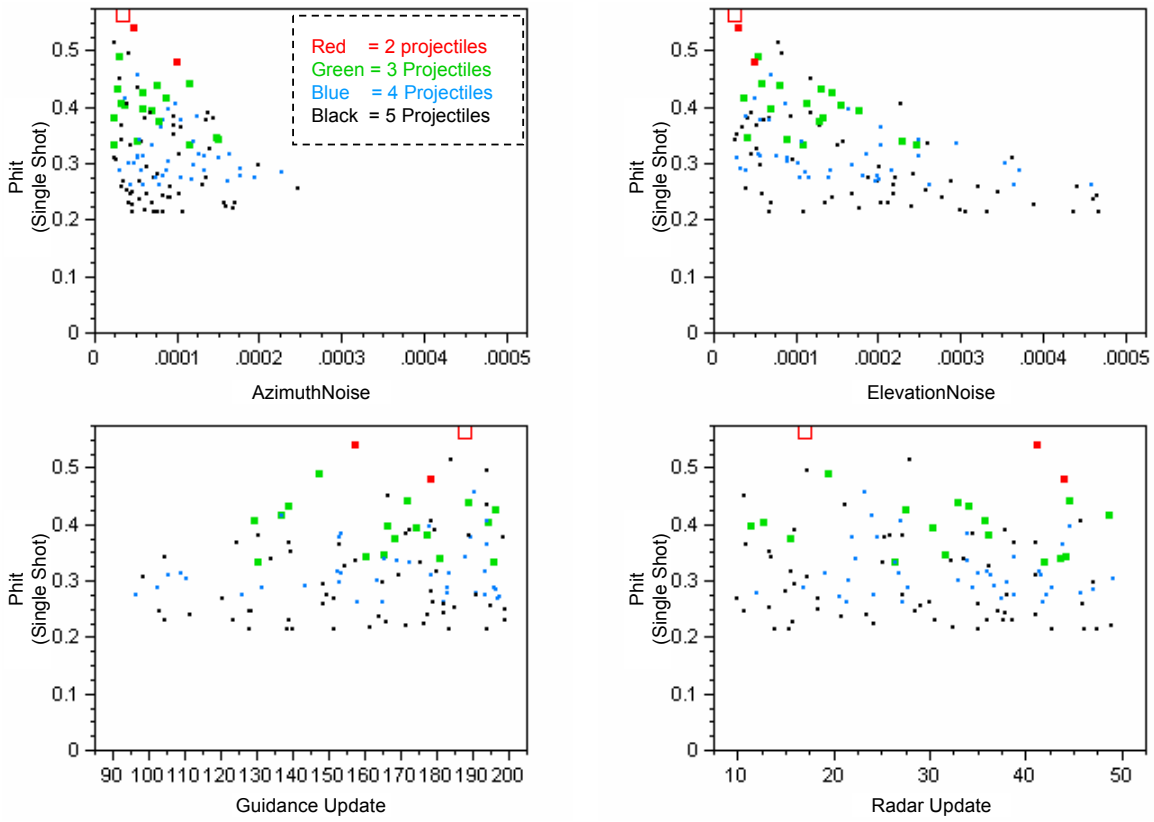

Figure 86: Multiple Projectiles Study - SSPH vs. Radar Properties, Grouped by Shots Fired

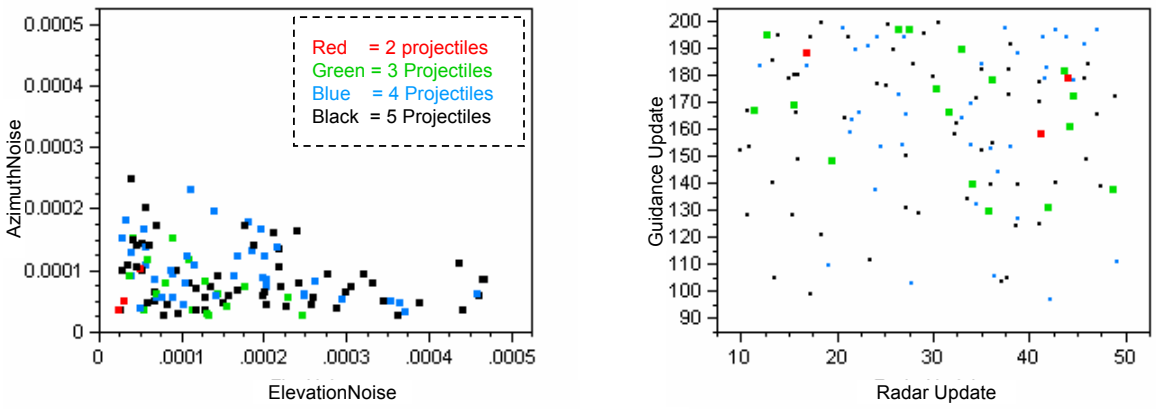

Figure 87: Multiple Projectiles Study - Radar Accuracies (L) & Update Rates (R), Grouped by Shots Fired

in Figure 87 show that there is not much distinction between the design spaces of using 4 versus 5 projectile shots. This is where the decision maker can decide whether the increased cost of firing another shot (i.e. making use of the maximum possible rate of fire) is worth a very minimal increase in MSPH (as first shown in Figure 85).

6.6 Subsystem Level Radar Properties

The goal of this section is to capture the design space of the radar system properties that drive the radar noise errors, as well as radar size and cost. The ultimate goal is to incorporate these elements into the completed system-of-systems hierarchy, and have the ability to study how radar subsystem level properties affect radar performance, which directly affect the defense system's overall performance capability. The radar properties considered for the design space exploration are the ones discussed in Section 2.7 for signal-to-noise given in Equation 14, and the measurement error standard deviation for an interferometer radar given in Equation 18. Table 18 lists the variables used for the radar subsystem level study. The bounds selected were based on a study conducted by Holder [76] to select the radar properties for a command guided bullet. Using those variable bounds, the equations used describe radar capability and can be manipulated using the prediction profiler shown in Figure 88, similar to the type used

Table 18: Variables Used for Radar Subsystem Study

Property	Minimum	Maximum	units
Power (average)	100	250	W
Gain (transmit)	12	50	dB
Gain (receive)	15	40	dB
Frequency	14	18	GHz
Range	500	2000	m
RCS	-25	-15	dBsm
Dwell Time	0.001	0.005	sec
Distance between Antenna Element Arrays	0.5	10.0	m

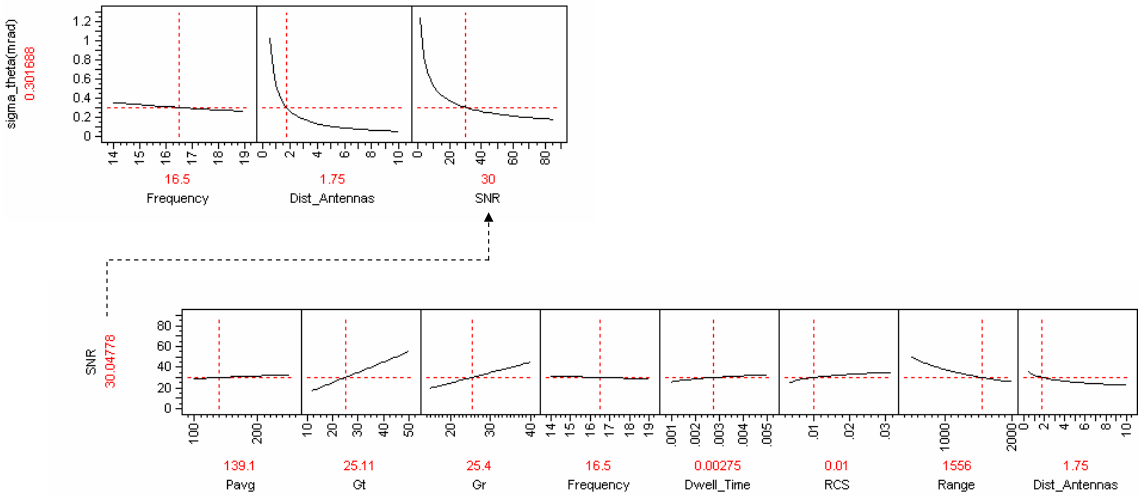

Figure 88: Prediction Profiler for Radar Subsystem Study

to manipulate surrogate models. In this case however, direct equations are used in lieu of a modeling and simulation tool, and surrogate models are not necessary. Note that many of the radar properties are used to calculate signal-to-noise ratio, which in turn is used to calculate the measurement standard deviation error (referred to as "sigma_theta" in many of the graphics in this section). Linking the equations together in a prediction profiler environment allows for direct calculation of measurement error using the radar properties, with the in between step of calculating signal-to-noise ratio handled internally.

The design space for the radar subsystem is explored using a Monte Carlo simulation, and visualized using the multivariate scatter plot technique shown in Figure 89. Note that the dependent responses in this design space are included in the red box, and are the radar signal-to-noise ratio, the angular measurement error standard deviation ("sigma_theta" on the multivariate plot), the antenna aperture area, and the radar cost. The dependent variable values outlined in the red box are calculated using the independent variables in the blue box, which are samples from a uniform distribution. Each of the remaining scatter plots show the design space of each of the response/variable combinations. Even at this level in the hierarchy, the same top-down design methodology can be applied, as is shown in Figure 90 where a maximum acceptable angular measurement error capability is defined at 0.05 mrad, and then a very tight cost constraint is applied at $4M (blue points) to differentiate from the more expensive design that meet the accuracy constraint (red points). The remaining design points that do not meet these standards are hidden for clarity.

Figure 91 shows some of the interesting findings from this example, comparing the design points of two capability definitions (low angle measurement at low and high acceptable cost). The top left plot shows the variation of radar cost and aperture area. There is a clear trend of limiting aperture area when limiting cost. The top right plot shows the variation of the distance between antennas and the signal-to-noise ratio. For feasible design points that meet the radar noise constraints, a lower signal-to-noise ratio is tolerable only with an increase in the distance between antenna element arrays (i.e. a larger radar), with a dashed line included to accentuate the trend. However, comparing the two cost constraints, we see clearly that having a lower cost constraint limits how close the antennas can be, in this case there are no blue (low cost) points below about 6 m antenna array separation. The bottom right plot shows the desired capability in terms of antenna transmit and receive gains. For all solutions shown there is a clear tradeoff frontier between the gains, however limiting

cost places an upper limit on the receive gain, leaving the remaining blue trend as the feasible space (recall from Section 5.3.3 that receive gain directly impacts the number of radar antenna element arrays, therefore also the cost of the radar). The last plot on Figure 91 on the bottom left shows the distance between antennas tradeoff with antenna receive gain. The desire to limit cost clearly limits the receive gain, however this drives the distance between antennas higher. By comparing the bottom left and top left plots in Figure 91, it is clear that the difference between the high and low cost constraints in the distance between antennas is very minimal (about 1 m), but would come a very large cost (the low cost constraint was set at \$4M, but the remaining design points range up \$50M).

This example shows the important tradeoff between radar capability and radar *size*; i.e. the larger the distance between radar antenna array elements, the larger the radar, hence the more accurate the radar. This example is another good argument for this approach: when the design space is filled using a Monte Carlo simulation, using the multivariate scatter plot to visualize the design space allows any combination of variables and responses to be studied simultaneously - and every term, both variable and response can be treated as independent variables.

Regions of low and high radar frequencies are selected in the design space in Figure 92, with all intermediate frequencies hidden for clarity. Interesting tradeoff spaces are shown in bivariate selections in Figure 93. The top left plot shows that for a given radar cost, a higher frequency tends toward a small antenna aperture area. The top right plot shows that for a given measurement accuracy, a higher frequency allows for a smaller distance between antenna element arrays. On the bottom left plot, for a given receive gain, a higher frequency reduces the aperture size. The bottom right plot serves almost as a histogram, showing the maximum aperture area for the two frequencies.

Another example of exploring the effects of selecting radar properties is shown

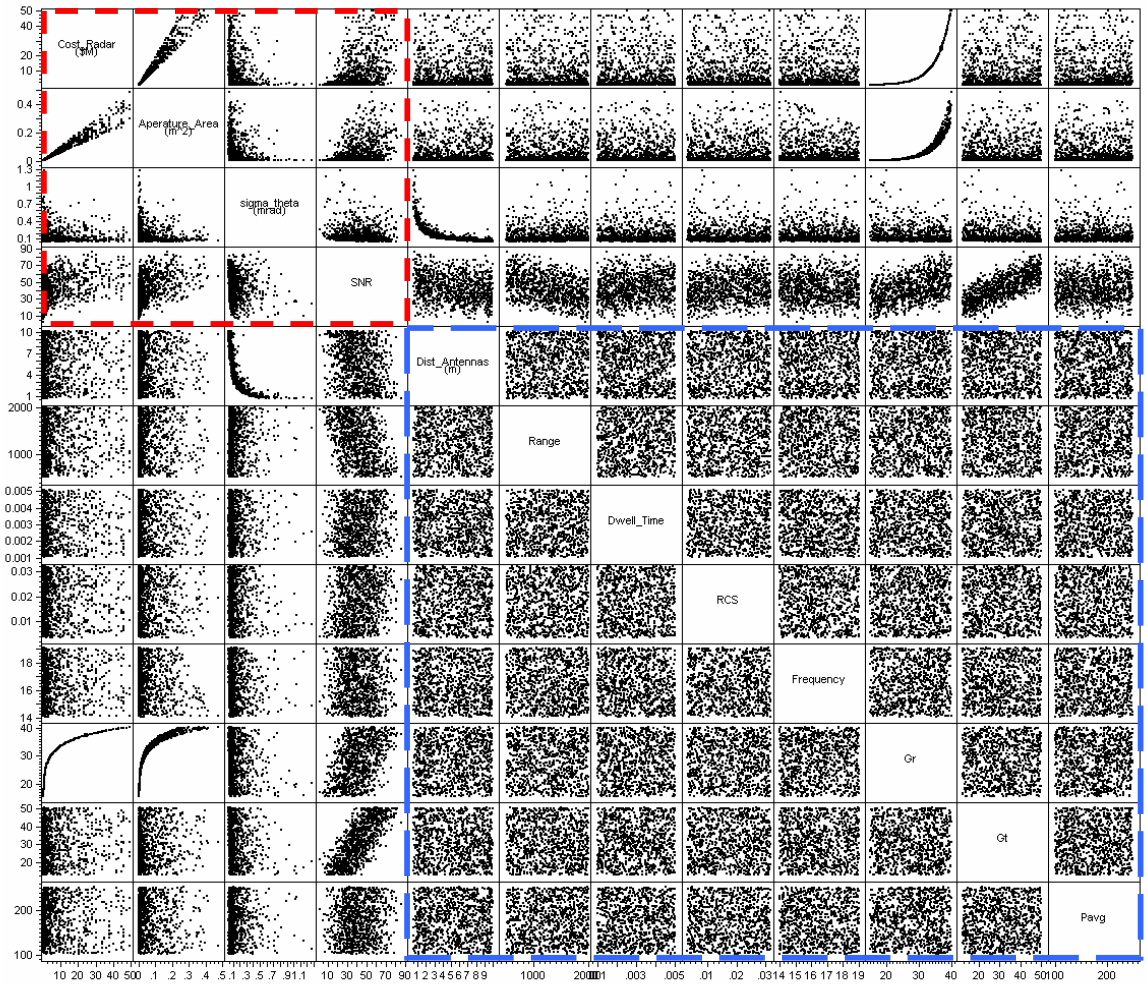

Figure 89: Radar Subsystem Study - Multivariate Scatter Plot Design Space Exploration

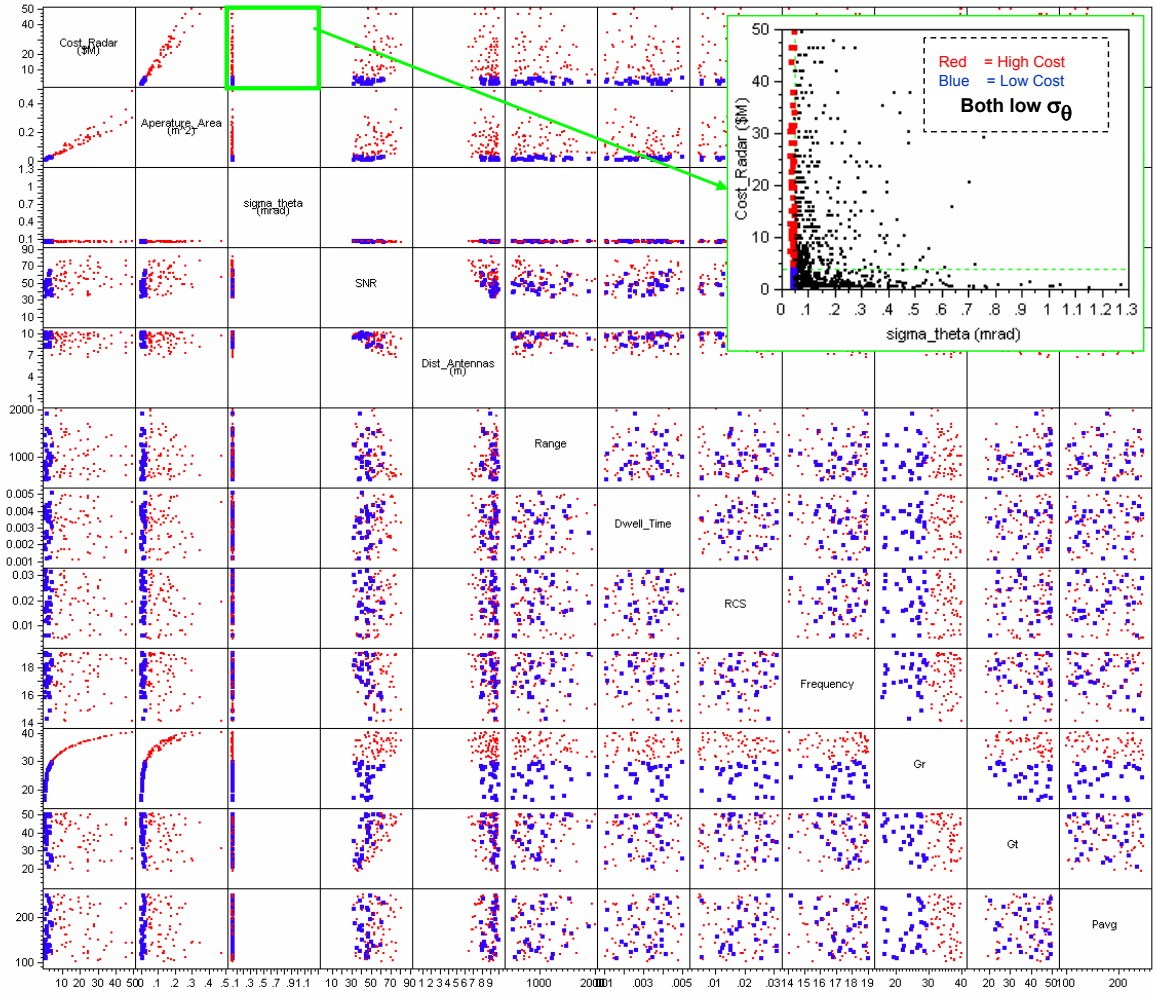

Figure 90: Radar Subsystem Study - Radar Error Capability Defined

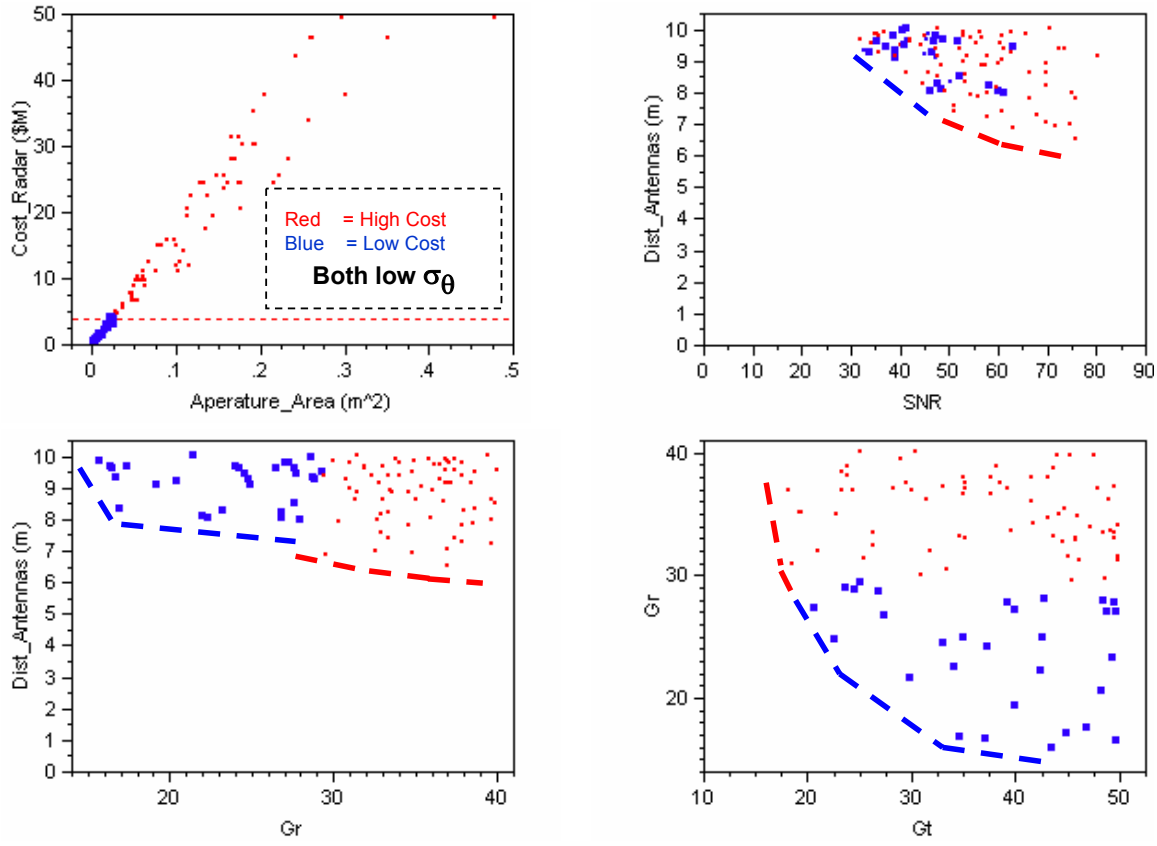

Figure 91: Radar Subsystem Study - Design Space for Radar Error Capability Requirement

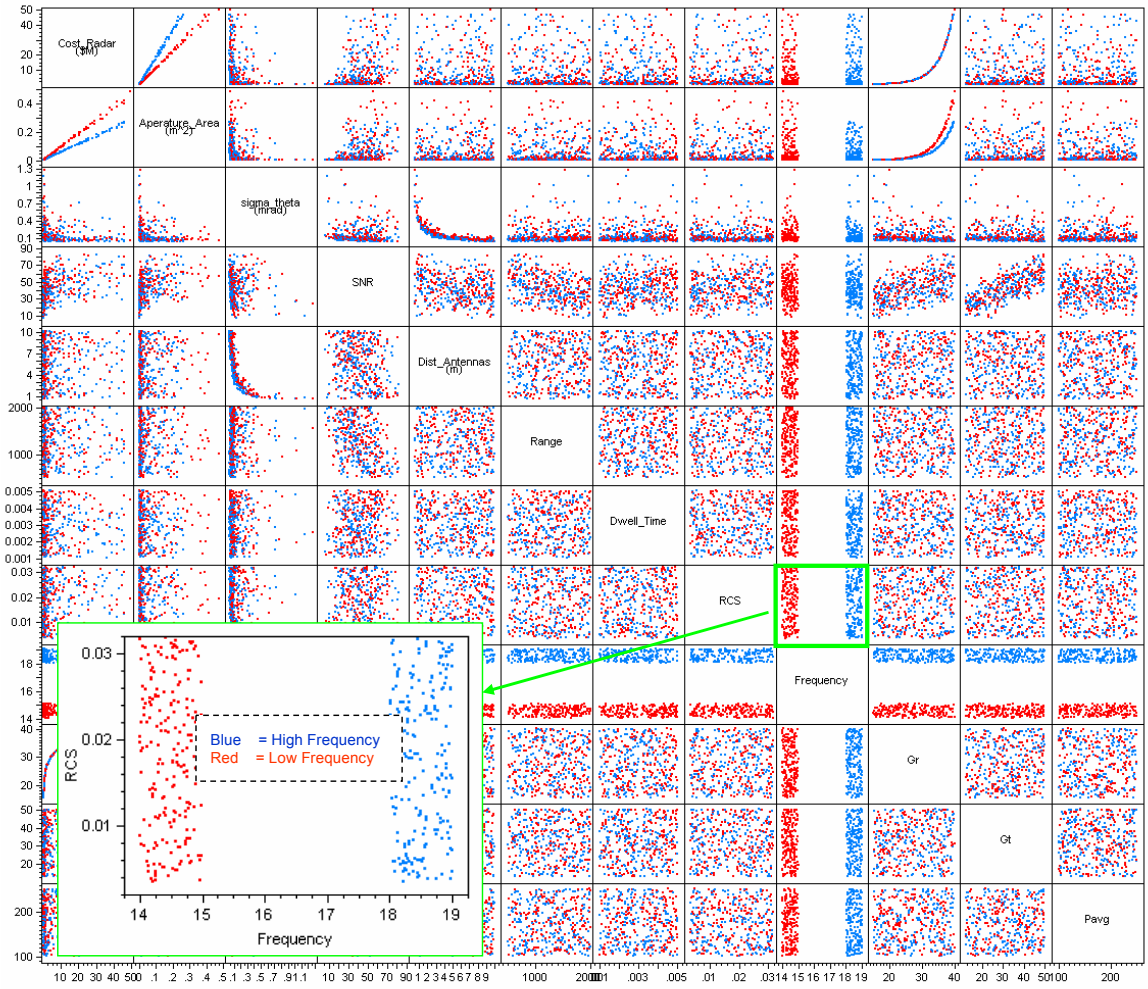

Figure 92: Radar Subsystem Study - Regions of Low and High Frequencies are Selected

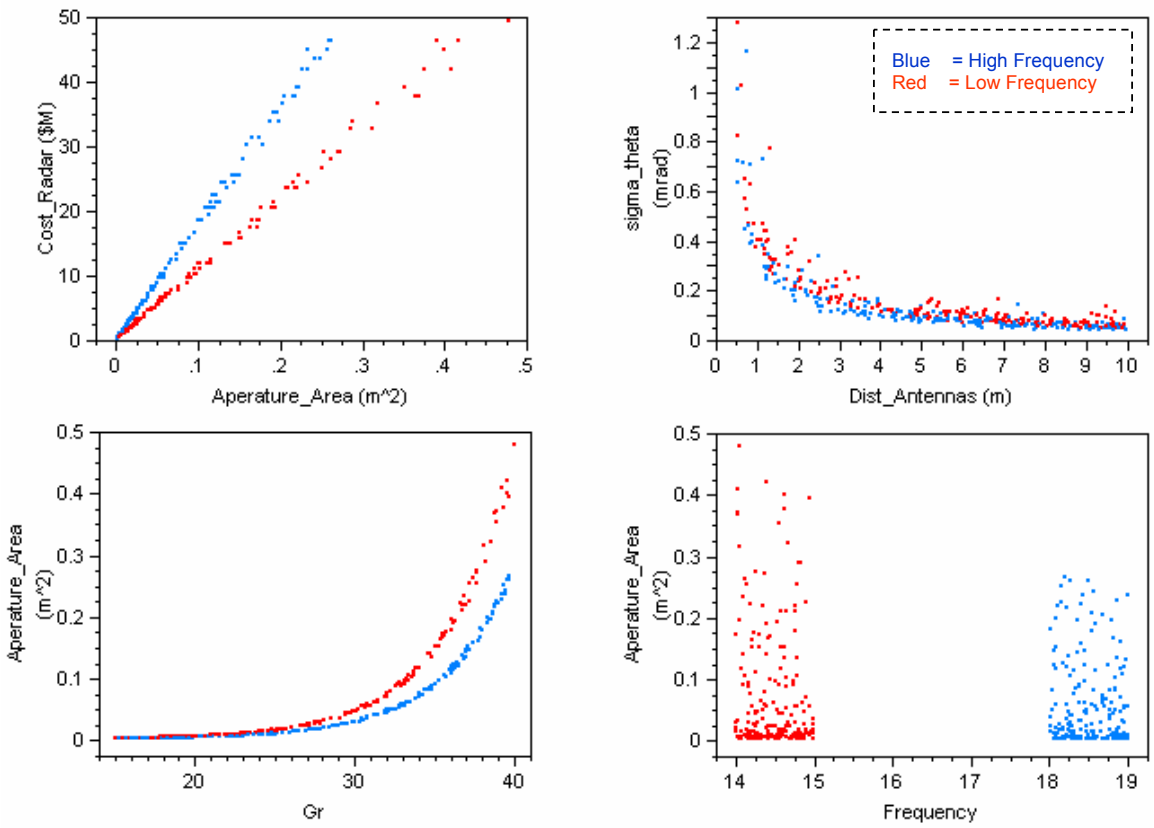

Figure 93: Radar Subsystem Study - Regions of Low and High Frequencies are Selected

in Figure 94 in which regions of low and high antenna gains (both transmit and receive) are selected. Important findings that emerged from the multivariate scatter plot are shown as bivariate plots in Figure 95. The top left plot shows the tradeoff between radar noise and the distance between antennas. At the lower bound of the distance between antennas, a higher gain allows for less measurement noise, however this impact is less evident as antenna separation increases. Therefore, higher gains allow for a smaller radar with same capability - however cost is not shown here, but examining the entire multivariate plot in Figure 94, there is a clear order of magnitude increase in cost for the higher gains selected. The top right plot of Figure 95 shows the variation of radar noise with range. Looking at all of the solutions, as range increases there is more spread of radar measurement error, i.e. increased potential for more radar noise. It is evident that with increased antenna gain, there is less variation of radar noise with range. This means that *higher gains enable a more robust solution* - a radar with accuracy that operates independent of the range of the projectile it is tracking. The bottom left graphic shows the tradeoff space between radar noise and signal-to-noise ratio. Here it is evident that radar noise is more sensitive to signal-to-noise at low antenna gains, and clearly higher gains provide less error and a higher signal-to-noise ratio. The group of low gain design points was identified at the extreme corner of high noise and low signal-to-noise, which identifies a clear trend in the plot in the bottom right corner, showing the variation of RCS with frequency. Without the high noise/low signal-to-noise designs identified, there does not seem to be any trends. However with those points identified, a clear trend emerges showing how with decreased target RCS, the design space opens to lower radar frequencies (this again is for the low gain, high noise, low signal-to-noise designs).

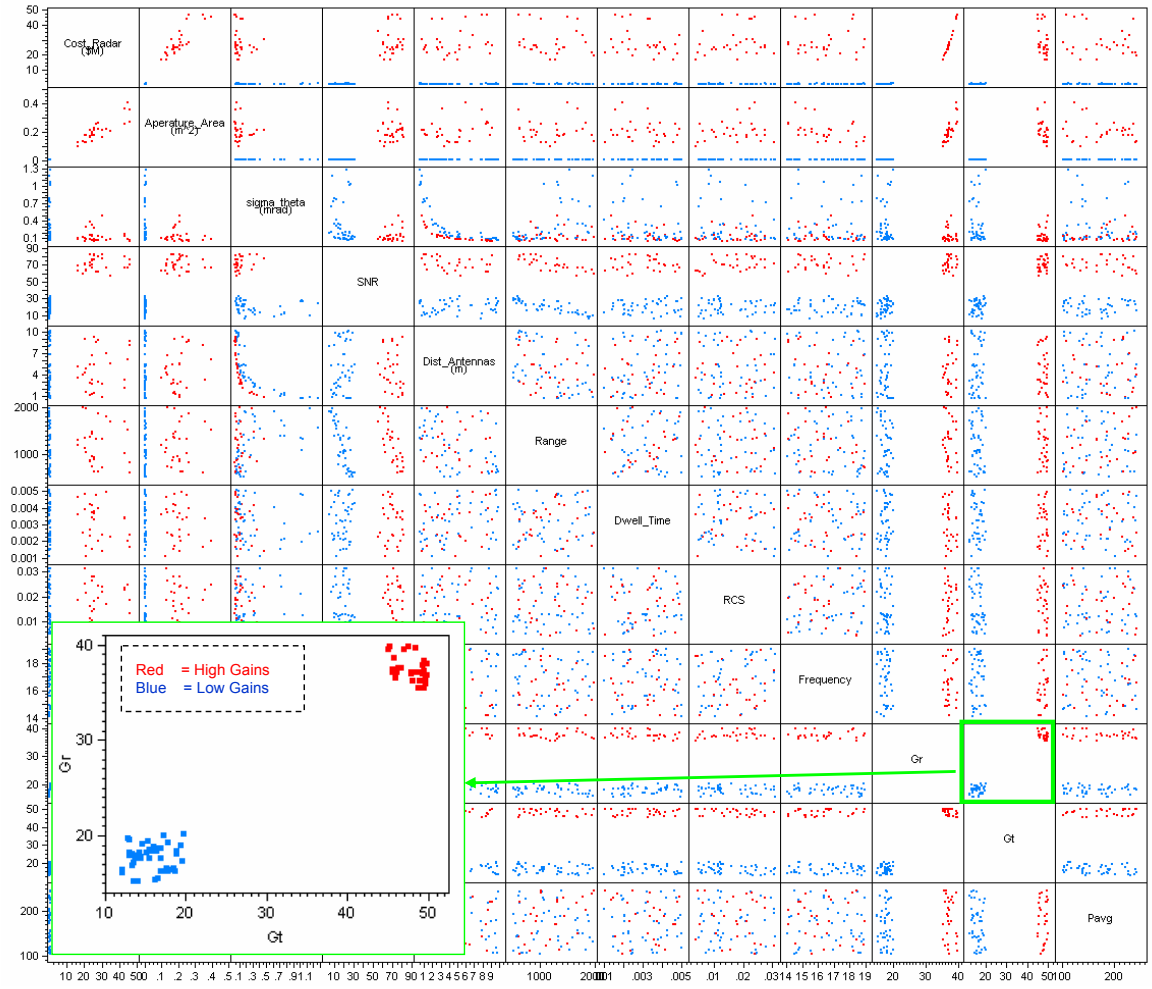

Figure 94: Radar Subsystem Study - Regions of Low and High Antenna Gains are Selected

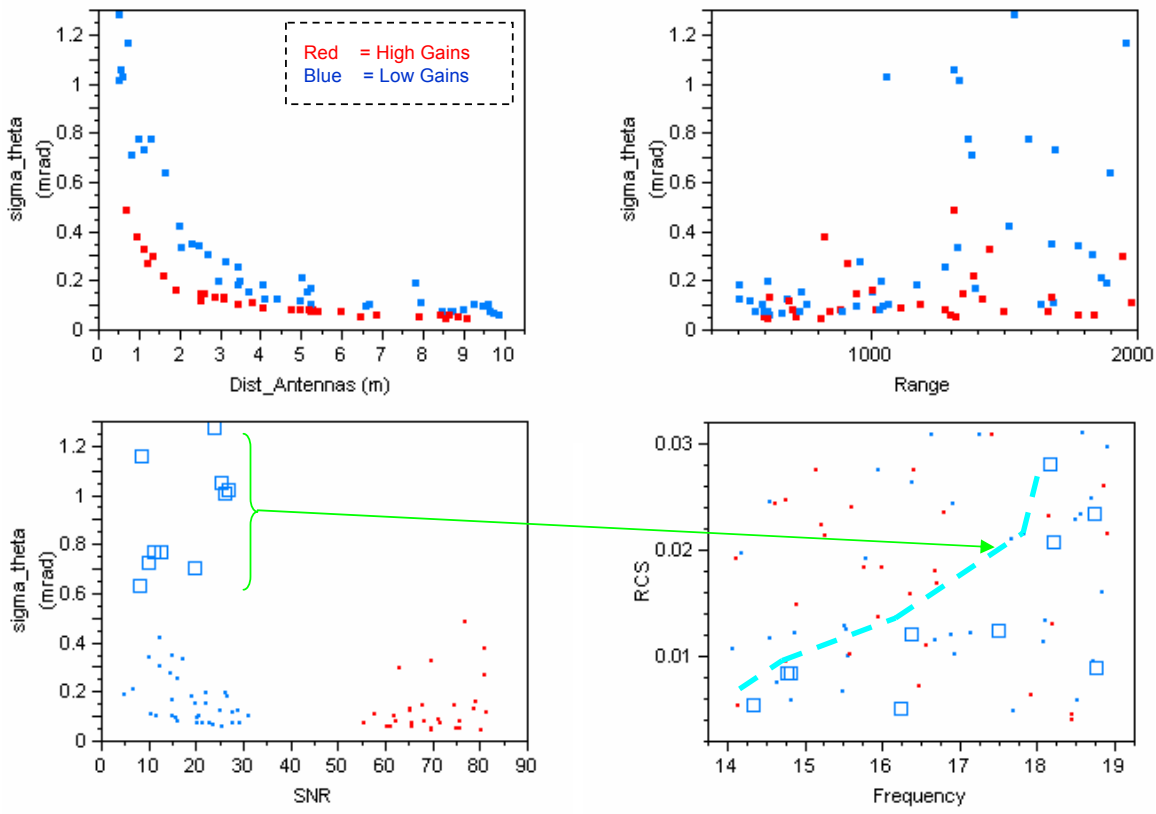

Figure 95: Radar Subsystem Study - Capabilities and Properties for Low and High Antenna Gains

6.7 Detailed 6-DoF Model

6.7.1 Variable Listing

This section will attempt to refine the parametric model using the findings from the initial study, in which the key variables were identified. The parameters for this study were defined with the help of appropriate committee members [24] [25]. The previous studies did not assume the use of a fire control solution. For a given intercept range and gun muzzle velocity, the gun firing elevation necessary to cause an intercept had to be determined iteratively (assuming head on shot with no error anywhere in the system). Therefore for the initial study, intercept range was treated as a discrete variable along with bore, and the DoE created for the remaining variables had to be run for every combination of range and bore. This detailed study will employ the use of a fire control solution, allowing the treatment of intercept range as a continuous variable. Therefore, this portion of the study will examine intercept ranges between 500-1500 m. All of the variables used for the remainder of the implementation portion of this thesis will be discussed in the following sections and are summarized in Tables 19 and 20.

6.7.1.1 Projectile

Regarding the projectile, this study will examine three different kill techniques by comparing an unguided projectile, a guided hit-to-kill projectile, and a guided projectile carrying a small warhead. The guided hit-to-kill projectile is the same one discussed in the initial study, using a pin firing mechanism to steer into the target. The main difference in this portion of the study is that the projectile will now employ a *bang-bang* controller that is more representative of how an actual guided projectile would be implemented, as opposed to the PID control employed in the earlier study; a PID would provide better control, but is far more complex to actually implement than a bang-bang controller, especially in a small projectile with clear volumetric

constraints. The unguided projectile will effectively be the same as the guided hit-to-kill projectile, except it will not receive any radar or guidance updates once it leaves the gun, and the pin firing mechanisms will therefore not be used. This is done in order to compare the use of a guided round to an unguided round. Ideally, a spin-stabilized round would be used (as opposed to the guided fin-stabilized hit-to-kill round). However, for the sake of simplifying the simulation this assumption was made. For these first two projectile types, a direct hit is required to destroy the target, and the probability of hit is the measure of merit for both.

The third kill mechanism involves using a guided projectile with a small warhead, and will require using a different aerodynamic shape conducive to carrying a warhead, shown graphically in Figure 96. For the sake of example, an assumption is made that the warhead has a 0.25 m lethal radius against the target type studied (any other value could have been used, using the CDF of the minimum miss distance as was done for the initial study). This effectively means that the measure of merit for this kill mechanism of the probability of hitting within 0.25 m of the target. For control, this projectile uses a small thruster that can fire only once to divert the projectile, graphically shown in Figure 97. Once an acceleration threshold is reached, the controller checks to see where the thrust action line is relative to the desired angle of acceleration. If the thruster line of action is outside of the desired acceleration arc, then the thruster is armed. The thruster is fired once the thruster line of action is inside the desired acceleration arc. It is assumed that the thruster is located at the projectile center of gravity, and that it fires for a very short duration, resulting in thrust force uniform in time [25].

One of the purposes of conducting this more detailed study was to reintroduce different bore sizes, which directly affect the rate of fire of the gun (discussed in the next section). For the two guided rounds (kinetic-kill/pin-control and warhead-kill/thruster-control), only the two larger bore sizes examined in the initial study will

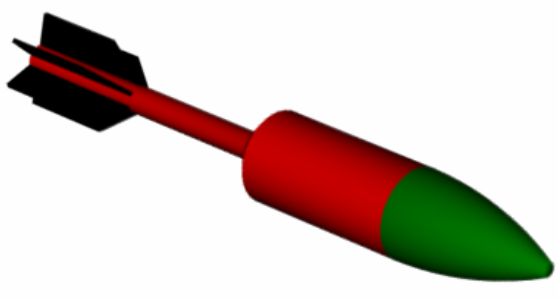

Figure 96: Warhead Round for Detailed 6-DoF Study [25]

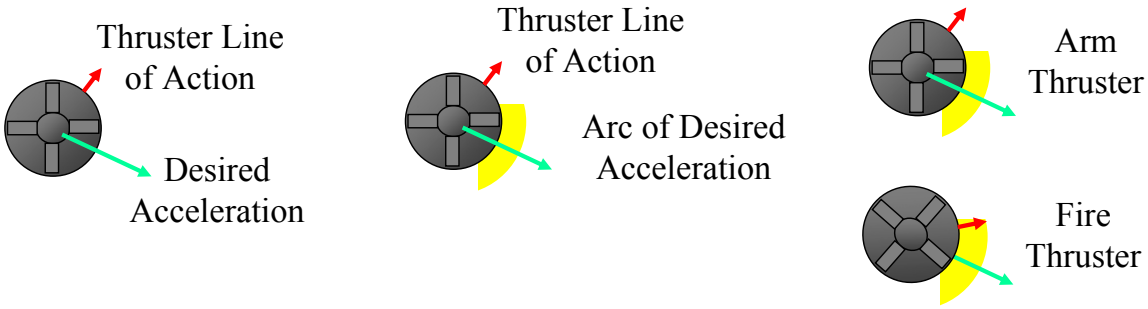

Figure 97: Thruster Controller for Warhead Round [25]

be used, 50 mm and 57 mm. For the unguided round, it was desired to include the use of a smaller bore, 30 mm, that enables a high rate of fire, in addition to the two bore sizes used for the guided rounds. The 40 mm bore examined in the initial study will not be examined here in an effort to provide a more realistic depiction of a gun firing small unguided projectiles at a high rate of fire. Because there is no control logic implemented on the 30 mm round, there were no issues with control authority such as that encountered in the initial study.

6.7.1.2 Gun

The initial study showed very little sensitivity of intercept miss distance to gun firing accuracy. When this occurs, there are two basic options when progressing to a more detailed study. The first option would be to fix the gun accuracies, and not allow any parametric variation. The other option is to open the bounds to see if values beyond those studied in the initial study would in fact contribute to the variability of performance. However, this was only studied for a guided round. For an unguided round, the gun firing error may play a more important role, and will therefore be studied for all three kill mechanisms. The original 6-DoF tool used in the initial study did not run a Monte Carlo simulation internally on the gun noises. Rather, for the initial study the gun error was treated as a controlled bias from the ideal firing position. A Monte Carlo simulation was conducted on surrogate models of the deviations from the ideal firing position to make intercept miss distance a function of gun noise, as described in Section 6.3.3. For this study, the 6-DoF tool will actually run the Monte Carlo simulation internally, and just as was done for the radar noises, the parametric surrogate models will be a direct function of gun noise. A more simplified approach will be taken to parameterize gun firing accuracy. Here, the gun firing azimuth and quadrant elevation will be coupled, meaning that the same value will be used for both. Muzzle velocity error will not be varied, and will be fixed at

a specific value of 0.4% (1σ) of the muzzle velocity. Because the 6-DoF tool only simulates a one-on-one intercept, the gun rate of fire will be taken into account after the fact in the assembled hierarchical model.

Also different from the initial study, this detailed study will examine three discrete gun firing muzzle velocities: 1000, 1325, and 1650 m/s. This is done to determine if one of the kill mechanisms has an advantage over another at a different muzzle velocity, and to determine how much of an effect the gun itself has on the entire interception process. Because most large caliber guns are designed to fire at specific muzzle velocities, there was no need to treat it as a continuous variable in this study.

6.7.1.3 Radar

The radar accuracy will be represented by coupling the azimuth and elevation noises (i.e. both use the same value). From the previous studies, there was little contribution to miss distance variability from the radar roll and range noises. For this study, roll noise will be fixed, however, range noise will vary. As shown in the previous study, the radar update rate contributes heavily to the performance of a guided projectile, and will remain a variable for this final study. The guidance update rate, however, will remain fixed at 1kHz. Much attention has been given to the radar properties in the previous sections, therefore there is no need to elaborate further about radar properties here.

6.7.1.4 Summary of Variables for Detail Study

Each of the variables discussed in this section along with their bounding values is given in Table 19 for the continuous variables, and Table 20 for the discrete variables.

6.7.2 Surrogate Modeling

A five variable DoE was created for the continuous variables listed in Table 19. An 81 run DoE was assembled using a 27 run CCD to capture the corners of the design

Table 19: Detailed Study - List of Variables

Property	Minimum	Maximum	units
Gun Pointing Error (Az, QE)	0.5	1.5	mrad
Radar Noise (Az, QE)	0.05	1.0	mrad
Radar Range Noise	0.05	1.0	m/km
Radar Update Rate	10	100	Hz
Range	500	1500	m

Table 20: Discrete Variable Settings for Detailed Study

Kill Mechanism	Bore (mm)	Muzzle Velocity (m/s)
Kinetic-Kill/Pin-Control	30	1000
Warhead/Thruster-Control	50	1325
Kinetic-Kill/Unguided	57	1600

space, a 27 run LHS to capture the space throughout the design space, and 27 random runs for model validation. This 81 run DoE had to be repeated for each combination of kill mechanism, bore, and muzzle velocity desired, shown in Table 20. For each of the three kill mechanisms, three gun muzzle velocities were studied, and each of the guided rounds were studied at two different bore sizes, and the unguided at three bore sizes. Additionally, as with the initial studies conducted, each DoE run executed a Monte Carlo simulation within the 6-DoF code. There was a desire to increase the number of internal 6-DoF Monte Carlo simulations in order to increase the fits of the surrogate models. For each of the two guided rounds, 750 Monte Carlo samples were run for each DoE case - for an 81 run DoE at three discrete bores and two discrete muzzle velocities - resulting in a total of 364,500 6-DoF runs for each. For the unguided round, 250 Monte Carlo runs were used, resulting in 182,250 6-DoF runs. Therefore, a total of 911,250 6-DoF executions were used in the data presented in this section and used in the remainder of this thesis. The 10 seconds per 6-DoF execution required about 2500 computational run hours distributed over several computers.

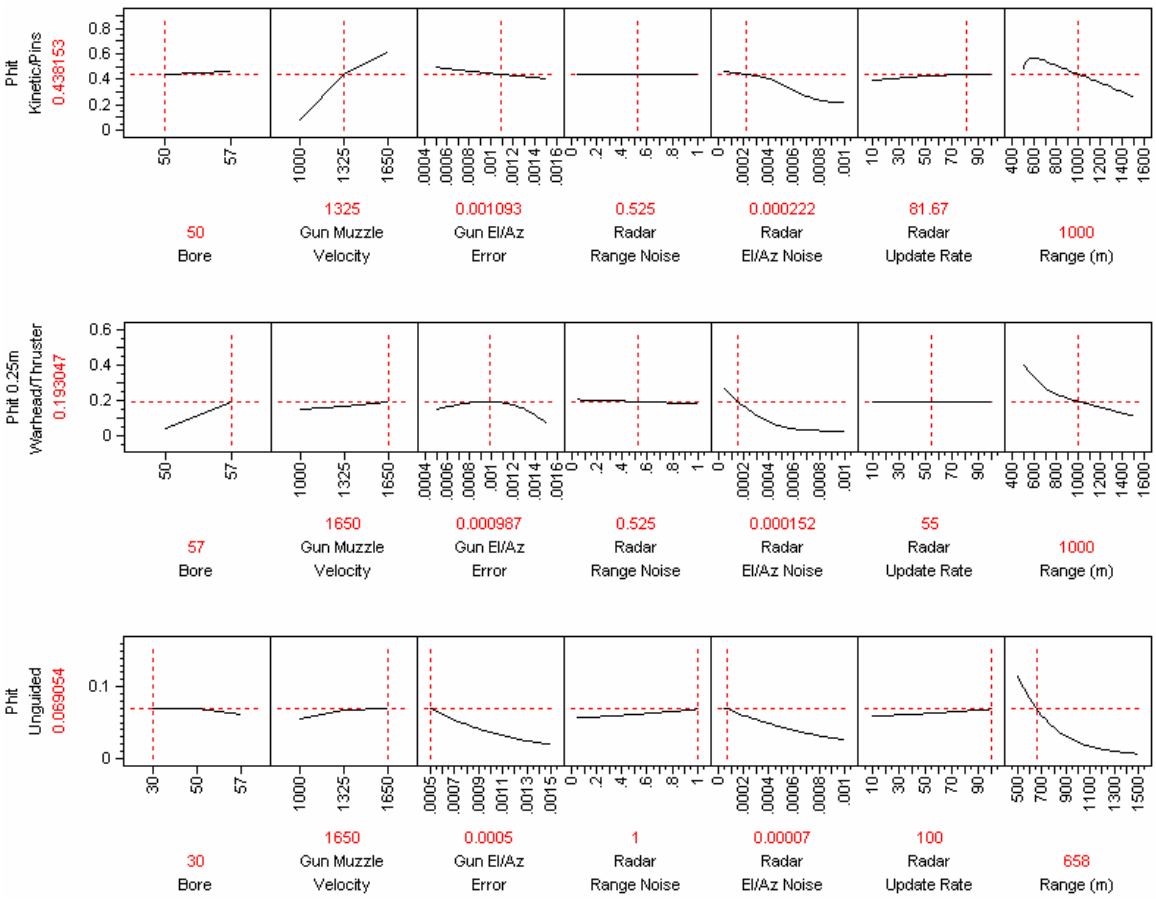

Figure 98: Detailed Study - Prediction Profiler for Three Projectile Kill Mechanisms

A prediction profiler used to manipulate the surrogate models is shown for each of the three kill mechanisms in Figure 98. Note again that the measure of merit for the kinetic kill weapons is probability of hit, where as for the warhead round, the probability of hitting within 0.25 is used. The analysis used to determine the goodness of these fits is given in Appendix D.2

6.8 Assembled Hierarchal Environment

This section will show how the various models described up to this point can be assembled in to a hierarchical decision making environment. The ultimate goal of this section is to be able to manipulate the entire hierarchy, from the highest level measures of merit, all the way down to the lowest subsystem level variables.

The complete hierarchical design space is populated using a Monte Carlo simulation and visualized using the multivariate scatter plot in Figure 99. At the bottom right corner within the red box are the radar properties, including its subsystem level variables, accuracy capability, and update rate. The gun properties are shown in the orange box, and are simply the pointing accuracy error, the muzzle velocity, and bore. However, the gun pointing error is also a function of the radar measurement accuracy, therefore there is an overlap at the radar measurement for both radar and gun properties. In the green box are the projectile properties, including the discrete bore sizes and kill mechanisms. Note the other overlap between projectile and gun bore; recall how gun rate of fire is directly a function of bore. Finally at the top left corner in the blue box are the operational level properties. Here one can view the intercept range and corresponding single shot probability of hit for all variables selected below the hierarchy. Using that single shot probability of hit and the number of rounds fired (based on rate of fire and bore), the multiple shot probability of hit is given. Additionally, as a measure of cost, the radar cost is given at the very top of the hierarchy as an operational level variable.

This is the assembled hierarchy that gives operational level properties decomposed into the systems that drive those properties, with one of those systems decomposed down to the subsystem level. Here a decision maker can manipulate the design space at any level of the hierarchy. For example, a high level decision maker or war planner can sit at the very top and decide he or she is only interested in solutions that meet a given multiple shot probability of hit, and must stay within a given budget. By eliminating the unwanted design space in those metrics of interest, the remaining design space will appear at each and every other level in the hierarchy.

The design space in Figure 100 is sorted by kill mechanism in order to help differentiate between them. Here very obvious trends appear in many of the individual plots, some of which are given for clarity as bivariate plots in Figures 101 and 102. In

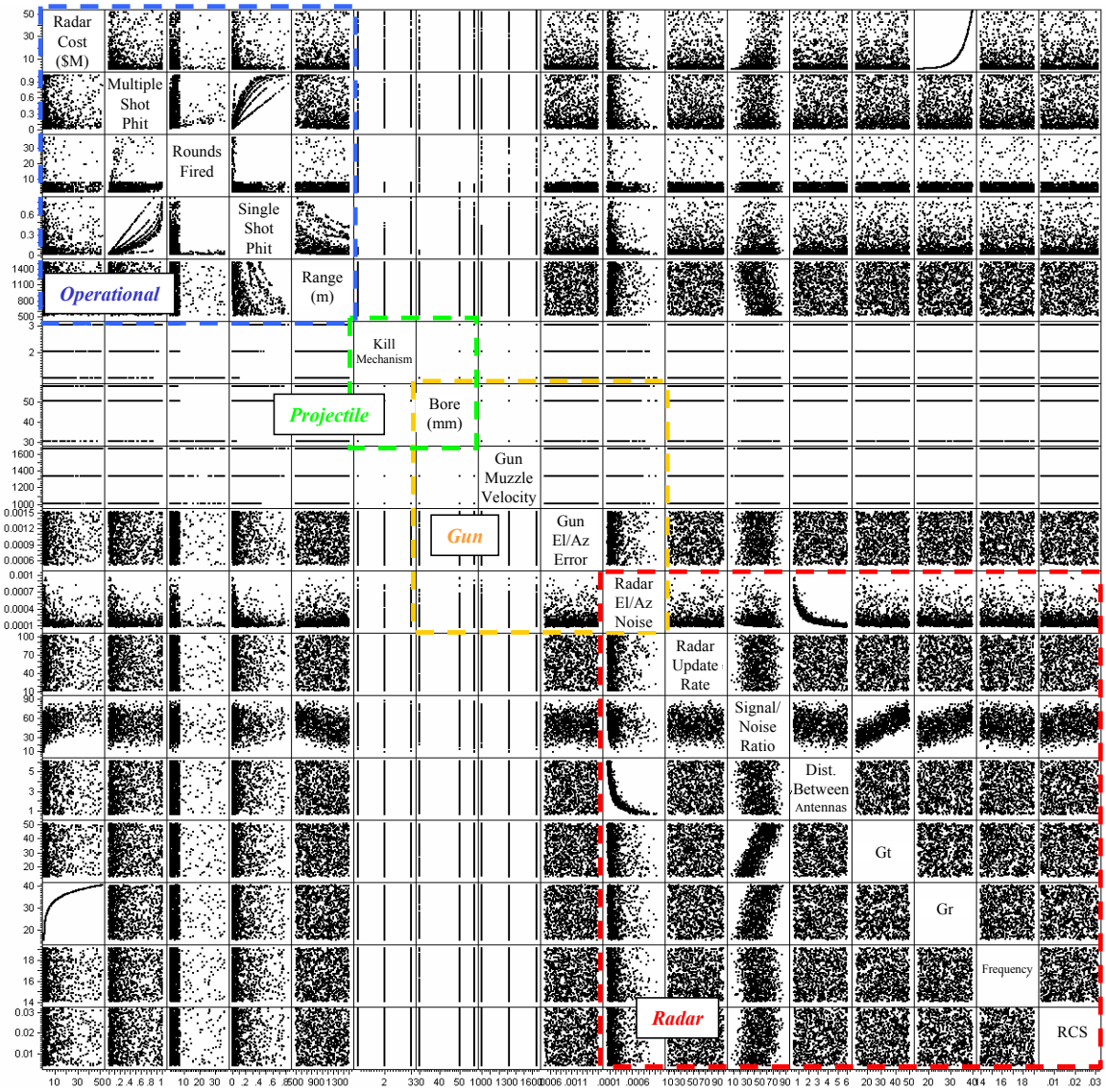

Figure 99: Assembled Hierarchical Environment - Complete Design Space

Figure 101, the operational level properties are shown, all versus MSPH. Note that for each plot, a line is drawn to differentiate the design space meeting or exceeding a MSPH of 0.90. Looking at the top right plot, it is clear that it would require at least two of the kinetic/pin rounds to achieve a MSPH of 0.90, five of the warhead/thruster rounds, and at least 34 of the unguided rounds[1]. Clearly, the kinetic/pin round is capable of reaching a higher MSPH using fewer shots than the other two rounds. The corresponding plot on the top left shows MSPH versus the SSPH, for curves of corresponding number of rounds fired. For the desired MSPH line drawn on the plot, one can determine the required SSPH for each projectile type, and for number of shots fired. The plot on the bottom left shows the tradeoff between MSPH and intercept range. Very clear trends appear for each of the three kill mechanisms (with dashed lines added for emphasis). The unguided round (black points) are capable of reaching high MSPH values at the low ranges, but as range is increased, the MSPH rapidly decays. Actually the highest range that the unguided round can achieve a MSPH of 0.90 is about 600 m. The warhead/thruster round also has a MSPH decaying with range, however not as rapid as the unguided round, and can achieve a MSPH of 0.90 up until a range of 700 m. The almost even distribution of kinetic/pins points on the lower left plot of Figure 101 shows that even at high ranges, a very high MSPH is achievable. Finally, the plot on the bottom right shows radar cost versus MSPH. Clearly the most desirable region is the high MSPH, low cost region (further discussed later).

One thing that was noted even just by grouping the design space by kill mechanism is that one of the bore/muzzle-velocity/kill-mechanism combinations stood out from the others. From manipulating the environment, it was evident that a 50 mm bore,

[1]Recall from the relation given in Appendix C that the maximum number of rounds fired is a function of bore size; for the assumption used in this example, the 50 and 57 mm guns can fire off a maximum of 6 and 7 rounds respectively, and the 30 mm bore, which applies only to the unguided round, can fire off a maximum of 37 rounds.

1650 m/s gun muzzle velocity (the fastest of the three), kinetic-kill/pin-control option provided the greatest SSPH and MSPH at every intercept range, as shown in Figure 102. These are bivariate plots from the same completed design space given back in Figure 100, just with this particular bore/muzzle-velocity/kill-mechanism option emphasized, and will be emphasized in many of the remaining graphics.

One of the greatest benefits of using an assembled hierarchical environment is to study the impacts of high level decision making on even the lowest level parameters. For example, at the operational use level, a decision maker may only care about having a given capability within a given cost. Shown in Figure 103, an example is given where a decision maker wants a MSPH of at least 0.90 and radar cost under $5 million. The remaining undesired designs are eliminated, including all of the unguided and most of the warhead/thruster options. Taken from the larger multivariate plot, Figure 104 shows the impact on the radar subsystem level variables. The top left plot with radar update rate and RCS clearly shows a trend for the warhead/thruster round. With higher radar update rate, the warhead/thruster round is able to achieve the desired MSPH with smaller projectile RCS. There are no noticable trends for the kinetic/pin round. The top right plot showing distance between antenna element arrays and intercept range shows several interesting trends. Clearly the warhead/thruster round is very sensitve to the distance between the antenna arrays in its ability to intercept the target with increased range.

Of course, a smaller radar is desirable for mobility reasons, and minimizing that distance between antenna arrays is therefore also desirable. Several designs stand out at the low distance between antenna arrays, and high intercept range corner - the green circles indicating the 50 mm bore, 1650 m/s gun muzzle velocity, kinetic/pin round. The bottom right plot shows radar frequency and average power. Again, there are no noticeable trends for the kinetic/pin round, however a clear trend showing that as frequency is reduced, a higher power is required for the warhead/thruster round to

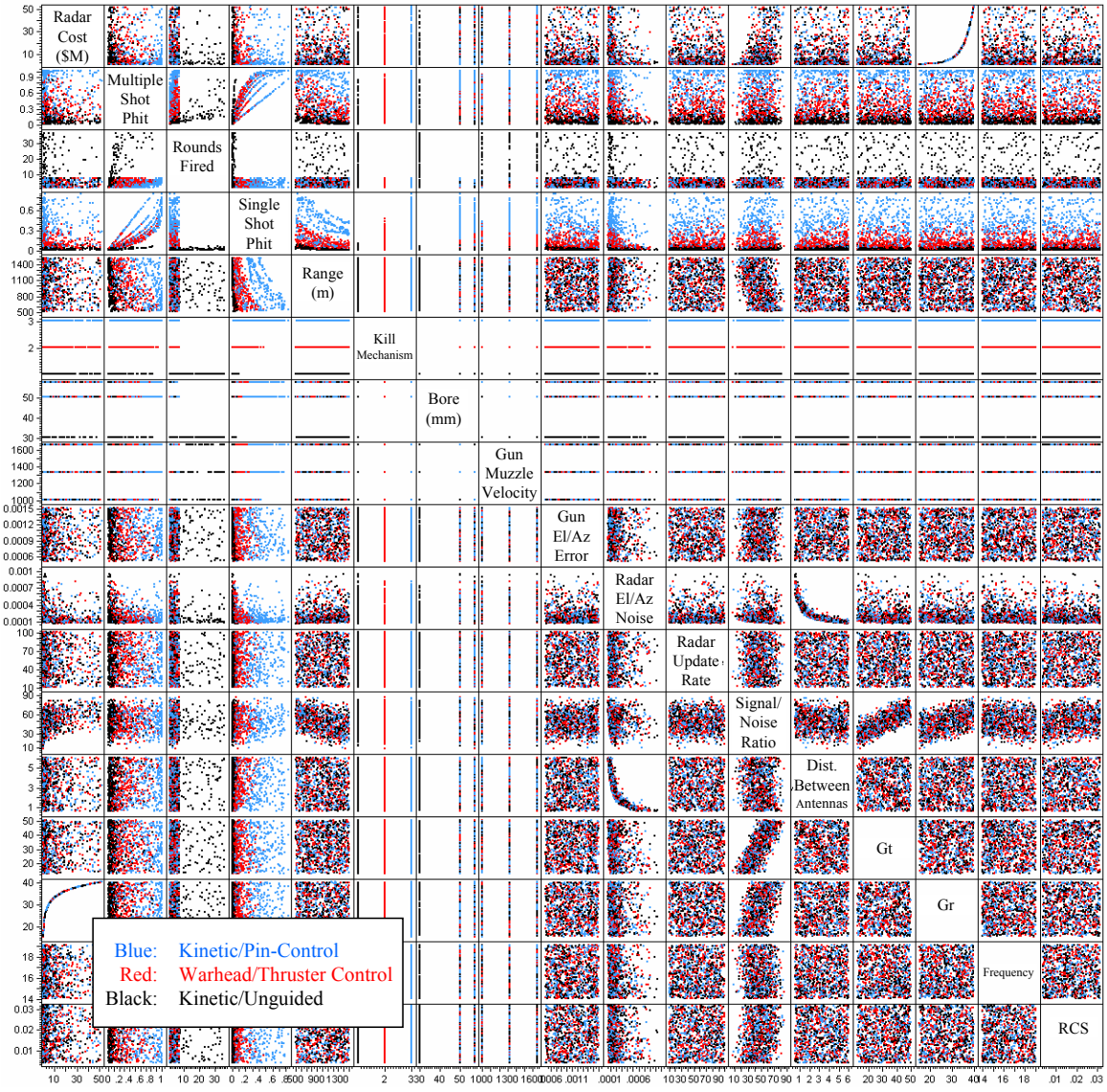

Figure 100: Assembled Hierarchical Environment - Design Space Sorted by Kill Mechanism

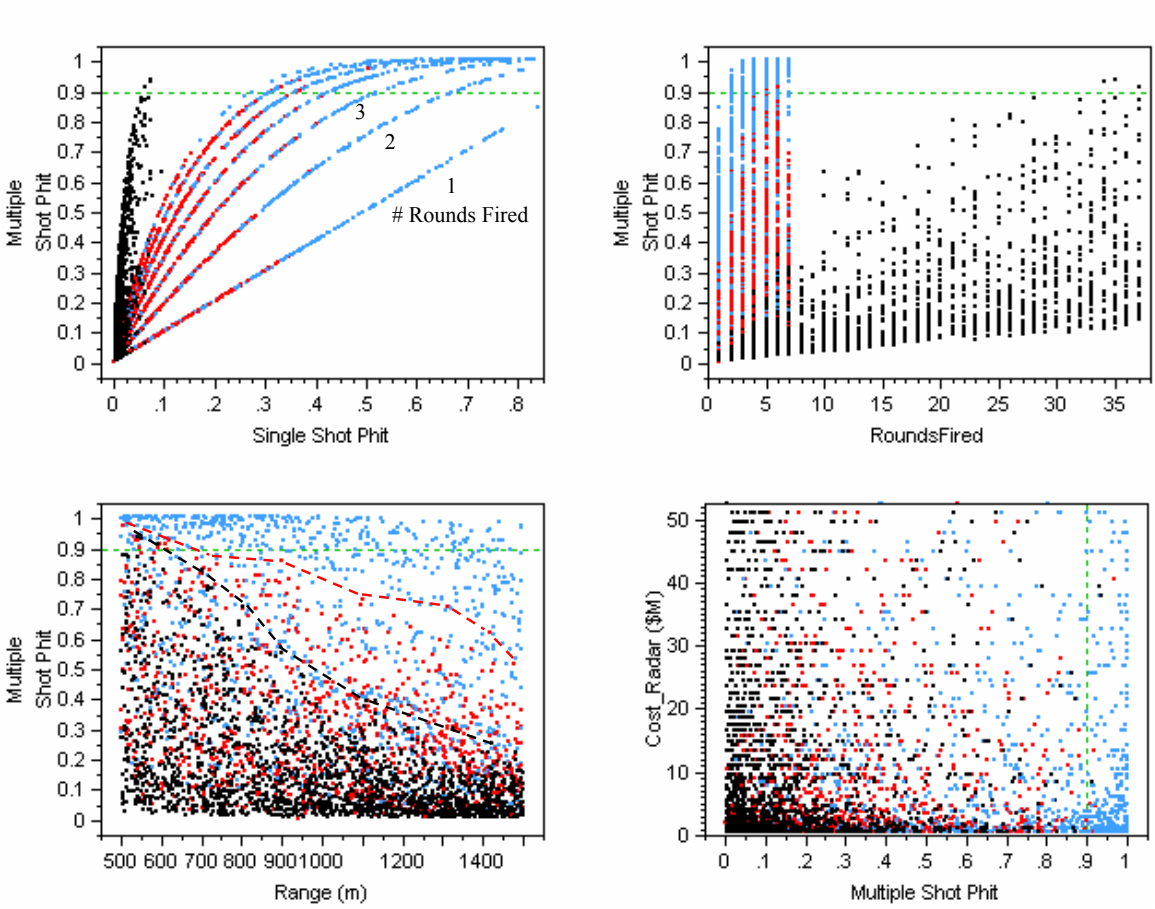

Figure 101: Assembled Hierarchical Environment - Operational Level Bivariate Plots

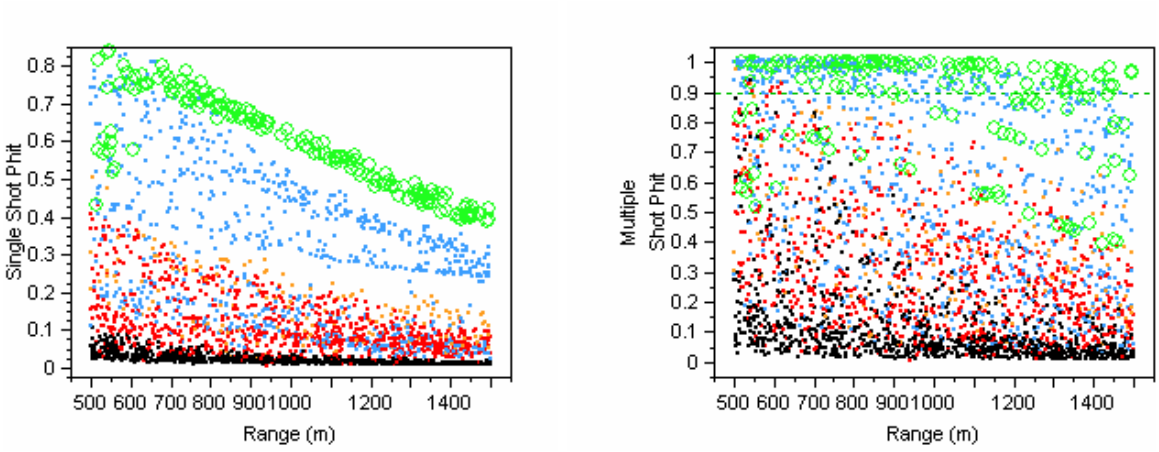

Figure 102: Assembled Hierarchical Environment - Emphasizing a Discrete Option

achieve the desired MSPH and cost requirements. Finally for the bottom left corner of Figure 104, SNR and the distance between antenna arrays are shown. There is a clear trend for all the design points where a higher SNR is required as the distance between antenna arrays is reduced, and low SNR are tolerable at the higher antenna array separations. However, now a radar expert can decide that any SNR values above a given value, say 35, are unreasonable for any given reasons, and a line can be drawn to differentiate between the designs that do and do not meet this SNR limit. Clearly the warhead/thruster rounds require a higher antenna array separation than the kinetic/pin rounds. This even allows the ability to isolate one particular design, such as the kinetic/pin rounds that achieve the highest MSPH at highest range (the green circles), and noting that the lowest antenna array separation achievable with those rounds is about 2.25 m.

Another desired attribute on the battlefield would be to minimize the number of rounds required to be fired against a target. Even looking back at Figure 101, if enough unguided rounds are fired at the target, it would be hit. However, the war fighter would rather not carry many ammunition stores, or wear out the gun barrel

with excessive firings. Figure 105 examines the rounds fired trade space on the 0.9 MSPH and $5 million constraints. Clearly as more rounds are fired, a greater intercept range is achievable. For one or two rounds, only the kinetic/pin round achieves the requirements, and beyond that, the 50 mm bore, 1650 m/s muzzle velocity, kinetic/pin round has the clear range advantage. The top right plot shows the radar accuracy tradeoff with rounds fired, and it is apparant that with more rounds fired, higher radar noise is tolerable. The bottom right plot shows how the required SSPH can be reduced with increased shots fired, and note how the warhead/thruster round is at the lowest SSPH for the rounds fired in which they appear. Finally, the bottom left plot of Figure 105 shows how the distance between antenna arrays varies with rounds fired. As the antenna arrays are brought in closer, more shots are required to achieve the operational level requirements.

The final tradeoff examined in this chapter is the gun muzzle velocity selection, given in Figure 106. Note that now the green circles are used to differentiate between the 50 and 57 mm kinetic/pin rounds. There were three muzzle velocities included in the detailed study, and the effects of which one used has a very defined impact. For the given high level requirements, note that at the slowest muzzle velocity, more rounds fired are required, and are only able to achieve intercept ranges up to about 700 m. For minimizing the number of rounds fired to achieve the high level requirements, a 57 mm kinetic/pin fired at the middle muzzle velocity option is the best. However as discussed earlier, the 50 mm kinetic/pin fired at the highest muzzle velocity had the greatest high range MSPH. Looking at the right side plot in Figure 106, there is not that much range benefit of using the smaller kinetic/pin bore, but this of course might assume firing more rounds. However, it may be more difficult to design the electronics and internal packaging for a smaller guided bullet, making the large bore more desirable.

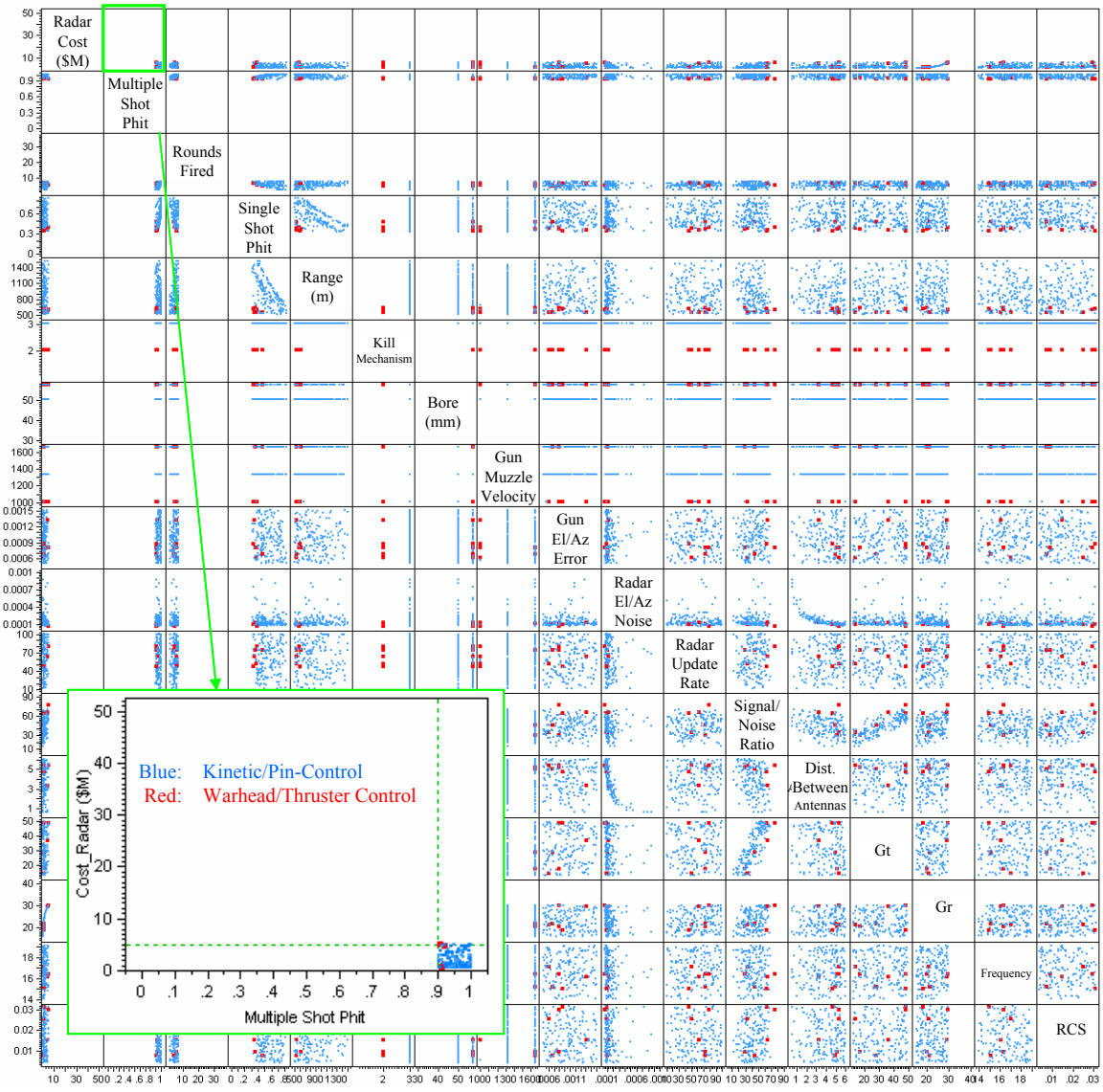

Figure 103: Assembled Hierarchical Environment - Selected Desired Phit and Radar Cost Operational Constraints

Green: *50mm, Kinetic/Pin, Fastest Muzzle Vel*
Blue: Kinetic/Pin-Control
Red: Warhead/Thruster Control

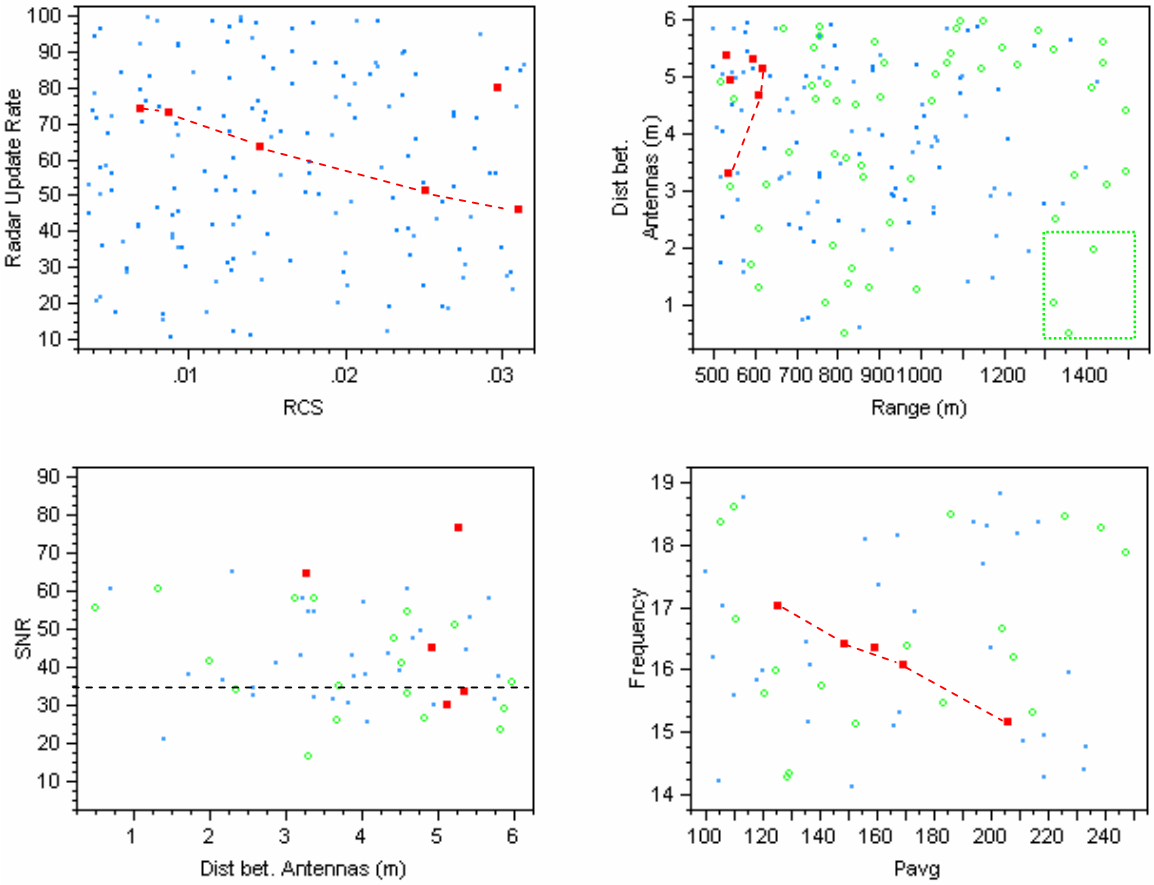

Figure 104: Assembled Hierarchical Environment - Radar Properties Due to Operational Level Constraints

Green: *50mm, Kinetic/Pin, Fastest Muzzle Vel*
Blue: Kinetic/Pin-Control
Red: Warhead/Thruster Control

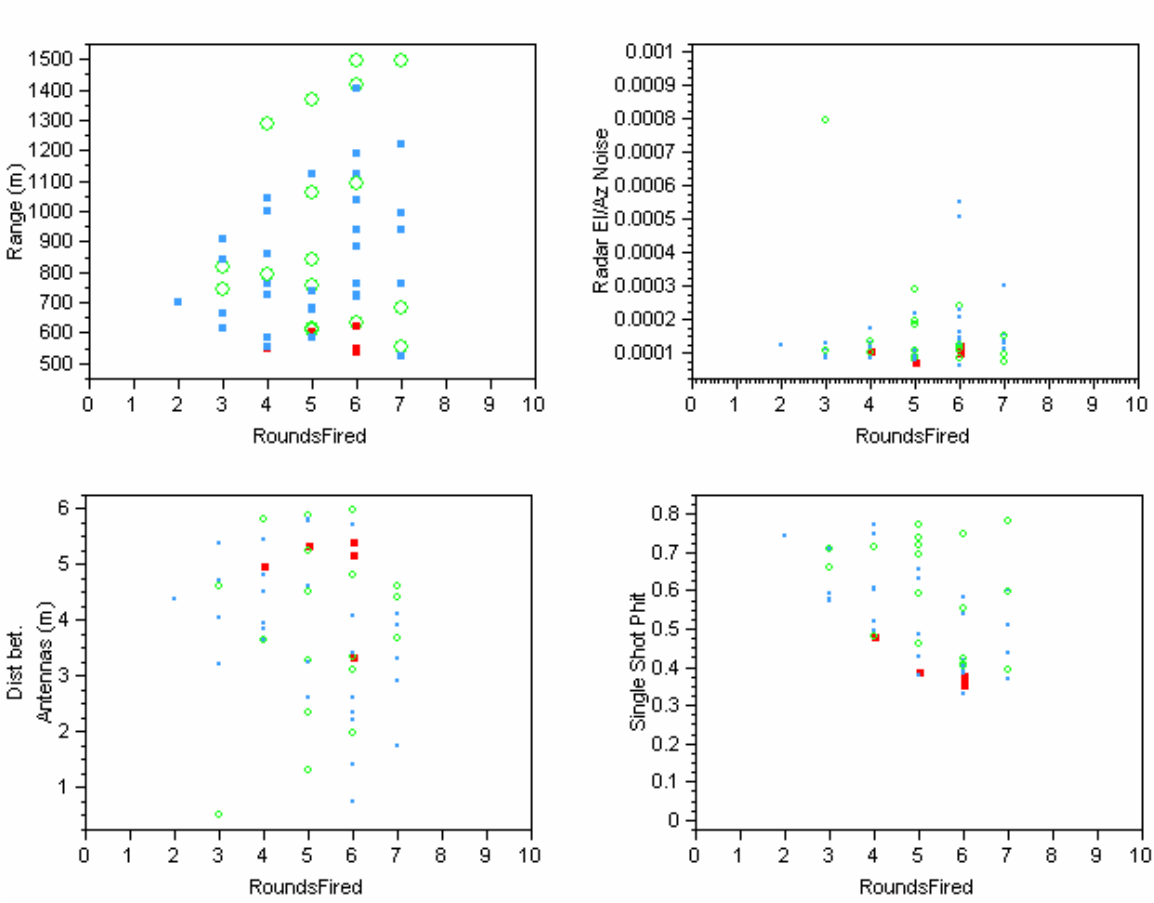

Figure 105: Assembled Hierarchical Environment - Number of Rounds Fired Trade Space

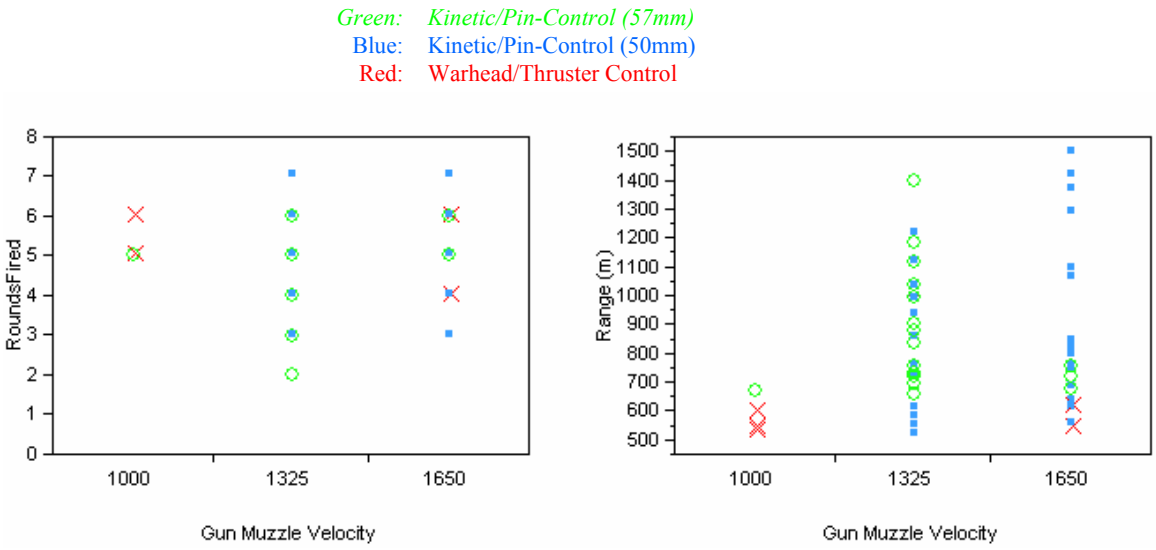

Figure 106: Assembled Hierarchical Environment - Gun Muzzle Velocity Trade Space

6.9 Chapter Conclusions

The assembled environment in Section 6.8 showed how the qualitative metrics of interest for an air defense system identified in Section 5.2 - lethality, mobility, and cost - can be represented across a system-of-systems hierarchy, using a top-down design approach to directly manipulate any property in that hierarchy. The measure of lethality was represented by the probability of directly intercepting the target using one or more projectiles, or using the measured confidence of impacting within a certain distance from that target. That measured lethality was a function of every property of the functionally decomposed environment discussed in Chapter 5, however as first discussed in Section 1.2.2.2, the radar capability would drive a guided projectile's effectiveness. Several of the radar subsystem properties that define the radar accuracy would then be used to represent the other two qualitative measures of effectiveness. The desired lethality capability would drive the radar accuracy, which in turn would drive the distance between antenna element arrays, which is a measure of the weapon system size, or mobility. That radar accuracy would also drive the radar properties that greatly affect its cost, which was shown to be of significant

value. This chapter first proved this approach one hierarchical level at a time with detail, and finally showed how the entire environment can be manipulated, flowing top level requirements directly to system and subsystem level properties. Examples were given throughout this chapter showing how requirements at any level in the hierarchy affect all other properties, as well how this can be used to discover interesting tradeoff spaces that exist between any combination of variables and responses that might have not otherwise been known.

CHAPTER VII

CONCLUSIONS

7.1 Review of Research Questions & Hypotheses

The very first research question was asked in order to determine the deficiencies the systems engineering process as applied to complex hierarchical systems. With those deficiencies identified, such as the inability to flow information across nonadjacent levels, the second research question expressed the desire to create a process in which those deficiencies could be overcome. The research questions asked in Chapter 4 helped focus the scope of this thesis and were based on the problem introduced in the motivation chapter, as well as information learned throughout the literature search effort. The hypotheses presented attempted to directly answer those questions using only knowledge gained during the literature search. This section will show how the approach laid out in Chapter 5 and associated methodology implementation from Chapter 6 proved the hypotheses, therefore answering the questions presented in Chapter 4.

7.1.1 First Hypothesis

The first hypothesis laid out a basic approach to answering Research Question 2, and served as the primary research objective for this thesis.

> **Research Question 2:** *How can a process be created that enables rapid manipulation across a hierarchy of decision making levels?*

> **Hypothesis 1:** *A system-of-systems approach can be used to create an environment that will allow for both weapon requirements definition and*

system optimization from top-down requirements that take into account operational environment characteristics, as well as for analyzing the impacts of subsystem level changes on top level metrics from the bottom-up.

The motivation for this thesis discussed in Chapter 1 led to the second research question, which was asked before any literature search was conducted. This question was meant to address the deficiencies associated with the systems engineering process discovered in Section 1.1.2. This desired process needed to include more than just generalized requirements for a method to design this type of weapon, but also a process to assemble an integrated hierarchical environment, based on accepted modeling and simulation methods, for the various components that need to interact and allow for rapid manipulation to enable decision making at any level within the hierarchy.

Therefore, the first hypothesis proposed creating a system-of-systems inspired approach for a hierarchical decision making design environment, where multiple interacting and independent systems affect an overall measure of effectiveness. This first hypothesis was realized in both the approach (Chapter 5) and implementation (Chapter 6) portions of this thesis. In Chapter 5, the problem of interest was hierarchically decomposed to the functions that enable the entire process, which served two purposes. First, the scope of the problem of interest was focused such that a sufficient methodology can be applied to address depth and breadth. Second, the hierarchical interdependencies were established showing which properties of the independent systems interact to drive operational measures of effectiveness. This process also showed the breakdown of the degrees of freedom across the entire system-of-systems hierarchy, from the lowest level subsystem properties all the way up to the highest level of decision making. The idea here was that once this environment is constructed, the second hypothesis can be realized, answering the next set of research questions.

7.1.2 Second Hypothesis

The second hypothesis addressed the issues relating to Research Questions 3, 4, and 5.

> **Research Question 3:** *An ANOVA/Pareto plot technique can be used to quantify the contribution of each variable to the variability of a response, but is there a way to identify which variables drive each other?*
>
> **Research Question 4:** *Can a tradeoff space be identified interchangeably between variables and responses?*
>
> **Research Question 5:** *How can rapid design tradeoffs be assessed in a hierarchical environment composed of independent time consuming models if the design space between them is multimodal or discontinuous?*
>
> **Hypothesis 2:** *A hierarchical environment composed of neural network based surrogate models will enable multimodal and/or discontinuous design spaces to be accurately represented, allowing for rapid tradeoffs. These tradeoffs may be conducted with real time application of constraints at any level of the hierarchy, for both independent variables and dependent responses.*

Research Questions 3, 4 and 5 were asked in ascending detail, however methods had to be applied to answer the questions in reverse order as implied by the second hypothesis. In order to identify the variable combinations that drive each other (Question 3), a tradeoff space must be identified between all of the variables and responses (Question 4). Although polynomial surrogate models have emerged as a useful way to capture the design space of very complex codes and enable rapid manipulation and tradeoffs, they severely limit the topology of the design space captured in that that they are appropriate only when the design space is continuous and not

highly multimodal. Research Question 5 was addressed using neural network based surrogate models that were able to capture very complex design spaces required for exploring across a system-of-systems hierarchy. For example, neural networks were used to capture the discontinuous design space surrounding the quantification of the probability of hit (i.e. a successful collision between interceptor projectile and target). This required sampling from an error distribution for every noise variable set prescribed by a Design of Experiments (DoE), and fitting to discontinuous cases were sometimes there was a successful target intercept, and many times when there was not an intercept.

To create the tradeoff space discussed in Question 4, a Monte Carlo simulation was used to uniformly fill the design space in the system-of-systems hierarchy using those neural network surrogate models. Using an interactive multivariate scatter plot, the design space of every variable and every response were viewed simultaneously, and *interchangeably*. This brings back the notion of viewing the design space in the context of the total (or full) derivative. Rather than extract single curves to show the pertinent tradeoff space between responses and variables for all other variables fixed, as with partial derivatives, this method keeps all degrees of freedom open throughout the design hierarchy. This allows for constraints to be placed anywhere in the hierarchy, regardless of whether they were variables or responses, clearly identifying the feasible design options and tradeoffs between any combination of variable/variable, variable/response, and even response/response. This method enables treating every variable and response as an independent variable. In doing this, the remainder of the second hypothesis was realized, answering Research Question 3. As constraints or requirements were imposed on metrics of interest within the hierarchy, the independent variables that were key drivers to the variability of those metrics could be identified, as well as the tradeoff spaces between those variables. The tradeoff space

that emerged as a result of placing constraints on responses was important in identifying which variables are dependent on the settings of *other* variables. This was the realization of the hierarchical top-down environment desired as a result of the first hypothesis.

7.1.3 Third Hypothesis

The third hypothesis addressed Research Question 6.

> **Research Question 6:** *How can the effects of uncertainty propagation at any level within a hierarchical decision making design environment be assessed?*
>
> **Hypothesis 3:** *A properly constructed system-of-systems environment will allow for the rapid assessment of the effects of uncertainty at any level in the hierarchy on any other level in the hierarchy.*

This thesis approached the subject of uncertainty in the design hierarchy in a number of ways. The first was from the bottom-up, where it was desired to determine the effects of uncertainty in a design variable on the ability to achieve a certain response. The traditional way to achieve this is to run a Monte Carlo simulation sampling from a distribution on the design space of those given variables, and quantifying the confidence of achieving a given response using a cumulative distribution function (CDF). The most straight forward method to achieve this in this thesis was the quantification of the probability of direct interceptor/target hit and of the CDF curve resulting in variation of the noise variables of various systems in the hierarchy. This enables the quantification of the bounds of variables that are random functions to an acceptable CDF

However, having the methodology in place for constructing a hierarchical decision making environment (as was realized in support of the first two hypotheses), a design

variable region of interest could easily be defined. This region of interest may encompass a region of uncertainty within a variable design space, or even as shown in many cases, several regions. With the interactive multivariate scatter plot, the resulting design space for every other variable and response are identified. The second major approach to uncertainty was done by identifying regions of acceptable responses and seeing how that constrains the remaining design space from the top-down. In other words, for a given region of uncertain desired response, this thesis showed the acceptable dependent variable design space.

7.2 Summary of Contributions

As discussed in the motivation for this thesis, in order to evaluate complex systems such as revolutionary applications for air defense weapons, there is a need for rapid manipulation of the systems engineering process across nonadjacent levels of a design hierarchy. This thesis did not try to provide a specific design solution to the general example problem presented in the motivation chapter. Rather, a portion of this problem was addressed to show how the methods developed could be applied to a problem of current interest for which there is no existing or programmed system with the ability to negate these threats after they are launched. One of the major contributions of this thesis to the field of aerospace systems design is the introduction of a methodology that enables decision makers anywhere across a system-of-systems hierarchy to rapidly and simultaneously manipulate the design space, however complex. This process eliminates the iterative steps that usually occur when dealing with flowing requirements from one level to next lower in the systems engineering process. By removing the internal constraints local to one level in the systems hierarchy, the design space could be manipulated from the top-down of a design environment directly, without having to deal with the iterations involved in optimizing a system or subsystem one level at a time.

The application of the process developed to the example problem enabled the identification of interesting phenomena that might not have been possible otherwise. This was due to the fact the data representing the design space was presented in bulk, rather than just static curves showing a response as a function of one variable, with all other variables (and assumptions) held constant. For example, the effects of the application of overall capability requirements at the highest decision making level could be instantly flowed down to carve out the feasible design space not only at the lower system capability level, but directly to the subsystem property level which enable that particular system capability. Using this new methodology, regions emerged among those variables where either subsystem design properties were either insensitive to high level requirements, or where trends among those variables could be easily identified.

Additionally, this process allows different decision makers to all explore the design space simultaneously each with their own set of assumptions. This is primarily possible because the neural network surrogate models allow for freedom in the variable design space, while still accurately representing a complex computer simulation. Therefore, as was shown in the implementation chapter, a user has the ability to define or eliminate regions of assumptions of variable design space, and observe the effects on each and every other variable and response in this interacting hierarchical environment. This also includes the ability to bound variables that are random functions. Prior to this new formulated methodology, these capabilities were not available on such a rapid manner.

7.3 Recommendations for Further Study

One of the most beneficial improvements to the actual methods developed in this thesis would be to mathematically define the Pareto frontier discovered during the

real time application of requirements and constraints on the interactive multivariate scatter plot. Recall that in many cases where a region of interest was defined on a multivariate scatter plot, several tradeoff spaces emerged in the remaining response/variable design space. There have been many studies into the definition of a response versus response Pareto frontier for given variable design space. This defines the region where an improvement in one response degrades another response. What is suggested for future work is the definition of the tradeoff space for the variables, given a response design space, such that any combination of variables along that frontier result in a feasible space. This should be done in real time while the user is constraining the response design space. Additionally, in order to further develop the systems engineering process, the author recommends a more thorough mathematical understanding of the multivariate analysis nature of the process.

There is much potential to expand the scope of the specific problem addressed in this thesis to deal with more issues relating to the EAPS issue. The system-of-systems methodology can be expanded to include multiple projectiles fired at multiple targets simultaneously. This may even be expanded to include engaging multiple target *types* simultaneously. Here the problem can become more complex due to the different errors associated with each target type. Additionally, this thesis examined targets flying at a zero angle trajectory in relation to the projectile interceptor. In essence, a two dimensional problem was set up in the 6-DoF code, and was only perturbed perpendicular to the direction of forward flight due to the errors in gun firing and radar azimuth. One could certainly apply this to off-axis trajectory targets, i.e. design a single gun to defend an area from targets coming in from many directions - and setting up a true three dimensional problem.

In the same manner discussed where top level requirements are flowed down to radar subsystem variables, having access to the gun attributes that result in a certain gun accuracy would allow for the subsystem manipulation of the gun accuracy that

is used in the 6-DoF simulation. However, the problem to overcome here would be the same encountered during the literature search for this thesis - there is not much open source information available on medium or large caliber gun design. A much deeper investigation into the field of gun design would be required.

The role of the tracking radar may be expanded to include the role of target recognition, and several useful sources were discovered that describe the techniques and methods, such as that by Nebabin [118], but were not used in this thesis as they were beyond the scope of this thesis. However, this is a topic that is pertinent to the problem discussed in the motivation chapter in that the remainder of the upstream kill chain could be quantified, rather than just assume that a valid target has been identified and tracked. Another excellent application of the power of capturing very complex design spaces with neural network based surrogate surrogate models is to capture the actual radar cross section of target in three dimensions, and even as a function of radar frequency. This way the the fluctuation in target RCS relative to the radar can be taken into consideration as the target travels along its flight path, and the associated radar noise errors which are a function of RCS, can be accounted for.

APPENDIX A

PROBABILITY DISTRIBUTIONS

This Appendix is meant to introduce some background for several of the important probability distributions discussed in this study. There are certainly many different types of probability distributions, such as those given in Figure 107, and each one has its strengths and weaknesses when used for a particular application. Here the *uniform* and *normal* continuous distributions, as well as the discrete *binomial* distribution is introduced. A good statistics book [70] [74] should certainly be consulted for a more in depth explanation.

A.1 Uniform Distribution

The uniform distribution is the simplest of all continuous distributions, in that any number within the sample bounds is equally likely to be selected in a random number draw. The uniform distribution has a constant probability density function (PDF) between its only two parameters, the minimum a and the maximum b bounds, as given in Equation 30. The standard uniform distribution has the parameters $a = 0$

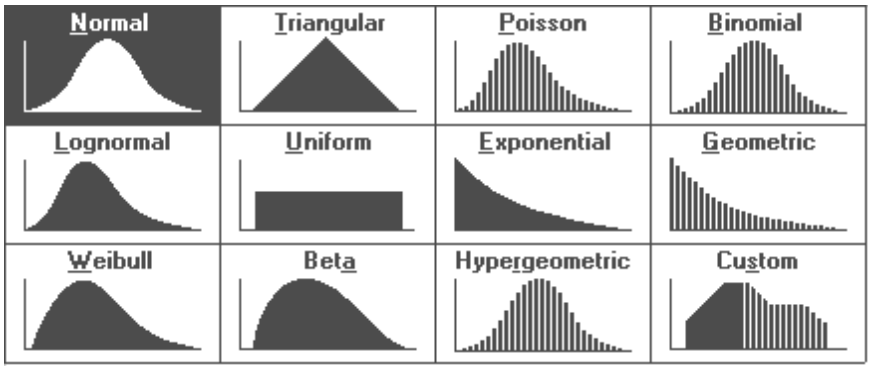

Figure 107: Sample Probability Distributions [52]

Table 21: Area Captured Under a Normal Distribution for Standard Deviation Multipliers

Standard Deviations	Area Captured Under Curve
1σ	68.27%
2σ	95.45%
3σ	99.73%
4σ	99.9994%

and $b = 1$, i.e. selecting a random number between 0 and 1 with equal likelihood.

$$\begin{aligned} f(x) &= \tfrac{1}{b-a} \quad a \leq x \leq b \\ &= 0 \qquad \text{otherwise} \end{aligned} \tag{30}$$

A.2 Normal Distribution

The normal distribution, sometimes referred to as the Gaussian distribution in honor of Carl Freidrich Gauss who developed it around 1820, is considered one of the most important of all continuous probability distributions, and is used frequently in statistics [70]. The PDF for the normal distribution is given in Equation 31,

$$f(x) = \frac{1}{\sigma\sqrt{2\pi}} e^{-\frac{(x-\mu)^2}{2\sigma^2}} \tag{31}$$

where the random variable x is bounded -$\infty \leq x \leq \infty$ and depends on the mean μ and variance σ^2 (where σ is the standard deviation). This distribution is symmetric about the mean μ, and for this reason occasionally referred to as a "bell" curve. The number of standard deviations away from the mean value can describe the amount of are under the distribution curve captured, as given in Table 21.

A.3 Binomial Distribution

Many types of problems have only two types of outcomes for a single trial, or can have one of two types of states, for example the success or failure of a projectile to

intercept a target. A set of these repeated trials of the same experiment in which each of the trials are independent is called a *Bernoulli trial* [74]. The *binomial distribution* given in Equation 32, was derived by James Bernoulli in 1713 to model the total number of successes in repeated trials from an infinite population, given the following conditions [103]:

- Only two outcomes are possible on each of n trials
- Probability of success for each trial p is held constant
- Each of the trials is independent of each other

$$f(x) = \binom{n}{x} p^x (1-p)^{n-x} \tag{32}$$

where

$$\begin{aligned} \binom{n}{x} &= \frac{n!}{(n-x)!x!} \\ x &= 0, 1, 3, \cdots, n \end{aligned}$$

It is known as the binomial PDF because the coefficients in the fraction are successive terms of the binomial expansion. Note that the PDF has a dependence on both p and n, and that it is a discrete, rather than continuous, distribution since the required number of trials, x can only take integer values.

APPENDIX B

PRELIMINARY RESULTS

This chapter will introduce some relevant research conducted by the author that serves as a proof-of-concept of the application of the methodologies introduced in Chapters 2 and 3, as applied to the problem of interest introduced in Chapter 1.

B.1 Skyshield/Ahead Ammunition Study

B.1.1 Introduction

A study by Ender et al. [60] was conducted to measure the effectiveness of firing an air bursting projectile munition against very small targets by quantifying the weapon system uncertainties inherent to a medium caliber weapon. The goal was to determine how accurate the projectile must be fired to burst close enough to the inbound target such that enough submunitions hit the target with the necessary kinetic energy to defeat it. Additionally, only those submunitions that hit an even smaller portion of the target, such as it's fuze, would count as effective hits. A Monte Carlo simulation was used to quantify the uncertainties associated with arriving at a desired point in three dimensional space with a certain velocity as a result of error associated with gun firing elevation, azimuth, muzzle velocity, and crosswind. The values used for error are listed in Table 22. The target intercept locations defined for this preliminary study were between 500 m and 2000 m downrange and between 1000 m and 3000 m in altitude.

The parameters in the design space consisted of a 35 mm unguided round containing submunitions, based on the Ahead round described in Section 1.2.3.2. This round is presently designed to defeat larger and softer targets than the target type of

Table 22: Ahead Study - Errors Used to Quantify Miss Distance

Variable	Error (1σ values)	units
Elevation	$\pm$ 1.25	milliradians
Azimuth	$\pm$ 1.25	milliradians
Muzzle Velocity	$\pm$ 2.50	m/s
Crosswind Gusts	$\pm$ 2.50	m/s

interest in this proposal study, thus its effectiveness against the smaller and harder targets, such as mortar rounds, was the focus of this study. The munition under investigation disperses 152 small tungsten cylinders where the dispersion density of the submunitions depends upon several factors, such as the distance the projectile is fuzed ahead of the target, the velocity degradation due to the projectile burst, and the dispersion pattern maintained by the submunitions as they cross the target plane. Quantifying the uncertainty due to the combined effects of the error in the weapon system and the change in dispersion density will yield the confidence in hitting the target with a certain number of submunitions, as well as the resulting kinetic energy delivered.

PRODAS [29] was used as the six degree-of-freedom trajectory analysis tool, with variations on firing conditions used to model the effects of several types of error. A Monte Carlo analysis was used to quantify uncertainty, where variability in input variables and/or assumptions was tracked by adding distributions to the nominal values. Many cases with randomly selected points from these distributions provided a statistical indication of the probability with which each response occurred. For this study, the probability of arriving at a position in three-dimensional space, and the resultant velocity at impact of the altered trajectory, was quantified as a function of error in gun elevation, azimuth, muzzle velocity, and crosswind. The best way to run a Monte Carlo simulation is to sample the actual analysis tool many times, preferably thousands of times. But with codes that require several seconds to run a single

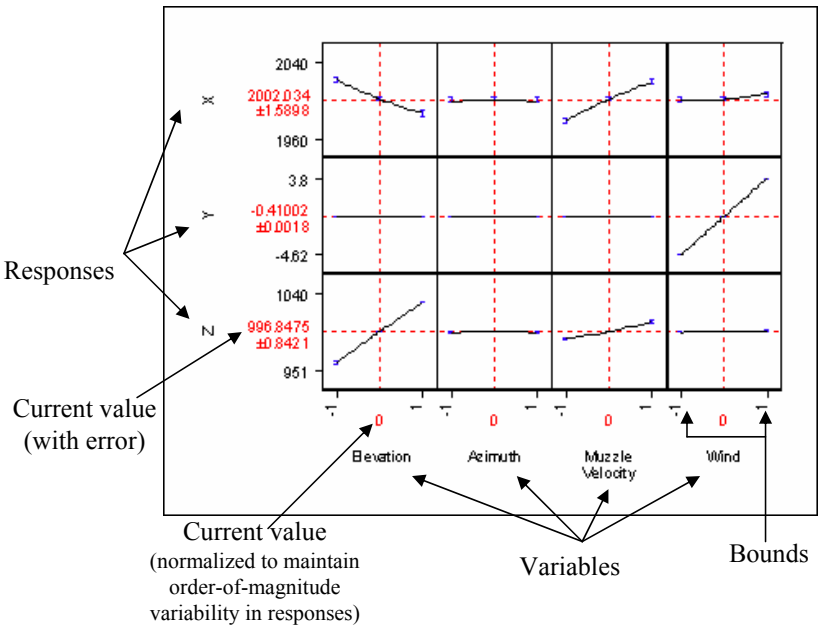

Figure 108: Ahead Study - Interactive Prediction Profiler of Response Surface Equations

case, this may not prove feasible, especially with limited processor capability and the desire to try many different conditions. Therefore, polynomial based surrogate models of the PRODAS simulation tool were created in order to reduce the run time of the thousands of necessary simulation trials, using a Design of Experiments to create representative polynomial response surface equations. A static example of these surrogate models are graphically shown using a JMP [127] prediction profiler in Figure 108.

B.1.2 Miss Distance Quantification

The first use of the advanced design methodology approach in this study was in the quantification of the miss distance between the intended trajectory to intercept the target, and the trajectory resulting from the errors in the weapon system. This step only examines the flight trajectory of the entire projectile *without* submunition dispersion. A Monte Carlo simulation was run in which the error distributions placed on the variables were sampled 10,000 times, each time using those values as the

inputs to the surrogate models that calculate the distance from actual target position and the resultant projectile location in three dimensional space, and the velocity of the projectile when it reaches the target point as a result of the system errors. Figure 109 shows the results of a miss distance Monte Carlo study run on the closest notional target trajectory (500 m down range; 1000 m altitude), where X is the downrange distance, Y is the cross range distance, and Z is altitude. For each of the 10,000 samples, the results are tracked and plotted on a histogram, the peaks of which form a Probability Density Function (PDF) that closely follows a normal distribution with the intended target (zero miss distance) as the mean. This shows that the input error does not bias the projectile in any particular one-dimensional direction. The integration of the PDF gives the Cumulative Density Function (CDF), and the probability of reaching within a certain distance of the intended target can be quantified. The CDF plots the confidence of reaching within a certain distance in 1-D space around the intended target. Because there is no skewness in the PDF, the likelihood of missing the target the same amount on either side is just as likely. Final velocity is presented to show the effects that position error has on final velocity. This plot shows that with these errors, there is still a 90% confidence that the velocity with which the projectile would hit the intended target would be within about 1.5 m/s of the mean value of the PDF. This small variation may not significantly affect the kinetic energy delivered if the target is hit.

Here, the CDF's have a use analogous to the circular error probable (CEP) metric used in the field of missile design, which is the radius of a circle within which 50% of the flight trajectories with the closest miss distance are expected to occur. An assumption used by Fleeman [63] in the conceptual design of missiles is that these miss distances are normally distributed around the intended target (as was the case in Monte Carlo results in Figure 6). In terms of standard deviation, the probability that the miss distance would be less than 1σ value of the normal distribution is 39%

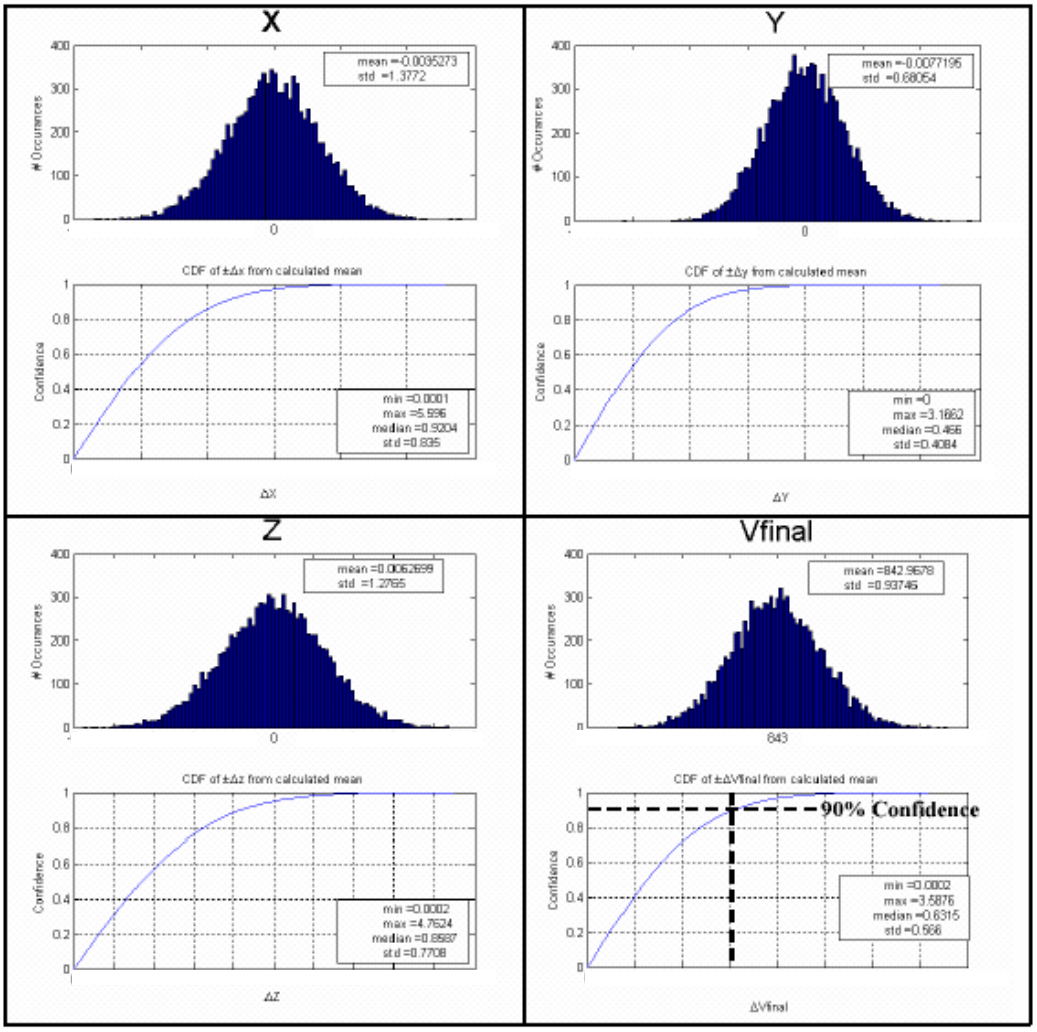

Figure 109: Ahead Study - PDF (top) and CDF (bottom) for Miss Distance and Velocity at Target Intercept

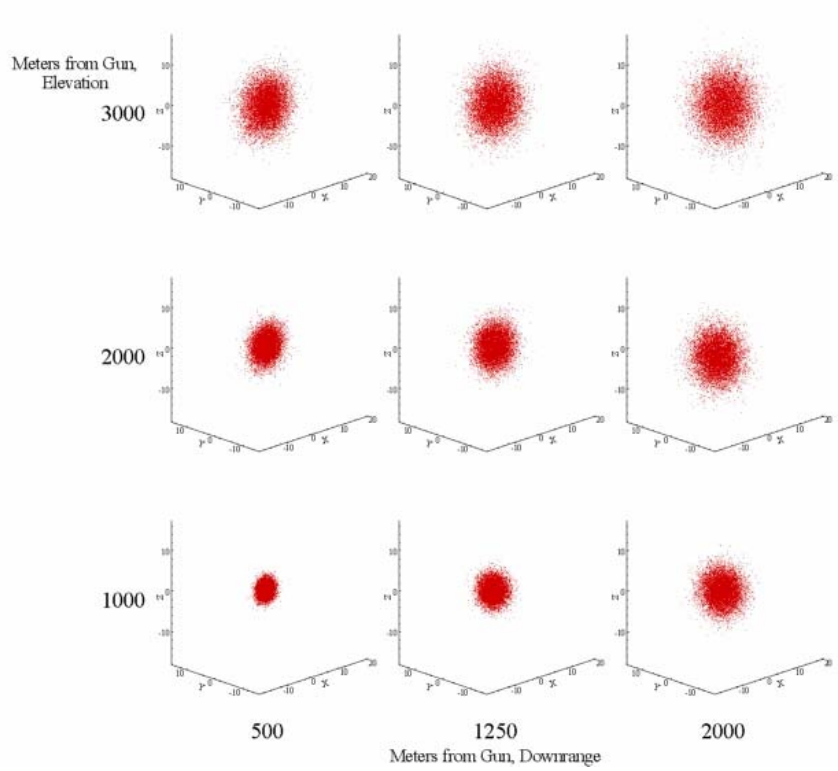

Figure 110: Ahead Study - Miss Distance Point Cloud Dispersion Results

. Similarly, the probability of being within a 2σ miss distance is 86% , and a 3σ miss distance is 99%. For example, a blast fragmentation warhead design may be set so that the warhead lethality radius is equal to the guidance estimate of the 3σ miss distance to provide a comfortable margin for miss distance uncertainty. Fleeman states that a common assumption in the conceptual design of missiles is to interchangeably use the CEP and 1σ terminology, consistent with design accuracy. In this study, the Monte Carlo simulation was used to create point cloud dispersion plots as shown in Figure 110, but instead of two-dimensional circles, the point clouds are three-dimensional ellipses. The point clouds' relative sizes indicate an increase in dispersion with increasing range.

B.1.3 Fuze Distance

A submunition dispersion model was needed to describe how the submunitions propagate through space after the fuze sets off the airburst. Using information from the manufacturer Oerlikon Contraves, several simplifying assumptions were made. After fuzing, the submunitions disperse at a constant 10° angle. Additionally, the submunitions disperse according to a standard witness plate trial, shown in Figure 111. This dispersion pattern was dimensionally scaled by radius to fit into the target plane striking area shown in Figure 112, depending on how far the projectile was fuzed ahead of the target. The main assumption is that the witness plate submunition distribution maintains its normalized shape regardless of fuzing distance, and that all the submunitions cross the target plane at the same time. Additionally, a random spin was added, meaning that the entire dispersion pattern was rotated at an arbitrary angle. The degradation in kinetic energy delivered by the individual submunition hits was taken into account by the velocity profile shown in Figure 112. For example, if the submunitions travel 10 m after the projectile is fuzed, their velocity is degraded to 93% of the velocity at fuzing. This is a simple drag model based on tests conducted by Oerlikon Contraves. Another simplifying assumption was made in that all of the projectiles that were fired in a burst to engage the inbound target arrived at the same time. In other words, the entire engagement occurred in a single plane.

Figure 113 shows a sample dispersion of 10 projectiles fuzed several meters from a 14 mm diameter target, projected in the plane of the target located at the origin. Note the different sizes of the dispersion patterns due to the various errors described earlier. The zoomed in portion of the figure shows the dispersion around the target and highlights the difficulty in hitting such a small target, as will be addressed in the accuracy requirement section. Many of the submunition dispersion patterns from each of the projectiles overlap. Therefore, if several submunitions from different projectiles hit the intended target, each will deliver a different kinetic energy due to each

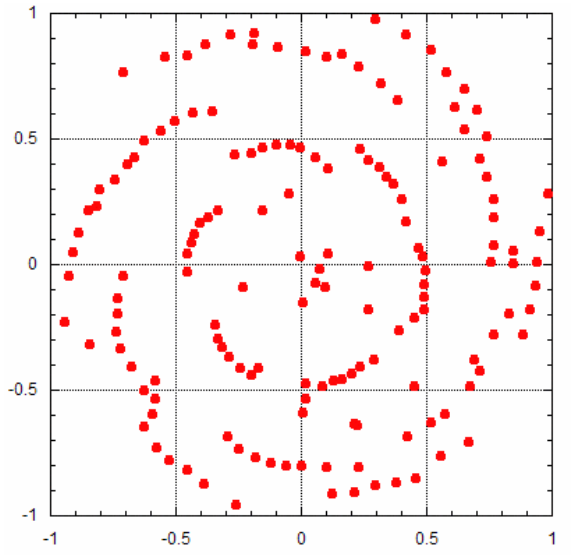

Figure 111: Ahead Study - Normalized Submunition Witness Plate Dispersion Pattern

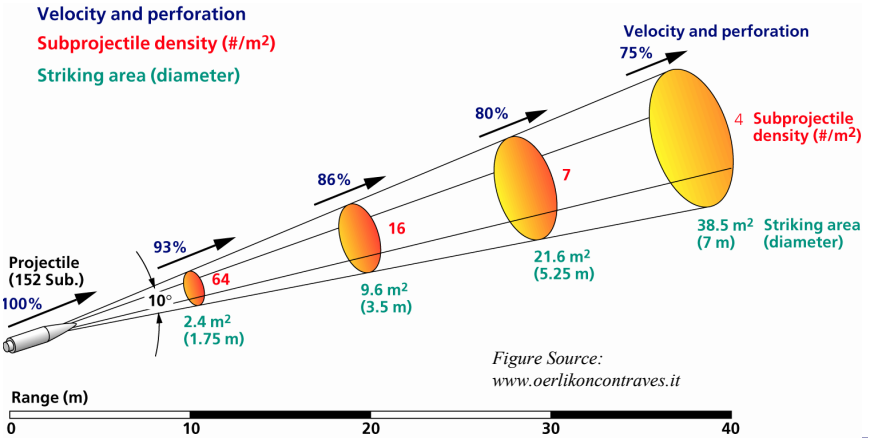

Figure 112: Ahead Study - Velocity Degradation Due to Submunition Dispersion [2]

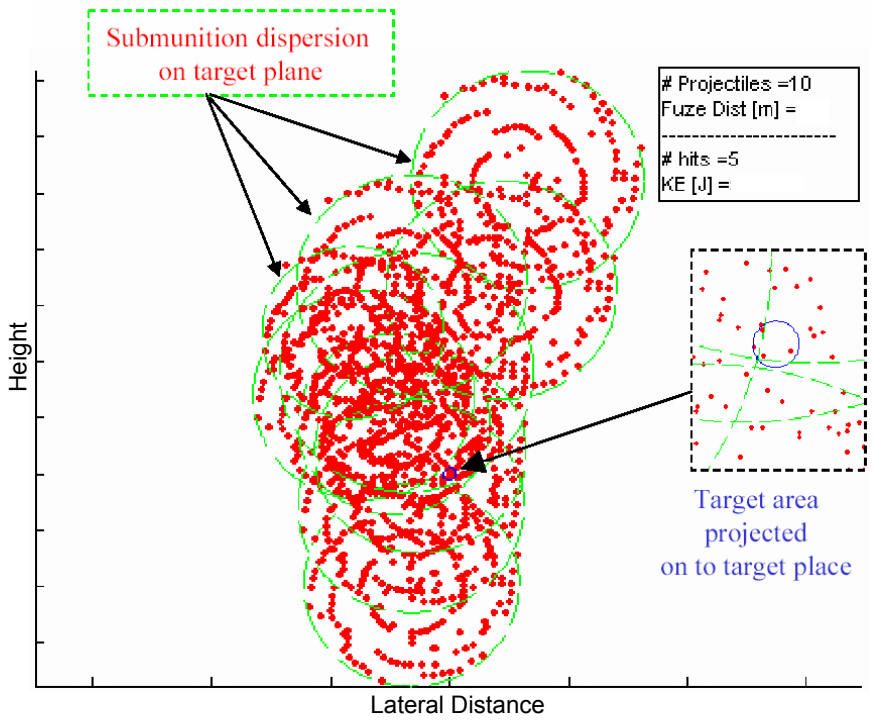

Figure 113: Ahead Study - Submunition Dispersion Clouds from Multiple Projectiles

projectiles final velocity as it crosses the target plane due to the errors applied in the Monte Carlo simulation. Monte Carlo trials conducted at various fuze distances ahead of the target will result in the optimal fuze distance required to hit the target with a required number of submunitions (i.e. kinetic energy) with quantifiable confidence.

B.2 CIWS study

The goal of this study was to determine the probability of hitting an 81 mm moving target *as it approaches* the defended area, while accounting for miss distance caused by random gun errors. The target was to be intercepted between 250-1000 m, and as shown in Figure 114, the range bounds were divided to four discrete cases that the simulation was run. Just as for the previous study, PRODAS [29] was used as the six degree-of-freedom trajectory analysis tool, with variations on firing conditions used

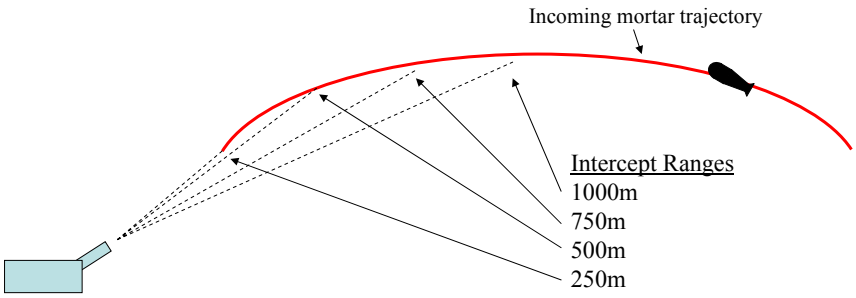

Figure 114: CIWS Study - Target Intercept Ranges

to model the effects of several types of error. The ultimate goal was to determine the probability of hitting the target due to the cumulative effect of tracking the target along its flight path, given the randomness in gun and crosswind error. For this study, randomness was introduced into five variables, the bounds of which will not be presented. These variables include:

1. Gun firing elevation
2. Gun firing azimuth
3. Crosswind gusts
4. Initial pitch
5. Initial yaw

Although a three dimensional problem, this particular study only focused on the two dimensional plane around the circular cross section of the target. This method was used since PRODAS can not model the trajectory of two objects simultaneously, i.e. a target and interceptor, and determine whether a hit occurred in three dimensional space. Polynomial RSE's were created for the actual point in space when it crosses the cross range/altitude plane of the target. Therefore, the prediction profiler in Figure 115 does not include down range (X) responses, but only cross range (Y) and altitude (Z) at each of the intercept ranges.

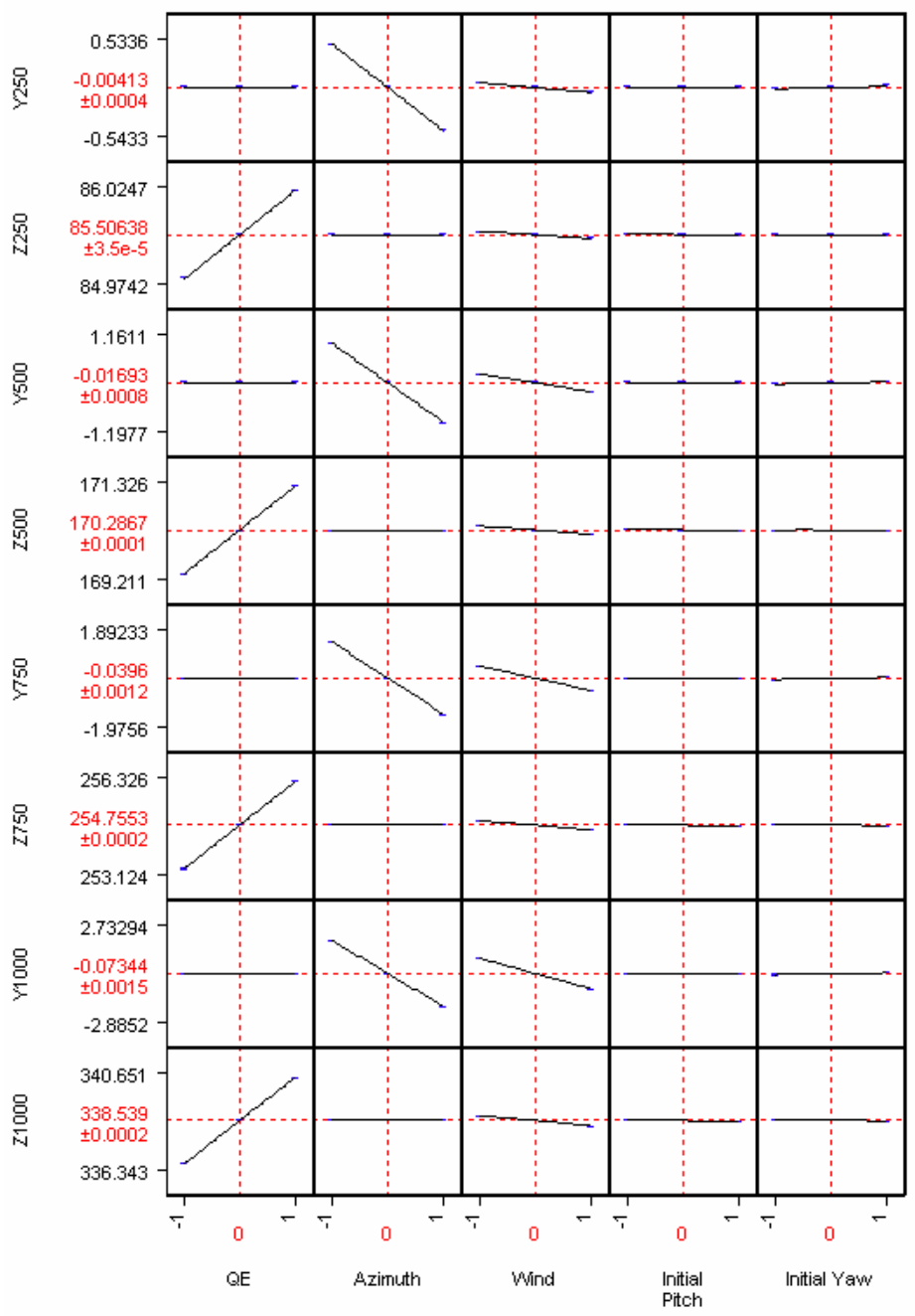

Figure 115: CIWS Study - Prediction Profiler of Surrogate Models

A Monte Carlo analysis was run to determine the probability of target intercept by a single round at the four notional ranges. A scatter plot showing where each round crosses the target plane can be used to calculate the 50% and 90% CEP's. The ratio of rounds crossing the target plane within the radius of the target (from the center of the target) to the total rounds examined in the Monte Carlo study indicates the probability of hitting the target, for a single round. Figure 116 shows the results of a Monte Carlo simulation run for each of the target intercept ranges. The blue circle represents the diameter of the target, the green circle represents the area comprising 50% of the projectiles, and the red circle represents the area comprising 90% of the projectiles. Note that as intercept range increases, the number of projectiles within the target area diminishes, as expected.

To quantify the confidence of arriving within a certain distance of the target, the CDF was calculated using the Monte Carlo simulations. The plots given in Figure 117 show the confidence of a single round arriving at a distance away from the center of the target, or the probability of a single hit. The red line represents the target radius, therefore the intersection of the red line with the CDF yields the probability of directly hitting the target, P_H. The curve may also be discretized by the total number of desired projectiles fired as the target travels, assuming that the single shot probability of hit at any range in between the four ranges listed earlier can be determined by simple linear interpolation. For an accurate cumulative hit probability, Equation 9 should be used. However, for simplicity Macfadzean [92] states that for very small single shot probabilities of hit, the cumulative probability of hit can be simply approximated by summing the individual single shot probabilities. Figure 118 shows the curve discretized for 100 rounds, meaning that some firing rate was assumed that resulted in 100 rounds being fired, the first one cross the target plane at 1000 m, and each subsequent round evenly spaced. Note that the study was only conducted at four discrete ranges. Certainly more test points would be required to define the space

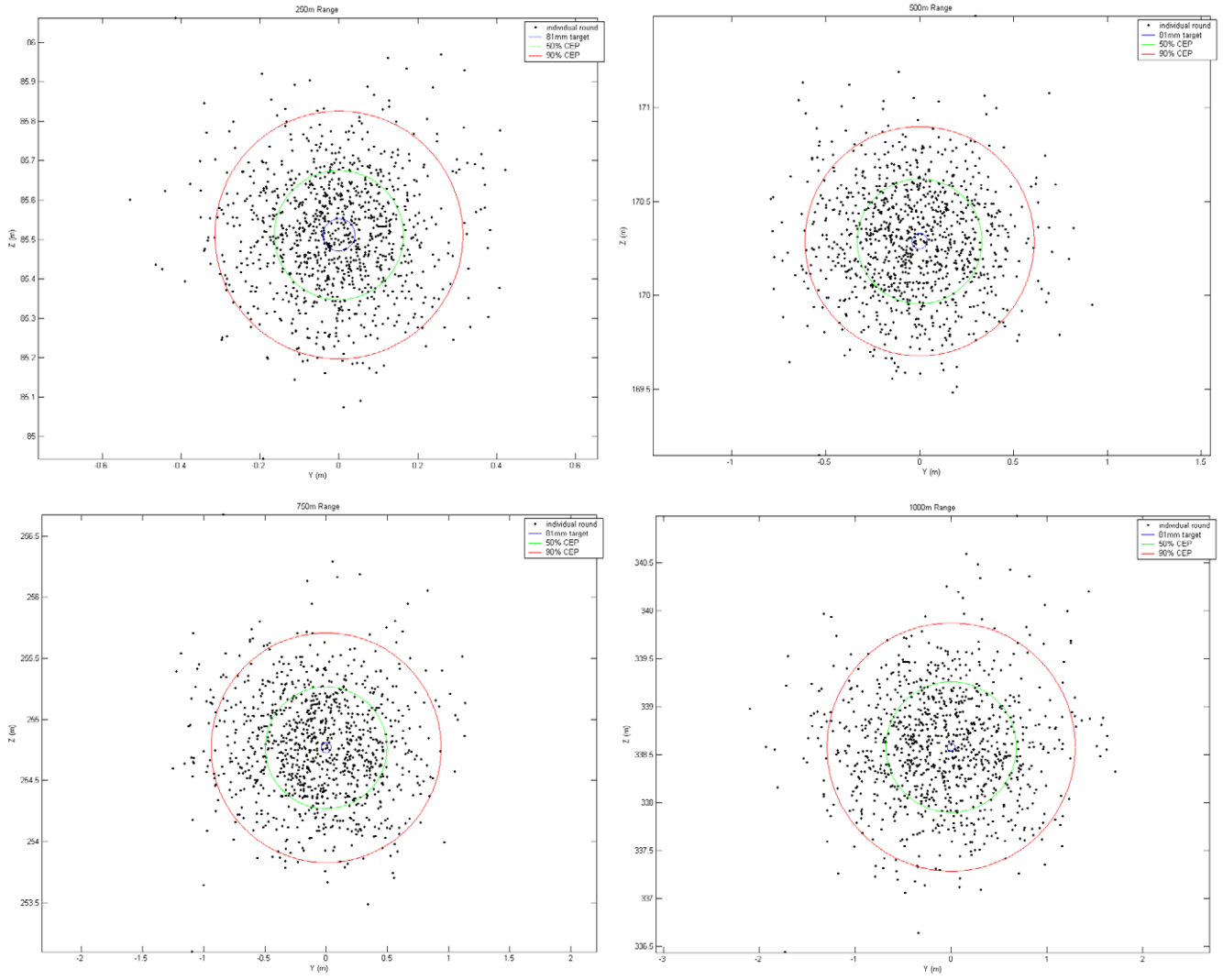

Figure 116: CIWS Study - Monte Carlo CEP Results Single Round Intercept at 250, 500, 750, and 1000 m

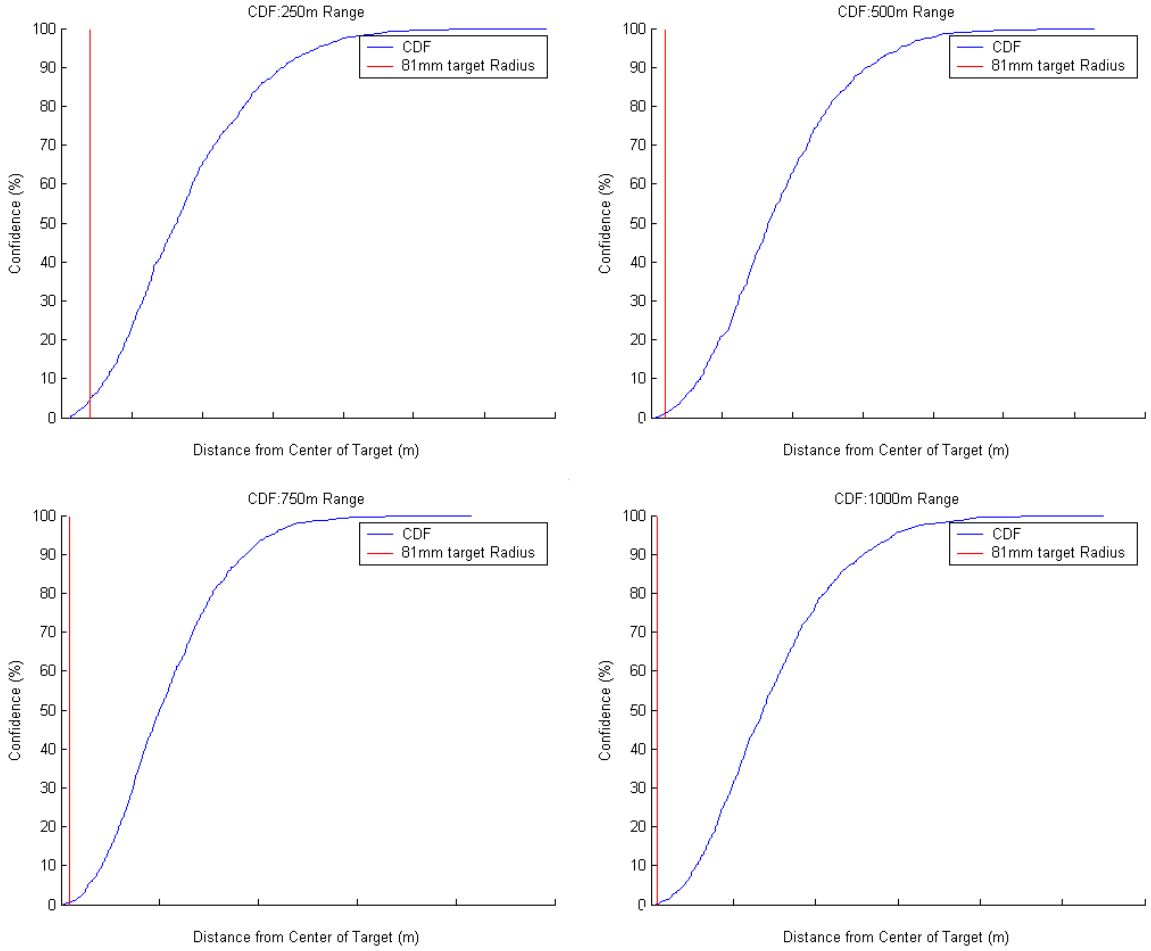

Figure 117: CIWS Study - CDF for 250, 500, 750, 1000 m Ranges

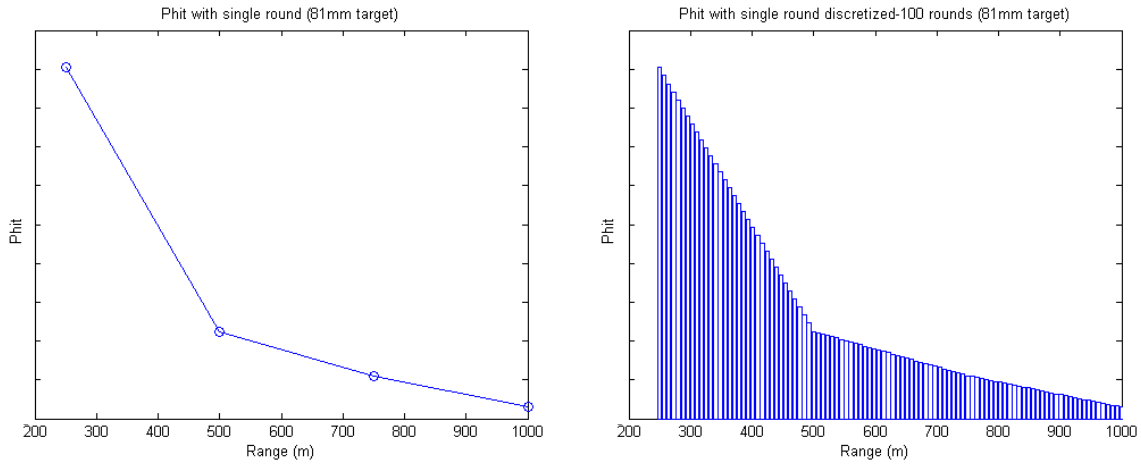

Figure 118: CIWS Study - Single Round P_H (L) and Discretized Single Round P_H (R)

between the 250 m and 500 m ranges, where the greatest difference between P_H values is. The cumulative probability of hitting the target with at least one projectile, or the confidence of intercepting the target as it approaches, is quantified in Figure 119. This simple curve now shows how the change in P_H varies as the target approaches the defended area.

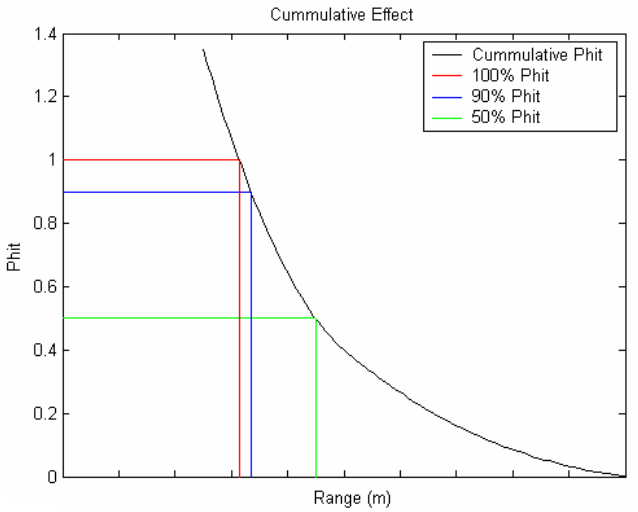

Figure 119: CIWS Study - Cumulative P_H of Approaching Target

APPENDIX C

GUN RATE OF FIRE REGRESSION

The historical data shown in Table 23 is based on a compilation of information collected by Massey [25]. The goal in assembling this database of historical information was to find a basic correlation between a gun's rate of fire and bore size. With the framework in place to create neural network surrogate models in place for most of the other work presented in this thesis, the author decided to fit a regression using the neural network methods. Equation 33 represents the method used to calculate rate of fire in this thesis. This equation calculates Rate of Fire (RoF) in rounds per minute, as a function of Bore size (in mm). Figure 120 shows the regression used with the data points used to create them overlaid and the distribution of error. This fit is certainly not excellent by most measures of merit, but considering that more than one data point (rate of fire) exist for many of the bore values input, this fit is an improvement over using a simple polynomial or logarithmic regression. Additionally, as overly complex as this equation make seem, it was very simple to create and implement in the simulation.

Table 23: Historical Data For Gun Rate of Fire [25]

Gun System	Caliber (mm)	Rate of Fire (RPM)	Barrels	RoF/Barrel (RPM)	Comment
Flak 38	20	450	1	450	1939 German
XM301	20	1500	3	500	Commanche gun
Phalanx C-RAM	20	4500	6	750	Gatling gun
m61 Vulcan	20	6000	6	1000	1960s
ZSU-23 Shilka	23	4000	4	1000	1965 Soviet Gun
GAU-12 Equalizer	25	4200	6	700	A-10 gun
Mk44	30	200	1	200	new
Flak 103/38	30	400	1	400	1944 German
GAU-8 Avenger	30	4200	7	600	F-18 gun
M230	30	625	1	625	1988 Apache gun
Aden Mk5	30	1600	1	1600	1954 Aden Mk1
Bushmaster III	35	160	1	160	New
Skysheild	35	1000	2	500	Growth version to 50mm
Flak 18	37	160	1	160	1935
Flak 36/37	37	160	1	160	1937
M1939 Type 55	37	180	1	180	1960s
Flak 43	37	250	1	250	1937
Bushmaster IV	40	160	1	160	
Mk44	40	200	1	200	Super 40
mk47	40	300	1	300	mk19 replacement
mk19	40	350	1	350	grenade launcher 1960s
Flak 41	50	130	1	130	1941
Bushmaster III	50	160	1	160	New
Great 58	55	140	1	140	1941
S-60	57	120	1	120	1950s Soviet
Bofors 57	57	220	1	220	
8.8cm Flak 18,37,37	88	15	1	15	1934
8.8cm Flak 41	88	20	1	20	1942
10.5cm Flak 38/39	105	15	1	15	1939
12.8cm Flak	128	12	1	12	1942

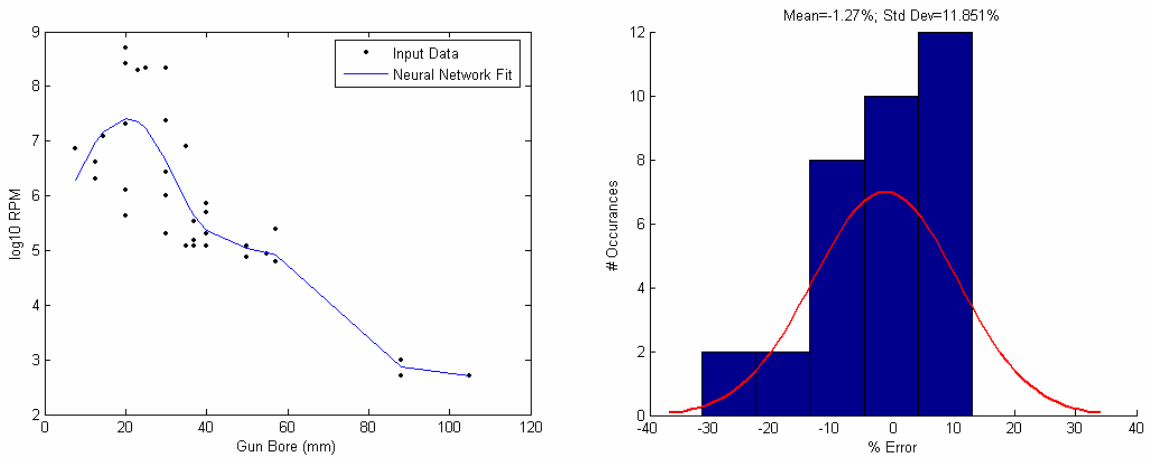

Figure 120: Firing Rate Curve Fit (L) and Associated Error Distribution (R)

$$\log_{10} RoF = 2.48490665 + 6.214608098 * \left[0.0300307957854 + \sum_{i=1}^{5} A_i * \frac{1}{1 + e^{-\left(B_i + C_i * \left(\frac{Bore - 7.62}{120.38}\right)\right)}}\right] \quad (33)$$

where

$$A_1 = 0.0606368589412 \quad B_1 = 27.9929448352691 \quad C_1 = -28.0070451148204$$

$$A_2 = 0.0295660006372 \quad B_2 = 21.0101869886458 \quad C_2 = -27.9880284206632$$

$$A_3 = 0.3500044429334 \quad B_3 = 14.1935862262056 \quad C_3 = -27.9214623686777$$

$$A_4 = 0.4375050999628 \quad B_4 = 5.6595893903830 \quad C_4 = -28.3736546079568$$

$$A_5 = -0.409428487125 \quad B_5 = 0.2901708320125 \quad C_5 = -27.9617886232176$$

APPENDIX D

SUPPORTING DATA

D.1 Initial Study Pareto Plots

This Appendix provides the complete set of Pareto plots referenced in Section 6.3.4. Figures 121, 122, and 123 include a Pareto plot for each discrete bore/range combination examining the response variability in the initial 6-DoF study.

D.2 Detail Study Surrogate Model Fit Results

Figure 124 shows the fit results for the neural network surrogate models created in the Detail Study in Section 6.7 and used in the Assembled Hierarchical Environment in Section 6.8. Note that for the two guided rounds (the kinetic-kill/pin-control and warhead-kill/thruster-control), the fits are fairly good. However, the unguided round has a relatively poor fit. The main reason for this is that unlike the two guided rounds that used 750 Monte Carlo simulations per 6-DoF execution, the unguided trials only executed 250 runs. With fewer Monte Carlo trials per DoE run, the data was very coarse, as can be seen in the bottom left plot of Figure 124, showing the actual data by predicted results for the unguided fits. As discussed in Section 6.7, close to one million 6-DoF trials were necessary to generate the fits shown in Figure 124, and towards the end of this process, the computational resources were less available. However, as the unguided results were used only for the purposes of comparison against the guided rounds, and the unguided trends made sense, these fit results were considered sufficient.

Bore: 40mm
Range: 250m

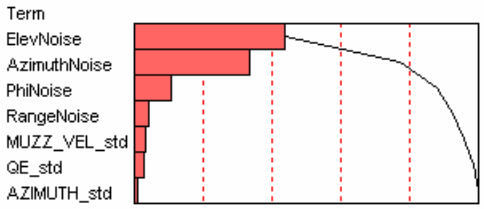

Bore: 40mm
Range: 500m

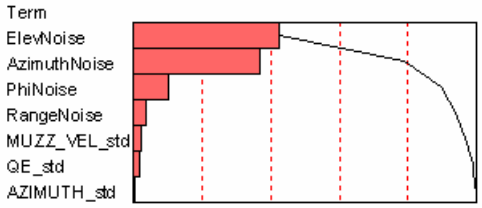

Bore: 40mm
Range: 1000m

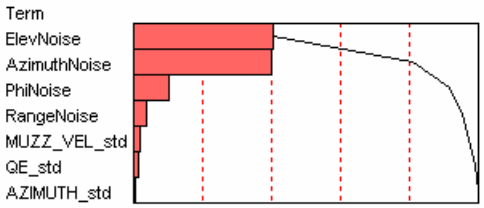

Bore: 40mm
Range: 1500m

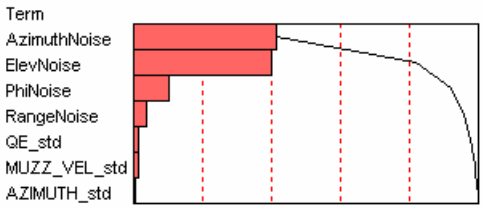

Bore: 40mm
Range: 2000m

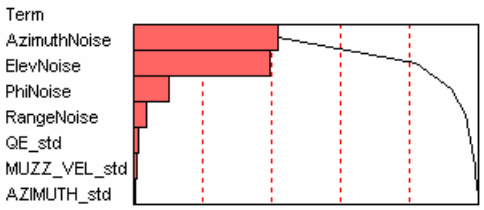

Figure 121: Initial Study - Pareto Plots for 40 mm Bore, All Ranges

Bore: 50mm
Range: 250m

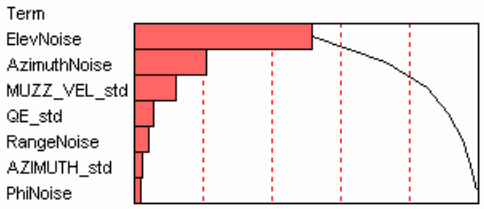

Bore: 50mm
Range: 500m

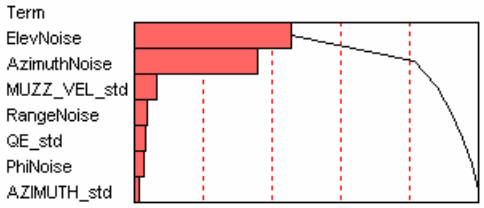

Bore: 50mm
Range: 1000m

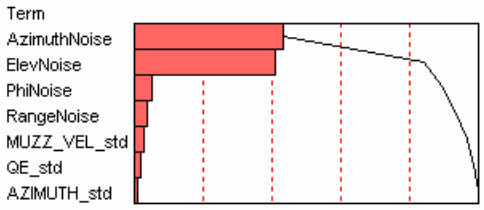

Bore: 50mm
Range: 1500m

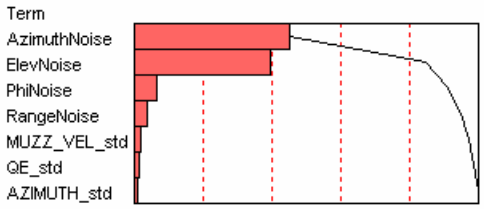

Bore: 50mm
Range: 2000m

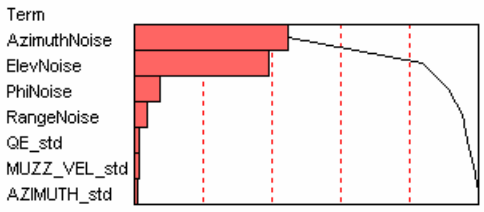

Figure 122: Initial Study - Pareto Plots for 50 mm Bore, All Ranges

Bore: 57mm
Range: 250m

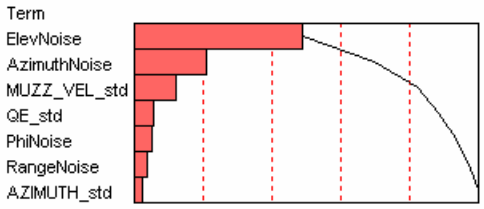

Bore: 57mm
Range: 500m

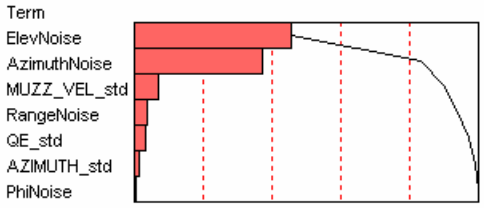

Bore: 57mm
Range: 1000m

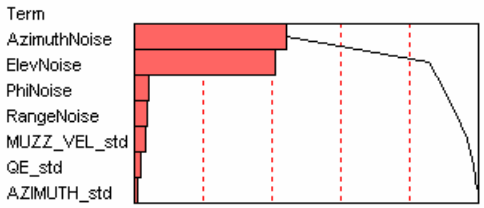

Bore: 57mm
Range: 1500m

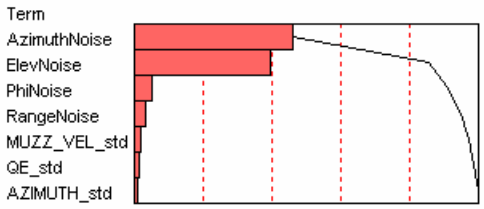

Bore: 57mm
Range: 2000m

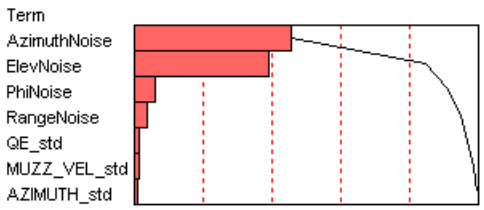

Figure 123: Initial Study - Pareto Plots for 57 mm Bore, All Ranges

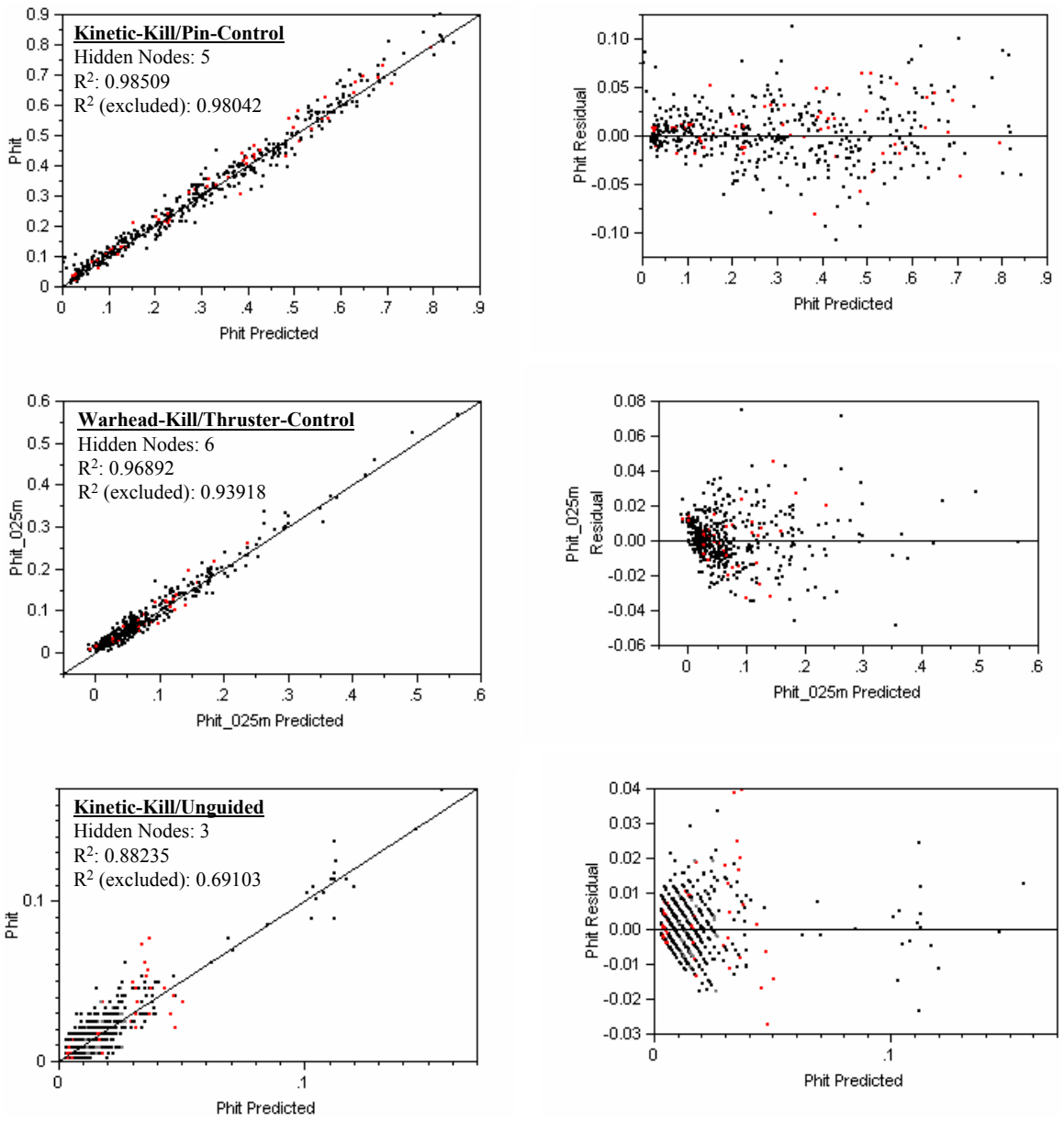

Figure 124: Detailed Study - Actual by Predicted and Residual Plots for Neural Network Fits

REFERENCES

[1] Federation of American Scientists. http://www.fas.org. [Date accessed: June, 2005].

[2] Oerlikon Contraves. http://www.oerlikoncontraves.com. [Date accessed: June, 2005].

[3] Webster online dictionary. http://www.webster.com. [Date accessed: June, 2005].

[4] Risk Glossary. http://www.riskglossary.com. [Date accessed: June, 2005].

[5] Aerospace Systems Design Laboratory, School of Aerospace Engineering, Georgia Institute of Technology. http://www.asdl.gatech.edu/. [Date accessed: July, 2006].

[6] ArrowTech Associates. http://www.prodas.com. [Date accessed: June, 2006].

[7] "Small Low-cost Interceptor Device (SLID)." Boeing Website. http://www.boeing.com/defense-space/missiles/slid/slid.htm. [Date accessed: January, 2006].

[8] "Tactical High Energy Laser (THEL)." MissileThreat.com, A Project of the Claremont Institute, http://www.missilethreat.com/systems/thel.html. [Date accessed: June, 2005].

[9] "Survivability, Aircraft, Nonnuclear, General Criteria." Vol. 1, Dept. of Defense, MIL-HDBK-336-1, Washington, DC, October 25, 1982.

[10] "DARPA Neural Network Study," tech. rep., M.I.T. Lincoln Laboratory, Lexington, MA, 1988.

[11] "USAF Intelligence Targeting Guide." Air Force Pamphlet 14-210, 1 February, 1998. http://afpubs.hq.af.mil. [Date accessed: January, 2006].

[12] "Tactical High Energy Laser ACTD." Federation of American Scientists., November 1998. http://www.fas.org/spp/starwars/program/thel.htm. [Date accessed: June, 2005].

[13] "Battle Command Training Program," tech. rep., United States Army Training and Doctrine Command, Fort Monroe, Virginia, 1 April 1999. TRADOC Regulation 350-50-3.

[14] "MK 45 5-inch / 54-caliber (lightweight) gun." Federation of American Scientists, Nov 1999. http://www.fas.org/man/dod-101/sys/ship/weaps/mk-45.htm. [Date accessed: January, 2006].

[15] "Department of Defense Dictionary of Military and Associated Terms." Joint Chiefs of Staff, U. S. Dept. of Defense, Joint Publication 1-02, April 2001. www.dtic.mil/doctrine/jel/doddict/. [Date accessed: June, 2005].

[16] "ASAR Product Handbook." Issue 1.2, European Space Agency, September 2004. http://envisat.esa.int/dataproducts/asar/CNTR.htm. [Date accessed: June, 2005].

[17] "Mobile / Tactical High Energy Laser (M-THEL) Technology Demonstration Program." Defense Update: An International Online Defense Magazine, May 7 2004. http://www.defense-update.com/directory/THEL.htm. [Date accessed: June,2005].

[18] "THEL Mortar Shootdown." Northrop Grumman Press Release, 2004. http://www.st.northropgrumman.com/media/VideoInfo.cfm?VideoID=34. [Date accessed: June, 2005].

[19] "AMSAA Supports Current Operations Through Counter Mortar Collateral Damage Estimation." RDECOM Magazine, submitted by U.S. Army Materiel Systems Analysis Activity, February 2005.

[20] "AHEAD Air defense Gun System, Oerlikon Contraves (Switzerland)." Defense Update: An International Online Defense Magazine, January 2005. http://www.defense-update.com/products/a/ahead.htm. [Date accessed: June, 2005].

[21] "Pentagon Fast-Tracks Mortar Defense System." Fox News, March 29 2005. http://www.foxnews.com/story/0,2933,151712,00.html. [Date accessed: June, 2005].

[22] "Green Zone." Global Security, June 2005. http://www.globalsecurity.org/.../baghdad-green-zone.htm. [Date accessed: June, 2006].

[23] "Counter Rocket, Artillery, and Mortar (C-RAM)." Global Security, June 2005. http://www.globalsecurity.org/military/systems/ground/cram.htm. [Date accessed: June, 2005].

[24] Discussions with thesis committee member Dr. E. Jeff Holder, Chief Scientist, Sensors and Electromagnetic Applications Laboratory, Georgia Tech Research Institute, Jan-June 2006.

[25] Discussions with thesis committee member Dr. Kevin Massey, Senior Research Engineer, Aerospace, Transportation, and Advanced Systems Laboratory, Georgia Tech Research Institute, Apr 2005 - June 2006.

[26] "Quadrennial Defense Review Report." United States Department of Defense, February 2006.

[27] "Neural Networks." StatSoft, Inc., Copyright 1984-2003. `http://www.statsoftinc.com/textbook/stneunet.html`. [Date accessed: June, 2005].

[28] Alexander, R., Hall-May, M., and Kelly, T., "Characterisation of Systems of Systems Failures," Proceedings of the 22nd International System Safety Conference, University of York, 2004.

[29] ArrowTech Associates, South Burlington, VT, *PRODAS Version 3 Technical Manual*, 2002.

[30] Baker, A. P., "Assessing the Simultaneous Impact of Requirements, Vehicle Characteristics, and Technologies During Aircraft Design," 39th Aerospace Sciences Meeting & Exhibit, Reno, NV, 8-11 January, 2001. AIAA-2001-0533.

[31] Baker, A. P., *The Role of Mission Requirements, Vehicle Attributes, Technologies and Uncertainty in Rotorcraft System Design*. PhD thesis, Georgia Institute of Technology, 2002.

[32] Ball, R. E., *The Fundamentals of Aircraft Combat Survivability Analysis and Design*. AIAA, 2003.

[33] Barr, M., "Closed-Loop Control," *Embedded Systems Programming*, pp. 55–66, August 2002.

[34] Barton, D. K., *Modern Radar System Analysis*. Artech House, 1988.

[35] Baumann, J., "Systems Engineering," Session 1-2. Presented at the 2nd AIAA Tactical Interceptor Technology Symposium, Huntsville, AL, 20-21 January, 2005.

[36] Benson, D., Ryan, B., and Drzewiecki, T., "An Optofluidic Control System for Tactical Missiles and Guided Munitions," AIAA Guidance, Navigation, and Control Conference, New Orleans, LA, 11-13 August, 1997. AIAA-1997-3834.

[37] Berglund, N., "The Full Derivative Matrix & Jacobian." Calculus III Lecture Notes, Georgia Institute of Technology, Spring, 2006. `http://www.math.gatech.edu/\~berglund/teaching.html`. [Date accessed: April, 2006].

[38] Biltgen, P. T., Ender, T. R., and Mavris, D. N., "Development of a Collaborative Capability-Based Tradeoff Environment for Complex System Architectures," 44th AIAA Aerospace Sciences Meeting and Exhibit, Reno, Nevada, Jan. 9-12, 2006. AIAA-2006-0728.

[39] Bird, J., "Air and Missile Defense Transformation: Where We Were, Where We Are Today, and Where We Are Going." Air Defense Artillery (ADA) Magazine Online, January 2006. `http://airdefense.bliss.army.mil/.../WhereWeAreGoing.htm`. [Date accessed: January, 2006].

[40] Blanchard, B. S., *System Engineering Management*. John Wiley & Sons, Inc., 1991.

[41] Blanchard, B. S., *Logistics Engineering and Management*. Prentice Hall Inc., 5th ed., 1998.

[42] Buede, D. M., *The Engineering Design of Systems*. John Wiley & Sons, Inc., 2000.

[43] Burnett, D., Brekke, K., Locke, J., and Frederick, R. A., "Shark Workshop Report," Session 4-2. Presented at the 2nd AIAA Tactical Interceptor Technology Symposium, Huntsville, AL, 20-21 January, 2005.

[44] Buzzett, J., Nixon, D., and Horwath, T., "Investigation of Guidance Technologies for Spinning Projectiles," presented at the 36th Annual Gun & Ammunition Symposium & Exhibition, San Diego, CA, 9-12 April, 2001. `http://www.dtic.mil/ndia/2001gun/2001gun.html`. [Date accessed: January, 2006].

[45] Cantor, M., "Thoughts on Functional Decomposition." IBM online magazine "The Rational Edge", 2003.

[46] Cave, D. R., "Systems Effectiveness Analysis Tool for Evaluating Guided Interceptors," Aerospace Sciences Meeting and Exhibit, 32nd, Reno, NV, 10-13 January, 1994. AIAA-1994-210.

[47] Chapman, W. L., Bahill, A. T., and Wymore, A. W., *Engineering Modeling and Design*. CRC Press, 1992.

[48] Chen, P., Gori, R., and Pozgay, A., "Systems and Capability Relation Management in Defence Systems-of-System Context," (Copenhagen, Denmark), Proceedings of The Ninth International Command and Control Research and Technology Symposium, 2004.

[49] Clare, T. A., "The Engineering and Acquisition of Systems of Systems," in *Proceedings from the 3rd Annual Systems Engineering & Supportability Conference*, Department of Defense, Research Development and Acquisition Office, Oct 2000.

[50] Clements, P., Krut, R., Morris, E., and Wallnau, K., "The Gadfly: An Approach to Architectural-Level System Comprehension," Fourth IEEE Workshop on Program Comprehension, Berlin, March, 1996.

[51] Costello, M., "Rigid Body Projectile Exterior," Session 3-2. Presented at the 2nd AIAA Tactical Interceptor Technology Symposium, Huntsville, AL, 20-21 January, 2005.

[52] Decisioneering, Inc., Denver, CO, *Crystal Ball User Manual*, 2004.

[53] Demuth, H. and Beale, M., *MATLAB: Neural Network Toolbox User's Guide Version 4*. The MathWorks, Inc., 2004.

[54] Despotou, G., Alexander, R., and Hall-May, M., "Key Concepts and Characteristics of Systems of Systems," Tech. Rep. DARP-HIRTS Strand 2, University of York, 2003.

[55] Dew, J., "Computer Models: Current Uses and Future Requirements." Presentation given at Systems Integration Branch, Defense Threat Reduction Agency, 18 November, 2003.

[56] Dieter, G. E., *Engineering Design: A Materials and Processing Approach*. McGraw Hill, 2000.

[57] Driels, M. R., *Weaponeering: Conventional Weapon System Effectiveness*. Reston, VA: AIAA Education Series, 2004.

[58] Du, X. and Chen, W., "Methodology for Managing the Effect of Uncertainty in Simulation-Based Design," *AIAA Journal*, vol. 38, pp. 1471–1478, August 2000.

[59] Einstein, A., "Collected Quotes from Albert Einstein." Copyright Kevin Harris, 1995.

[60] Ender, T. R., Mavris, D. N., Massey, K. C., Holder, E. J., OLeary, P., and Smith, R. A., "Predicting the Effectiveness of an Air Bursting Munition Using Uncertainty Quantification," Presented at the AIAA 2004 Missile Sciences Conference, Monterey, CA, November 16-18, 2004.

[61] Ender, T. R., McClure, E. K., and Mavris, D. N., "A Probabilistic Approach to the Conceptual Design of a Ship-Launched High Speed Standoff Missile," Presented at the AIAA 2002 Missile Sciences Conference, Monterey, CA, November 5-7, 2002.

[62] Ender, T. R., McClure, E. K., and Mavris, D. N., "Development of an Integrated Parametric Environment for Conceptual Hypersonic Missile Sizing," Presented at the 2nd AIAA ATIO Forum, Los Angeles, CA, October 1-3, 2002.

[63] Fleeman, E. L., *Tactical Missile Design*. Reston, VA: American Institute of Aeronautics and Astronautics, 2001.

[64] Frame, M., Mandelbrot, B., and Neger, N., "Fractal Geometry." Yale University, April 2005. http://classes.yale.edu/fractals/CA/NeuralNets/NeuralNets.html. [Date accessed: June, 2005].

[65] Gajda, W. J. and Biles, W. C., *Engineering Modeling and Computation*. Boston: Houghton Mifflin Company, 1978.

[66] Geswender, C., "Guided Projectiles Theory of Operations," presented at the 36th Annual Gun & Ammunition Symposium & Exhibition, San Diego, CA, 9-12 April, 2001. http://www.dtic.mil/ndia/2001gun/2001gun.html. [Date accessed: January, 2006].

[67] Gompert, D. and Isaacson, J., "Planning a Ballistic Missile Defense System of Systems: An Adaptive Strategy," Tech. Rep. Paper IP-181, RAND National Defense Research Institute, 1999.

[68] Group W Inc., Fairfax, VA, *THUNDER: Multi-Service Campaign Analysis Tool*, http://www.group-w-inc.com/. [Date accessed: June, 2005].

[69] Hartlage, B., Owen, M., Dimeler, H., Robert A. Frederick, J., and Davis, C., "Enhanced Counter Air Projectile," 40th AIAA/ASME/SAE/ASEE Joint Propulsion Conference and Exhibit, Fort Lauderdale, Florida, 11-14 July, 2004. AIAA 2004-4086.

[70] Hayter, A. J., *Probability and Statistics for Engineers and Scientists*. Boston: PWS Publishing Company, 1996.

[71] Heller, A., "Simulation Warfare Is No Video Game," *Science & Technology Review*, pp. 4–11, January/February 2000. National Nuclear Security Administration's Lawrence Livermore National Laboratory.

[72] Hewitt, D. J., "Notional System - Shark I," Session 4-1. Presented at the 2nd AIAA Tactical Interceptor Technology Symposium, Huntsville, AL, 20-21 January, 2005.

[73] Hines, N. R. and Mavris, D. N., "A Parametric Design Environment for Including Signatures Analysis in Conceptual Design," 2000. AIAA-2000-01-5564.

[74] Hines, W. W. and Montgomery, D. C., *Probability and Statistics in Engineering and Management Science*. John Wiley & Sons, Inc., 3rd ed., 1990.

[75] Holder, E. J., "Fire Control Radar Requirements for RAM Defense," Session 2-5. Presented at the 2nd AIAA Tactical Interceptor Technology Symposium, Huntsville, AL, 20-21 January, 2005.

[76] Holder, E. J., "Command vs Semi-Active Projectile Guidance." Review Presentation for U.S. Army Customers, Georgia Tech Research Institute, Atlanta, GA, 2006.

[77] Hollis, P. S., "Transforming the Force - From Korea to Today. Robert H. Scales, Jr. - Major General Retired - Interview," *Field Artillery Journal*, July 2001.

[78] Horwath, T. G. and Barnych, G., "Low Cost Course Correction Cost Course Correction (LCCC) Technology Applications," NDIA International Armaments Technology International Armaments Technology Symposium, 14-16 June, 2004.

[79] Hughes, Wayne P., J., *Military Model for Decision Makers*. Military Operations Research Society, 1997.

[80] Huyse, L., "Solving Problems of Optimization Under Uncertainty as Statistical Decision Problems," in *AIAA-2001-1519*, 2001.

[81] Johnson, C., "Introduction to Neural Networks in JMP, Version 2.0." May 2004.

[82] Johnson, C., "Function Approximating Neural Network Generation System (FANNGS) Documentation Version 1.2." June 2005.

[83] Kapper, F. B., "Wargaming," *Defense*, 1981. Department of Defense.

[84] Kirby, M. R. and Mavris, D. N., "Forecasting the Impact of Technology Infusion on Subsonic Transport Affordability," 1998. AIAA-98-5576.

[85] Kirby, M. R. and Mavris, D. N., "Forecasting Technology Uncertainty in Preliminary Aircraft Design," 1999. AIAA-99-01-5631.

[86] Knott, E. F., *Tactical Missile Aerodynamics*. AIAA Tactical Missile Series, 1992.

[87] Koller, R., *Konstruktionslehre fuer den Maschinenbau*. Berlin: Springer-Verlag, 1985.

[88] Kuhne, C., Wiggs, G., Beeson, D., Madelone, J., and Gardner, M., "Using Monte Carlo Simulation for Probabilistic Design," Proceedings of the 2005 Crystal Ball User Conference, 2005.

[89] Lanchester, F. A., *Aircraft in Warfare: The Dawn of the Fourth Arm*. London: Constable, 1916.

[90] Lloyd, R. M., *Conventional Warhead Systems Physics and Engineering Design*, vol. 179 of *Progress in Astronautics and Aeronautics Series*. AIAA, 1998.

[91] Lloyd, R. M., *Physics of Direct Hit and Near Miss Warhead Technology*, vol. 194 of *Progress in Astronautics and Aeronautics*. Reston, VA: AIAA, 2001.

[92] Macfadzean, R. H. M., *Surface-Based Air Defense System Analysis*. Boston: Artech House, 1992.

[93] Maier, M. W., "Architecting Principles for Systems of Systems," in *Proceedings of the Sixth Annual International Symposium, International Council on Systems Engineering, Boston, MA*, 1996.

[94] Maier, M. W., "Integrated Modeling: A Unified Approach to System Engineering," *Journal of Systems and Software*, vol. 32, Feb 1996.

[95] Maier, M. W. and Rechtin, E., *The Art of Systems Architecting*. Boca Raton, FL: CRC Press, 2nd ed., 2000.

[96] Martin, S. G., "Phalanx Block 1B CIWS: Ready For The Fleet." Defense Technical Information Center, May 2000. `http://www.dtic.mil/ndia/ammo/martin.pdf` [Date accessed: June, 2005].

[97] Marx, W. J., Mavris, D. N., and Schrage, D. P., "A Hierarchical Aircraft Life Cycle Cost Analysis Model," 1st AIAA Aircraft Engineering, Technology, and Operations Conference, Los Angeles, CA, September 19-21, 1995. AIAA-95-3861.

[98] Marx, W. J., Mavris, D. N., and Schrage, D. P., "Effects of Alternative Wing Structural Concepts on High Speed Civil Transport Life Cycle Costs," 1996. AIAA-96-1381.

[99] Massey, K. C., McMichael, J., Warnock, T., and Hay, F., "Design and Wind Tunnel Testing Of Guidance Pins For Supersonic Projectiles," Presented at the 24th Army Sciences Conference, 2004. CO-04.

[100] Massey, K. C. and Silton, S. I., "Testing the Maneuvering Performance of a Mach 4 Projectile," Presented at the 24th AIAA Applied Aerodynamics Conference, San Francisco, California, June 5-8,, 2006. AIAA-2006-3649.

[101] Massey, K., Heiges, M., DiFrancesco, B., Ender, T., and Mavris, D., "The Use of Simulations and System-of-Systems Design to Investigate a Guided Projectile Mortar Defense System," Presented at the 36th AIAA Fluid Dynamics Conference and Exhibit, 24th Applied Aerodynamics Conference, San Francisco, CA, June 5-8, 2006. AIAA-2006-3652.

[102] Massey, K., Holder, J., Ender, T., and Heiges, M., "6-DOF and Guided Projectile System Requirements." Review Presentation for U.S. Army Customers, Georgia Tech Research Institute, Atlanta, GA, February 2006.

[103] The MathWorks, Inc., *MATLAB: Statistics Toolbox User's Guide Version 5*, 2004.

[104] Mavris, D. N., Baker, A. P., and Schrage, D. P., "Implementation of a Technology Impact Forecast Technique on a Civil Tiltrotor," Presented at the American Helicopter Society 55th Annual Forum, Montreal, Quebec, Canada, May 25-27, 1999. AHS-99-AB.

[105] Mavris, D. N. and DeLaurentis, D. A., "A Stochastic Design Approach for Aircraft Affordability," Presented at the 21st Congress of the International Council on the Aeronautical Sciences (ICAS), Melbourne, Australia, September, 1998. ICAS-98-6.1.3.

[106] Mavris, D. N., DeLaurentis, D. A., Bandte, O., and Hale, M. A., "A Stochastic Approach to Multi-disciplinary Aircraft Analysis and Design," Presented at the 36th Aerospace Sciences Meeting and Exhibit, Reno, NV, January 12-15, 1998. AIAA-98-0912.

[107] Mavris, D. N., DeLaurentis, D. A., Hale, M. A., and Tai, J. C., "Elements of an Emerging Virtual Stochastic life Cycle Design Environment," Presented at the 4th World Aviation Congress and Exposition, San Francisco, CA, October 19-21, 1999.

[108] Mavris, D. N. and Garcia, E., "Affordability Assessment for a Subsonic Transport," Presented at the 2nd Joint ISAP/SCEA International Conference, San Antonio, TX, June, 1999.

[109] Mavris, D. N., Kirby, M. R., and Qiu, S., "Technology Impact Forecasting for a High Speed Civil Transport," 1998. AIAA-98-5547.

[110] Mavris, D. N., Biltgen, P. T., Ender, T. R., and Cole, B., "Technology Assessment and Capability Tradeoff Using Architecture-Based Systems Engineering Methodologies," 1st International Conference on Innovation and Integration in Aerospace Sciences, Queens University Belfast, Northern Ireland, UK, 4-5 August, 2005. CEIAT 2005-0048.

[111] Mavris, D., Soban, D., and Largent, M., "An Application of a Technology Impact Forecasting (TIF) Method to an Uninhabited Combat Aerial Vehicle," 1999. AIAA-1999-01-5633.

[112] McCullers, L. A., *FLOPS Users Guide Ver. 5.94*. NASA Langley Research Center, January 1998.

[113] MIL-STD-499A, "Engineering Management," May 1974. Military Standard published by the Department of Defense.

[114] Miller, D., *The Illustrated Directory of Modern American Weapons*. Salamander Books Ltd., 2002.

[115] Montgomery, D. C., *Design and Analysis of Experiments*. New York: John Wiley & Sons, Inc., 1976.

[116] Myers, R. H. and Montgomery, D. C., *Response Surface Methodology: Process and Product Optimization Using Designed Experiments*. New York: John Wiley & Sons, Inc, 1995.

[117] Naval Air Systems Command, Avionics Department, AIR-4.5, EW Class Desk, Washington, D.C. 20361, *Electronic Warfare and Radar Systems Engineering Handbook*, April 1999. NAWCWPNS-TP-8347.

[118] Nebabin, V. G., *Methods and Techniques of Radar Recognition*. Boston: Artech House, 1995.

[119] Nelson, R. C., *Flight Stability and Automatic Control*. McGraw-Hill, 2nd ed., 1998.

[120] Nourse, B., "Extended Area Protection and Survivability," Session 1-1. Presented at the 2nd AIAA Tactical Interceptor Technology Symposium, Huntsville, AL, 20-21 January, 2005.

[121] Owen, M., "Experimental Design and System Analysis using the Response Surface Method," Session 4-3. Presented at the 2nd AIAA Tactical Interceptor Technology Symposium, Huntsville, AL, 20-21 January, 2005.

[122] Pahl, G. and Beitz, W., *Engineering Design*. London: Springer-Verlag, 1996.

[123] Papp, D. S., Johnson, L. K., and Endicott, J., *American Foreign Policy: History, Politics, and Policy*. Pearson Education, Inc., 2005.

[124] Parsch, A., "Raytheon ERGM (5" Projectile MK 171)." Directory of U.S. Military Rockets and Missiles, 2003. `http://www.designation-systems.net/dusrm/app4/ergm.html`. [Date accessed: January, 2006].

[125] Paterson, J., "Overview of Low Observable Technology and its Effects on Combat Aircraft Survivability," *Journal of Aircraft*, vol. 36, March-April 1999.

[126] Przemieniecki, J., *Mathematical Methods in Defense Analysis*. AIAA, 3rd ed., 2000.

[127] SAS Institute Inc., Cary, NC, *JMP, Computer Program and Users Manual*, 1994.

[128] Scharl, J. and Mavris, D., "Building Parametric and Probabilistic Dynamic Vehicle Models Using Neural Networks," Presented at the AIAA Modeling and Simulation Conference and Exhibit, Montreal, Canada, August 6-9, 2001. AIAA 2001-4373.

[129] Science Applications International Corporation, San Diego, CA, *Integrated Theater Engagement Model (ITEM)*, 1999.

[130] Shonkwiler, R., "Math 4225 Class Notes." School of Mathematics, Georgia Institute of Technology, 2004.

[131] Silton, S. I., "Comparison of Predicted Actuator Performance for Guidance of Supersonic Projectiles to Measured Range Data," 2004. AIAA-2004-5195.

[132] Silton, S. I. and Massey, K. C., "Integrated numerical and experimental investigation of actuator performance for guidance of supersonic projectiles," Army Sciences Conference, 2004.

[133] Skolnik, M. I., *Introduction to Radar Systems*. McGraw-Hill Publishing Company, 1980.

[134] Soban, D. S., *A Methodology for the Probabilistic Assessment of System Effectiveness as Applied to Aircraft Survivability and Susceptibility*. PhD thesis, Georgia Institute of Technology, 2001.

[135] Tidd, J., Bessant, J., and Pavitt, K., *Managing Innovation: Integrating Technological, Market, and Organizational Change*. John Wiley and Sons, 2nd ed., 2001. Online Innovation Management Toolbox `http://www.wiley.co.uk/.../forecastingtools.htm` [Date accessed: June, 2005].

[136] Tournes, C., "Shark-Flight Control," Session 4-5. Presented at the 2nd AIAA Tactical Interceptor Technology Symposium, Huntsville, AL, 20-21 January, 2005.

[137] Twiss, B. C., *Forecasting for Technologists and Engineers: A Practical Guide for Better Decisions*. London: Peter Peregrinus, Ltd., 1992.

[138] United States Department of Defense (DOD), Department of the Army, U.S. Army Aviation and Missile Command (AMCOM), "Extended Area Protection and Survivability Architecture Study." U.S. Government Printing Office FedBizOpps, Research and Development Procurement, September 2004. `http://fedbizopps.cos.com/cgi-bin/getRec?id=20040913a5`. [Date accessed: January, 2006].

[139] Vanderplaats, G. N., *Numerical Optimization Techniques for Engineering Design*. Colorado Springs, CO: Vanderplaats Research & Development, Inc., 3rd ed., 1999.

[140] Weisstein, E. W., "Monte Carlo Method." MathWorld–A Wolfram Web Resource, `http://mathworld.wolfram.com/MonteCarloMethod.html`. [Date accessed: June, 2005].

[141] Weisstein, E. W., "Total derivative." From MathWorld–A Wolfram Web Resource, `http://mathworld.wolfram.com/TotalDerivative.html`. [Date accessed: April, 2006].

[142] Whyte, J., "Projectile Rocket Ordnance Design and Analysis Software (PRODAS Version 3) Capabilities - Part 1," Session 3-3. Presented at the 2nd AIAA Tactical Interceptor Technology Symposium, Huntsville, AL, 20-21 January, 2005.

[143] Whyte, J., "Projectile Rocket Ordnance Design and Analysis Software (PRODAS Version 3) Capabilities - Part 2," Session 3-4. Presented at the 2nd AIAA Tactical Interceptor Technology Symposium, Huntsville, AL, 20-21 January, 2005.

[144] Williams, J., Brekke, K., Patrick, S., Crosswy, R., Hahna, P., and Frederick, R. A., "Conceptual Design of a Guided Interceptor," 41st AIAA/ASME/SAE/ASEE Joint Propulsion Conference & Exhibit, Tucson, Arizona, 10-13 July, 2005.

[145] Zang, T. A., Hemsch, M. J., Hilburger, M. W., Kenny, S. P., Luckring, J., Maghami, P., Padula, S. L., and Stroud, W. J., "Needs and Opportunities for Uncertainty-Based Multidisciplinary Design Methods for Aerospace Vehicles," Tech. Rep. TM-2002-211462, NASA Langley Research Center, Hampton, VA, 2002.

VITA

Tommer Ender was born on September 28, 1978 in Englewood, NJ. He was raised in South Florida where he attended Cooper City High School, graduating in 1996. He then went on to enroll at the Aerospace Engineering program at the Georgia Institute of Technology in Atlanta, GA, where he earned a Bachelor's degree in 2001. He worked as an undergraduate research assistant at the Aerospace Systems Design Laboratory through which he eventually earned a Master's degree in 2002, and subsequently began pursuing a Ph.D. His professional experience includes working as an undergraduate cooperative student at Pratt & Whitney Government Engines and Space Propulsion in West Palm Beach, FL, and has had the opportunity to work with various government entities during his graduate school tenure. Beyond his technical experience, Mr. Ender was selected as a Pre-Doctoral Fellow for the 2004-2005 Sam Nunn Security Program, through the Sam Nunn School of International Affairs at Georgia Tech.